



UFBA

UNIVERSIDADE FEDERAL DA BAHIA
ESCOLA POLITÉCNICA
PROGRAMA DE PÓS GRADUAÇÃO EM
ENGENHARIA INDUSTRIAL - PEI

MESTRADO EM ENGENHARIA INDUSTRIAL

ANA PAULA ALVES AMORIM

Optimizing Microgrid Design and Operation in Brazil:
A Decision-Making Framework for
Residential Distributed Energy Systems



SALVADOR
2023



UNIVERSIDADE FEDERAL DA BAHIA
ESCOLA POLITÉCNICA
PROGRAMA DE PÓS-GRADUAÇÃO EM ENGENHARIA INDUSTRIAL

ANA PAULA ALVES AMORIM

**Optimizing Microgrid Design and Operation in Brazil: A Decision-Making
Framework for Residential Distributed Energy Systems**

Salvador

2023

Ficha catalográfica elaborada pelo Sistema Universitário de Bibliotecas (SIBI/UFBA),
com os dados fornecidos pelo(a) autor(a).

Alves Amorim, Ana Paula
Optimizing Microgrid Design and Operation in
Brazil: A Decision-Making Framework for Residential
Distributed Energy Systems / Ana Paula Alves Amorim. -
- Salvador, 2023.
227 f. : il

Orientadora: Karen Valverde Pontes.
Coorientador: Bogdan Dorneanu.
Dissertação (Mestrado - Programa de Pós-Graduação em
Engenharia Industrial) -- Universidade Federal da
Bahia, Universidade Federal da Bahia, 2023.

1. Distributed Energy Systems (DES). 2. Microgrid.
3. MINLP. 4. Clustering. I. Valverde Pontes, Karen.
II. Dorneanu, Bogdan. III. Título.

OPTIMIZING MICROGRID DESIGN AND OPERATION IN BRAZIL: A DECISION-MAKING FRAMEWORK FOR RESIDENTIAL DISTRIBUTED ENERGY SYSTEMS

ANA PAULA ALVES AMORIM

Dissertação submetida ao corpo docente do programa de pós-graduação em Engenharia Industrial da Universidade Federal da Bahia como parte dos requisitos necessários para a obtenção do grau de mestre em Engenharia Industrial.

Examinada por:

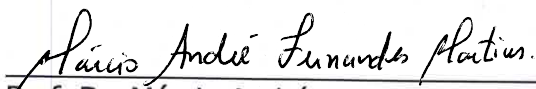


Prof. Dr.-Ing. Harvey Arellano-Garcia, Chemical and Process Engineering, Technische Universität Berlin, Germany, 2006.



Dr. Bogdan Dorneanu

Doutor em Engenharia Química, Delft University of Technology, Netherlands, 2011



Prof. Dr. Márcio André Fernandes Martins

Doutor em Engenharia Química, Universidade de São Paulo, Brasil, 2014.



Prof^a. Dr^a. Karen Valverde Pontes

Doutor em Engenharia Química, Universidade Estadual de Campinas, Brasil, 2008.

Salvador, BA - BRASIL
Abril/2023

ACKNOWLEDGEMENT

I would like to extend my sincerest gratitude to Professor Dr. Harvey Arellano Garcia and all the team at the Department of Process and Plant Technology of the Brandenburgische Technische Universität Cottbus-Senftenberg for providing me with the opportunity to participate in an exchange program in Germany and for their unwavering support throughout my stay. I am deeply grateful for the knowledge and experience I have gained from this opportunity.

I am also incredibly grateful to my advisors, Dr. Karen Valverde Pontes and Dr. Bogdan Dorneanu, for their guidance and support throughout the research process. Their expertise and encouragement have been invaluable to me and have contributed greatly to the completion of this thesis.

I thank God and Holy Mary for their infinite kindness to me throughout my life. My faith has been a constant source of strength and inspiration, and I am deeply grateful for the grace and protection that I have received.

I would also like to extend my sincere thanks to my family, who have always been my rock and my source of strength. Their unwavering love and support have been a constant source of inspiration, and I could not have done this without them.

I would also like to thank Leonardo for his love and support during this challenging time. His patience and understanding have been truly invaluable, and I am so grateful to have him by my side. I also thank my friends in Brazil and also those I gained in Germany and France. Your friendships have been a constant source of inspiration and motivation, and I am deeply grateful for the memories we have shared together.

Lastly, I would like to thank all the people who have supported me in one way or another throughout my academic journey. Your support has been invaluable, and I am deeply grateful for your kindness and encouragement.

This work was carried out with the support of the Coordenação de Aperfeiçoamento de Pessoal de Nível Superior - Brazil (CAPES) - funding code 001.

Abstract of the Master Thesis presented to PEI/UFBA as part of the requirements needed to obtain the degree of Master in Science (M.Sc.).

Optimizing Microgrid Design and Operation in Brazil: A Decision-Making Framework for Residential Distributed Energy Systems

Ana Paula Alves Amorim

Advisor: Prof^ª. Dr^ª. Karen Valverde Pontes

Dr. Bogdan Dorneanu

Distributed Energy Systems (DES) with renewable energy sources were conceived as a way to reduce the emission of polluting gases into the atmosphere and have become a major incentive for self-producers of energy. Although Brazil has a large availability of natural resources, which creates a strong potential for the application of microgrids based on renewable energy sources such as solar, wind, and biomass, it is still little explored in relation to other countries. This study aims to bridge the gaps in the current literature regarding microgrid design by addressing the impact of energy demands in the sizing of a microgrid and the impact of climate on renewable resource efficiency. The study pioneers the application of biogas to all residential energy demands in a microgrid and offers a new approach to analyzing the effects of varying input variables over time in an on-grid microgrid. Therefore the study proposes a decision-making framework for designing and operating residential DES in Brazil, based on mixed-integer nonlinear programming (MINLP) problems that take into account the particularities of the country, such as the availability of various renewable resources and the impact of COVID-19 on energy demand. The models optimize the cost of designing and operating a microgrid with integrated pipelines and consider the varying efficiency of different technologies over time, as well as different options for renewable incentive policies. Additionally, it proposes a systematic, cluster-based method to split the time horizon of the model, allowing for a more accurate representation of the dynamics of the input variables of the optimization problem such as energy demand, wind speed, and solar irradiation over time. The framework is tested on a case study of a residential DES of 5 and 10 houses in Salvador, Brazil, comparing pre- and post-COVID-19 scenarios. The results show that the use of distributed energy resources has turned out to be economically and environmentally advantageous compared to using only non-renewable resources. The study also demonstrates the economic viability of using biogas and the new energy trends emerging during the pandemic, and how this impacts the sizing of microgrids. By not considering time-dependent efficiency in the analysis, there may have been a

positive impact on the economic gain of around 90% in relation to the baseline scenario, but it may also have contributed to the underestimation of power generation. Also, although the empirical method showed a greater reduction in environmental costs (60%), the clustering method had a greater reduction (80%) in total costs. This highlights the relevance of the innovative approaches utilized in the optimization problem for designing a microgrid.

Keywords: Distributed Energy Systems (DES); Microgrid; MINLP; Clustering

Summary

ACKNOWLEDGEMENT	4
CHAPTER I- INTRODUCTION.....	11
I.1. Introduction	11
I.2. Objective	14
I.3. Justification	14
I.4. Structure of the master thesis	15
CHAPTER II- State-of-the-art Review	17
II.1. Introduction	17
II.2. International agreements to promote sustainable development	17
II.3. Incentive policies for Distributed Generation (DG).....	19
II.4. Incentive policies for Distributed Generation (DG) in Brazil	23
II.5. Energy and electric matrix of Brazil and the world	27
II.6. Renewable energy sources	32
II.6.1. Solar	32
II.6.2. Wind	36
II.6.3. Biomass	38
II.6.4. Biopropane (BioLPG)	43
II.6.5. Hydroelectricity	44
II.6.6. Oceanic.....	46
II.6.7. CHP	48
II.6.8. Geothermal	49
II.6.9. Energy storage.....	51
II.7. Microgrids	53
II.7.1. Optimal microgrid configuration.....	55
II.8. Conclusions	71
CHAPTER III- Formulation of the Optimization Problem.....	73
III.1. Introduction	73
III.2. Problem Definition	74
III.3. Splitting the Time Horizon.....	76
III.4. Optimization problem formulation	82
III.4.1. Objective Function	82
a. Investment	82
b. Operation and maintenance (O&M) cost.....	86

c.	Environmental Cost	91
d.	Electricity Cost	92
e.	Natural Gas Cost	92
f.	Policy revenue	93
III.4.2.	Electricity balance	94
III.4.3.	Hot water balance	95
III.4.4.	Air cooling balance	95
III.4.5.	Cooking gas balance	96
III.4.6.	Natural gas consumption	96
III.4.7.	Design and operation constraints	96
III.5.	Model Implementation	112
III.6.	Conclusion	112
CHAPTER IV – RESULTS AND DISCUSSION		114
IV.1.	Introduction	114
IV.2.	Description of the case study	115
IV.2.1	Parameters	115
IV.3.	Splitting the Time Horizon	120
IV.4.	Results and discussions	122
IV.4.1.	S1E5: Scenario without time-dependent profile for efficiency of the DER and cluster method during pre-COVID for five houses	123
IV.4.2.	S2E5: Scenario with time-dependent profiles for efficiency of the DER and empirical method during pre-COVID for five houses	125
IV.4.3.	S3E5: Scenario with time-dependent profile for efficiency of the DER and clustering method during pre-COVID for five houses	126
IV.4.4.	S3O5: Scenario with time-dependent profile for efficiency of the DER and clustering method during post-COVID for five houses	128
IV.4.5.	S3E10: Scenario with time-dependent profile for efficiency of the DER and clustering method during pre-COVID for ten houses	129
IV.4.6.	S3O10: Scenario with time-dependent profile for efficiency of the DER and clustering method during post-COVID for ten houses	131
IV.5.	Costs and revenues	132
IV.6.	Sensitivity analysis for battery use	137
IV.7.	Sizing	137
IV.8.	The Effect of Time-Varying Efficiency Profiles on power generation	143
IV.9.	The Effect of Time Horizon Division with the Clustering Method on power generation	145

IV.10.	Differences between Pre and Post-COVID on power generation	146
IV.11.	The Influence of the Number of Houses on Power Generation.....	147
IV.12.	Numerical Statistics.....	148
IV.13.	Conclusion	149
CHAPTER V – CONCLUSIONS AND FUTURE WORK.....		151
V.1.	Conclusion	151
V.2.	Suggestions for future work.....	153
APPENDIX A- Parameters and Costs		155
APPENDIX B- Python code for period clustering.....		158
APPENDIX C - Discussion of the Time Clustering Result.....		160
APPENDIX D - Discussion of the results for each scenario.....		165
S1E5: Scenario 1 during pre-COVID for five (5) houses.....		165
S2E5: Scenario 2 during pre-COVID state for five (5) houses.....		170
S3E5: Scenario 3 pre-COVID for five (5) houses.....		174
S3O5: Scenario 3 post-COVID for five (5) houses.....		179
S3E10: Scenario 3 during pre-covid state for ten (10) houses		183
S3O10: Scenario 3 during post-COVID state for ten (10) houses.....		190
APPENDIX E – Variables and Parameters.....		197
REFERENCES.....		203

List of Figures

Figure 1 – Global fossil fuel consumption. Source: Ritchie, Rosado and Roser (2022).....	11
Figure 2 – Industrial Revolution Timeline. Source: Vaidya (2023)	11
Figure 3 - Historical CO ₂ emissions from fossil fuels in the world. Source: Ritchie, Roser and Rosado (2021).	12
Figure 4 - Increase in global temperature over the years. Source: Ritchie, Roser and Rosado (2021).	12
Figure 5 - Warming scenarios of greenhouse gas emissions. Source: Ritchie, Roser, and Rosado (2021).	18
Figure 6 - Distribution of greenhouse gas emissions by sector in 2020. Source: Ritchie and Roser (2020).	19
Figure 7 – Brazil Regions Map. Source: Mappr (2023).	23
Figure 8 - History of the main policies/mechanisms to encourage renewable energy in Brazil. 24	
Figure 9 - Brazilian and world energy matrix in 2019. Source: Ritchie, Roser (2019).	28
Figure 10 - Renewable and non-renewable energy consumption profile in Brazil and the world in 2019. Source: MME (2020).	28
Figure 11 - Brazilian Electric Matrix 2020. Source: MME (2021).	29
Figure 12 - Diagram of photovoltaic energy in a residence. Source: GBS (2022).	33
Figure 13 - Cumulative profile of distributed and centralized generation by PV worldwide in the decade 2009-2019. Source: Masson et al. (2020).	34
Figure 14 - Solar thermal energy production diagram. Source: Greenriverside (2022).	36
Figure 15 - Diagram of solar energy production in hybrid PV/T systems. Source: Ramos (2017).	36
Figure 16 – Representation of wind energy in a residence. Source: Rowan House (2022).	37
Figure 17 - Distribution of onshore and offshore wind installations worldwide. Source: GWEC (2021).	37
Figure 18 – Diagram of a biomass thermoelectric plant. Source: Salix Renewable (2018).	39
Figure 19 – Diagram of thermal energy generation through biomass. Source: Herschel Infrared (2022).	39
Figure 20 - Diagram of biogas and biomethane production. Source: Reurasia (2020).	40
Figure 21 - Historical and forecasted increase in installed capacity by biomass in Brazil in MW. Source: Unica (2020).	41
Figure 22 - Historical biogas installed capacity in the world in MW	41
Figure 23 - Biomass distribution in electric generation in Brazil.....	42
Figure 24 - Monthly LPG consumption in Brazil. Source: Sindigás (2021)	43
Figure 25 - Technological routes for biopropane production. Source: Adapted from Hopwood, Mitchell, Sourmelis (2019).	44
Figure 26 - Diagram of operation of a hydroelectric plant. Source: U.S. Department of Energy (2022).	45
Figure 27 – Capacity of hydroelectric generation in the world between 2000 and 2019. Source: IEA (2020).	46
Figure 28 - Diagram of the production of electricity through wave energy. Source: Stauffer (2009).	47
Figure 29 - Classification of the main CHP technologies. Source: Adaptado de Martinez et al. (2017).	48

Figure 30 - Schematic diagram of the operation of a CHP system. Source: Martinez, Michaux, Salagnac, nd Bouvier (2017).	49
Figure 31 - Geothermal energy operation. Source: Energizect (2022).	50
Figure 32 - Map of geothermal resource in Brazil. Source: Arboit et al. (2013).	51
Figure 33 - Operation of a battery in the electrical system. Source: Nikolaidis, Poullikkas (2017).	52
Figure 34 - Example of a microgrid. Source: Elinoff (2019).	53
Figure 35 - Classification of microgrids. Source: Adapted from Eluri and Naik (2021).	54
Figure 36 - Optimization techniques used to define the best configuration for distributed generation systems. Source: Adapted from Tan et al. (2013).	68
Figure 37 – General sketch of all technologies considered in the microgrid.	74
Figure 38 - Operation scheme for hot water generation in each residence.	76
Figure 39 - The annual time horizon for operating the microgrid	77
Figure 40 - The time horizon for operating the microgrid divided into seasons(m) and periods (p)	77
Figure 41 - Profile of the electricity demand before time division.	78
Figure 42- K-means method to cluster the data set. Source: Sharma (2022).	79
Figure 43 - Exemplification of the elbow method. Source: Yse (2019).	80
Figure 44 – Algorithm for the clustering process to split the time horizon.	81
Figure 45 - Operation of an electric shower. Source: Adapted from Lara (2019).	99
Figure 46 - Behavior of the weather in Brazil: (a) Solar irradiation; (b) Temperature; (c) Wind speed; (d) Wind power. Source: World Bank Group (2022); DTU Wind Energy (2022)	117
Figure 47 - Electricity rate (R\$/kW) from the central grid in Bahia for the pre- and post-COVID scenario. Source: BRASIL, 2019; BRASIL, 2022.	118
Figure 48 - Average energy demand in Salvador, Brazil in the pre- and post-COVID scenarios for: (a-b) electrical demand (kW); (c-d) cooling demand (kW); (e-f) hot water (L); (g-h) gas for cooking (kW).	119
Figure 49 - Time period during the year and the day for the pre-COVID state with empirical method.	121
Figure 50 - Time period during the year for the pre-COVID scenario.	122
Figure 51 - Time period during the day for the post-COVID state.	122
Figure 52 - Optimal energy resources and connections between houses for Scenario 1 during pre-COVID for five houses (S1E5).	124
Figure 53 - Optimal energy resources and connections between houses for Scenario 2 during pre-COVID for five houses (S2E5).	125
Figure 54- Optimal energy resources and connections between houses for Scenario 3 during pre-COVID for five houses (S3E5).	127
Figure 55 - Optimal energy resources and connections between houses for Scenario 3 post-COVID for five houses (S3O5).	128
Figure 56 - Diagram of energy resources and connections between houses for the microgrid with 10 houses pre-COVID for Scenario 3 (S3E10).	131
Figure 57 - Diagram of energy resources and connections between houses for the microgrid with 10 houses post-COVID for Scenario 3 (S3O10).	132
Figure 58 - Total cost for each scenario and its respective baseline.	133

Figure 59 - Impact of battery capital cost on the objective function and number of batteries installed in S3E5.	137
Figure 60 - Profile of resources used to meet the electrical demand in Scenario S1E5 houses: a)i1; c) i4 and in Scenario S3E5 houses: b)i1; d)i5.....	144
Figure 61 - Distribution of resources used to meet the hot water demand for house i5 in the case: a) S1E5; b) S3E5.....	145
Figure 62 - Profile of resources used to meet the electrical demand in house i1 in the case: a)S2E5; b)S3E5.....	145
Figure 63 - Profile of the resources used to meet the electrical demand in house i2 Scenario S3O5 expressed in: a) kW; c)percentage and in house i2 Scenario S3E5 expressed in: b)kW; d) percentage.	147
Figure 64 - Profile of resources used to meet the electrical demand in house i2 in the case: a)S3E10; b)S3E5.....	148
Figure 65- Graphical method for selecting the best amount of clusters during the year in the pre-COVID scenarios.	160
Figure 66 – Clustering the period during the year in the pre covid state	161
Figure 67 - Graphical method for selecting the best amount of clusters during the day in the pre-COVID scenarios	161
Figure 68 - Clustering the period during the day in the pre-COVID scenarios.....	162
Figure 69 - Graphical method for selecting the best amount of clusters during the year in the post-COVID scenarios.....	163
Figure 70 - Clustering the period during the year in the post-COVID scenarios.....	163
Figure 71- Graphical method for selecting the best amount of clusters during the day in the post-COVID scenarios.....	164
Figure 72 - Clustering the period during the day in the post-COVID scenarios	164
Figure 73 - Profile of resources used to meet the electrical demand in Scenario 1 pre-COVID for a microgrid with 5 houses: a) i1; b) i2; c) i3; d) i4; e) i5.	166
Figure 74 - Distribution of electricity generation by distributed renewable resources for Scenario 1 pre-COVID for a microgrid with 5 houses: a) i1; b) i2; c) i3; d) i4; e) i5.....	168
Figure 75 - Profile of resources used to meet the hot water demand for Scenario 1 pre-COVID for a microgrid with 5 houses: a) i2; b) i3; c) i4; d) i5.....	169
Figure 76 - Biogas and natural gas consumption behavior for Scenario 1 pre-COVID for a microgrid with 5 houses for house i5.....	170
Figure 77 - Profile of resources used to meet the electrical demand in Scenario 2 pre-COVID for five houses: a) i1; b) i2; c) i3; d) i4; e) i5.....	171
Figure 78 - Distribution of electricity generation by distributed renewable resources for Scenario 2 pre-COVID for a microgrid with five houses: a) i1; b) i2; c) i3; d) i4; e) i5.....	173
Figure 79- Profile of resources used to meet the hot water demand in Scenario 2 pre-COVID for a microgrid with five houses: a) i1; b) i2; c) i3; d) i4; e) i5.	174
Figure 80 - Profile of resources used to meet the electrical demand in Scenario 3 pre-COVID for a microgrid with five houses: a) i1; b) i2; c) i3; d) i4; e) i5.	175
Figure 81 - Distribution of electricity generation by distributed renewable resources in Scenario 3 pre-COVID for a microgrid with five houses: a) i1; b) i2; c) i3; d) i4; e) i5.....	177
Figure 82 - Profile of resources used to meet the hot water demand in Scenario 3 pre-COVID for a microgrid with five houses: a) i1; b) i2; c) i3; d) i4; e) i5.....	178

Figure 83 - Biogas and natural gas consumption behavior in Scenario 3 pre-COVID for a microgrid with five houses for house i5.....	179
Figure 84 - Profile of resources used to meet the electrical demand for Scenario 3 post-COVID for five houses: a) i1; b) i2; c) i3; d) i4; e) i5.	180
Figure 85 - Distribution of electricity generation by distributed renewable resources for Scenario 3 post-COVID state for five houses: a) i1; b) i2; c) i3; d) i4; e) i5.....	182
Figure 86 - Profile of resources used to meet the hot water demand for Scenario 3 post-COVID state for five houses: a) i1; b) i2; c) i3; d) i4; e) i5.	183
Figure 87 - Profile of resources used to meet the electrical demand in the pre-COVID scenario 3 for ten houses: a) i1; b) i2; c) i3; d) i4; e) i5; f) i6; g) i7; h) i8; i) i9; j) i10.....	185
Figure 88 - Distribution of electricity generation by distributed renewable resources in the pre-COVID scenario 3 for ten houses: a) i1; b) i2; c) i3; d) i4; e) i5; f) i6; g) i7; h) i8; i) i9; j) i10... ..	187
Figure 89 - Profile of resources used to meet the hot water demand in the pre-COVID scenario 3 for ten houses: a) i1; b) i2; c) i3; d) i4; e) i5; f) i6; g) i7; h) i8; i) i9; j) i10.	189
Figure 90 - Biogas and natural gas consumption behavior for house i5 for the microgrid of 10 houses in the pre-COVID scenario 3.....	190
Figure 91 - Profile of resources used to meet the electrical demand in the post-COVID scenario 3 for ten houses: a) i1; b) i2; c) i3; d) i4; e) i5; f) i6; g) i7; h) i8; i) i9; j) i10.	192
Figure 92 - Distribution of electricity generation by distributed renewable resources in the post-COVID scenario 3 for ten houses: a) i1; b) i2; c) i3; d) i4; e) i5; f) i6; g) i7; h) i8; i) i9; j) i10.	194
Figure 93 - Profile of resources used to meet the hot water demand in the post-COVID scenario 3 for ten houses: a) i1; b) i2; c) i3; d) i4; e) i5; f) i6; g) i7; h) i8; i) i9; j) i10.	196

List of Tables

Table 1 - Comparison of Incentive Policies for Distributed Generation: Advantages and Disadvantages	22
Table 2 - Overview by region of contracted power in the first phase of PROINFA. Source: MME (2009).	25
Table 3 - Energy amount and cost for PAP 2020. Source: Eletrobrás (2020).	25
Table 4 - Installed capacity of Electric Generation in Brazil (GW). Source: MME (2021).	30
Table 5 - Percentage of installed energy supply according to energy production systems - 2020 (%). Source: MME (2021).	31
Table 6 - Electricity generation profile by self-producer (APE) - 2020 (GWh). Source: MME (2021).	31
Table 7 - Top 10 countries for distributed PV installed in 2020. Source: IEA (2021).	34
Table 8 - Installed power by state in Brazil in 2020. Source: Godoi (2021).	38
Table 9 - Classification of biogas plants for energy purposes in Brazil in 2020. Source: CIBlogas (2020).	42
Table 10 - Theoretical energy potential of oceanic sources. Source: Modified from Saavedra (2016).	47
Table 11 - Countries in the top 5 of energy generation by geothermal sources. Source: Campos et al. (2016).	50
Table 12 - Microgrid configuration optimization studies.....	56
Table 13 - Size and computational performance of optimization problems.	66
Table 14 - Advantages and disadvantages of DRG placement methods. Source: Tan et al. (2013)	70
Table 15 – Technologies adopted in the optimization problem.	75
Table 16 - Distance between houses in meters for the scenario with 10 houses.	116
Table 17- Cost of natural gas in Bahia for the pre-covid and post-covid states	118
Table 18 - Scalar of the demand for each house.....	120
Table 19 – Simulated cases	123
Table 20 - Costs and revenues for all scenarios	134
Table 21 - Resource size at baseline for all scenarios	138
Table 22 - Size of renewable resources distributed for all scenarios.....	140
Table 23 - Results for the scenarios with energy resources distributed at a 0% gap	149
Table 24 – Costs of energy resources and their operational parameters.....	155
Table 25 – Carbon intensity for each resource	157
Table 26 – Feed in Tariff for generating electricity for each resource	157
Table 27 - Time period during the year for the pre-COVID scenarios.....	161
Table 28 - Time period during the day for the pre-COVID scenarios.....	162
Table 29 - Time period during the year for the post-COVID scenarios	163
Table 30 - Time period during the day for the post-COVID scenarios	164
Table 31 - Continuous variables for the model.	198
Table 32 - Binary variables used in the model.	200
Table 33 – Parameters used in the model.	201
Table 34 – Input variables used in the model.	202

List of Abbreviations

AC: Air Conditioning

ACc: Alternating Current

ACL: Ambiente de Contratação Livre (Free Contracting Environment)

ACR: Ambientes de Contratação Regulada (Regulated Contracting Environment)

AI: Artificial Intelligence

ANEEL: *Agência Nacional de Energia Elétrica* (National Agency of Electric Energy)

ANP: *Agência Nacional do Petróleo, Gás Natural e Biocombustíveis* (National Petroleum, Natural Gas and Biofuels Agency)

APE: Autoprodutor de Energia Elétrica (Self-Producer of Electric Energy)

BARON: Branch-And-Reduce Optimization Navigator

BD: biodigester

BG: biogas electricity generator

BH: biogas heater

BT: battery

C: cooking gas

CCEE: Câmara de Comercialização de Energia Elétrica (Chamber of Commercialization of Electric Energy)

CDM: Clean Development Mechanism

CER: Certified Emission Reductions

CGHs: *Centrais Geradoras Hidrelétricas* (Hydroelectric Generating Plants)

CHP: Combined Heat and Power

CHP: Combined Heat and Power

COE: Cost of Electricity

COPs: Conference of the Parties

CRF: Capital Recovery Factor

CSP: Concentrated Solar Power

DC: Direct Current

DES: Distributed Energy Systems

DG: Distributed Generation

DNI: direct solar irradiation

DOC: Depth of discharge

DRG: distributed renewable generation

EL: electricity line

EPE: *Empresa de Pesquisa Energética* (Energy Research Company)

ES: electric shower

FIT: Feed-in-Tariff

GAMS: General Algebraic Modelling System

GH: gas heater

GHG: Greenhouse gas

GRID: grid energy

HVO: Hydrogenated Vegetable Oil

HW: hot water

IBGE: Instituto Brasileiro de Geografia e Estatística (Brazilian Institute of Geography and Statistics)

ICE: Internal Combustion Engine

IEEE: Institute of Electrical and Electronics Engineers

I-RECs: International REC Standard

LPG: Liquefied Petroleum Gas

LPSP: Loss of Power Supply Probability

MG: cost with the microgrid

MILP: mixed integer linear programming

MINLP: Mixed Integer Nonlinear Programming

MOPSO: Multiple Objective Particle Swarm Optimization

MPC: Model Predictive Control

NDC: Nationally Determined Contribution

NEM: Net Energy Metering

NG: natural gas energy

NLP: Nonlinear Programming

O&M: Operation and maintenance

OTEC: Ocean Thermal Energy Conversion

PAP: *Plano Anual do Proinfa* (Annual Plan of Proinfa)

PCH: *Pequenas Centrais Hidrelétricas* (Small Hydroelectric Plants)

PEE: Programa de Eficiência Energética (Energy Efficiency Program)

PEM: Proton Exchange Membrane

PESA II: Pareto Swarm Optimization

PLD: Preço da Liquidação das Diferenças (Price for the Settlement of Differences)

PP: hot water piping

ProGD: Programa de Desenvolvimento da Geração Distribuída de Energia Elétrica (Program for the Development of Distributed Generation of Electric Energy)

PV: Photovoltaic panel

REC: Renewables Energy Certificates

RHI: Renewable Heat Incentive

SC: Solar Collector

SDGs: Sustainable Development Goals

SE: Stirling Engine

SIN: *Sistema Interligado Nacional* (National Interconnected System)

SOFC: Solid Oxide Fuel Cell

SPEA2: Strength Pareto Evolutionary Algorithm

ST: storage tank

TS: thermal storage

UHES: *Usinas Hidrelétricas de Energia* (Hydroelectric Power Plants)

UN: United Nations

UNFCCC: United Nations Framework Convention on Climate Change

WT: Wind Turbine

CHAPTER I- INTRODUCTION

I.1. Introduction

After the emergence of the first industrial activities and energy processes, greenhouse gas (GHG) emissions increased significantly. This is due to the burning of fossil fuels for energy production. Figure 1 shows the increase in fossil fuel consumption from 1800 to 2021, doubling in value from 1970 to 2021 when the Third and Fourth industrial revolutions took place. As seen in Figure 2, the third industrial revolution began around 1970 and lasted until around 2000, with the introduction of electronics and information technology in manufacturing. The fourth industrial revolution began soon after, with the fusion of digital technologies and physical systems, leading to a transformative impact on various sectors through advancements such as artificial intelligence, automation, big data, and the Internet of Things.

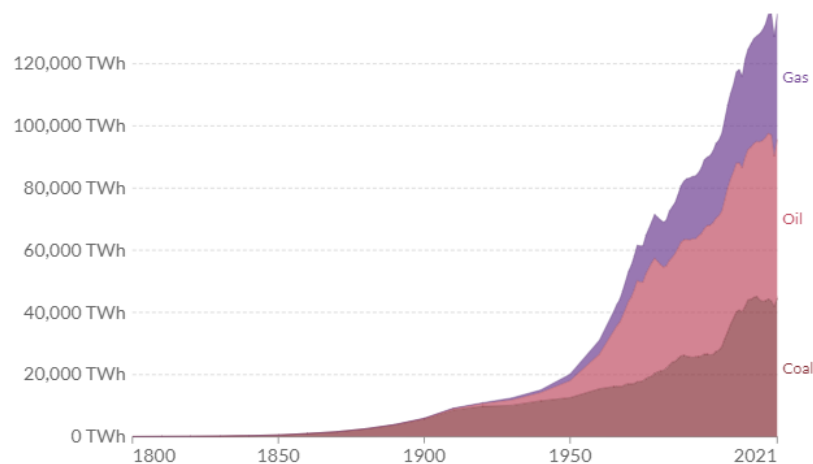


Figure 1 – Global fossil fuel consumption. Source: Ritchie, Rosado and Roser (2022).



Figure 2 – Industrial Revolution Timeline. Source: Vaidya (2023)

Similarly, as can be seen in Figure 3, there has been an increase in GHG emissions, with the most economically developed countries making the largest contributions to this increase. Over the years, the emissions from human activities have been contributing to the rise in global temperatures (Figure 4) This, in turn, has led to an increase in the frequency of natural disasters such as cyclones, floods, tornadoes, and droughts. The reduction in air quality further causes respiratory problems in the population (HOUGHTON, 2005).

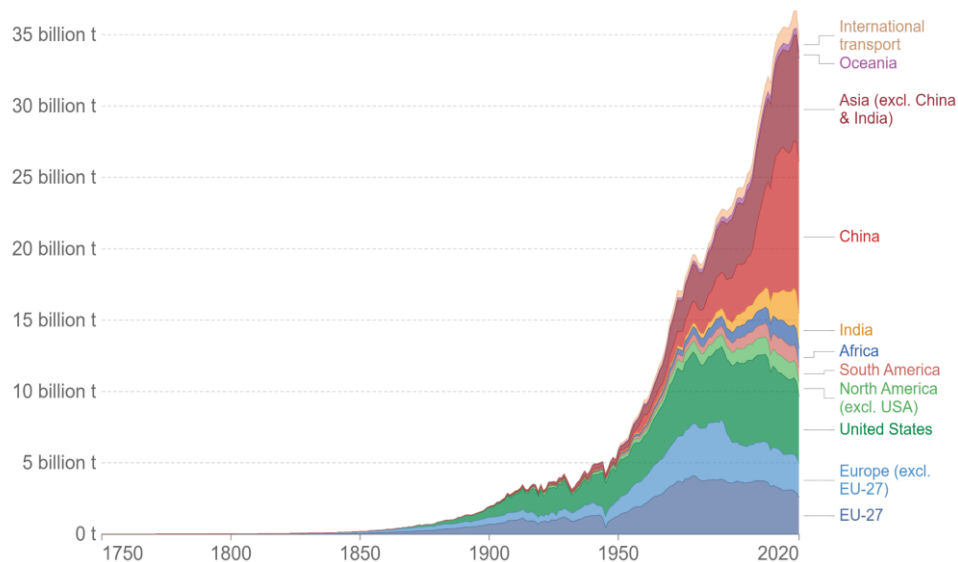


Figure 3 - Historical CO₂ emissions from fossil fuels in the world. Source: Ritchie, Roser and Rosado (2021).

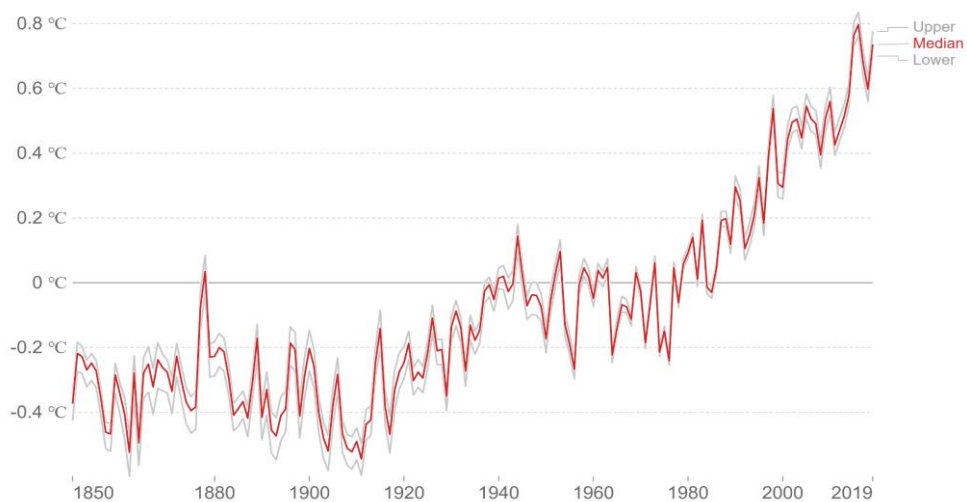


Figure 4 - Increase in global temperature over the years. Source: Ritchie, Roser and Rosado (2021).

The need to reduce atmospheric GHG emissions from burning fossil fuels to generate electricity is driving the development of microgrids. These systems correspond to the

production of energy at or near the place of consumption by means of renewable sources, so they are considered distributed generation systems.

Microgrids provide an alternative to traditional centralized power systems and require less technical expertise to operate, making them an effective solution for modernizing existing power grids over time (LEE et al., 2015). From this perspective, the use of distributed renewable energy production contributes to the reduction of pollutant gases emitted into the atmosphere, making the use of resources more efficient, diversifying the energy matrix, reducing losses in energy transmission, creating jobs, along with others (LEE et al., 2015). However, microgrid planning can be a complex task as it involves balancing a variety of factors such as the availability of renewable energy sources, which can be highly variable, the environment, technology, geography, and regulatory constraints. One of the main challenges in microgrid planning is managing the variability of renewable energy sources such as solar and wind power, which can fluctuate depending on weather conditions. This requires careful forecasting and real-time monitoring to ensure that the microgrid can adjust to changes in the availability of energy. Additionally, the integration of different energy sources and technologies, as well as compliance with local regulations, can add to the complexity of microgrid planning. The geographic location also plays a significant role in the planning as well, as it affects the availability of different energy sources and the environmental conditions that the microgrid will operate in (GAMARRA and GUERRERO, 2015).

Inappropriate allocation and combinations of distributed renewable resources can lead, among other things, to energy losses, necessary reconfiguration of protection systems, and increased costs (TAN et al., 2013). To reap all the benefits, a detailed study is required to determine the optimal configuration of the system before implementing a microgrid.

Microgrid configuration optimization problems can be structured in terms of cost minimization, reliability maximization, electrical losses minimization, to cite a few (TAN et al., 2013). Because it is such a broad field, there are still gaps in the literature regarding the impact of varying energy demands on microgrid design, the influence of time-dependent efficiency profiles of renewable resources on energy sharing behavior, the selection of appropriate time periods for optimization, and the use of biogas to meet all the energy demands in a residential microgrid, combined with other renewable sources. Additionally, there is a need to customize incentive policies for renewable distributed energy systems based on local conditions and characteristics.

These are important to realistically define the problem under study. Therefore, it is necessary to conduct a thorough analysis of these factors in order to determine the optimal configuration for microgrids.

I.2. Objective

I.2.1. General Objective

The objective of this work is to propose a decision-making framework that utilizes mixed nonlinear programming models to design and operate residential distributed energy systems, while incorporating innovative analyses to better understand the system.

I.2.2. Specific Objectives

- i. Propose a systematic method, based on clustering, to split the time periods of the energy demand profile for the model, and compare the effectiveness of this method with the empirical method;
- ii. Formulate and solve an optimization model of a microgrid that encompasses all the main energy demands of a residence;
- iii. Analyze the impact of pre- and post-COVID demand scenarios on microgrid design;
- iv. Identify the best incentive policy for residential microgrids;
- v. Identify how the time-dependent profile of efficiency of renewable sources influence the cost and the design of the microgrid;
- vi. Evaluate the feasibility of utilizing biogas as a renewable energy source in microgrids, and propose a combination of biogas with other renewable sources.

I.3. Justification

Energy demand is an essential parameter when optimizing the microgrid's configuration, since it characterizes the system. However, the literature does not provide yet an analysis of how different demands may affect microgrid design. Taking into consideration the COVID-19 pandemic that has considerably affected the energy consumption in residences around the world due to the popularization of working from home and distance learning systems, this work analyzes post- and pre-COVID demand scenarios and their impact on microgrid design. In addition, variations in climatic conditions can impact the energy supply when using renewable resources such as photovoltaic panels, solar collectors, and wind turbines. These variations can affect the efficiency of these technologies in real-time (WOUTERS et al., 2015). Currently, there is a lack of the literature regarding the influence of the time-dependent efficiency profile of renewable resources on energy sharing behavior in microgrids, as well as the differences in adopting this consideration or not in the design of a microgrid. Therefore, a comparison is made between a scenario without consideration of the time-dependent profile of the efficiency of solar and wind sources, and a scenario that takes into account the changes in efficiency over time for a microgrid of 5 houses.

The continuous time scale (day, month and year) needs to be discretized into time periods in the optimization problem, in order to reduce the computational effort and facilitate the numerical solution of the problem. Therefore, due to the importance of this step for solving the optimization problem, this work uses the systematic clustering method to determine the time period taking into account important data in the system characterization, such as energy demands and/or environmental data (ZATTI et al., 2019). Thus, this work investigates the applicability of the systematic clustering method for the presented optimization problem, and compares it with the empirical method, based on system observation and manual division of the time horizon, used by Clarke et al. (2021) and Sidnell et al. (2021a). Furthermore, this work analyzes how the clustering method impacts microgrids with varying amounts of houses, as well as the allocation and sizing of renewable resources within these systems.

Certain energy sources may not yet be fully utilized in distributed energy systems. One of them is the biogas, which can generate electricity and thermal energy. It can be produced from the decomposition of organic waste, therefore offers low environmental impact and is a good alternative to replace non-renewable fuels such as natural gas (COELHO et al., 2018). Thus, a new approach to the sizing of a biogas plant within a microgrid was evaluated to meet the demands of electricity, hot water and gas for cooking food. In addition, a combination of biogas with other renewable sources was proposed: solar and wind energy. In the available literature, the utilization of a combination of biogas, wind energy, and photovoltaic sources is not widely examined.

The adoption of incentive policies for the production of renewable distributed energy has contributed to the increase in the adhesion of these systems all over the world (FREITAS and HOLLANDA, 2015). However, an incentive policy must be customized to offer good results, taking into account the conditions and characteristics of each country. With this in mind, the main policies currently adopted in the market for self-consumption generation (i.e. Feed in Tariff, Net Energy Metering) are considered in formulating the optimization problem, in order to identify the best incentive policy for the system.

I.4. Structure of the master thesis

This dissertation is divided into five chapters. Chapter I presented the contextualization of the theme, the general and specific objectives, the justification of the work and its structure.

Chapter II presents the review of the state-of-the-art, discussing the international agreements to promote sustainable development, the incentive policies for Distributed Generation (DG) and the characterization of the electric energy matrix adopted in Brazil and in the world. In addition, it presents the main renewable energy sources, as well as

reviews the studies reported in the area of optimization of micro-grid configuration. The critical analysis of these studies was essential to analyze the gaps in the literature on the subject to be considered for defining the optimization problem.

Chapter III aims to present the formulation of the optimization problem. For this, the methods used to determine the time period of the optimization problem are defined, as well as the optimization problem and, namely the objective function and its constraints. After that, the method to solve the problem is presented.

Chapter IV presents the case study for the city of Salvador, Brazil. First, the behavior of the environmental variables (wind speed and solar irradiation) of the site is exposed, as well as the behavior of the energy demands. Then the time periods used in the problem are presented. After that, the results for all cases and scenarios are presented and discussed, exposing the selection of energy resources in each house, as well as the interaction between a set of 5 and 10 houses. After that, the results for each scenario are compared with each other in terms of total costs, environmental cost and energy resource sizing. Finally, a numerical analysis of the model are performed in order to verify the computational effort for each scenario and case.

Finally, Chapter V presents the conclusions, as well as suggestions for future work.

CHAPTER II- State-of-the-art Review

II.1. Introduction

As previously discussed, the prolonged use of fossil fuels has led to a substantial rise in greenhouse gas emissions. In light of this, this chapter will explore the incentive policies for Distributed Generation adopted in Brazil and in the world in order to mitigate the effects of the prolonged use of fossil fuels, as well as the influence of these policies on the energy scenario in Brazil. In addition, it discusses the main renewable energy sources used in Brazil and in the world, also introduces the contributions of microgeneration adoption. To this end, studies are presented that explain the optimization of microgeneration configuration, using various renewable energy sources, in terms of minimizing costs, minimizing energy losses, maximizing reliability, among other factors.

II.2. International agreements to promote sustainable development

The impact of human action began to gain global prominence in 1972 with the Stockholm Conference. Since then, the scientific community and political leaders have been meeting to discuss solutions to minimize and contain environmental impacts and promote sustainable development worldwide. One of the agreements that gained prominence due to the mobilization of several countries was the United Nations Framework Convention on Climate Change (UNFCCC), which was proclaimed at the United Nations Conference on Environment and Development in 1992, in Rio de Janeiro, with the participation of 178 countries. This convention had the proposal to hold frequent conferences (Conference of the Parties - COPs) on climate in order to monitor and review the progress of the measures taken by countries in reducing the global emission of greenhouse gases (GHGs) (MOREIRA; GIOMETTI, 2008).

The third Conference of the Parties, COP3, held in Kyoto, Japan in December 1997, brought together the discussions held in previous meetings and conferences and enacted the Kyoto Protocol. This agreement approved goals and deadlines for GHG reduction, legitimizing the carbon credit market between developed and undeveloped countries. Certified Emission Reductions (CER) or carbon credits are acquired after a developing country voluntarily undertakes activities that reduce carbon emissions through the Clean Development Mechanism (CDM). CERs can be sold to developed countries to help them meet their environmental GHG emission reduction targets

(BITTENCOURT et al., 2017). Based on the historical and current contribution of each country to the increase of GHG in the atmosphere, the international meetings decided that developed countries have the greatest responsibility for reducing emissions, while developing countries do not necessarily have an obligation to reduce greenhouse gases (MENEGUELLO, DE CASTRO, 2007).

The Kyoto Protocol became the main environmental agreement between countries until 2016, when it was replaced by the Paris Agreement signed at the 21st COP by 195 countries. The Paris Agreement established the commitment to limit the increase in global temperature by 1.5 to 2°C by the year 2100, through measures taken by each nation according to their conditions and historical contributions. Each country must outline and communicate their actions being known as their Nationally Determined Contribution - NDC (EULER, 2016). Regarding Brazil, the following renewable targets were agreed with the UN (United Nations): reducing CO₂ emissions in 43% by 2030 compared to the 2005 levels; achieving 28% to 33% of renewable energy sources, other than hydroelectric, in the share of the Brazilian electricity matrix and achieving 10% efficiency in the electricity system by 2030 (MME, 2015). As seen in Figure 5, current policies to reduce GHGs will have an impact on the reduction of the global temperature, but more effort is still needed to reach the goal set for 2100. Thus, the expansion in the use of renewable sources with the consequent substitution of fossil fuel burning processes becomes more and more urgent.

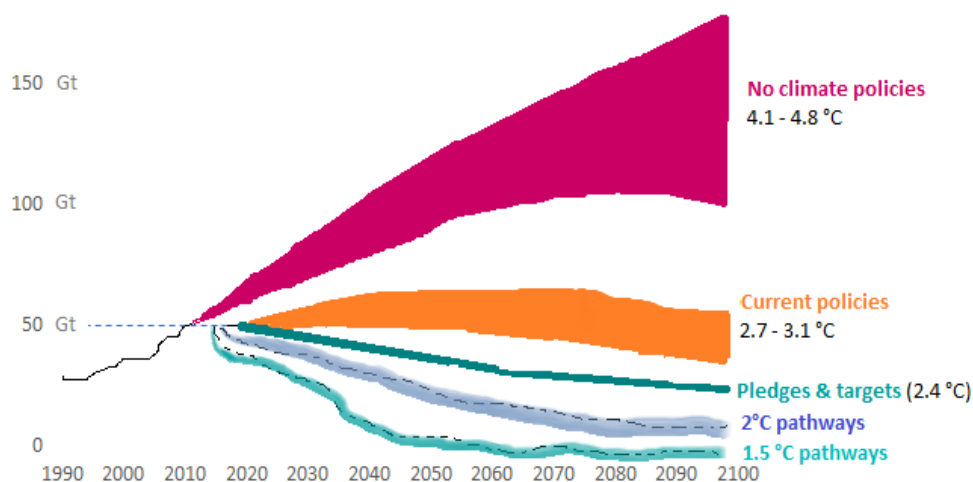


Figure 5 - Warming scenarios of greenhouse gas emissions. Source: Ritchie, Roser, and Rosado (2021).

Furthermore, most of the world's GHGs come from the energy sector, which includes residential, commercial, and transportation power generation. It corresponded to 73% in 2020, as Figure 6 shows. To reduce their emission, the countries seek to substitute fossil fuel energy by renewable sources in the energy matrix. As a result, distributed generation, i. e., the generation of energy from renewable sources in the same place of consumption, has been intensified. With the development of distributed generation,

countries around the world have proposed incentive policies that allow self-producers to access renewable energy sources.

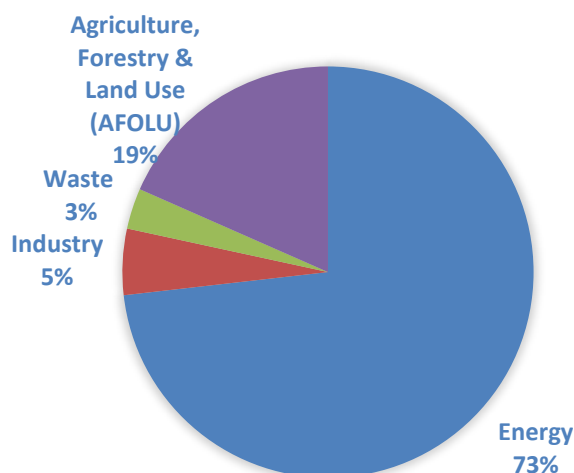


Figure 6 - Distribution of greenhouse gas emissions worldwide by sector in 2020. Source: Ritchie and Roser (2020).

II.3. Incentive policies for Distributed Generation (DG)

There are currently many incentive policies for Distributed Generation (DG) of renewable energy in international markets. The most prominent are: the Feed-in-Tariff (FiT), Net Energy Metering (NEM), Renewables Energy Certificates (REC), Tender System and Renewable Heat Incentive (RHI) (FREITAS and HOLLANDA, 2015).

The FiT is a policy to encourage the generation of energy from renewable sources, which establishes the contracting of long-term tariffs for periods that vary between 10 and 20 years. The value of this tariff is established according to the generation costs, the source used, the type of installation, among other factors. Because of this, the energy exported to the central grid by these means of generation is passed on at a higher value than the energy acquired from the central grid. This value is reduced over time as the generation costs also decrease. Thus, the FiT provides the stimulus for distributed microgeneration by renewable energy sources on site (JUÁ STECANELLA et al., 2021).

Dalvi et al. (2017) describe that after Germany and Japan have adopted FiT as a policy to encourage distributed microgeneration, there was a considerable increase in the admission of renewable energy sources in the countries. In Germany, after the adoption of the FiT policy, there was an expansion of 35.83 GW in the installed power of photovoltaic systems, equivalent to more than a 31,433% increase, and 27.66 GW in the onshore wind system, equivalent to more than a 453% increase, between 2000 and 2013. In Japan, in 2012, the installed power from renewable sources was 12 GW (DALVI

et al., 2017). When well managed, the FiT has good results in encouraging the inclusion of renewable energy sources in the countries' energy matrix.

Net Energy Metering (NEM), on the other hand, is a policy that is mostly adopted in European and Asian countries, in which photovoltaic energy producers receive credits (in kWh) for the surplus energy injected into the central grid. These credits are used when local energy production is lower than demand, thus requiring energy from the central grid (SERGICI et al., 2019). In this configuration there is no energy trading, the main objective is to relieve the central grid, especially at times of high energy demand (AQUILA et al. 2017). Therefore, there is no return in a profitable way for the owner of the DG systems, since only the decrease in energy costs is obtained in the long term.

Another policy adopted around the world is the REC, Renewable Energy Certificate. This is an instrument to promote the generation of renewable energy, which consists of a title that certifies that the energy was generated by a renewable source. The REC emerged after changes in the legislation of some countries such as India, which began to require that part of the electricity produced by energy companies originate from renewable sources (KUMAR; AGARWALA, 2013). In this way, energy companies can buy RECs from owners of DG systems and meet the country's legal requirements.

There is also the Tender System, characterized by the commercialization of energy, where entrepreneurs interested in selling their energy from renewable sources propose tariff bids. For this to occur, the competent body previously determines the amount of energy that must be contracted, as well as the publication of the rules and organization of auctions (MARTINS, 2010). This system favors the transfer of better rates to the end consumer, since the auction is won by the proposal with the lowest bid in increasing order until the amount of energy previously defined is completed.

The Renewable Heat Incentive (RHI) is a government financial support to encourage the generation of heat from renewable sources. Households that meet the required criteria, which vary from country to country, receive an annual amount for producing heat from renewable sources; the rate for each source is calculated taking into account factors such as type and size (VISHNUBHOTLA, 2022).

Table 1 provides a comprehensive overview of the theses different incentive policies available for distributed generation. In addition, it presents the main countries that have already adopted them. It is possible to infer that the selection of each policy will be determined by the objectives and needs of each country. For example, the adoption of renewable energy certificates is mandatory for developed countries, but for emerging countries, i.e. India, it can be used as a source of income. Among the policies listed, Feed-in Tariff and Net Energy Metering can be considered the most successful and well-defined in the market for self-consumption generation. This is attributed to their long-

term presence in the market and the growth in installed capacity of renewable resources within each country (JUNLAKARN et al., 2021).

Table 1 - Comparison of Incentive Policies for Distributed Generation: Advantages and Disadvantages

Policy	Characteristics	Advantages	Disadvantages	Application	Reference
Feed-in-Tariff	Provide financial incentives for renewable energy production, including guaranteed payment, long-term contracts, premium pricing, and declining rates, as part of a government-supported policy.	<ul style="list-style-type: none"> • Encourages renewable energy production • Stable and predictable returns • Promotes local economic development 	<ul style="list-style-type: none"> • Increased costs for ratepayer • Administrative complexities • Potential for market distortions • Limited effectiveness in reducing emissions 	Germany, Japan, Spain, France, Italy, Portugal, Australia, Canada, United States, China	Kërçi, Tzounas, Milano (2022)
Net Energy Metering	Allows those who generate their own renewable energy to receive credit on their utility bills for excess electricity they produce and feed back into the grid, which offsets the cost of the electricity they consume from the grid.	<ul style="list-style-type: none"> • Encourages renewable energy installations • Reduces greenhouse gas emissions • Improve grid stability 	<ul style="list-style-type: none"> • Shifts maintenance costs to non-participants • Regulatory challenges 	United States, Germany, Australia, India, Thailand, France, Brazil	Roux and Shanker (2018)
Renewables Energy Certificates	RECs are tradeable certificates that represent proof that one MWh of electricity was generated from a renewable energy source. They can be bought and sold, and are a way to support renewable energy and meet renewable energy targets. They vary in price and quality, and are not the same as carbon offsets.	<ul style="list-style-type: none"> • Help meet renewable energy targets • Provide a source of revenue for renewable energy producers • Reduce greenhouse emissions 	<ul style="list-style-type: none"> • The price of RECs can be volatile and subject to market fluctuations • The quality and verification of RECs can vary, leading to confusion for buyers 	United States, Canada, Australia, United Kingdom, South Korea, European Union member countries, India	Zhu et al. (2022)
Tender System	Commercialization of energy, where entrepreneurs interested in selling their energy from renewable sources propose tariff bids	<ul style="list-style-type: none"> • Potential cost savings for the entity seeking goods or services • Transparent selection process 	<ul style="list-style-type: none"> • Bureaucratic requirements may be a barrier to entry for some suppliers • Tendering can be costly for suppliers, with no guarantee of being awarded the contract 	United States, United Kingdom, Canada, Germany, Japan, India, China	Toke (2015)
Renewable Heat Incentive	Provides financial incentives to encourage the use of renewable energy for heat generation.	<ul style="list-style-type: none"> • Reduces greenhouse gas emissions • Stimulates the economy • Encourages renewable energy adoption 	<ul style="list-style-type: none"> • Program Complexity • Create uncertainty for participants, as changes to the program or funding levels may occur over time 	United Kingdom, Ireland, Germany, Italy, Spain, Sweden, Denmark	Abu-Bakar et al. (2013)

II.4. Incentive policies for Distributed Generation (DG) in Brazil

There are two systems that supply the energy demand of the Brazilian regions: the National Interconnected System (SIN: *Sistema Interligado Nacional*) and the Isolated System. The SIN supplies the Northeast, Center-West, South, Southeast and part of the North regions (Figure 7). It is mostly composed of large hydroelectric plants and a vast transmission network that interconnects all regions. In contrast, there are 270 locations that, for technical or economic reasons, are not part of the SIN. These are called Isolated Systems, and are regulated by Decree No. 7246, of July 28, 2010, and distributed in the Northern region, in the region of Mato Grosso and in the region of Fernando de Noronha. The supply of electricity in these markets is ensured by the Energy Research Company (EPE: *Empresa de Pesquisa Energética*) through studies that identify the current supply and generation from consumption, load and demand forecasts for each location made available by local energy distributors.



Figure 7 – Brazil Regions Map. Source: Mappr (2023).

Figure 8 provides a brief history of the main incentive policies for renewable energy in Brazil that will be detailed later. Among these policies, it is possible to observe the main approaches also adopted in the international market, such as the auction system, the use of RECs and NEM.

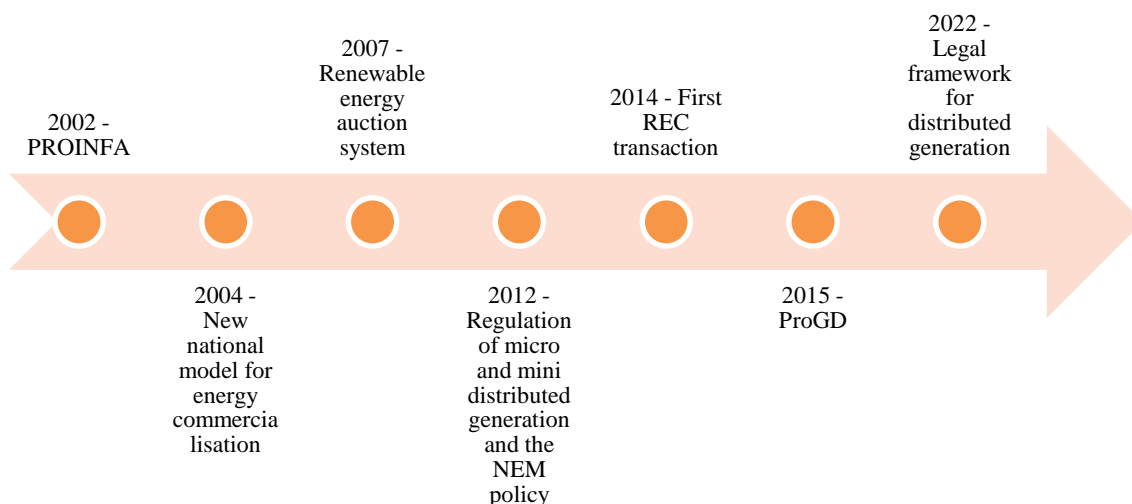


Figure 8 - History of the main policies/mechanisms to encourage renewable energy in Brazil.

In 2002 the Program of Incentive to Alternative Sources (PROINFA: *Programa de Incentivo às Fontes Alternativas*) was instituted by Law No. 10.438. This had as strategic objectives the diversification of the energy matrix, the search for the reduction of greenhouse gases in order to meet the Kyoto Protocol and the generation of jobs in the country (MARTINS, 2010). PROINFA consists of Independent Autonomous Producers that make up the SIN. They produce electricity based on wind sources, Small Hydroelectric Plants (PCH: *Pequenas Centrais Hidrelétricas*) and biomass. It is one of the pioneer programs in Brazil to encourage the generation of energy from renewable sources. In the first stage of the program, the aim was to implement 3,300 MW of capacity, with the contracting of 1,100 MW per energy source. The contracts were intermediated by *Centrais Elétricas Brasileiras S.A. - ELETROBRÁS* and had a duration of 20 years, thus the FiT policy was adopted to encourage generation from renewable sources (CCEE, 2010).

In this phase, for the selection of producers, public calls were made taking into consideration criteria such as: the oldest Environmental Installation License and hiring limits per State. The latter was intended to stimulate regional development and foster local jobs (MARTINS, 2010). Table 2 shows the distribution of contracted power for each region of the country, where Qty is the quantity of plants installed. For the operation of the program, the administrative costs, financial costs, tax charges of PROINFA and the amount paid for electricity by ELETROBRÁS are passed on to the final consumers, in proportion to their energy consumption, except for the Low Income Residential Sub-class, which has a consumption equal to or less than 80 kWh/month (MME, 2004).

Table 2 - Overview by region of contracted power in the first phase of PROINFA. Source: MME (2009).

SOURCE		NORTH	NORTH EAST	CENTRAL WEST	SOUTH EAST	SOUTH	TOTAL
PCH	Qty	6	3	25	15	14	63
	Power (MW)	102.20	41.80	498.94	285.20	263.10	1,191.24
BIOMASS	Qty	-	6	6	11	4	27
	Power (MW)	-	119.20	128.92	332.02	105.10	685.24
WIND POWER	Qty	-	36	-	2	16	54
	Power (MW)	-	805.58	-	165.05	454.29	1,422.92
	Qty	6	45	31	28	34	144
TOTAL	Power (MW)	102.20	966.58	627.86	780.27	822.49	3,299.40

Each year Eletrobrás prepares the Annual Plan of Proinfa (PAP: *Plano Anual do Proinfa*), which is approved by the National Agency of Electric Energy (ANEEL: *Agência Nacional de Energia Elétrica*). The Annual Plan includes, among other information, the calculation of quotas to fund the program (ELETROBRÁS, 2020). Table 3 shows the amount of energy and costs considered for the PAP 2020. These values are considered for the calculation of tariffs that are passed on to end users, in order to provide for the maintenance of the program.

Table 3 - Energy amount and cost for PAP 2020. Source: Eletrobrás (2020).

Source	Number of installations	Energy (MWh)	Annual Cost (R\$)
Biomass	19	1,182,057.00	267,143,373.77
Wind	52	3,525,426.00	1,675,292,617.55
PCH	60	6,494,664.00	1,819,153,937.14
TOTAL	131	11,202,147.00	3,761,589,928.46

In 2004, the commercialization of electric energy in the country was regulated by Decree nº 5,163, of July 30, 2004. This occurs through the Regulated Contracting Environment (ACR: *Ambientes de Contratação Regulada*) and the Free Contracting Environment (ACL: *Ambiente de Contratação Livre*). In the ACR, the energy generation agents sell to energy distribution agents by means of auctions organized by the Chamber of Commercialization of Electric Energy (CCEE: *Câmara de Comercialização de Energia*

Elétrica), with the objective of transferring the lowest tariff to the final users. In ACL, on the other hand, the sale value is agreed upon according to specific commercialization rules between the producer and the free consumers. The latter are companies with high consumption and can be classified as Conventional Free Consumer and Special Free Consumer. The special one must consume energy from renewable energy sources.

The difference between the energy that was contracted (in the ACR and ACL) and that which was actually generated and consumed by each agent is negotiated in the Short Term Market. The trading value of this market is determined by the CCEE from mathematical models, and the value found is called the price for the settlement of differences (PLD: Preço da Liquidação das Diferenças). In this market there are no contracts, there is multilateral contracting (CCEE, 2004).

From Decree nº 6.048 of February 27, 2007, which altered Decree nº 5.163, of July 30, 2004, the auction (tender system) of energy from renewable sources was promoted. In this way, the producers contracted in PROINFA and also the Self-Producer of Electric Energy (APE: Autoprodutor de Energia Elétrica) individuals, legal entities or companies that are authorized to produce energy for their own consumption and that may eventually commercialize energy, sell energy to buyers participating in the CCEE auction.

In 2012, the Normative Resolution No. 482 (RNE482) was approved, subsequently amended by Normative Resolution No. 687 of 2015 and Normative Resolution No. 786 of 2017, which provides for the regulation of distributed micro and mini generation in Brazil. Through the last published resolution, distributed microgeneration is considered to be the power plant with installed power less than or equal to 75 kW that uses qualified cogeneration or renewable energy sources. For distributed minigeneration, on the other hand, power plants with installed capacity greater than 75kW and less than or equal to 5MW are considered.

In addition, RNE482 regulates the Net Energy Metering (NEM) system, in which the enterprise that meets the requirements proposed in the resolution may inject the surplus energy, which was not consumed, into the distribution network. This will account for credits that can be deducted from the energy bill, with a period of up to 60 months to be used.

In 2014, there was the first transaction of REC in Brazil. In the country there are two types: I-RECs (International REC Standard), the same used in the international market and I-RECs with REC Brazil seal. The international seal provides, in addition to the renewable energy certificate to the company, the certificate according to the criteria of the Sustainable Development Goals (SDGs) of the United Nations, proving its social and environmental impact. In 2019, more than 2.5 million certificates were traded and

their numbers have grown considerably since then, assisting in achieving the environmental goals of large companies (ECON ENERGIA, 2021).

In 2015, the Program for the Development of Distributed Generation of Electric Energy (ProGD: Programa de Desenvolvimento da Geração Distribuída de Energia Elétrica) was launched in order to stimulate distributed generation by renewable sources, through incentive actions with financial incentives (credit lines, permission to sell energy) and fiscal facilitation (legal, regulatory, and tax improvements). In this way, the program helps to fulfill the Nationally Determined Contribution (NDC) agreed with the UN.

In 2022, the legal framework for distributed generation was instituted through Law no. 14.300/2022. One of the innovations in this law is the gathering of energy consumers through voluntary civil and building condominiums, characterizing shared generation, in addition to the consortiums and cooperatives already included in the REN 482. Furthermore, the acquired right and the transition rules for distributed generation installations were established, in which, in the first 12 months after the date of publication of the law, the billing will be done in the same way as it was already being done, with the tariffs falling on the positive difference between the consumption of the central network and the electric energy deposited in the network. At the end of this period, the costs related to the distribution service that will be charged on the compensated energy will be passed on to the distributed energy generation producers, following the transition rule, the percentage in relation to the tariff components of this service will be (i) 15% in 2023; (ii) 30% in 2024; (iii) 45% in 2025; (iv) 60% in 2026; (v) 75% in 2027; (vi) 90% in 2028; and (vii) 100% in 2029.

Furthermore, in 2022 the Social Renewable Energy Program was created, with the purpose of facilitating the acquisition of renewable energy systems for the low-income population. This program will promote investments for this part of the population with resources coming from the Energy Efficiency Program (PEE: Programa de Eficiência Energética) (TAUIL, CHEQUER, 2022).

II.5. Energy and electric matrix of Brazil and the world

The energy matrix corresponds to all means of energy generation including locomotion, while the electric matrix corresponds to the means of generating only electric energy. The Brazilian and world energy matrices in 2019 are shown in Figure 9. It can be seen that the resource with the largest share in both matrices is oil, with 42% in the national matrix and 31% in the world matrix, respectively. The second most used source in the Brazilian matrix is hydroelectricity, which stands out with 31% against only 6% in the world matrix. On the other hand, mineral coal is the second most used source in the world energy matrix. This has a strong influence on the profile of use of renewable

sources in Brazil in relation to the world, as illustrated in Figure 10. This may be due to the abundance and availability of renewable resources in the country.

Figure 9 also shows that the participation of other renewable sources including solar and wind is still more restricted. This may be due to the lack of efficient generation technology, as well as the high costs in installation and maintenance of renewable sources. The same challenges occur in the installation of technologies such as geothermal and ocean energy, or new technologies that are still in the implementation phase, such as bioLPG.

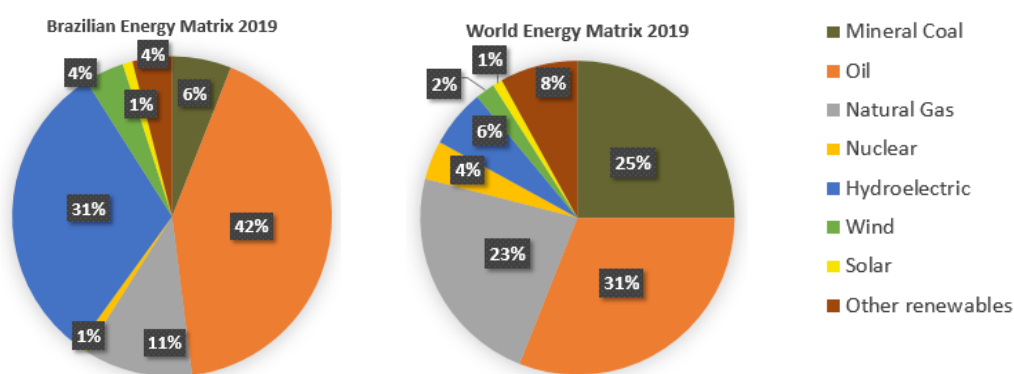


Figure 9 - Brazilian and world energy matrix in 2019. Source: Ritchie and Roser (2019).

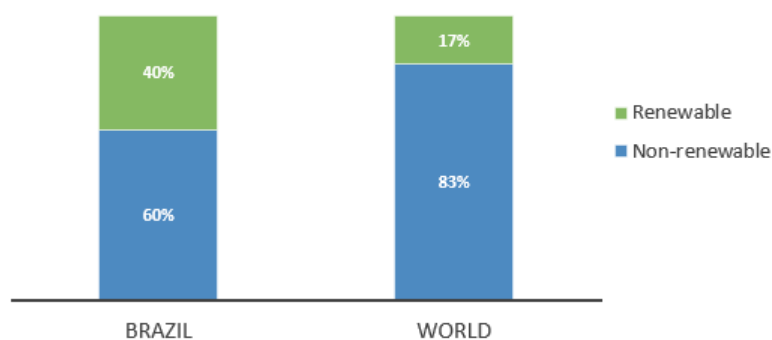


Figure 10 - Renewable and non-renewable energy consumption profile in Brazil and the world in 2019. Source: MME (2020).

With regard to the distribution of resources that are aimed solely at electricity generation, hydroelectricity represents the largest national percentage with 64%, followed by wind and solar with 15% and biomass with 9%, according to data from 2020 (Figure 11). In this scenario renewable resources represent 88% of all installed capacity against 40% of the energy matrix.

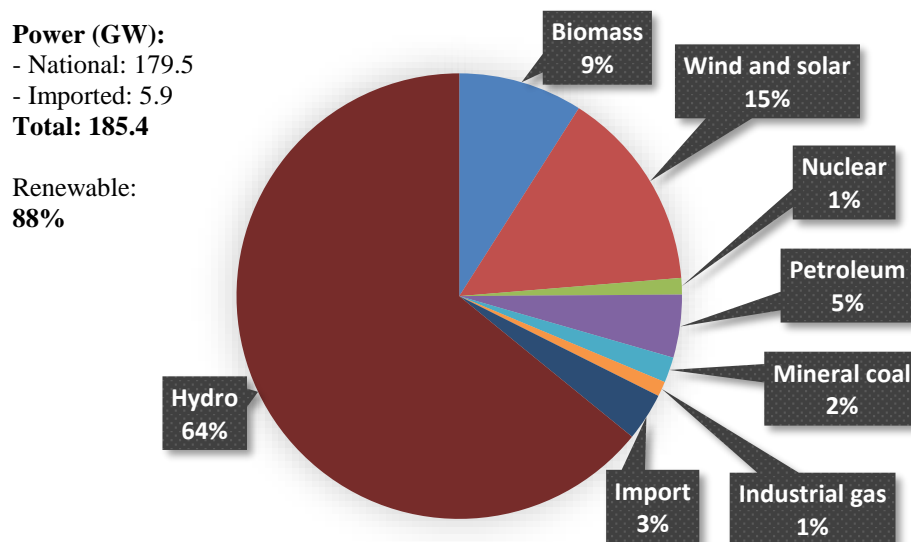


Figure 11 - Brazilian Electric Matrix 2020. Source: MME (2021).

In 2020, the installed capacity of hydroelectric power in the country was 109.27 GW, which represented an increase of 76% in relation to the year 2002, when it achieved 62.02 GW (ANEEL, 2002). The year 2002 was marked by the beginning of incentive policies for renewable energy in Brazil. This suggests that the public policies adopted since then have contributed to the increased participation of renewable sources in the Brazilian electricity matrix. This high impact was also observed in wind energy, since in 2020 the country reached 17.13 GW of installed capacity, an increase of 17,131% in relation to the previous decade, when the capacity was 1 GW (ANEEL, 2002).

Table 4 represents the distribution of installed electric generation capacity in the country in the years 2019 and 2020. From the total 179.5 GW of installed capacity in 2020 only 4.77 GW correspond to distributed generation. This shows that, even after RNE482, the Normative Resolution for regulating distributed micro and mini generation in Brazil, mini and micro generation in the country still represented 2.66% of all installed capacity. However, there was an increase of approximately 23% in relation to 2019, even with the low representativeness in relation to the national total. According to EPBR (2022), in 2022 among the sources of mini and micro electricity generation systems, solar energy accounted for 97.7% of the total; followed by thermoelectric (1.2%), hydroelectric generating plant - CGH (0.87%) and wind (0.18%). For decentralized applications, then, the use of solar energy is more pronounced.

Table 4 - Installed capacity of Electric Generation in Brazil (GW). Source: MME (2021).

Source	2019	2020
Hydro	109,058	109,271
<i>Power Plants</i>	102,999	103,027
<i>Small Plants and Generating Plants</i>	6,059	6,244
Biomass	14,978	15,306
<i>Cane Bagasse</i>	11,438	11,712
<i>Biogas</i>	186	206
<i>Bleach and others</i>	3,354	3,388
Wind	15,378	17,131
Solar	2,473	3,287
Uranium	1,990	1,990
Gas	15,304	16,825
<i>Natural Gas</i>	13,385	14,927
<i>Industrial Gas</i>	1,919	1,899
Oil	7,670	7,696
<i>Of which Fuel Oil</i>	3,316	3,256
Mineral Coal	3,228	3,203
Unknown	40	27
Subtotal	170,118	174,737
Distributed Generation	2,140	4,768
<i>Solar</i>	1,970	4,635
<i>Wind</i>	10	15
<i>Hydro</i>	97	23
<i>Thermal</i>	63	95
Nacional Total	172,258	179,505
<i>Of which renewable</i>	144,067	149,764
<i>Availability with import</i>	178,130	185,355

Table 5 illustrates the installed power offer ratio in 2020 for each generation system. The largest share comes from the SIN whose main source is hydroelectric. In the isolated systems, the use of thermal sources such as diesel oil predominates because these are places with difficult access, which makes it difficult to connect to the SIN and use other sources. Likewise, the largest percentage of the APE (*Auto-Produtor de Energia* - Energy Self-Producer) comes from a thermal source, mainly from biomass since the majority of self-producers work with qualified cogeneration. Table 6 summarizes the electricity generation profile by self-producer in 2020. The main source is the sugar and alcohol sector, followed by the pulp and paper sector.

Table 5 - Percentage of installed energy supply according to energy production systems - 2020 (%). Source: MME (2021).

Source	SIN	Isolated	Captive APE	Total
Hydraulics	66.7	25.6	7.5	62.1
<i>National</i>	63.4	0.6	7.5	59.0
<i>Imported</i>	3.3	24.9		3.2
Thermal	18.5	74.4	79.8	23.3
Nuclear	1.2			1.1
Wind	10.0		0.009	9.3
Solar	3.6		12.8	4.3
Total (%)	100.0	100.0	100.0	100.0
Total (GW)	170.9	0.8	13.7	185.4

Table 6 - Electricity generation profile by self-producer (APE) - 2020 (GWh). Source: MME (2021).

Sector	Total generation (GWh)
Sugar and Alcohol	37,831
Pulp and Paper	16,666
Petroleum	12,963
Siderurgia	11,538
Others	9,941
Non-Ferrous	8,861
Agriculture and Livestock	3,684
Mining	3,249
Chemistry	1,719
Total	106,452

Energy self-production can occur in two ways: on-site or off-site. When it occurs outside the place of consumption it uses the distribution networks of the SIN so that the energy generated can reach the consumption unit. What differentiates energy self-production from distributed generation in Brazil (mini- and micro-generation) is that self-production is allocated to the free market and distributed generation to the

regulated market. Thus, self-producers follow the rules for contracting and selling energy in the free market, and distributed generation follows the policy of compensation of credits for the excess of energy injected into the grid according to the RNE482.

II.6. Renewable energy sources

According to the panorama presented, there is a favorable scenario in the country and in the world for the promotion of distributed generation, as well as the increased participation of renewable sources in the national and global energy and electricity matrices. With this in mind, this section will address a review with a greater level of detail about the main renewable sources used in Brazil and in the world, along with their energy potential and the main generation technologies.

II.6.1. Solar

The Planet Earth receives 9.5×10^4 TW of solar energy daily, which is equivalent to 3,167 times more than the energy the population will consume in the year 2050 (MACHADO, MIRANDA, 2015). Thus, technologies have been developed to convert solar energy into electrical and thermal energy to cope with the global demand. This can be generated by two methods: photovoltaic and heliothermal systems, also known as Concentrated Solar Power (CSP) systems.

Photovoltaic (PV) energy comes from the excitation of electrons in semiconductor materials by sunlight, producing an electric current. Because the material used has electrons that are weakly bounded to the parent atom, high irradiance is not required for power generation. During the night there is an interruption of power generation and a reduction in efficiency on cloudy days. One of the possible solutions to this problem is the adoption of a system of batteries for storing the energy produced in sunny periods; however, the very high cost of acquisition and low life of the batteries often makes the adoption of this system unfeasible (MACHADO, MIRANDA, 2015). Figure 12 represents the operation of a photovoltaic panel in a household.

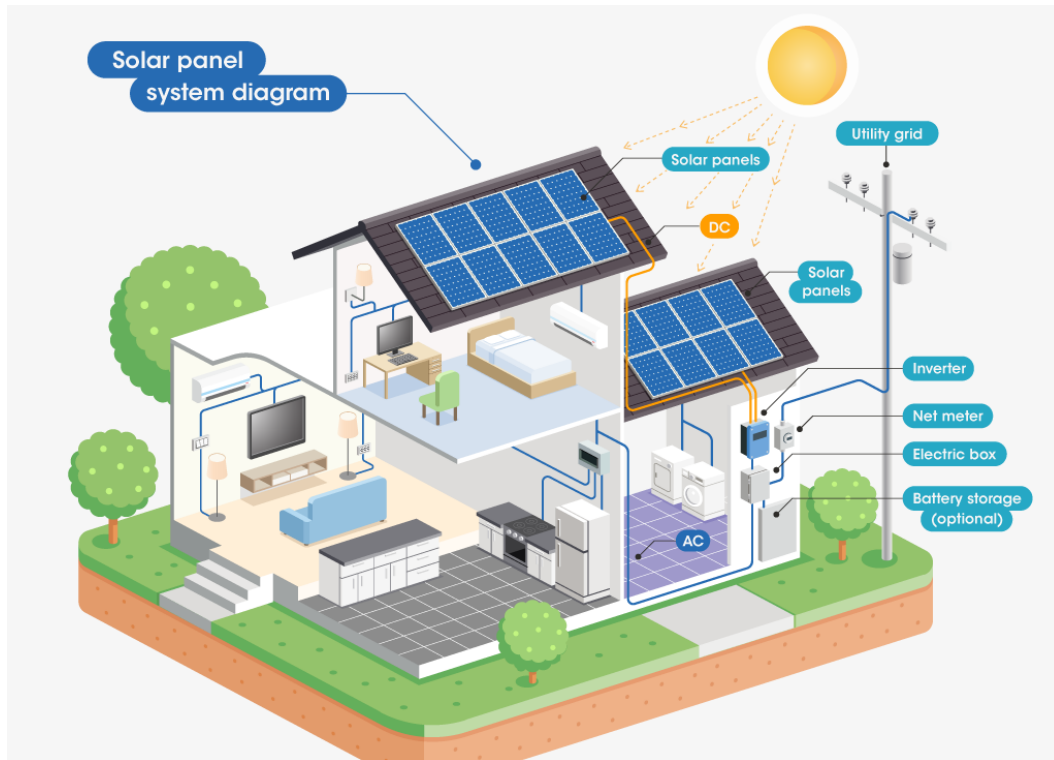


Figure 12 - Diagram of photovoltaic energy in a residence. Source: GBS (2022).

Due to the development of new technological routes, access to photovoltaic energy has grown considerably. In 2019, the worldwide installed capacity grew by 115 GW, 22.5% over the previous year (NASSA, 2020). Figure 13 expresses the cumulative global profile of distributed and centralized PV generation during the decade from 2009 to 2019. Over the years, the share of centralized PV generation has increased by almost 60% of all the energy generated. This may be due to increased governmental investments in order to meet the environmental goals.

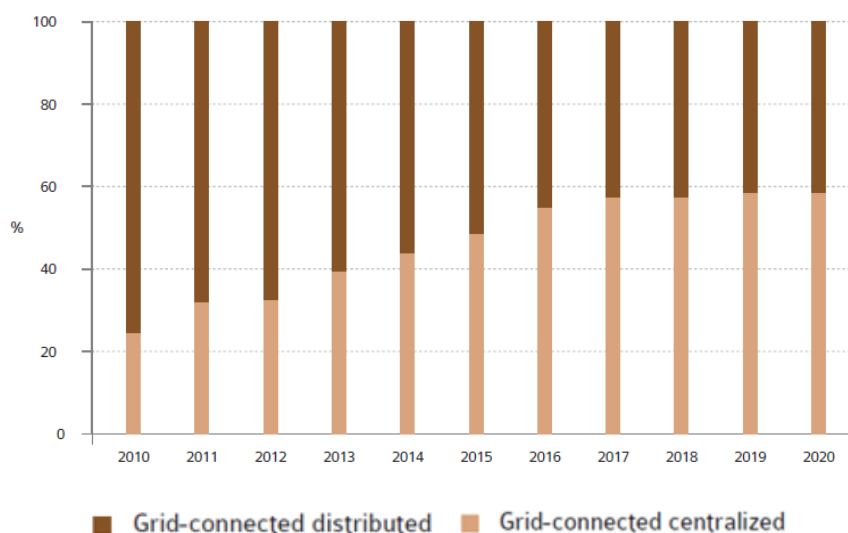


Figure 13 - Cumulative profile of distributed and centralized generation by PV worldwide in the decade 2009-2019. Source: Masson et al. (2020).

Brazil occupied the 7th position in the world ranking of installed capacity of distributed generation of PV in the year 2020 with capacity addition of 2.26 GW (IEA, 2021), as Table 7 shows. Brazil is ahead of countries like the Netherlands (1.09 GW), Belgium (1.03 GW) and India (0.86 GW).

Table 7 - Top 10 countries for distributed PV installed in 2020. Source: IEA (2021).

	Country	Capacity(GW)
1°	China	15.5
2°	Vietnam	9.58
3°	United States	5.27
4°	Japan	3.82
5°	Germany	3.69
6°	Australia	3.06
7°	Brazil	2.26
8°	Netherlands	1.09
9°	Belgium	1.03
10°	India	0.86

Regarding the total installed capacity in the country, of the 7.7 GW of installed photovoltaic capacity, 3.1 GW are centralized generation and 4.67 GW are distributed generation (ABSOLAR, 2021b). This number, according to ABSOLAR (2021a), meets only

0.5% of the 85 million electricity consumers in the country. This indicates that there is still a great potential for growth of photovoltaic energy in the country.

Heliothermal energy uses normal direct solar irradiation (DNI), as in photovoltaics, to heat a fluid that undergoes an expansion in order to convert the heat into work and subsequently into electrical energy via an electromechanical generator (SORIA, SCHAEFFER and SZKLO, 2014). This technology can be used with or without heat storage. Heat storage enables the plant to operate in periods when there is no solar incidence. For the use of CSP technology, it is necessary that the installation site has special conditions such as: DNI higher than 1,800 kWh/m²/year, low velocity winds, and adequate topographical conditions. The high costs of equipment as well as the installation costs, which depends on the labor force of each country, still makes the heliothermal energy an expensive technology. The authors Vieira, Guimarães and Lisboa (2018) report that, due to these limitations, there are only 94 systems in operation in the world, corresponding to 5,206 MW of installed power. According to Cunha and Weiss (2021), CSP technology costs, in 2019, was 3 times greater than photovoltaics. Thus, in Brazil, despite having favorable regions for installation, this technology is still little explored for electricity generation due to the high costs associated with its implementation, with a little representative value in the national electric matrix (VIEIRA, GUIMARÃES, LISBOA, 2018).

Solar energy can also be used as a source of heat to supply the demand for hot water in houses and industrial processes. This system is exemplified in Figure 14, where the solar collector is responsible for capturing the heat of the sun that is transferred to the water pipe inserted inside the collector, as in heliothermal technology. The heated water is then transferred to a container where it will be stored until used.

According to the 2020 report of the International Energy Agency's Collaborative Program on Solar Heating and Cooling Technology, the global thermal capacity of water collectors, that has a specific goal of only producing hot water, has grown from 62 GWth (89 million m²) in 2000 to 479 GWth (684 million m²) in 2019 (WEISS, SPÖRK-DÜR, 2020). In the world ranking, Brazil occupies the 6th position of growth in the implementation of this technology. Furthermore, this is responsible for part of the electrical energy savings in Brazilian homes, since the electricity that would be required to heat water, with the use of electric showers, is no longer necessary. Data from the beginning of the year 2000 show that this source was responsible for saving 44% of the electrical energy consumption in Brazilian residences (WEISS, SPÖRK-DÜR, 2020).

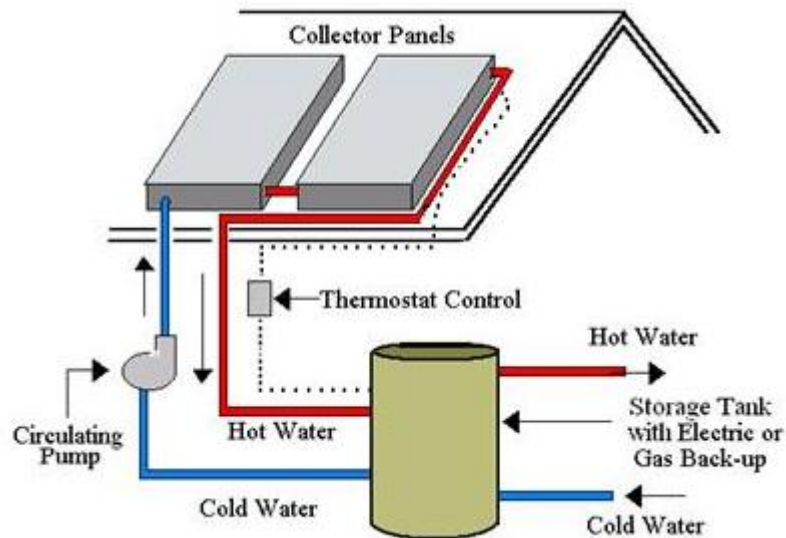


Figure 14 - Solar thermal energy production diagram. Source: Greenriverside (2022).

Another solar energy technology relates to hybrid PV/T systems that produce thermal energy and electrical energy at the same time. This system is a combination of photovoltaics and solar collectors, so they feature the same components seen in both technologies (Figure 15). This technology is interesting because in photovoltaic systems only a part of the energy is transformed into electricity and the rest is lost to the environment, but in this system the energy not used for electricity generation is used for water heating, providing a greater use of the captured solar energy (OLIVEIRA, 2017).

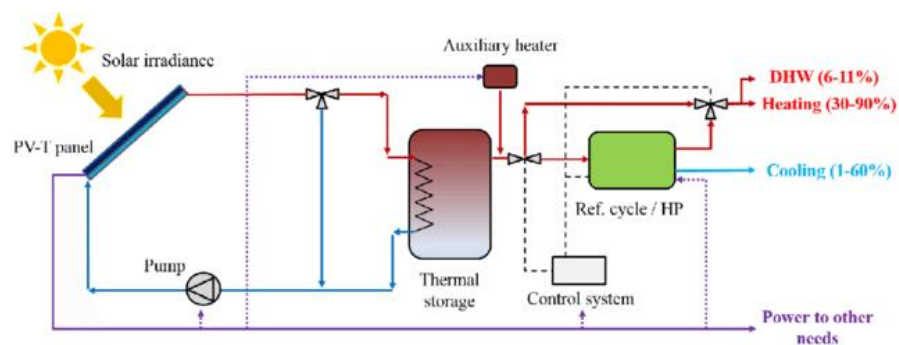


Figure 15 - Diagram of solar energy production in hybrid PV/T systems. Source: Ramos (2017).

II.6.2. Wind

Wind energy is obtained by means of a wind turbine that converts the kinetic energy of air flow into electrical energy (Figure 16). An inexhaustible source of energy, it can be produced both onshore and offshore. In addition, it has low environmental impact and occupies a relatively small area, and its perimeter can be used for farming or grazing (COSTA, CASOTTI, AZEVEDO, 2009).

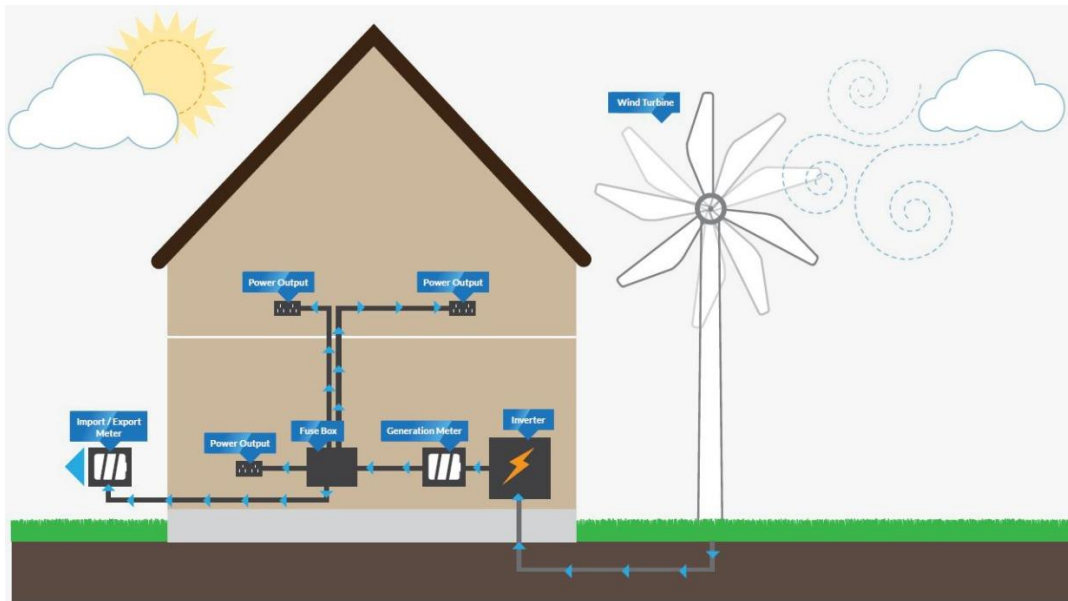


Figure 16 – Representation of wind energy in a residence. Source: Rowan House (2022).

According to GWEC (2021), the total onshore and offshore wind power installations in the world is 742.7 GW, of this total 93 GW were installed in the year 2020, 2.79 GW of which in Brazil. Figure 17 shows the worldwide distribution of onshore and offshore wind power installations. China has the highest percentage of onshore installations with 39% equivalent to 275.9 GW, while the UK leads in offshore installations with 30%, equivalent to 10.59 GW.

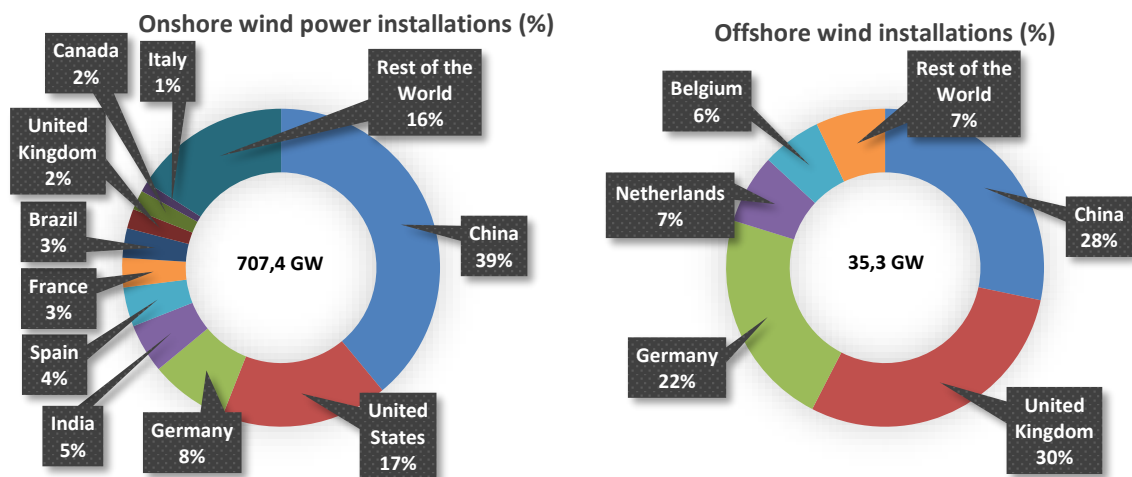


Figure 17 - Distribution of onshore and offshore wind installations worldwide. Source: GWEC (2021).

Due to policies to encourage the acquisition and improvement studies of wind technologies in order to reduce expenses and increase energy yield, Brazil is one of the five fastest growing countries in the deployment of wind resources. Regarding the wind potential in the country, its estimated capacity is 326 W/m², with the largest potential

located in the Northeast region (DTU, 2019). Thus, in addition to the financial incentive regarding its use, there is also the climatic feasibility for the use of wind energy in Brazil.

Table 8 shows the installed capacity of wind energy by state in the country. The Northeast region has the largest number of wind farms. Rio Grande do Norte is the most representative, with 182 farms and an installed capacity of 5,154.2 MW, followed by Bahia with 184 farms and 4,879.6 MW of installed capacity.

Regarding distributed generation in Brazil, wind energy corresponds to 19.8 MW in 2022, corresponding to 0.18% of all distributed generation in the country (EPBR, 2022). This low percentage can be attributed to the limited availability of wind in some regions of the country, which would require investment in larger wind turbines to capture more energy, and also due to the low popularity of residential wind turbines. Therefore, more studies are needed to show the viability of these resources for use in distributed generation.

Table 8 - Installed power by state in Brazil in 2020. Source: Godoi (2021).

State	Installed Power (MW)	Parks
RN	5,154.20	182
BA	4,879.60	189
PI	2,275.90	79
CE	2,179.30	81
RS	1,835.90	80
PE	798.4	34
MA	426	15
SC	238.5	14
PB	157.2	15
SE	34.5	1
RJ	28.1	1
PR	2.5	1
Total	18,010.1	695

II.6.3. Biomass

Biomass energy can be converted into electric (Figure 18) and thermal (Figure 19) energy by means of direct burning in thermoelectric plants. Figure 18 shows an example of a biomass thermoelectric plant. The heat produced by burning biomass heats a liquid

(water), which produces work and moves a turbine, that feed an electric generator. Figure 19 represents the thermal energy generation. The biomass is burned, but the heated liquid is directly used for its applications, such as supplying the hot water demand in the residence. Burning biomass, though, can be harmful to humans due to the release of particles that can harm the respiratory system. Therefore, additional investments in equipment are often required to remove this particulate material (DANTAS, 2010).

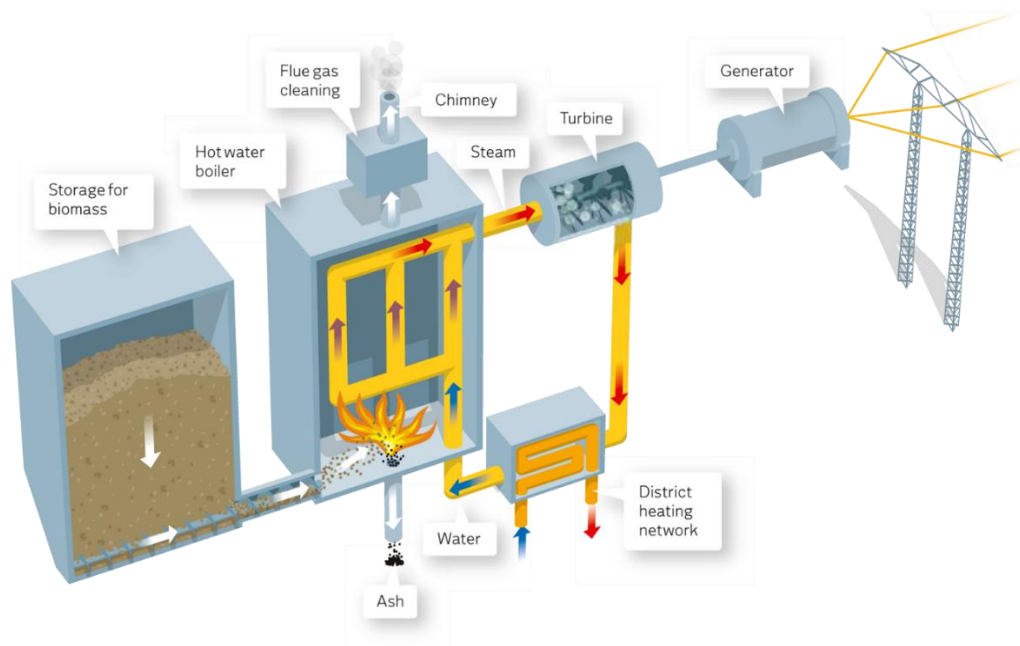


Figure 18 – Diagram of a biomass thermoelectric plant. Source: Salix Renewable (2018).

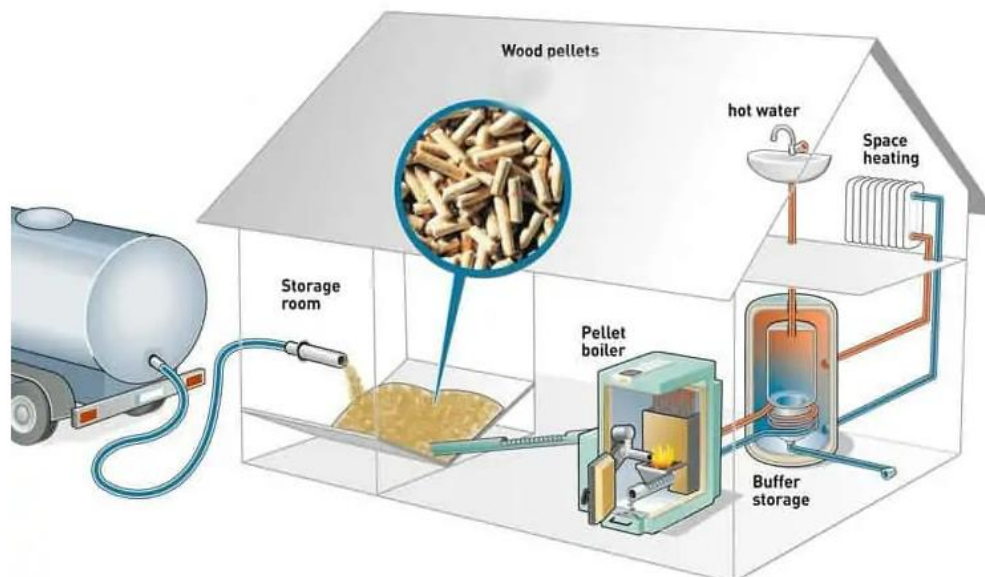


Figure 19 – Diagram of thermal energy generation through biomass. Source: Herschel Infrared (2022).

Due to the low energy efficiency of some systems, requiring large quantities of inputs to meet the demand, different mechanisms have been investigated to reduce the costs of transportation of inputs, such as the use of waste in cogeneration plants. In addition,

the development of new technologies has sought to increase the energy efficiency of biomass generators (MACEDO, 2001).

Fermentation is an alternative process for obtaining thermal and electrical energy from biomass. It produces biogas, a mixture of CH_4 and CO_2 and small amounts of waste gases (COELHO et al., 2018). Figure 20 shows some technological routes of biogas production and its improved version, the biomethane, as well as their respective applications. As noted, biogas can be used directly as cooking gas to produce heat and electricity or after the upgrading process it can be used as transportation fuel. The upgrading process, in addition to the production of biomethane, is important to prevent corrosive substances found in biogas, such as hydrogen sulfide (H_2S), from reducing the life of engines and generators, as well as increasing the calorific value of the gas (COELHO et al., 2018).

For biogas production, it is necessary to install an anaerobic biodigester that is fed with various organic sources, from animal waste to food waste. In the biodigester there is a reduction of organic matter with the consequent production of biogas. The residue generated in this process, called digestate, can be used as biofertilizer or animal bedding (REURASIA, 2020). For the production of electricity, a generator is used to convert the chemical energy of the gas into mechanical energy through a combustion process.

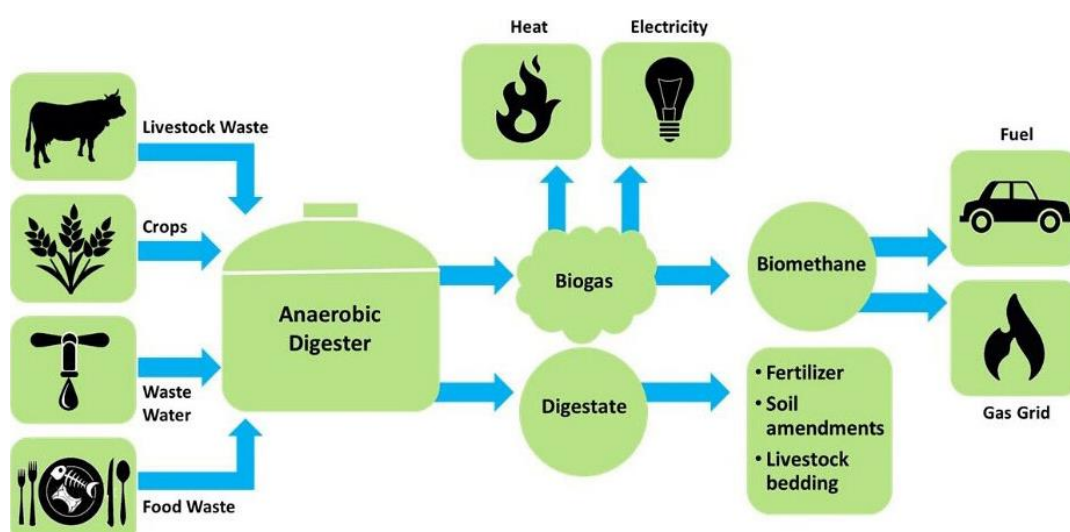


Figure 20 - Diagram of biogas and biomethane production. Source: Reurasia (2020).

In 2020, the world installed capacity of energy generation by biomass, which includes all forms of thermal generation by this source (biogas digesters and biomass power plants), was approximately 140 GW, of which 15.320 GW corresponds to Brazil (UNICA, 2020; SÖNNICHSEN, 2020). Figure 21 shows the increase in installed power per year of this source in the national scenario. In the period between 2009 and 2016 there is a rapid growth of installed power, which may be due to the increase in national investment in biomass in the period. From 2017, a decrease in the deployment of installed power was observed. This can be attributed to the increased priority given to

other energy sources, such as wind, as well as due to budgetary constraints and the need to reduce government subsidies (BRASIL, 2017).

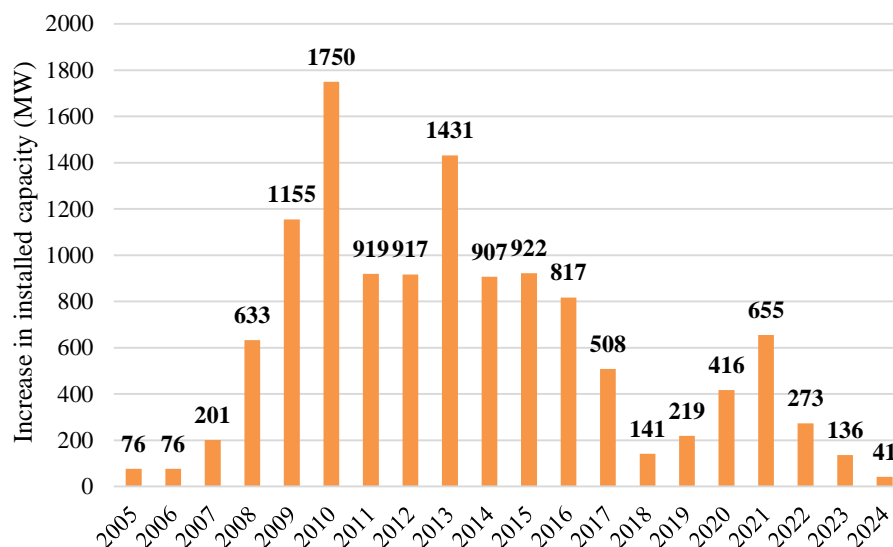


Figure 21 - Historical and forecasted increase in installed capacity by biomass in Brazil in MW. Source: Unica (2020).

As regards biogas alone, the global installed capacity in 2020 was 20,150 MW, approximately 120% higher than a decade earlier, whose value was 9,519 MW. Figure 22 shows the roughly linear growth trend of this source over the last decade.

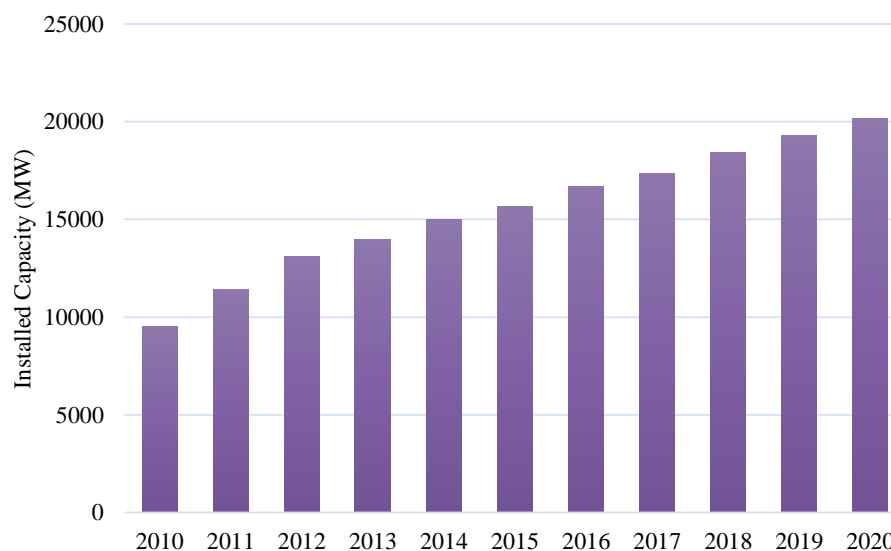


Figure 22 - Historical biogas installed capacity in the world in MW Source: Irena (2020).

Figure 23 shows the participation of each type of biomass for electricity generation in Brazil. In 2019, 52 TWh of biomass energy was produced, with 68% coming from sugarcane bagasse, 24% from bleach, 4% from firewood, 2% from biogas, and 2% from other renewables. Regarding the biogas production, in 2020 there were 638 biogas plants, most of which (78%) were small plants up to 1,000,000 Nm³/year. However, as

observed in Table 9, these plants represent only 8% of all annual biogas production in the country, with large plants being responsible for the largest production volume.

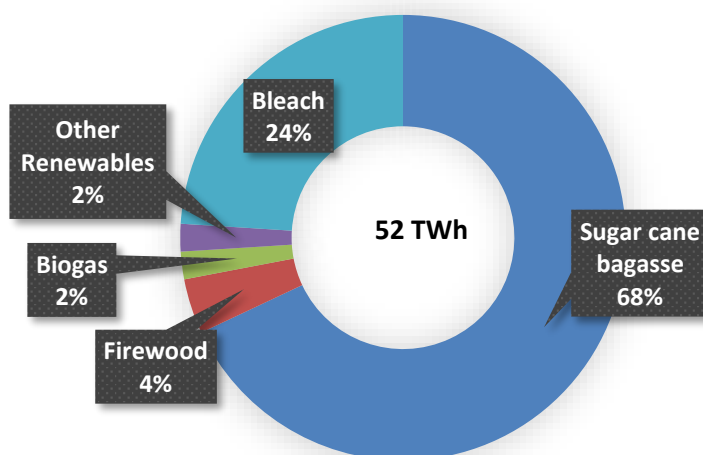


Figure 23 - Biomass distribution in electric generation in Brazil
Source: Coelho (2020).

Table 9 - Classification of biogas plants for energy purposes in Brazil in 2020. Source: CIBlogas (2020).

Plant size	Number of plants		Biogas volume Nm ³ /year	
Small size	496	78%	150,849,096	8%
<500,000 Nm ³ /year – Size 1	406	64%	90,937,686	5%
500,001 to 1,000,000 Nm ³ /year – Size 2	90	14%	59,911,410	3%
Medium size	104	16%	239,360,738	13%
1,000,001 to 3,500,000 Nm ³ /year – Size 3	78	12%	135,507,781	7%
3,500,001 to 5,000,000 Nm ³ /year – Size 4	26	4%	103,852,957	6%
Large size	38	6%	1,438,855,500	79%
5,000,001 to 30,000,000 Nm ³ /year – Size 5	25	4%	312,221,282	17%
30,000,001 to 125,000,000 Nm ³ /year – Size 6	10	2%	688,634,218	38%
>125,000,000 Nm ³ /year – Size 7	3	0.5%	438,000,000	24%
Total	638		1,829,065,334	

With a 10% share in the national energy matrix in 2022, biomass energy becomes a good alternative for Brazil, since the country is a large producer of agricultural inputs and these, in turn, generate waste, as in the production of soy, corn, and sugar cane (DE MIRANDA, MARTINS, LOPES, 2019; ENGIE, 2022). This scenario favors the promotion of self-producers of energy, since the waste can be used in the same place it is produced, without logistical and transportation problems.

II.6.4. Biopropane (BioLPG)

LPG (Liquefied Petroleum Gas) is used to prepare daily meals in 65.9 million Brazilian households (91% of total households). Its consumption, as observed in Figure 24, follows a steady trend over the months, but still corresponds to only 3.1% of the national energy matrix (EPBR, 2020). This can be attributed to the legal restrictions imposed on its application according to Law 8.716, of 8/2/1991, sanctioned when the country was dependent on the external market and went through supply crises. This defined as a crime against the economic order the use of LPG in any application that was not essential such as use in boilers, saunas and engines. However, even after reaching self-sufficiency in LPG supply, this law remains in force, because there has been no reform in the constitution since then (SINDIGÁS, 2008).

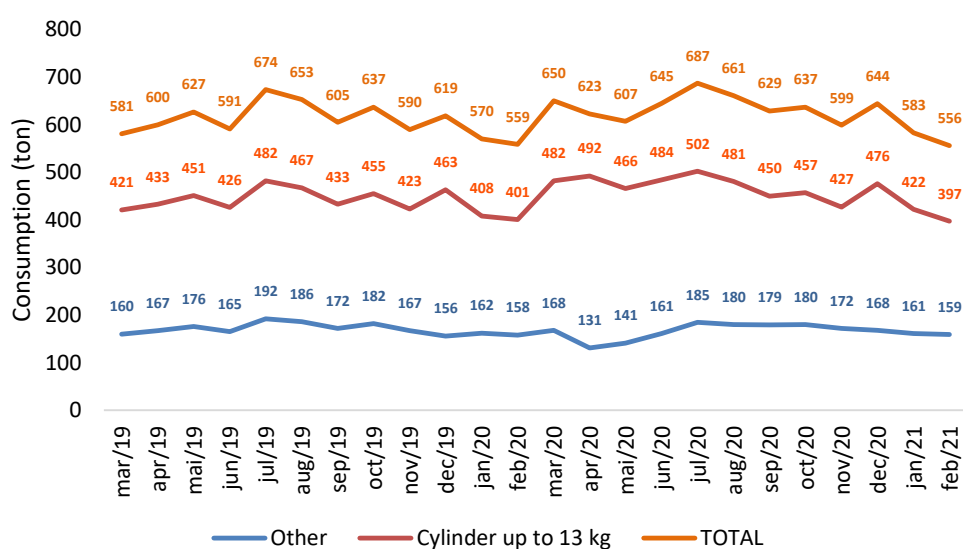


Figure 24 - Monthly LPG consumption in Brazil. Source: Sindigás (2021)

Biopropane, also known as bioLPG, has the same chemical composition as liquefied petroleum gas (LPG), but is about 94% less polluting than conventional LPG due to the production process, and can be used for the same applications such as cooking food and heating water in the residential sector (APETRO, 2019). There are several technological routes for biopropane production, and the main ones are represented in Figure 25. Among them, the most widely used is the process of hydrotreating oils (HVO: Hydrogenated Vegetable Oil) that can be of both plant and animal origin and has biopropane as a co-product.

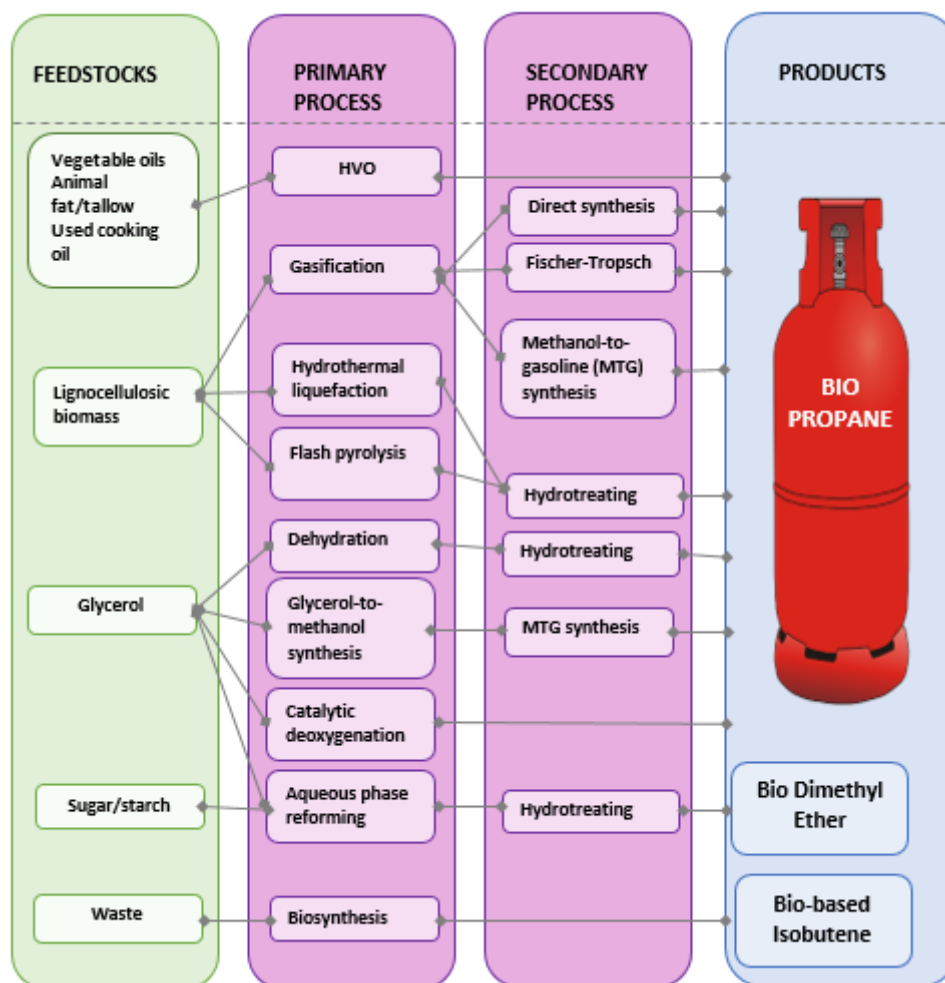


Figure 25 - Technological routes for biopropane production. Source: Adapted from Hopwood, Mitchell, Sourmelis (2019).

The potential for bioLPG production could reach 20 to 25 million tons per year in Europe by 2050. This would be enough to handle the continent's entire demand for LPG for power generation. With investments and incentive policies, which enable the production of biopropane, this production potential can be exploited and thereby achieve a complete decarbonization of the LPG distribution chain (APETRO, 2019).

With a reform in the legislation, and Brazil being a potential producer of green diesel (HVO) through the new HVO specification regulation prepared by the National Petroleum, Natural Gas and Biofuels Agency (ANP: *Agência Nacional do Petróleo, Gás Natural e Biocombustíveis*), the replacement of conventional LPG by bioLPG may contribute to thermal and electric generation in a more sustainable way in the country (CHIAPPINI, 2020).

II.6.5. Hydroelectricity

Hydroelectricity comes from the conversion of hydraulic potential energy into electrical energy. The installed capacity of a power plant is determined by the height and flow of the waterfall in the region or the force of the flow, for run-of-river

hydroelectric plants. In Figure 26, the operation of a hydroelectric plant is exemplified, where the kinetic energy of the waterfall drives a turbine, which in turn drives a generator that produces electricity, and through a transformer, this energy is directed to the energy transmission system of the central network.

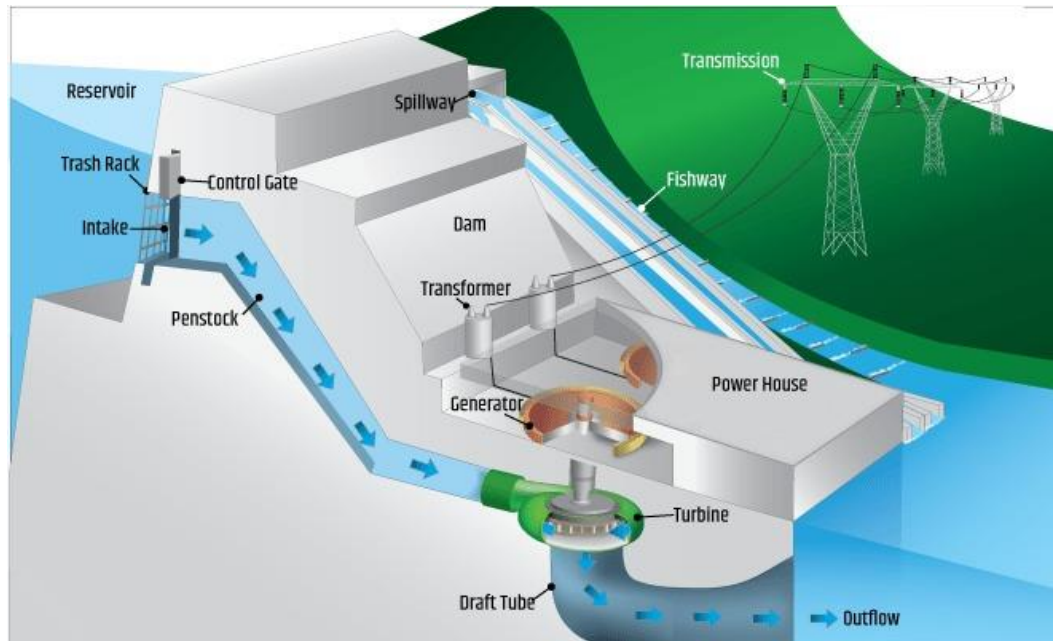


Figure 26 - Diagram of operation of a hydroelectric plant. Source: U.S. Department of Energy (2022).

According to the National Agency for Electric Energy (ANEEL: *Agência Nacional de Energia Elétrica*), hydroelectric plants are classified into three groups according to size and installed capacity: Hydroelectric Generating Plants (CGHs: *Centrais Geradoras Hidrelétricas*) are hydroelectric plants with up to 5 MW of installed capacity; Small Hydroelectric Plants (PCHs: *Pequenas Centrais Hidrelétricas*) have installed capacity of 5 MW to 30 MW; and Hydroelectric Power Plants (UHEs: *Usinas Hidrelétricas de Energia*) have more than 30 MW of installed capacity. According to ANEEL (2021), currently 739 CGHs, 425 PCHs and 219 UHEs are in operation in Brazil, which together correspond to 109.3 GW of installed capacity. Among the hydroelectric plants in the country, three are among the ten largest in the world: Itaipu Binacional with 14 GW, Belo Monte 11.23 GW and Tucuruí with 8.37 GW. In the world scenario, Brazil is the second largest producer of hydropower worldwide with 11.9%, behind China occupying the first place, with 15.4%, and Canada the third, with 11.7% (LIMA et al., 2018, NUNEZ, 2019). Figure 27 shows the evolution of electric generation capacity since 2000 by hydro source in the world. In 2030 the generation is estimated to reach 5,722 TWh (IEA, 2020).

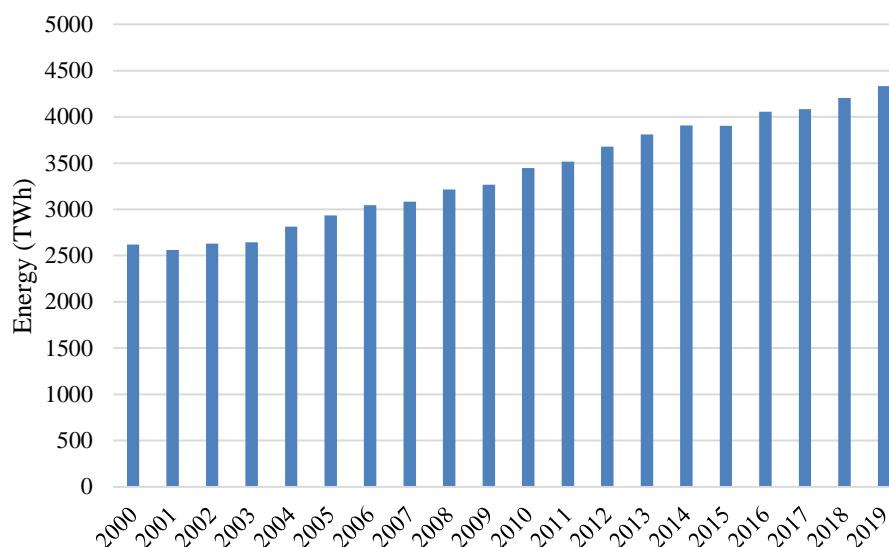


Figure 27 – Capacity of hydroelectric generation in the world between 2000 and 2019.

Source: IEA (2020).

Despite being considered a renewable resource due to the use of water as an energy source, studies show that hydroelectric plants can negatively impact the environment, depending on the installation site, such as in the Amazon where it has a vast area of vegetation. This occurs by flooding areas with organic materials that produce greenhouse gases due to the decomposition of these materials (DE FARIA et al., 2015). In addition, periods of drought can impact energy generation. In these periods, countries that have hydroelectric plants as their main energy source can suffer from energy crises, as happened in Brazil between 2000 and 2002, when it was necessary to implement an energy rationing plan to manage the crisis (AUGUSTO, 2020). In 2021, Brazilians saw the scenario of almost two decades ago repeat itself. Due to the lowest level of rainfall in 91 years, the government was forced to implement new measures to mitigate the energy crisis, among them: the expansion of thermoelectric generation and water rationing in reservoirs (AMATO, 2021). This highlights the importance of a country having a more diversified electricity matrix.

II.6.6. *Oceanic*

Ocean energy comes in four forms: wave energy, tidal energy, current energy, Ocean Thermal Energy Conversion (OTEC). Wave, tidal and current energies work by converting kinetic or potential energy into electrical energy.

As can be seen in Figure 28, the movement of the tides activates the electric turbine. The energy from the temperature gradient of warm surface water and cold deep water can be converted into thermal energy (FLEMING, 2012).

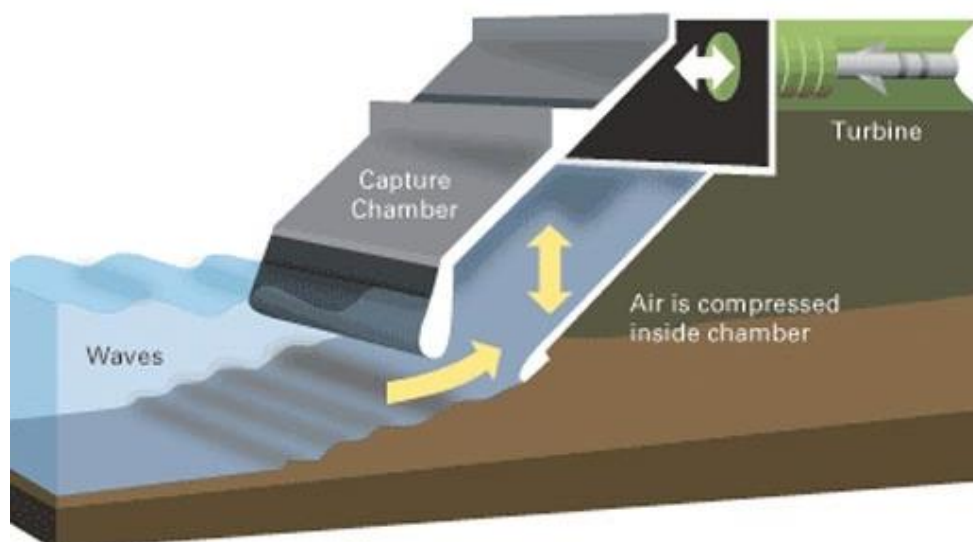


Figure 28 - Diagram of the production of electricity through wave energy. Source: Stauffer (2009).

The estimated theoretical potential for each source is summarized in Table 10. According to CIA (2015), the annual electricity consumption in the world is 21.78 TWh. Considering the sources that produce electricity (tides and waves), their potential represents about 1,836 times more than what is consumed in the world. However, due to the high cost of implementing these technologies, this potential is still little exploited, with about 600 MW of installed capacity in the world (EDENHOFER et al., 2011).

Table 10 - Theoretical energy potential of oceanic sources. Source: Modified from Saavedra (2016).

Source	TWh/year
Tides	22,000
Waves	18,000
OTEC	2,000,000
Salinity Gradient	23,000
TOTAL	2,063,000

According to Oliveira and Saavedra (2016), Brazil has a potential of 27 GW of energy generation by oceanic sources and presents a pilot plant project for the Estuário do Bacanga in Maranhão. However, due to the lack of incentives and a development policy for this source, there is still no participation of ocean energy in the country's electricity matrix.

II.6.7. CHP

Combined Heat and Power (CHP) is used to provide electrical and thermal energy simultaneously. This system is designed to reduce heat losses in the conventional electricity generation process. During electricity production, waste heat from the process is captured and can be used for water heating in homes or steam production in industrial processes (MOTEVASEL, SEIFI, NIKNAM, 2013).

CHP systems can be classified according to maximum electrical capacity into three categories: as micro cogeneration if their capacity is less than 50kWe, mini cogeneration if it is between 50kWe to 1MWe, and cogeneration if it is greater than 1 MWe (MARTINEZ et al., 2017). CHP technologies can be divided into two major groups, those that are based on thermodynamic cycles and those that are not based on thermodynamic cycles, as schematized in Figure 29.

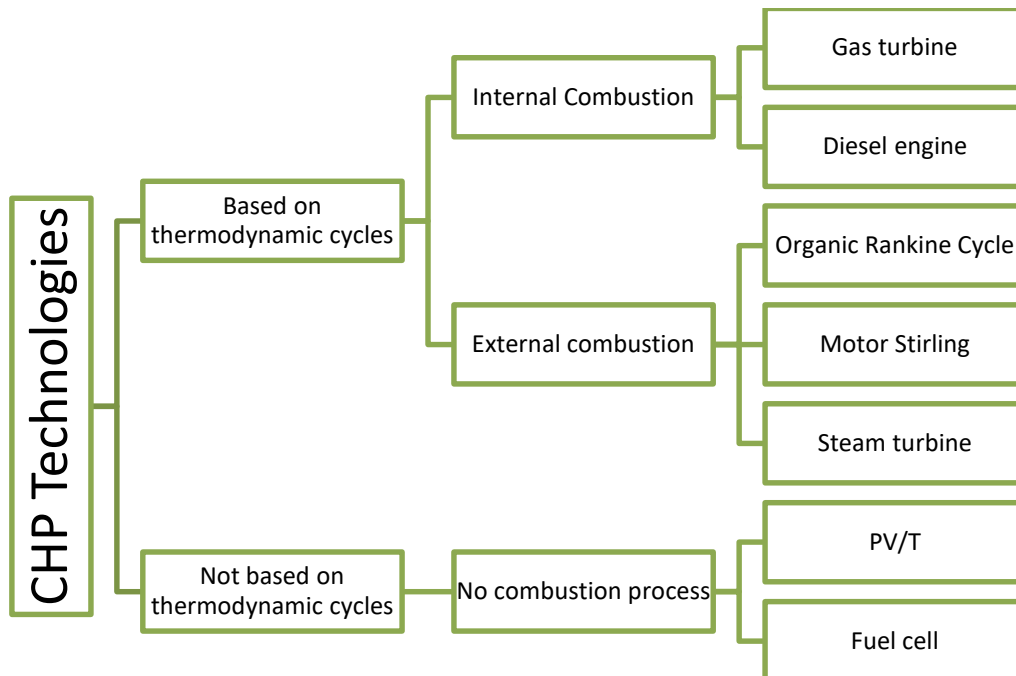


Figure 29 - Classification of the main CHP technologies. Source: Adaptado de Martinez et al. (2017).

Internal combustion and external combustion are classified as technologies based on thermodynamic cycles, which can use fossil fuel sources such as natural gas or renewable sources such as biogas. On the other hand, technologies that do not have a combustion process are not based on thermodynamic cycles and can be used from other renewable sources such as the hybrid solar photovoltaic/thermal (PV/T) collector and fuel cells (MARTINEZ et al., 2017). The latter converts the Gibbs energy of a chemical reaction into electrical energy and, depending on the technology adopted, does not emit GHGs (ALVES, 2012). In Figure 30 the operation of a CHP system is synthesized. In this case, one of the technologies in Figure 29 can be used as prime mover additionally with a heat storage system, piping and cables for heat and electricity transmission to the residence, respectively.

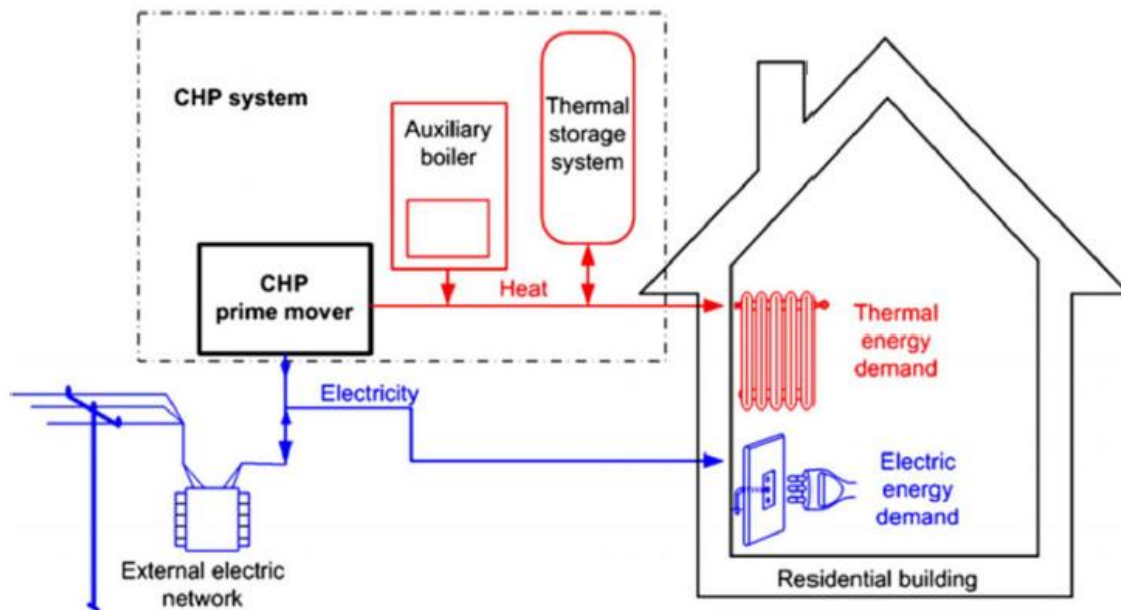


Figure 30 - Schematic diagram of the operation of a CHP system. Source: Martinez, Michaux, Salagnac, nd Bouvier (2017).

The adoption of CHP technologies with renewable sources promotes greater efficiency of the electricity and heat generation system, compared to other energy production systems. In addition, there is a reduction of GHG emissions and waste heat in the environment (MOTEVASEL, SEIFI, NIKNAM, 2013).

II.6.8. Geothermal

Geothermal energy is thermal energy originating from the Earth's interior. In areas of tectonic plate transition, thermal zones are more intense and therefore have a great potential for geothermal energy. However, studies show that geothermal energy can be harnessed even in places where high earth temperatures do not occur (ARBOIT et al., 2013). There are two ways of using this energy, the direct mode, when the heat is used directly, as an example, for heating water, or the indirect mode, in which the heat is used to generate electricity. Figure 31 shows an example of a geothermal energy system for heating water in a residence, in which a pumping system is used to make the water circulate inside the earth and absorb the heat.

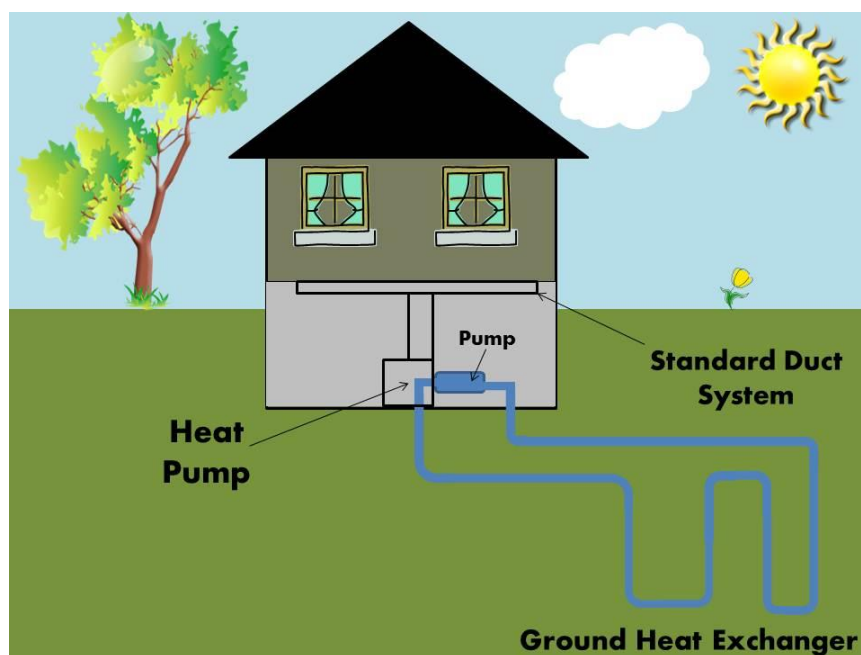


Figure 31 - Geothermal energy operation. Source: Energizect (2022).

Because it is a renewable source, it does not harm the soil where it is exploited, it does not emit GHGs, and its production capacity does not depend on climate variations, geothermal energy is being adopted by many countries (CAMPOS et al., 2016). Table 11 shows the five countries that most exploit this energy source. Although the United States has the largest installed capacity (3,094 MW), Iceland has achieved the title of most self-sustainable country with 70% of its energy matrix from hydroelectric plants and 30% from geothermal (CAMPOS et al., 2016).

Table 11 - Countries in the top 5 of energy generation by geothermal sources. Source: Campos et al. (2016).

	1°	2°	3°	4°	5°
Investment in 2015	Turkey	United States	Mexico	Kenya	Germany and Japan
Installed capacity at the end of 2015	United States	Philippines	Indonesia	Mexico	New Zealand
Heating capacity	China	Turkey	Japan	Iceland	India
Heating capacity (per capita)	Iceland	New Zealand	Hungary	Turkey	Japan

However, the percentage of geothermal energy use is still low compared to other energy sources, representing only 0.3% of all global installed capacity (KEATING, 2017). This may be due to the high costs involved in its implementation, around \$2,500 and \$5,300/kWh. This can be circumvented by the development of new technologies and government incentives, since the other costs, i.e., operational and maintenance, are relatively low (CAMPOS et al., 2016; STATISTA, 2021). However, other issues must be

observed when one intends to harness geothermal energy, such as the high heating of the extraction site and the possibility of release into the environment of hydrogen sulfide gas, extremely harmful to human health. In this sense, investments are required to mitigate these disorders (CAMPOS et al., 2016).

Brazil, despite not being located in tectonic plate transition zones, has some areas with high earth temperatures, as observed in Figure 32, which corresponds to an energy potential of 5.2×10^{22} J accessible for exploitation (CORRÊA, 2019). However, this source is little explored in the country, and has no representativeness in the national energy matrix. This can be attributed to lack of investment, lack of policies to encourage the adoption of geothermal generation technologies in the country and the available potential is lower than other sources such as wind and solar. The use of geothermal energy in Brazil is restricted to recreational and tourism purposes in the regions of Caldas Novas (GO), Piratuba (SC), Araxá (MG), Olímpia, Águas de Lindóia and Águas de São Pedro (SP) (ARBOIT et al., 2013).

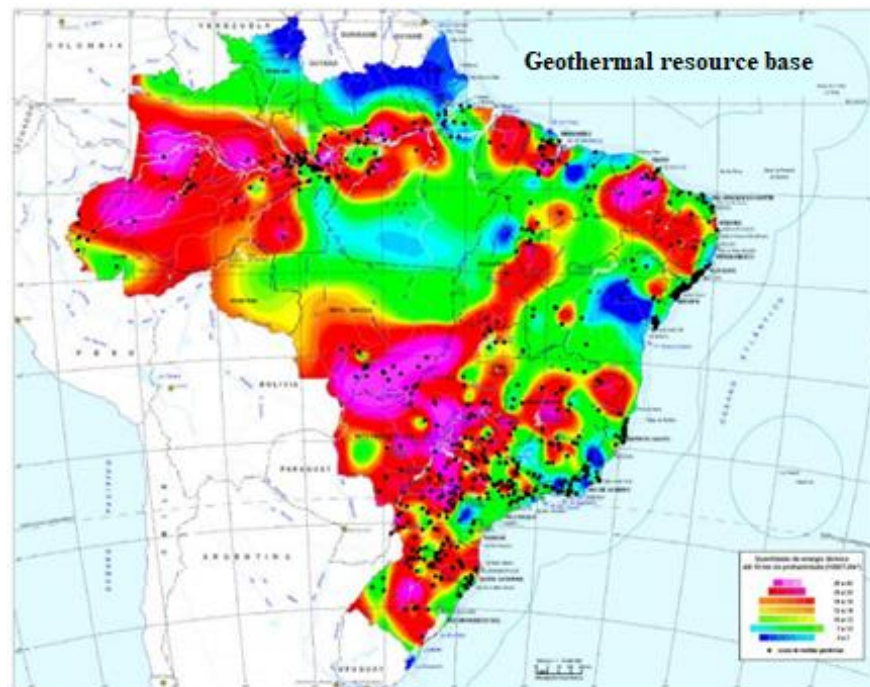


Figure 32 - Map of geothermal resource in Brazil. Source: Arboit et al. (2013).

II.6.9. Energy storage

In most cases the energy is not fully used at the time it is generated, as with solar and wind energy. Because of this, technologies have been developed to store it for later use. Energy storage can be either thermal or electrical. Thermal storage solutions keep energy in the form of heat that can be used for water heating, space heating or cooling, or even electricity production (GURUPRASAD et al, 2018). Currently several technologies

can be found, some of them are represented in Figure 14 and Figure 19, which use a boiler to store the hot water produced, such as biomass and thermal solar energy.

In electrical storage, electricity is converted into other forms of energy for later reconversion into electrical energy (World Nuclear Association, 2021). This also has several technologies with the most common being batteries. Batteries convert electrical energy into chemical energy and can convert chemical energy back into electrical energy by changing the direction of the oxiredution chemical process, represented by the arrow indicating the "discharge" of the battery in Figure 33.

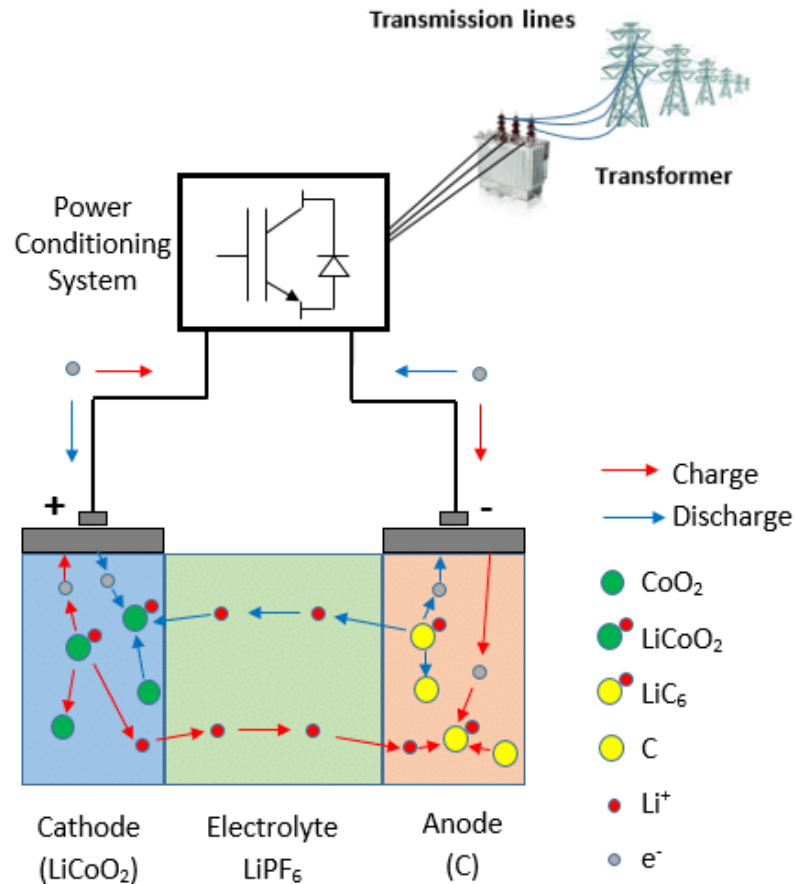


Figure 33 - Operation of a battery in the electrical system. Source: Nikolaidis, Poullikkas (2017).

Energy storage technologies are still very expensive and may not be feasible to use in some cases. However, according to the projection made in 2016 by the World Energy Council, the several technologies will have a drop in value in 2030, and the biggest drop will be the value of batteries, which may be 70% lower than in 2015 (World Nuclear Association, 2021).

II.7. Microgrids

Microgrids consist of power generation and consumption devices, energy management, and controllers, and can be entirely powered by renewable resources. (Figure 34). The microgrid controller is responsible for managing the generation, storage, and distribution of energy within the microgrid. In addition, the controller is responsible for monitoring the generation of power from renewable resources and ensuring that the power generated is always in line with the demand of the microgrid, as well as ensuring the safety and quality of the power generated.

The microgrid is located close to the place where the energy is used, which provides savings in the installation of distribution networks and reduction of energy loss in transportation. The microgrid differs from the minigrid only in size: while the microgrid is used for residential and small commercial and industrial purposes, the minigrid is used to supply larger configurations such as small islands.

The energy produced in the microgrid can be sold on the energy market becoming a source of income for those who produce it. In addition, distributed generation from renewable sources is beneficial not only because it allows for the reduction of greenhouse gas emissions, but also because it allows for independent operation from the centralized energy grid, which is usually powered by fossil fuel sources.

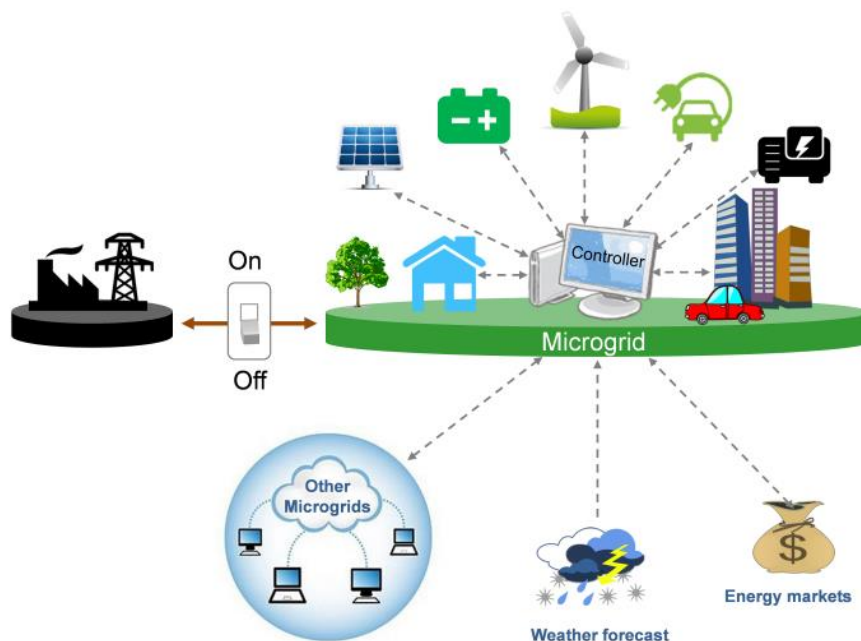


Figure 34 - Example of a microgrid. Source: Elinoff (2019).

Figure 35 illustrates the categories in which the microgrid can be classified regarding mode of operation, type, source and scenario:

- Mode of operation. The microgrid can be connected to the central energy grid, being able to inject the excess energy produced in the distribution network, or it can be isolated, when it operates without being interconnected to the network. In isolated operation, battery systems shall be used to store the excess energy to be used later, according to local demand.
- Type. The microgrid can be Alternating Current (ACc), Direct Current (DC) or hybrid, when it has both currents. Direct current is unidirectional, i.e., it follows a continuous flow in one direction, whereas alternating current is characterized by the variation of its direction periodically, so that the energy can be transported for great distances and with a high load. However, it is common for alternating current to be transformed into direct current, reducing its voltage, to be used in households.
- Source. Fossil fuels such as diesel and natural gas, renewable sources such as photovoltaic, wind power, and biomass, or more than one source, i.e., a hybrid condition, can be used.
- Scenario. The micro-grid can be used in homes, industries, and commerce in order to seek energy autonomy.

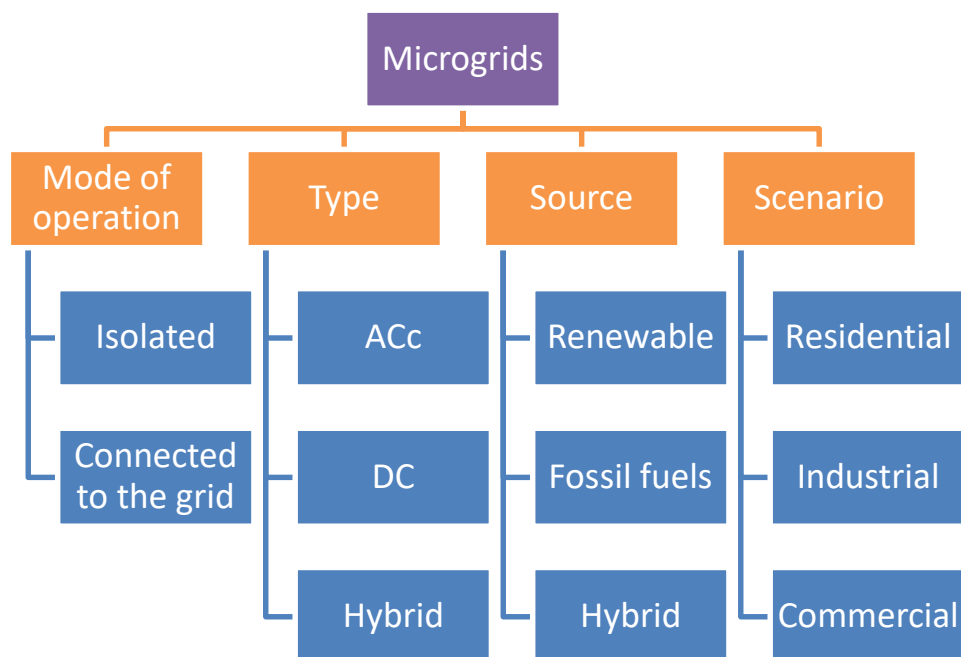


Figure 35 - Classification of microgrids. Source: Adapted from Eluri and Naik (2021).

The allocation of a microgrid involves choosing the location and size of the microgrid, as well as selecting and installing the energy sources and energy storage and distribution equipment. In addition, the allocation may also involve the definition of rules and mechanisms for managing and operating the microgrid, including the distribution of costs and benefits among participants.

Distributed generation devices which are poorly sized and allocated can cause several problems: energy losses, if the feeder line is poorly sized; reconfiguration of the protection system, if the distribution system of the central network is overloaded;

increased costs, when there is inadequate sizing and choice of energy source for the installation site; periods with discontinuation in energy supplementation, when the combination of resources is not done properly; among other factors (TAN et al, 2013). To enjoy all the benefits of the microgrid, therefore, the optimal configuration of the system must be determined.

II.7.1. Optimal microgrid configuration

For the optimal configuration of a microgrid, one must first define the challenges and problems associated with its implementation, as well as the benefits it intends to achieve. To define the optimization problem of a microgrid configuration, it is common to adopt the following steps: select the study site; define the initial considerations for the model; establish the renewable resources available at the site; delimit the constraints; propose the mathematical model; perform the optimization. In this way, it is possible to effectively characterize the problem under study.

A review of the state-of-the-art since 2006 was carried out focusing on optimization problems that seek to meet the energy demands of residences, sets of establishments or neighborhoods in order to provide the autonomy of these places. The keywords used in this search were: microgrid, design, optimization, energy distribution planning, distributed generation, optimal sizing, with the following combinations: microgrid AND (design OR optimization OR optimal sizing); design AND optimization AND (microgrid OR distributed generation); distributed generation AND design; energy distribution planning AND optimal sizing. The articles were also found by the references cited in these articles. This state-of-the-art review is expressed in Table 12.

Table 12 - Microgrid configuration optimization studies.

REFERENCE	OBJECTIVE FUNCTION	CONSTRAINTS	DEMAND	ENERGY/HEAT SOURCES	INCENTIVE POLICY	MODEL	STUDY CASE
Weber et al. (2006)	Min(Cost) AND Min(CO ₂ emissions)	Thermal and electric energy balance, mass balance and configuration	Electricity, heating	CHP	-	MINLP	Geneva – Switzerland
Hawkes, Leach (2009)	Min (Annual Cost equivalent)	Capacity, operational	Electricity, heating	Photovoltaic, Wind, CHP	-	MILP	United Kingdom
Atwa et al. (2010)	Min(Annual energy losses)	Operacional, configuration, capacity	Electricity	Photovoltaic, Wind, biomass	-	MINLP	Ontario – Canada
Weber and Shah (2011)	Min(Total Annual Costs)	Electric energy balance, configuration, operational	Electricity, heating, hot water, air cooling	Photovoltaic, wind, CHP, Gas boiler	-	MILP	United Kingdom
Porkar et al. (2011)	Min(Cost) AND Max(Total System Benefits)	Electric energy balance, operational, capacity	Electricity	Photovoltaic, wind, CHP, gas turbine, fuel cell, microturbine	-	MINLP	Central Western Region United States
Mehleri et al. (2012)	Min(Cost)	Thermal and electric energy balance, operational, configuration	Electricity, heating	Photovoltaic, natural gas boiler, CHP (fuel cells, gas engine, Stirling engine)	Feed in Tariff	MILP	Greece
Omu et al. (2013)	Min(Investment and Operational Costs)	Electric energy balance, operational, configuration, environmental targets	Electricity, heating	Photovoltaic, wind, biomass, natural gas	Feed in Tariff, Renewable Heat Incentive	MILP	United Kingdom
Wakui, Yokoyama (2014)	Min(Annual consumption of primary energy)	Thermal and electric energy balance, configuration, operational	Electricity, heating, hot water, air cooling	Boiler, CHP	-	MILP	Japan
Wouters et al. (2015)	Min(Cost)	Thermal and electric energy balance, configuration, operational	Electricity, heating	Photovoltaic, wind, CHP, Absorption Chillers	Feed in Tariff	MILP	Australia South
Zhang et al. (2015)	Min(Cost) AND Min(Global Warming Potential of the components)	Capacity, operational	Electricity, heating	CHP	Feed in Tariff	MILP	United Kingdom
Nasir and Mutale (2016)	Min(Cost)	Operational, capacity	Electricity, gas for cooking	Photovoltaic, battery, biogas generator	-	MILP	Kenya

Gabrielli et al. (2017)	Min(Cost)	Operational	Electricity, heating	Photovoltaic, thermal solar, battery	-	MILP	Zurich - Switzerland
Mashayekh et al. (2018)	Min(Investment) AND Min(Operating Costs) AND Min(CO ₂ emissions)	Operational, capacity, thermal energy balance	Electricity, heating, hot water, air cooling	Photovoltaic, CHP, Battery, boiler, Electric Chiller	-	MILP	Alasca
Schütz et al. (2018)	Min(Cost)	Configuration, operational, capacity	Electricity, heating	Photovoltaic, CHP, boiler, battery	Feed in Tariff	MILP	Bottrop - Germany
Mavromatidis et al. (2018)	Min(Cost)	Operational, environmental targets	Electricity, heating	Photovoltaic, CHP, biomass boiler, Gas boiler, battery	Feed in Tariff	MILP	Zurich – Switzerland
Mohammed et al. (2019)	Min(Cost)	Operational, realibility	Electricity	Photovoltaic, wind, tidal, battery	-	MINLP	Bretanha-France
Zatti et al. (2019)	Min(Cost)	Operational	Electricity, heating, cooling	Photovoltaic, Solar heating, Natural gas boiler, cogeneration Internal combustion engines, Heat storage	-	MILP	Italy
Pereira et al. (2019)	Min(Cost)	Energy balance, capacity, operational	Electricity	Photovoltaic, wind, tidal, diesel generator, battery	-	MINLP	Brazil
De Mel et al. (2020)	Min(Cost)	Configuration, operational	Electricity, heating	Photovoltaic, CHP, boilers	Feed in Tariff	MILP	United Kingdom
Recalde e Alvarez-Alvarado (2020)	Max(Realibility)	Configuration, operational	Electricity	Photovoltaic, wind, tidal	-	MINLP	Australia
Teichgraeber et al. (2020)	Min(Cost)	Operational	Electricity, heating	Photovoltaic, electric heater, battery	-	MILP	Germany
Karamov et al. (2021)	Min(Levelized cost of Electricity)	Operational, capacity	Electricity	Photovoltaic, diesel generators, battery	-	MINLP	Russia
Kharrich et al. (2021)	Min (Net Present Cost) AND Min (Cost of emitting CO ₂) AND Min(Amount de CO ₂)	Operational, capacity	Electricity	Photovoltaic, wind, Diesel generator, battery	-	MINLP	Morocco

Boucekara et al. (2021)	Min (Cost of electricity) AND Min(probability of loss of Power supply)	Capacity	Electricity	Photovoltaic, wind, Diesel generator	-	MINLP	Yanbu – Saudi Arabia
Clarke et al. (2021)	Min(Cost)	Energy balance, operational, capacity	Electricity, heating, hot water, air cooling	Photovoltaic, wind, CHP, batteries	Feed in Tariff	MILP	United Kingdom
Sidnell et al (2021a)	Min(Cost)	Energy balance, operational, capacity	Electricity, heating, hot water, air cooling	Photovoltaic, wind, CHP, Biomass Boiler, absorption chillers, gas heater, batteries	Feed in Tariff, Renewable Heat Incentive	MILP	United Kingdom
Sidnell et al (2021b)	Min(Cost)	Energy balance, operational, capacity Energy balance,	Electricity, heating, hot water, air cooling	Photovoltaic, biomass boiler, CHP, wind	Feed in Tariff, Renewable Heat Incentive	MILP	United Kingdom
Mechleri et al. (2022)	Min(Cost)	Energy balance, operational, capacity	Electricity, heating	Photovoltaic, CHP	-	MILP	Greece

Most authors adopted cost minimization as the objective function, since cost is a determining factor in the feasibility of a project. In addition, some authors (WEBER et al., 2006; MASHAYEKH et al., 2018; SACHS, SAWODNY, 2016; KHARRICH et al., 2021) also considered the minimization of CO₂ emissions, since it is an important aspect to be considered when implementing a microgrid at a site.

Regarding the constraints, usually thermal and electrical energy balances were considered. In addition, operational constraints such as interactions with the central grid, such as prohibiting the purchase and sale of energy in the same period to the central grid, were considered (MEHLERI et al., 2012). Environmental goals were also considered as operational constraints in Mashayekh et al. (2018), Sachs and Sawodny (2016), Mavromatidis et al. (2018), as well as voltage limits in Atwa et al. (2010) and Porkar et al. (2011). Configuration constraints have been presented as limitations in the allocation distributed generation units. In Mehleri et al. (2012) this constraint was exposed with the CHP unit centralized in a tree network structure. Similar to Omu et al. (2013), the capacity constraints were presented as the size, quantity of distributed generation units, and maximum and minimum power generation limits. In this way, the constraints were defined in order to satisfy the limitations of the site and the resources used.

Given the selection of renewable resources for each location studied, there was a predominance of the use of combined heat and power (CHP) systems, also known as cogeneration. Zhang et al. (2015) proposed an optimization study in environmental and economic terms for different scenarios where several CHP generation technologies are considered, among them: Proton Exchange Membrane (PEM); fuel cell; Solid Oxide Fuel Cell (SOFC); Stirling Engine (SE); and Internal Combustion Engine (ICE). The results found that PEM technology offers lower environmental impact with lower cost. Mashayekh et al. (2018) found the benefits of CHP technology by evaluating the optimal configuration of distributed renewable resources considering CHP, photovoltaics, and batteries. For places with scarce natural resources (solar, wind, tidal) the use of CHP technologies becomes a sustainable alternative, since CHP can use resources such as biogas, biomass, and even new technologies with low environmental impact such as PEM.

Regarding the incentive policy, some authors do not mention any incentive policy, either because they did not consider it for the country of study or because the country in question does not adopt any incentive policy. Although the authors Zhang et al. (2015) and Weber and Shah (2011) adopted the case study in the UK, which has the Feed in Tariff, they did not consider the policy in modeling the problem. Weber and Shah (2011) conclude that the system of renewable energy resources was not economically feasible to meet electricity demand. However, when comparing the authors who adopted this incentive policy (Clarke et al., 2021; Sidnell et al., 2021a; Sidnell et al., 2021b), the system was feasible. Omu et al. (2013) compare the economic and environmental impacts of

distributed energy systems with conventional centralized power generation systems, as well as analyze whether renewable energy subsidies in the UK increase the economic competitiveness of these systems. The authors concluded that the decision to install distributed renewable resources is strongly dependent on the regulatory economic landscape and building requirements. Furthermore, they exposed that the decision to adopt subsidies should be made when evaluating the technology that presents the greatest gain in terms of performance and CO₂ reduction for each site. Regarding the demand, there is not yet a study in the literature that covers all the demands of the residence such as air cooling, hot water, electricity, and gas for cooking.

Each reference sought to address gaps in the literature ranging from solving methods to combine different technologies, referred to as hybrid systems. Weber et al. (2006) developed a new method to configure district energy systems by decomposing the multi-objective optimization problem analogous to Bender's decomposition which is a mathematical technique used to solve extensive linear programming problems. They found that the method still needs adjustments to be able to better portray the optimal scenario in terms of financial and CO₂ emissions. In addition, they did not assume hot water and cooling demand.

Hawkes and Leach (2009) proposed a microgrid techno-economic modeling framework that explicitly defines the amount of time the microgrid is expected to operate autonomously and restricts the heat flow between the participants of the microgrid. The authors found that the deployment of the microgrid is more economically feasible than the use of the central grid and boiler. In addition, they noted that the microgrid in islanded mode can be more expensive and presents a greater complexity of operation than using the microgrid connected to the central grid. However, this analysis was conducted without assuming any type of government incentive.

Atwa et al. (2010) proposed a probabilistic planning technique to determine the optimal fuel mix of different types of renewable distributed generation (DG) units in the distribution system in order to minimize the annual energy loss. In addition, the uncertainties associated with renewable resources as in solar and wind energy were considered. The authors found that for all combinations performed of the renewable resources there was a significant reduction in energy loss.

Weber and Shah (2011) presented a tool for district energy system design and optimization to find the optimal combination of technologies that will simultaneously assist in reducing emissions while ensuring the resilience of the energy supply. The authors found that with regard to heat supply, CHP plants combined with heat pumps is a cheaper alternative to conventional heat pumps and helps to reduce CO₂. However, the uncertainties of renewable resources such as wind conditions and energy consumption profile, for example, were not considered in the optimization problem.

Porkar et al. (2011) proposed a two-stage scheduling for distributed generation (DG) allocation: minimizing total costs *versus* payback time and maximizing total system benefits *versus* lifetime of DG. The authors concluded that DG can be a good option when the distribution grid has congestion problem.

Mehleri et al. (2012) optimized the design of distributed power generation systems that satisfy heating and power demand at the level of a small neighborhood by including a network of heating ducts in the system to transport thermal energy between consumers. Because this network is not considered pre-existing, the problem covers all possible configurations. To better define the arrangement of the heating ducts, one should add to the model, besides the basic constraints of energy balance and unit operations, constraints that consider the design and operation of the network. This can be applied as constraints in order to avoid looping in the heat transfer between houses, in other words to avoid that heat from being transported in more than one direction at the same time.

Wakui and Yokoyama (2014) included several types of operating constraints of residential cogeneration units, such as operating the system with a constant power output, operating it using the daily start-stop mechanism, in which the system restarts automatically in order to reduce fuel consumption, and continuous operation with a minimum power output. The results show that, for the selection of a cogeneration power and heat unit, the operating constraints influence the choice more than the heat/power generation rate. The use of batteries was not considered in the problem, which could have allowed a better analysis of the energy supply capacity of renewable resources.

Wouters et al. (2015) presented a residential trigeneration approach: electricity, heat, and chilled water. In addition, feedback-free loop approaches were adopted. This allows each household to only receive or send heat to or from the heating and cooling grids and the operation of the microgrid. The authors demonstrated that the photovoltaic units provide a source of income when the Feed in Tariff policy is available. Furthermore, they found that variability in solar irradiance does not significantly impact the design of the microgrid.

Zhang et al. (2015) quantified and evaluated the environmental performance of a process for its entire life cycle with multi-objective modeling on economic and environmental metrics to design the optimal configuration of a microgrid. They observed that installing multiple CHP technologies provided a lower environmental impact at a lower cost compared to the scenario where only one technology was installed. However, interactions with the central power grid such as selling the excess power generated was not considered, neither variations in resource efficiency or adoption of renewable resources such as photovoltaics, wind for example.

Nasir and Mutale (2016) proposed a remote microgrid, which is not connected to the central energy grid, and use biogas to meet the gas demand for cooking food. The results showed that the proposed microgrid can meet the demand of remote rural communities. However, some limitations were observed in the model such as lack of energy sharing between the houses of the microgrid, the sizing of the technologies considering the demand behavior for each house. In addition, biogas was not used to meet other demands such as hot water, for example.

Gabrielli et al. (2017) proposed new methodologies to simplify the optimization problem in multi-energy systems with seasonal energy storage, which typically involve a large number of decision variables. The proposed techniques allow for a one-year time horizon with hourly resolution, which are validated using a computationally efficient system that does not rely on design days. However, the impact of the chosen time horizon method on the energy sharing interaction among the houses in the microgrid is not analyzed. In addition, the authors use the time-dependent efficiency profile of the PV panel to predict the best system sizing. The results show that the proposed approaches correctly size the energy storage and simplify the optimization problem, while achieving good agreement with full-scale optimization.

Mashayekh et al. (2018) proposed a configuration approach that determines the optimal combination, size, location, and dispatch of distributed fossil fuel-based and renewable energy resources in microgrids, i.e., the scheduling/planning of generation and energy availability. The authors observed that, when considering power supply security constraints, the adoption of renewable resources presented disadvantages due to generation variability and inability to increase generation after a system contingency. However, when evaluating economic and environmental aspects, the adoption of renewable resources would be advantageous.

Schütz et al. (2018) presented and analyzed a new method for solving the problem of optimizing the design, sizing, and operation of distributed power systems iteratively without having to change/simplify the original model. The method showed a significant improvement in the scalability of the model providing the adoption of larger amounts of energy resources.

Mavromatidis et al. (2018) proposed a two-stage stochastic model (design and operation decision) considering uncertainties in the parameters: energy carrier prices, emission factors, building heating and electricity demand, incoming solar irradiation patterns. After a comparison between deterministic and stochastic scenarios, a large deviation in costs, configuration and operation of the DER was observed. This showed the shortfalls of the deterministic DER model design.

Mohammed et al. (2019) proposed the application of particle swarm technique for optimization to reduce the computation time in hybrid renewable energy system

optimization problems (wind, tidal, photovoltaic and battery). The results showed that for the case study the optimal solution would be the adoption of wind turbines and battery. This is due to variables such as climatic conditions, constraints, demand profiles and costs adopted at the study site.

Zatti et al. (2019) proposed a Mixed Linear Program clustering model, k-MILP, to optimize the design of multi-energy systems. This model considers the operation strategy and the part-load behavior of the units in the optimization process and formulates it as a two-step problem. The k-MILP model allows the selection of representative and extreme periods for the optimization process and provides the flexibility to control the characteristics of the selected periods and set a maximum tolerance for deviation. The model has been tested on two different multi-energy systems and compared with other well-known clustering techniques, with results showing that k-MILP leads to a better representation of typical and extreme operating conditions, resulting in more efficient and reliable designs. However, it is worth mentioning that the work did not consider the residential energy profile and did not take into account the energy distribution between houses in the microgrid and the connection of the microgrid to the central grid, as well as seasonal variations in the energy profiles used in the application of the clustering method.

Pereira et al. (2019) presented the evaluation of the energy complementarity characteristics of photovoltaic, wind and tidal sources. It was observed that the problem of variability of sources can be solved when complementary sources are used in the system. For the case study presented, the best scenario was the use of photovoltaic energy together with wind energy.

De Mel et al. (2020) analyzed the impacts of uncertainties in electricity demand, heating demand, and solar irradiation on the total daily operating cost of distributed energy systems. The authors observed that heat demand has the greatest influence on the variation in total daily operating cost.

Recalde and Alvarez-Alvarado (2020) used an integrated reliability assessment based on the system state within the optimization method by means of probabilistic models as well as time-dependent models for each distributed renewable resource for central grid power supply and load demands. The results showed a tradeoff between cost, reliability and system losses for all optimal scenarios. Moreover, the best scenario considering higher performance at lower cost was the adoption of photovoltaic and wind power.

Teichgraeber et al. (2020) addressed the challenge of incorporating extreme events, such as peaks, in time-series clustering used in energy system optimization. Clustering methods typically remove such events, which can lead to suboptimal and unreliable system designs. The authors present a decision framework to include extreme events in

a set of representative periods and introduce a method to find extreme periods based on the slack variables of the optimization problem. The proposed method is evaluated on a residential energy supply system and benchmarked against other methods from the literature. The results show that using extreme periods improves the accuracy of the optimization results by up to 75%, depending on system constraints, compared to clustering only. This improvement reduces system cost and enhances system reliability.

Karamov et al. (2021) have developed a method for optimizing the structure and installed capacity of isolated power systems in specially protected areas such as Lake Baikal. The method is demonstrated by using a real tourist base as an example and involves forming a unified model of isolated power systems, taking into account the specific requirements and restrictions set by environmental laws and regulations. Mathematical models and control algorithms were selected based on the specifics of the problem and climate indicators. The nonlinear integral Volterra equation was used to optimize the charging and discharging processes of the storage batteries, taking into account their nonlinear dependence on efficiency. In addition, an equation that considers the efficiency as time dependent for the operation of the photovoltaic panel was considered. The results showed that the optimal solution involves the use of solar panels and storage batteries.

Kharrich et al. (2021) compared three algorithms (MOPSO: Multiple Objective Particle Swarm Optimization, PESA II: Pareto Swarm Optimization and SPEA2: Strength Pareto Evolutionary Algorithm) to optimize multi-objective hybrid renewable energy system (photovoltaic, wind, diesel generator and battery) based on Six Sigma tool in order to measure and evaluate the robustness of the method. The multi-objective problem was used to analyze the Net Present Cost, penalty cost of emission and CO₂ emissions. The authors found that in terms of robustness and reliability the best method was SPEA2. Furthermore, the microgrid studied presented a good cost-benefit ratio and proved to be able to guarantee power availability 98% of the time.

Boucekara et al. (2021) presented a new approach of using decomposition-based multi-objective evolutionary algorithm to optimally design the system considering load uncertainty. The optimization problem considers a Loss of Power Supply Probability (LPSP) and Cost of Electricity (COE) as objective functions. The results showed that the proposed method, which is the combination of four decomposition methods, performs better than adopting each of the methods individually.

Clarke et al. (2021) proposed a microgrid, in which, each house can generate thermal energy and store this energy in a tank located in another house. The biomass boiler is used to meet both hot water and space heating demands. In this system a lower environmental impact was observed due to the use of renewable sources at a lower cost.

Sidnell et al. (2021a) presented the optimization of a distributed renewable resource system with a larger number of technologies and energy demand options compared to similar work found in the literature. In addition, they included more than one government incentive option in the model. The authors also found that the distributed renewable resource system can produce cheaper energy than centralized generation. In addition, they demonstrated that renewable energy incentives such as the Feed in Tariff policy and Renewable Heat Incentives can make DERs even more cost-effective. They also found that the greater the number of homes in the system, the lower the average number of units needed to be installed per home, due to the possibility of sharing energy between homes. However, the effect of uncertainties and variations in renewable sources was not considered.

Sidnell et al. (2021b) presented a framework for identifying variable prices for distributed energy resources to control the electricity that is imported from, exported to, or exported into systems. The authors found that grids that produce most of the energy needed for their consumption and import little from the central grid are not greatly affected with dynamic import prices. However, these have a greater incentive to sell surplus energy at dynamic export prices.

Mechleri et al. (2022) proposed a new approach to find the optimal configuration of a microgrid based on Model Predictive Control (MPC). The results showed that there are benefits to installing the microgrid connected to the central power grid, as well as the use of electrical energy storage. However, the model did not consider the variation in the efficiency of renewable resources, as well as the state of charge for storage systems.

Table 13 expresses the problem size of each reference, along with the amount of single equations, single variables and discrete variables, and the computational performance in terms of CPU time. According to the GAMS directory, the term SINGLE indicates the number of individual rows and columns in the problem generated (GAMS, 2023). For some authors (ATWA et al., 2010; WEBER and SHAH, 2011; PORKAR et al., 2011; OMU et al., 2013; RECALDE and ALVAREZ-ALVARADO, 2020) the problem dimension was considered in terms of IEEE bus system, which consists of a representation of the generators, loads and power line parameters standardized by the Institute of Electrical and Electronics Engineers - IEEE (TIWARI et al., 2018). Each bus in this system can be represented as a load point, so to standardize the discussion of the Table 13 under study each bus was considered equivalent to a residence.

In addition, some authors such as Hawkes and Leach (2009) and Zhang et al. (2015), considered the study of different microgrids in order to compare the behavior of each demand. Hawkes and Leach (2009) considered the study of a microgrid with three different facilities: hospital, hotel and residence and found that in these scenarios the use of a microgrid is positive due to the gain in terms of reliability in energy supply and lower emissions of pollutant gases into the atmosphere. Zatti et al. (2019) considered a

university campus and a singles university building. Some authors (Mohammed et al., 2019; Pereira et al., 2019; Kharrich et al., 2021) did not specify the number of houses or establishments adopted in the microgrid under study, only the total amount of the microgrid load was presented. In addition to the number of facilities considered in the microgrid, the number of discrete and continuous variables as well as the number of equations adopted in the problem indicates the computational effort demanded to find the optimal solution. Comparing the work of Clarke et al. (2021) and Sidnell et al. (2021a), even considering the same number of facilities, the increase of 5% in the number of variables demands approximately 1190% more time to solve the problem. This infers that simplifications in the mathematical models can significantly impact the reduction in problem solving time due to less computational effort.

Table 13 - Size and computational performance of optimization problems.

REFERENCE	DIMENSION	SINGLE EQUATIONS	SINGLE VARIABLES	DISCRETE VARIABLES	CPU TIME (s)
Weber et al. (2006)	12 houses	NS	NS	NS	NS
Hawkes, Leach (2009)	3 installations	NS	NS	NS	NS
Atwa et al. (2010)	41 houses	NS	NS	NS	NS
Weber e Shah (2011)	35 installations	NS	NS	NS	NS
Porkar et al. (2011)	30 houses	NS	NS	NS	NS
Mehlerer et al. (2012)	5,10,20 houses	NS	NS	NS	1,275
Omu et al. (2013)	6 installations	NS	NS	NS	NS
Wakui, Yokoyama (2014)	1 house	18,900	13,120	3,847	NS
Wouters et al. (2015)	5 houses	31,421	23,553	3,686	63.399
Zhang et al. (2015)	5 installations	NS	NS	NS	NS
Nasir and Mutale (2016)	100 houses	NS	NS	NS	NS
Gabrielli et al. (2017)	NS	NS	NS	NS	NS
Mashayekh et al. (2018)	19 houses	NS	NS	NS	NS
Schütz et al. (2018)	136 installations	2,051,067	1,184,067	157,896	NS

Mavromatidis et al. (2018)	10 installations	NS	NS	NS	NS
Mohammed et al. (2019)	NS	NS	NS	NS	NS
Zatti et al. (2019)	2 installations	NS	NS	NS	NS
Pereira et al. (2019)	NS	NS	NS	NS	NS
De Mel et al. (2020)	9 houses	135	171	NS	56,520
Recalde and Alvarez-Alvarado (2020)	37 houses	NS	NS	NS	NS
Teichgraeber et al. (2020)	1 house	NS	NS	NS	NS
Karamov et al. (2021)	75 people	NS	NS	NS	NS
Kharrich et al. (2021)	NS	NS	NS	NS	NS
Boucekara et al.(2021)	5,10 houses	NS	NS	NS	NS
Clarke et al. (2021)	20 houses	85,160	169,882	1,500	396,390.66
Sidnel et al. (2021a)	20 houses	85,945	161,166	1,501	33,209.77
Sidnell et al. (2021b)	5 houses	NS	NS	NS	NS
Mechleri et al. (2022)	10 houses	NS	NS	NS	NS

NS: Not Specified

When the problems address the electrical aspect of the DRG system, considering the variability in the behavior of energy sources, as well as uncertainties in the process make the problem more complex. Most of these problems are represented by nonlinear equations, with quadratic and exponential constraints. Therefore, a Mixed Integer Nonlinear Programming (MINLP) results, as was observed by some authors cited in Table 12 (Atwa et al., 2010; Sachs, Sawodny, 2016; Pereira et al., 2019; Recalde Alvarez-Alvarado, 2020; Weber et al., 2006; Porkar et al., 2011, Mohammed et al., 2019, Kharrich et al., 2021, Boucekara et al., 2021).

On the other hand, problems that are restricted to the sizing of renewable resources and their allocation within the microgrid without taking into account electrical aspects and uncertainties, can be defined in terms of linear equations and constraints. Thus, a

mixed integer linear programming (MILP) results, as Mehleri et al. (2012) and other authors (HAWKES, LEACH, 2009; WEBER and SHAH, 2011; OMU et al., 2013; WAKUI, YOKAYAMA, 2014; SECCHI, 2015). Consequently, problems of this type will present a lower computational effort due to further simplification of the model.

Tan et al. (2013) conducted a survey of the most popular optimization methods for determining the best configuration of a microgrid system, as illustrated in Figure 36. Among them there are conventional methods (analytical methods, optimal power flow, SNOPT, BARON, etc.), Artificial Intelligence (AI) techniques, and hybrid intelligent systems, as Table 14 summarizes.

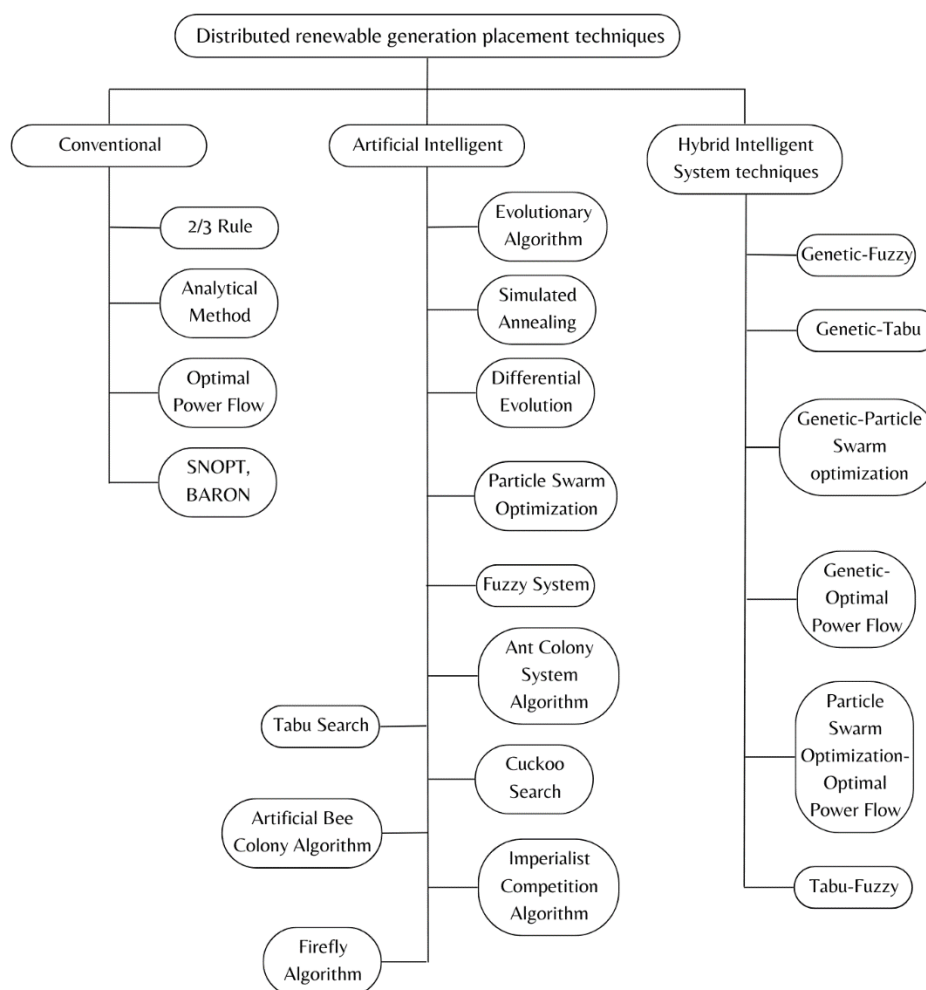


Figure 36 - Optimization techniques used to define the best configuration for distributed generation systems. Source: Adapted from Tan et al. (2013).

Regarding conventional methods, the 2/3 rule is usually used for problems that seek the proper location of shunt capacitors, responsible for improving the power factor of distributed systems (WILLIS, 2000). The analytical methods are commonly used when the objective is to reduce power loss and improve voltage profiles by finding the optimal

allocation and sizing for the system (ACHARYA et al., 2006). The optimal power flow method is used when one wants to determine the best operating levels of an electrical system to meet a given electrical demand (VOVOS et al., 2005).

SNOPT and BARON are powerful solvers for MINLP problems, which join continuous and integer variables and NL objective functions and/or constraints. Such solvers are available in GAMS software, which is a high-level modeling system for mathematical programming and optimization (EL- KHATTAM et al., 2005).

AI methods are commonly used for energy loss minimization problems (BORGES, FALCAO, 2006). The Evolutionary Algorithm is based on biological evolution concepts, and for an optimization problem the variables are manipulated following such concepts until a solution to the problem is found. This was used as the solving method for the problems proposed by Boucekara et al. (2021), for instance, expressed in Table 12. Simulated annealing is a probabilistic local search technique and can be used in distributed power system optimization problems (SUTTHIBUN, BHASAPUTRA, 2010). Differential Evolution is an algorithm based on natural selection and population genetics. The optimization problem is solved by sampling the objective function at several randomly chosen starting points. This can be used for multi-objective problems with technical and economic aspects to optimize a microgrid (GUNDA, KHAN, 2011). Particle swarm optimization is also a technique based on patterns in nature that, through an iterative method, tends to search for the optimal point. This method was used by Mohammed et al. (2019) and Kharrich et al. (2021) expressed in Table 12. The fuzzy system is a mathematical system that uses fuzzy control and logic (LALITHA et al., 2010).

Tabu Search is a combinatorial optimization algorithm. The Ant Colony Algorithm involves a fork path-finding problem, it is based on the foraging behavior of ants. The Artificial Bee Colony algorithm is based on the foraging behavior of the bee swarm. It can be applied to microgrid optimization problems, in order to find the optimal scenario that reduces losses and increases feed line capacity (ABU-MOUTI, EL-HAWARY, 2011). The Cuckoo Search Algorithm is based on the parasitic behavior of the Cuckoo bird that lays its eggs in other birds' nests. This type of algorithm can also be used to improve the voltage profile (MORAVEJ, AKHLAGHI, 2013). The Firefly Algorithm is inspired by the ability of fireflies to blink. This algorithm can be applied to optimize the configuration of distributed power resources, minimizing in addition to power loss, the line load and improving voltage profiles (SULLAIMAN et al., 2012). The Imperialist Competitive Algorithm is used to solve optimization problems and can be used to optimize microgrids, considering technical aspects of capacity and system allocation (SOROUDI, EHSAN, 2012).

Hybrid Intelligent System techniques are a combination of AI algorithms in order to improve their results. In microgrid optimization problems they can solve multi-

objective functions with economic and technical aspects in order to find the best system configuration (HARRISON et al., 2007).

According to TAN et al. (2013) the advantages and disadvantages of each method for distributed renewable generation (DRG) are those expressed in Table 14. Each methodology has its own characteristics, advantages and disadvantages depending on the gains to be achieved and the complexity of the system. In the table, all the genetic algorithms are encompassed in the Hybrid intelligent system.

Table 14 - Advantages and disadvantages of DRG placement methods. Source: Tan et al. (2013)

	DRG placement method	Advantages	Disadvantages
Conventional	2/3 Rule	Simple and easy to use approximate technique	Not suitable applied directly to non-uniform load network systems
	Analytical Method	Easy to implement, high precision factor, computational time efficiency	Few literature examples, lacks robustness, only can consider single objective and single DRG at a time
	Optimal Power Flow	Easy to find literature examples, high precision factor, computational time efficiency	Problem formulated in "closed" manner, hard to include different aspect into calculation
	Mixed Integer Nonlinear Programming	High precision factor, computational time efficiency	Hard to implement and understand
Artificial Intelligence	Evolutionary Algorithm	Efficient performance for finding the global optimum, easy to find literature examples	Relatively harder to code, premature convergence possibility of trapping into local optima, lower precision factor
	Simulated Annealing	Ease of implementation, ability to provide reasonably good solutions for many combinatorial problems, robustness	Relatively lower performance for finding the global optimum, fewer literature examples
	Fuzzy System	Easy to understand and suitable to model uncertainties for better compromised solution	Fewer literature examples
	Tabu Search	Efficient performance for achieve an optimal or sub optimal solution, capable to escape from local minimum	Relatively harder to code due to many parameters to be tuned, lower precision factor
	Ant Colony Search	Easy to understand and code	Probability distribution changes by iteration, uncertain time to convergence, few literature examples

	Artificial Bee Colony Algorithm	Capable of handling complex optimization problems, easy to code	Few literature examples
	Cuckoo Search	Easy to code, less parameters setting	Slow convergence, fewer literature examples
	Firefly Algorithm	Easy to understand and code	Slow convergence, fewer literature examples
	Imperialist Competition Algorithm	Capable of handling complex optimization problems	Relatively harder to code due to many parameters to be tuned, fewer literature examples
Hybrid	Hybrid Intelligent System	Efficient performance for finding the global optimum capable of handling complex optimization problems	Relatively harder to code, fewer literature examples

Therefore, the choice between a deterministic and a stochastic method for microgrid optimization may depend on several factors, including:

- Knowledge of the system: A deterministic method is more suitable when there is a high level of knowledge about the system and its variables, while a stochastic method is more suitable when there is uncertainty about these variables.
- Complexity: A deterministic method is generally less complex, while a stochastic method can be more complex due to the need to model and simulate uncertainty.
- Processing Time: A deterministic method generally requires less processing time, while a stochastic method may require more time due to the need to simulate multiple scenarios.
- Objective: If the objective is to obtain the best possible, or optimal, result with known information, the deterministic method is the best choice. Otherwise, a stochastic method may be more appropriate to evaluate the robustness of the solution against uncertainties.

II.8. Conclusions

This chapter presents the incentive policies in Brazil and in the world for the adoption of distributed generation, as well as the reason for proposing policies of this type as a result of international sustainability meetings and protocols. In addition, the main renewable energy sources were explained and a review of the state-of-the-art on modeling studies for the optimal configuration of microgrids was presented. The main conclusions of the chapter are:

- The adoption of distributed generation from renewable sources is still understated in Brazil compared to centralized generation and in other countries around the world. This can be attributed to regulatory challenges

and high acquisition costs of distributed renewable resources. For the use of the high energy potential that Brazil has, public policies and projects that aim to further encourage the installation of microgrids in the country should be feasible.

- The review of the state-of-the-art on microgrid configuration optimization modeling showed the effectiveness of using distributed energy resources to reduce GHG emissions and the technical and economic feasibility of these resources.
- At present, there is a lack of literature addressing how the time-dependent efficiency profile of renewable resources impacts energy sharing behavior in microgrids. Additionally, there is a need for more in-depth analysis to understand the differences between adopting the time-dependent efficiency profile *versus* not considering it in microgrid scenarios.
- Techniques for systematic time period determination have not yet been consistently analyzed in how it affects microgrids with different number of houses, as well as the allocation and sizing of renewable resources in these systems.
- Biogas has great potential as a renewable energy source to meet energy demands, but its underutilization in Brazil and globally, and limited research into optimal microgrid configurations pose a challenge. Furthermore, the potential use of biogas to meet hot water demands remains unexplored. Moreover, there has been a lack of literature on the complete biogas production process that considers the specificities and limitations in meeting all microgrid requirements.
- Studies that analyze the influence of demand behavior on the sizing of a microgrid have not yet been portrayed in the literature.
- There is a lack in the literature of modeling that addresses specific energy demand such as heating for food and the best allocation of sources at a community level considering their environmental impact in Brazil.
- The adoption of other policies to encourage renewable energy in Brazil can enable the increase of distributed generation in the country and the use of potential renewable sources.

In the next chapter, the optimization problem for designing a microgrid will be formulated in order to address some of the gaps found in the literature. In addition, several scenarios will be analyzed in order to verify the applicability of the proposed model.

CHAPTER III- Formulation of the Optimization Problem

III.1. Introduction

The state-of-the-art review exposed in the previous chapter raised some points that have been either hardly explored in the literature or not yet addressed. The model formulation proposed in the present work sought to address some of these gaps in the literature, more specifically, the following points:

- Adopt the clustering procedure for systematic time period determination in the model, considering seasonal and hourly distributions in order to determine the impact on the design of the microgrid;
- Consider time-dependent profile for efficiencies of renewable resources that are subject to weather conditions, such as photovoltaic panels, solar collectors, and wind turbines in order to determine the impact on the design of the microgrid;
- Given the potential of biogas as a renewable energy source to meet energy demands, its underutilization both in Brazil and globally, and the limited research into optimal microgrid configurations, there is a need to investigate the feasibility of implementing biogas in microgrids. Such an investigation could help identifying the best configuration for a microgrid (e.g. to determine the amount of organic material needed to meet the gas demand for cooking food, heating water and generating electricity), and thus help promote the use of this renewable energy source;
- Select the best renewable energy incentive policy among the main and well consolidated ones currently adopted in the market for self-consumption generation, namely Feed in Tariff, Net Metering for electric energy;
- Consider eleven (11) different technologies to meet the demand for electricity, air cooling, food heating, and water heating.

This chapter aims to present the definition of the optimization problem that will be solved, as well as its modeling. To do this, first the entire system configuration will be detailed, with its respective resources used. Next, the methods for dividing the time

periods of the problem are presented. Finally, the equations (objective function and constraints) involved in the model will be presented.

III.2. Problem Definition

The model considers the demands for electricity, hot water, cooking gas and cooling air in each household and aims to find the best combination of distributed renewable resources as well as their sizing for a set of houses. As a way to illustrate the problem, Figure 37 represents a case study with 3 houses, although the proposed model can be applied to a greater number of houses. The technologies that can be installed in the system are listed in Table 15, along with the legend of the symbols and connections expressed in Figure 37. The sharing of hot water between the houses is illustrated with the blue line, the sharing of electricity between the houses is illustrated with the black line, and the transfer of biogas from the biodigester to the houses is illustrated by the yellow line.

The electricity demand can be met by wind, photovoltaic, biogas, or purchased from the central grid. The electricity generated from renewable resources can be used for self-consumption, transferred to another household, fed into the central grid or stored in electric batteries.

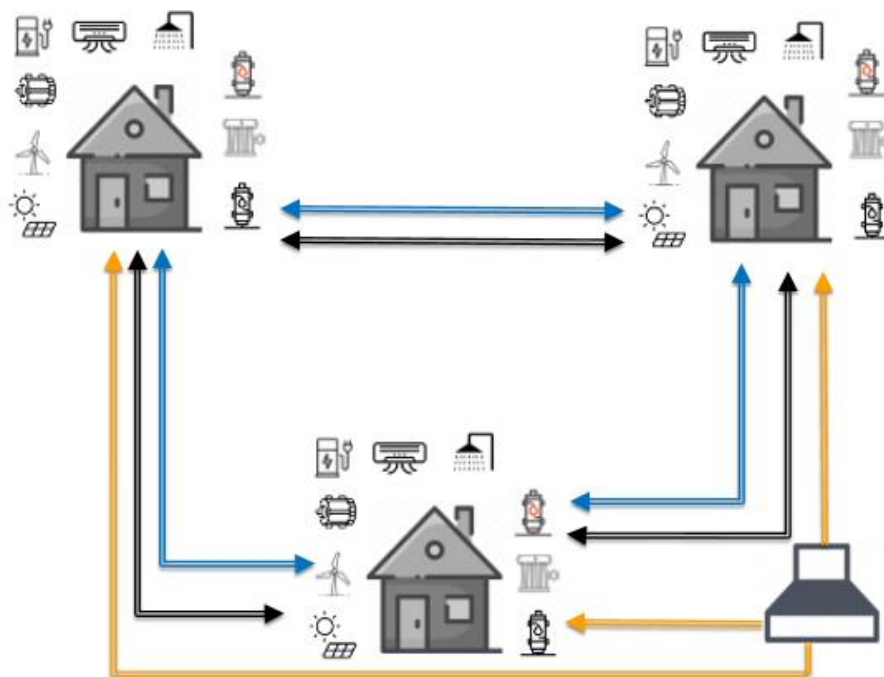







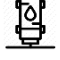







Figure 37 – General sketch of all technologies considered in the microgrid.

Table 15 – Technologies adopted in the optimization problem.

Tecnology	Abbreviation	Symbol	Demand	Connection
Photovoltaic panel	PV		Electricity	
Wind Turbine	WT			
Biogas generator	BG			
Battery	BT			
Electric Shower	ES		Hot water	
Gas Heater	GH			
Biogas Heater	BH			
Solar Collector/Thermal Storage	SC/TS			
Biodigester	BD		Gas for cooking, hot water, electricity	
Air conditioning	AC		Cooling air	not connected

To meet the hot water demand of the houses, an electric shower, biogas heater, solar collector or gas heater can be installed. The combination of installing these technologies in each house will be discussed in the constraints section. Because the electric shower, biogas heater and gas heater generate hot water at the moment of consumption, the storage of thermal energy by these technologies is not necessary. On the other hand, the solar collector depends on the solar irradiation and this in turn varies throughout the day; therefore, storage of hot water must be considered. The hot water supply is exemplified in Figure 38. Hot water can be transferred to another house to supply microgrid demand or used for self-consumption. The installation of an electric shower at home limits the usage to this particular technology, owing to its distinct operational needs. However, a biogas or gas heater can be used alongside a solar collector. The solar collector has the added advantage of storing hot water, which can also be shared with other houses in the micro-grid once the demand of the original house has been met.

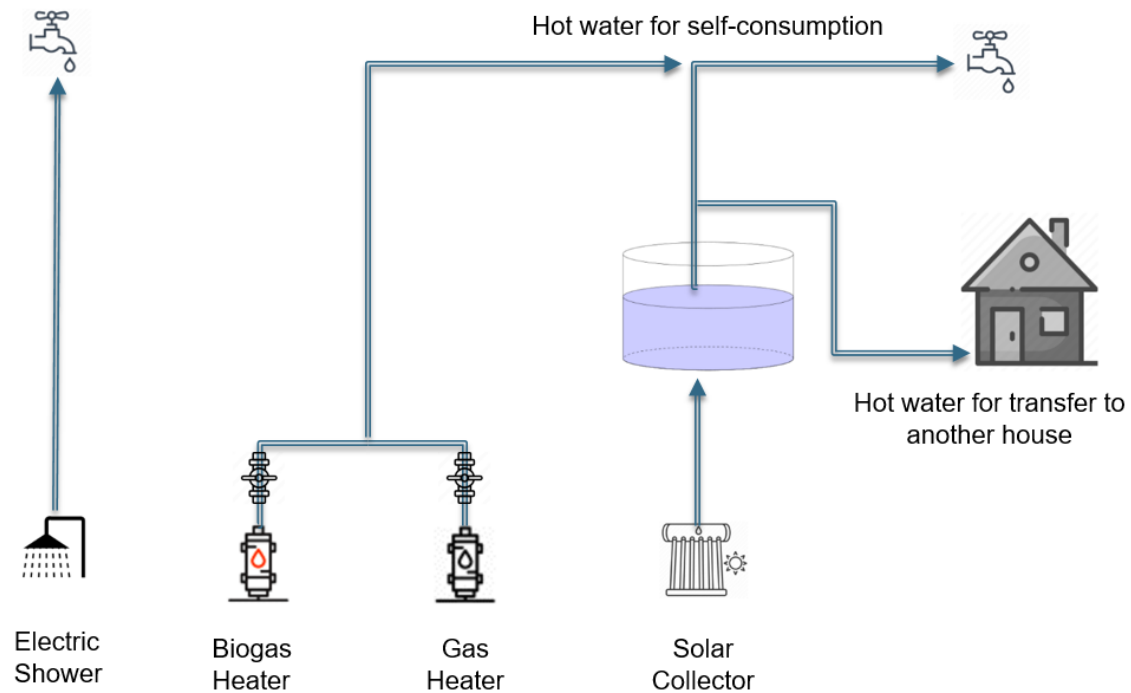


Figure 38 - Operation scheme for hot water generation in each residence.

The demand for cooking gas can be supplied by natural gas from the network or by biogas produced in a biodigester. Due to space limitations and in order to avoid unpleasant odors when installed inside the residences, the installation of a central biodigester was considered to serve the group of houses, which may or may not be installed in the micro-grid. This biodigester is connected to all the houses for the collection of organic material. However, the connection for the transportation of biogas between the biodigester and the residence is according to the demand of each residence. In addition, there is the possibility of purchasing extra organic material for use in the biodigester.

III.3. Splitting the Time Horizon

The microgrid is operated with an annual time horizon, considering months, days and hours of operation, as expressed in Figure 39. In order to characterize the consumption profile and keep the complexity of the model reasonable, and since each technology operates at distinct times, the year is divided into seasons, which comprehends a number of months (m). In each season, the months have a certain number of days, calculated by the average number of days in each month that makes up the season. The day, as far as it is concerned, is divided into periods of hours (p). Figure 40 illustrates the time horizon splitting.

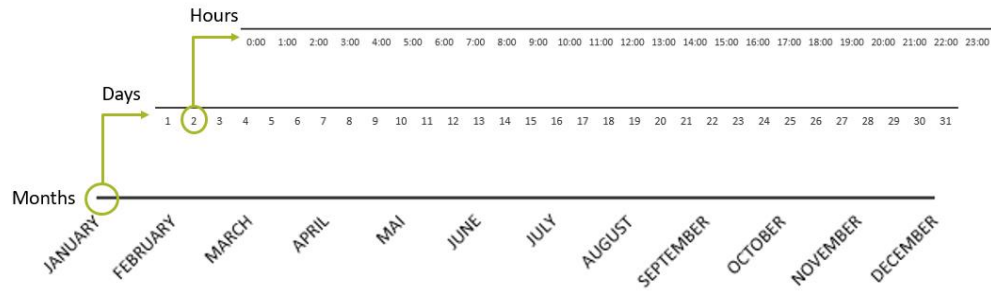


Figure 39 - The annual time horizon for operating the microgrid

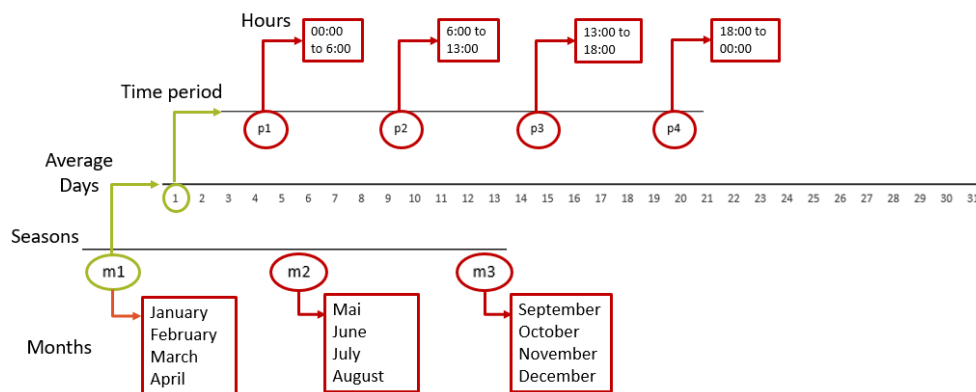


Figure 40 - The time horizon for operating the microgrid divided into seasons(m) and periods (p)

The electricity load data is illustrated in Figure 41 without time division. Periods in different months overlap, making it difficult to characterize the system. In the present work, two methods are proposed to split the time horizon: an empirical method and the clustering method. The electricity generation is responsible for the largest energy contribution in the system, in detriment of hot water, cooking gas and air cooling. In order to better characterize the time horizon, data on solar irradiation and wind speed were used since these data are essential to determine solar and wind power generation, respectively. In addition, the electricity load data and the price of electricity was considered, as it varies during the day.

This approach differs from the literature on the following points:

- Two-step clustering method for time horizon division: The proposed clustering method for energy system optimization involves a two-step process, where the first step partitions seasons and the second step identifies hourly periods. This approach aims to improve design accuracy and characterization of the system.
- Microgrid configuration: The proposed analysis also takes into account the overall system configuration. This includes an analysis of how the time period splitting clustering method impacts the capacity of the renewable energy sources, the energy storage capacity, and the layout of the microgrid.

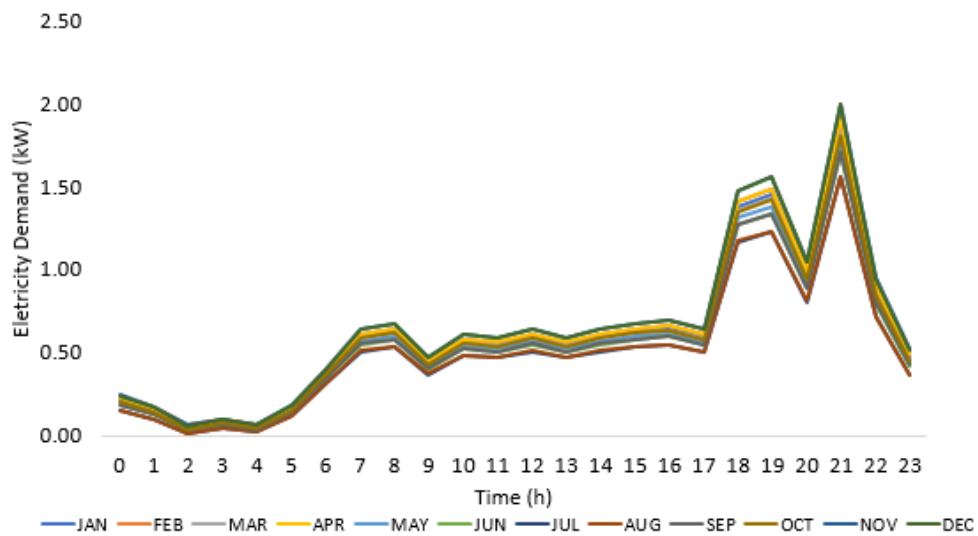


Figure 41 - Profile of the electricity demand before time division.

III.3.1. Empirical Method

The empirical method is based on system observation and manual selection. To determine each period, the temporal profiles of electric demand, electric energy prices and environmental data (wind speed and solar irradiation) are analyzed. The months belonging to a season were set according to the behavior of the environmental data. To set the number of days in a month of each season, the average of days in the months that make up the season was taken. The day was divided into periods of hours by identifying similar behavior in the electricity prices and demand profiles.

This method presents some limitations. As the analysis is done manually based on profiles visualization, some pattern that would impact the results might be overlooked, especially when analyzing more than two graphs simultaneously. In addition, because the method also depends on the previous knowledge of the evaluator on the region under study, the determination of the time periods may vary from evaluator to evaluator, resulting in poor repeatability and reproduction of results. To avoid these drawbacks, a systematic computational method, the clustering method, was used.

III.3.2. Clustering Method

The clustering method is proposed as a systematic tool to define the time periods discretization in the model. It identifies, using computational tools, patterns in the data series, in which there is a grouping of data that resemble each other into a cluster. Among

the several techniques available for clustering, the most widely used is the K-means method (YSE, 2019).

The K-means method assigns a centroid to each cluster that corresponds to the arithmetic mean of the data points. The algorithm then works iteratively so that each point is closer to the centroid of its cluster than to the other clusters, in order to minimize the intra-cluster distance in each interaction. The number of clusters is given by the user and then the arrangement of the data into that number of clusters is done (YSE, 2019). Figure 42 shows what happens after K-means is applied to a data set. The data that was part of a single set is separated and grouped into small sets, according to the similarity between them.

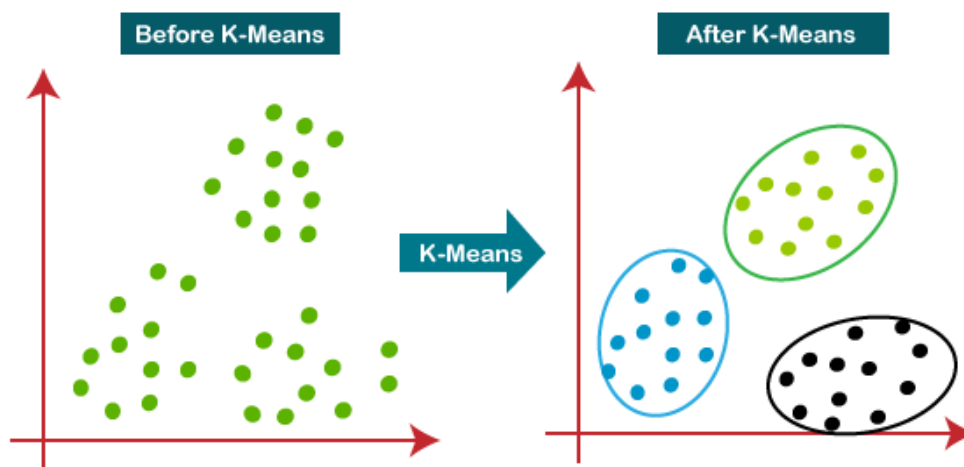


Figure 42- K-means method to cluster the data set. Source: Sharma (2022).

To define the best cluster number in the dataset, the Elbow method is usually used. This approach tests different numbers of clusters by measuring the resulting squared sum of the distance between the centroid and each cluster member, where the centroid is the center of a given cluster. The optimal cluster number is the "elbow point", i.e., the point where the sum of squared distance decreases asymptotically with the number of clusters, as illustrated in Figure 43. For a cluster number greater than 3, as represented in the Figure 43, the gradient of the sum of the squared distance is nearly zero; therefore, that point is chosen as the best cluster number for this data set.

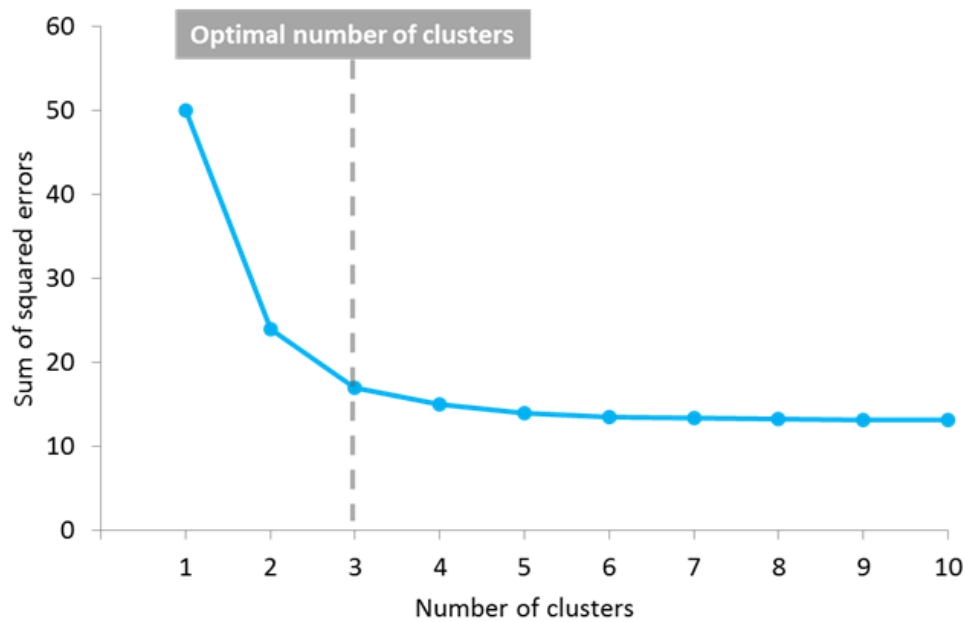


Figure 43 - Exemplification of the elbow method. Source: Yse (2019).

The algorithm in Figure 44 was used to divide the time horizon into seasons and periods. As the model was constituted in terms of months and hours, two clustering processes were performed, the first for the classification of months and the second for the hours of the day. Because the original data series is represented in different dimensions and units (electricity demand, environmental data and prices), the data was normalized. The optimal number of clusters was also adjusted considering that the time periods are consecutive, for example, period p1 corresponds to 00:00 to 12:00, period p2 corresponds to 12:00 to 18:00, and period p3 corresponds to 18:00 to 00:00. In addition, considering that the electric power taxation of the central grid varies throughout the day and, therefore, can influence the behavior and cost of the system, the hourly energy tariff data were included to define the time period for the model.

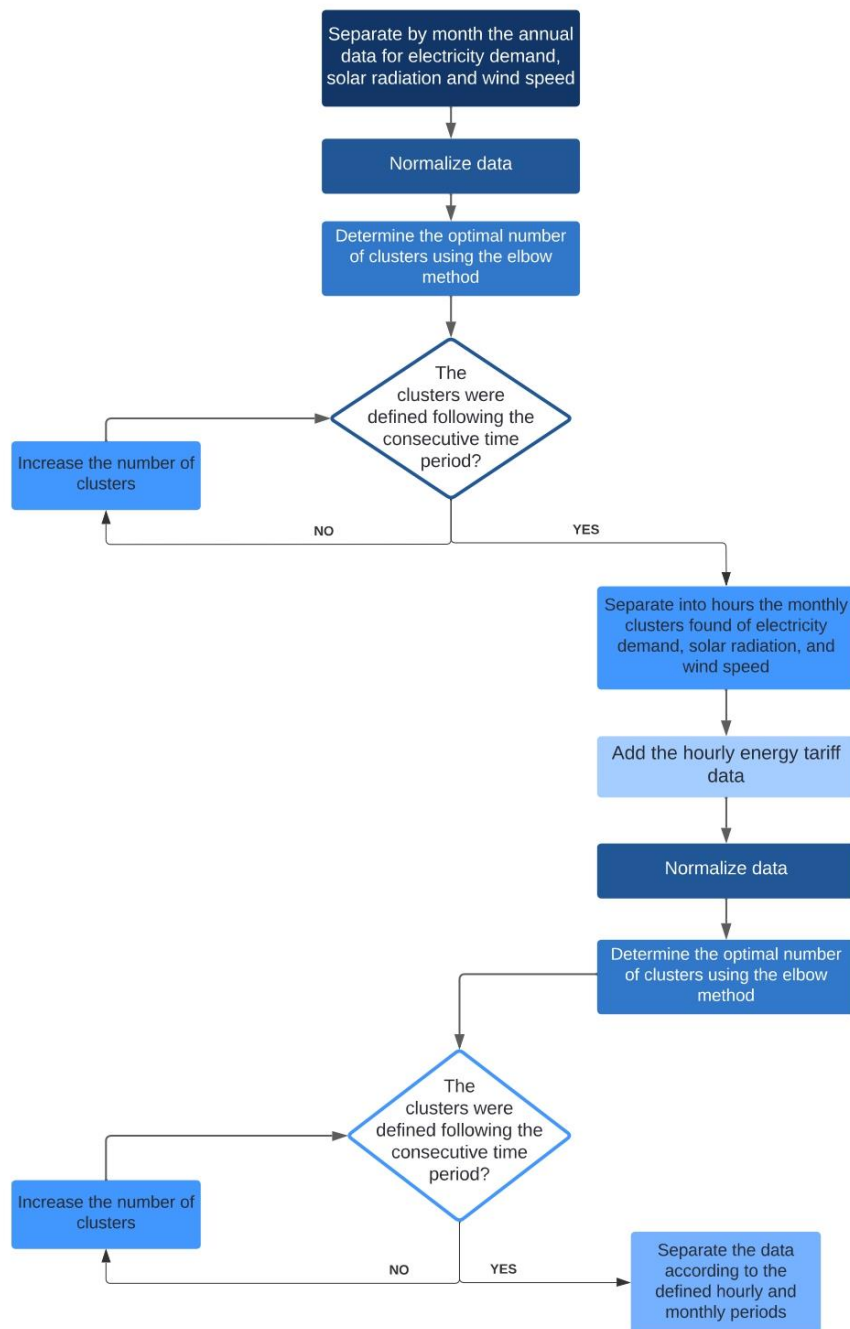


Figure 44 – Algorithm for the clustering process to split the time horizon.

The k-means technique was implemented in the Python language and developed using the *pandas*, *numpy* and *matplotlib* libraries (ROSSUM, DRAKE JR., 1995). The *pandas* library is mainly used for data manipulation and analysis and was used to read the data. The *numpy* library supports the processing of multi-dimensional arrangements and matrices which was used to apply the method and process more than two variables at the same time. The *matplotlib* library is used for data visualization and graph generation. The code used to define the time periods for each scenario for the case study are presented in Appendix B.

III.4. Optimization problem formulation

This section presents the objective function, detailing all its terms, followed by the energy balances for all demands (electricity, cooling air, hot water, cooking gas). Finally, the operational, design and capacity constraints for each technology used are described. The overview of variables and parameters can be found in Appendix E.

III.4.1. Objective Function

The objective function to be minimized is given by the total annual investment and annual operation cost, adapted from Sidnell et al. (2021a) (R\$):

$$C_{TOTAL} = C_{INV} + C_{OM} + C_{BUY}^{GRID} + C^{NG} + C^{ENV} - NEM - FIT \quad (1)$$

where C_{INV} is the total investment, C_{OM} is the operating and maintenance cost, C_{BUY}^{GRID} is the total cost of electricity purchased from the grid, C^{NG} is the cost to purchase natural gas from the grid, C^{ENV} is the the environmental costs, NEM is the credit revenue obtained by using the Net Metering policy, FIT is the amount received for adopting Feed in Tariff.

a. Investment

The investment is the sum of all the capital costs invested to acquire each technology:

$$C_{INV} = C_{INV}^{PV} + C_{INV}^{BG} + C_{INV}^{WT} + C_{INV}^{BD} + C_{INV}^{PPBD} + C_{INV}^{BT} + C_{INV}^{MG} + C_{INV}^{EL} + C_{INV}^{PP} + C_{INV}^{SC} + C_{INV}^{TS} + C_{INV}^{GH} + C_{INV}^{BH} + C_{INV}^{ES} + C_{INV}^{AC} \quad (2)$$

where C_{INV}^{PV} is the investment cost of photovoltaic panel (R\$), C_{INV}^{BG} the investment cost of biogas electric generator (R\$), C_{INV}^{WT} the investment cost of wind turbine (R\$), C_{INV}^{BD} the investment cost of biodigester (R\$), C_{INV}^{PPBD} the investment cost of biodigester pipeline (R\$), C_{INV}^{BT} the investment cost of battery (R\$), C_{INV}^{MG} the investment cost of microgrid (R\$), C_{INV}^{EL} the investment cost of electricity line (R\$), C_{INV}^{PP} the investment cost of hot water pipeline (R\$), C_{INV}^{SC} the investment cost of solar collector (R\$), C_{INV}^{TS} the investment cost of thermal storage (R\$), C_{INV}^{GH} the investment cost of gas heater (R\$), C_{INV}^{BH} the investment cost of biogas heater (R\$), C_{INV}^{ES} the investment cost of electric shower (R\$), C_{INV}^{AC} the investment cost of air conditioning (R\$). The total investment per each technology is given in the following paragraphs.

The Capital Recovery Factor (CRF) is a financial measurement utilized to calculate the yearly installment required to pay back a loan over a specific duration, expressed as:

$$CRF = \frac{r \cdot (1 + r)^n}{(1 + r)^n - 1} \quad (3)$$

and refers to the portion corresponding to the investment at the interest rate (r) to be paid during n period in years.

- Photovoltaic panel

The annual investment of the photovoltaic panel depends on the area of the photovoltaic panel installed at house i (A_i^{PV} , m²), the nominal capacity of the photovoltaic panel (Cn^{PV} , kWp/m²), the capital cost of the photovoltaic panel (C_c^{PV} , R\$/kW), and the Capital Recovery Factor (CRF), according to:

$$C_{INV}^{PV} = Cn^{PV} \cdot C_c^{PV} \cdot CRF \cdot \sum_i A_i^{PV} \quad (4)$$

- Biogas electric generator

The annual investment of the biogas generator depends on the capital cost of the biogas generator (C_c^{BG} , R\$/kW), the power of the biogas generator installed at each house i (k_i^{BG} , kW) and the CRF :

$$C_{INV}^{BG} = C_c^{BG} \cdot CRF \cdot \sum_i k_i^{BG} \quad (5)$$

- Wind turbine

The annual investment of the wind turbine depends on wind turbine area installed at each house i (A_i^{WT} , m²), the rated capacity of the wind turbine (kr^{WT} , kW/m²), the capital cost of the wind turbine (C_c^{WT} , R\$/kW) and the CRF .

$$C_{INV}^{WT} = C_c^{WT} \cdot kr^{WT} \cdot CRF \cdot \sum_i A_i^{WT} \quad (6)$$

- Biodigester

The annual investment of the biodigester depends on the capital cost of the biodigester (C_c^{BD} , R\$/m³), the biodigester volume (V^{BD} , m³) and the CRF . The equation is multiplied by the binary Y^{BD} because the cost is only considered when the biodigester is installed:

$$C_{INV}^{BD} = C_c^{BD} \cdot V^{BD} \cdot CRF \cdot Y^{BD} \quad (7)$$

- Biodigester pipeline

The investment of the pipeline to collect the organic material from the houses to the biodigester and to distribute the biogas from the biodigester to the houses, depends on the capital cost of a pipeline to distribute the biogas (C_c^{PPBio} , R\$/m), the distance from

the biodigester to the houses (l_{bio_i} , m) and the capital cost of a pipeline to collect the organic material from the houses (C_c^{PPOW} , R\$/m):

$$C_{INV}^{PPBD} = C_c^{PPBio} \cdot Y_i^{PPBio} \cdot \sum_i (l_{bio_i}) + C_c^{PPOW} \cdot Y^{BD} \cdot \sum_i (l_{bio_i}) \quad (8)$$

where Y_i^{PPBio} is the binary variable that expresses whether or not the biogas pipeline exists between house i and the biodigester and Y^{BD} is whether or not the biodigester exists. The cost of the biogas pipeline from the biodigester to house i only exists when the corresponding pipeline is installed, therefore the binary variable Y_i^{PPBio} is used. Regarding the piping of organic material, all the houses are connected to the biodigester if it is installed. Hence, the binary variable Y^{BD} is used to include the cost of the organic material pipeline when the biodigester is installed.

- Battery for electrical energy storage

The annual investment of the battery depends on the capital cost of the battery (C_c^{BT} , R\$/kW), the capacity of the battery installed at house i (k_i^{BT} , kW), the capital cost of the charge controller per battery ($C_c^{CONTROLLER,BT}$, R\$), which is considered only if the battery is installed (Y_i^{BT}) and the CRF :

$$C_{INV}^{BT} = \left(C_c^{BT} \cdot \sum_i k_i^{BT} + C_c^{CONTROLLER,BT} \cdot \sum_i Y_i^{BT} \right) \cdot CRF \quad (9)$$

- Microgrid

The annual investment of the microgrid depends on the capital cost of microgrid central controller (C_c^{CC} , R\$), whether or not the microgrid exists (Z), i.e., if there is sharing of electricity between the houses and the CRF :

$$C_{INV}^{MG} = C_c^{CC} \cdot Z \cdot CRF \quad (10)$$

- Electricity line

The annual investment of the cables to transmit the electricity produced from house i to house j depends on the capital cost of the electricity line (C_c^{EL} , R\$/m), the distance between the houses ($l_{i,j}$, m), if there is a connection between house i and house j ($Y_{i,j}^{MG}$) and the CRF :

$$C_{INV}^{EL} = C_c^{EL} \cdot CRF \cdot \sum_{i,j} (Y_{i,j}^{MG} \cdot l_{i,j}) \quad (11)$$

- Hot water pipeline

The annual investment of the pipeline to transmit the hot water from house i to house j depends on the capital cost of the pipeline (C_c^{PP} , R\$/m), the distance between houses ($l_{i,j}$, m), if there is a connection between house i and house j ($Y_{i,j}^{PP}$) and the CRF :

$$C_{INV}^{PP} = C_c^{PP} \cdot CRF \cdot \sum_{i,j} (Y_{i,j}^{PP} \cdot l_{i,j}) \quad (12)$$

- Solar collector for hot water production

The annual investment of the solar collector depends on the rated capacity of the solar collector (Cn^{SC} , kWp/m²), the capital cost of the solar collector (C_c^{SC} , R\$/kW), the CRF and the area of the solar collector installed at house each house i :

$$C_{INV}^{SC} = Cn^{SC} \cdot C_c^{SC} \cdot CRF \sum_i A_i^{SC} \quad (13)$$

- Thermal storage of hot water

The annual investment of the thermal storage depends on the amount of hot water produced for storage in each house i (k_i^{ST} , L/h), the capital cost of the storage tank (C_c^{TS} , R\$/L/h) and the CRF :

$$C_{INV}^{TS} = C_c^{TS} \cdot CRF \cdot \sum_i k_i^{TS} \quad (14)$$

- Natural gas heater for hot water production

The annual investment of the gas heater depends on the capital cost of the gas heater installed at each house i (C_c^{GH} , R\$/L/h), the capacity of the gas heater (k_i^{GH} , L/h) and the CRF :

$$C_{INV}^{GH} = C_c^{GH} \cdot CRF \cdot \sum_i k_i^{GH} \quad (15)$$

- Biogas heater for hot water production

The annual investment of the biogas heater depends on the capital cost of the biogas heater (C_c^{BH} , R\$/L/h), the capacity of the biogas heater installed at each house i (k_i^{BH}) (L/h) and the CRF :

$$C_{INV}^{BH} = C_c^{BH} \cdot CRF \cdot \sum_i k_i^{BH} \quad (16)$$

- Electric shower for hot water production

The annual investment of the electric shower depends on the capital cost of the electric shower (C_c^{ES} , R\$/kW), the capacity of the electric shower installed at each house i (k_i^{ES} , kW) and the CRF :

$$C_{INV}^{ES} = C_c^{ES} \cdot CRF \cdot \sum_i k_i^{ES} \quad (17)$$

- Air conditioning:

The annual investment of the air conditioning depends on the capital cost of the air conditioning (C_c^{AC} , R\$/kW), the capacity of the air conditioning installed at each house (k_i^{AC} , kW) and the CRF :

$$C_{INV}^{AC} = C_c^{AC} \cdot CRF \cdot \sum_i k_i^{AC} \quad (18)$$

b. Operation and maintenance (O&M) cost

The fixed and variable costs of operating and maintaining the system technologies are given by:

$$C_{OM} = C_{OM}^{PV} + C_{OM}^{BG} + C_{OM}^{WT} + C_{OM}^{BT} + C_{OM}^{BD} + C_{OM}^{PPBD} + C_{OM}^{MG} + C_{OM}^{TS} + C_{OM}^{SC} + C_{OM}^{GH} + C_{OM}^{BH} + C_{OM}^{ES} + C_{OM}^{AC} \quad (19)$$

where C_{OM}^{PV} is the O&M cost of photovoltaic panel (R\$), C_{OM}^{BG} the O&M cost biogas electric generator (R\$), C_{OM}^{WT} the O&M cost wind turbine (R\$), C_{OM}^{BD} the O&M cost biodigester (R\$), C_{OM}^{PPBD} O&M cost of biodigester pipeline (R\$), C_{OM}^{BT} the O&M cost of battery (R\$), C_{OM}^{MG} the O&M cost of microgrid (R\$), C_{OM}^{SC} the O&M cost of solar collector (R\$), C_{OM}^{TS} the O&M cost of thermal storage (R\$), C_{OM}^{GH} the O&M cost of gas heater (R\$), C_{OM}^{BH} the O&M cost of biogas heater (R\$), C_{OM}^{ES} the O&M cost of electric shower (R\$), C_{OM}^{AC} the O&M cost of air conditioning (R\$). The O&M cost is composed of fixed and variable operation and maintenance costs given by the nominal equipment capacity and operating cost, as detailed below for each technology (SIDNELL et al., 2021a):

- Photovoltaic panel

The operation and maintenance cost of the photovoltaic panels is given by:

$$C_{OM}^{PV} = C_{OMFix}^{PV} \cdot Cn^{PV} \cdot \sum_i A_i^{PV} + C_{OMVar}^{PV} \cdot \left(\sum_{i,m,p} (E_{i,m,p}^{SELF,PV} + E_{i,m,p}^{SALE,PV} + \sum_{j(j \neq i)} E_{i,j,m,p}^{TRANSFER,PV} + E_{i,m,p}^{STORAGE,PV}) \cdot day_m \cdot hours_p \cdot season_m \right) \quad (20)$$

where C_{OMFix}^{PV} is the fixed operational and maintenance cost of photovoltaic panel (R\$/kWp), Cn^{PV} is the nominal capacity of the photovoltaic unit (kWp/m²), A_i^{PV} is the area of the photovoltaic panel installed at house i , C_{OMVar}^{PV} is the variable operational and maintenance cost (R\$/kWh), $E_{i,m,p}^{SELF,PV}$ is the energy produced for self-consumption (kW) by house i during season m at time period p , $E_{i,m,p}^{SALE,PV}$ is the energy inserted into the central grid (kW), $E_{i,j,m,p}^{TRANSFER,PV}$ is the energy transferred from house i to all other houses j (kW) and $E_{i,m,p}^{STORAGE,PV}$ is the energy storage (kW). In order to find the annual variable cost, the total energy produced is multiplied by the number of months in each season m , number of days in season m and the total of hours within time period p .

- Biogas electric generator

The operation and maintenance cost of the biogas electric generator is given by:

$$C_{OM}^{BG} = C_{OMVar}^{BG} \cdot \sum_{i,m,p} (E_{i,m,p}^{SELF,BG} + E_{i,m,p}^{SALE,BG} + \sum_{j(j \neq i)} E_{i,j,m,p}^{TRANSFER,BG} + E_{i,m,p}^{STORAGE,BG}) \cdot day_m \cdot hours_p \cdot season_m + C_{OMFix}^{BG} \cdot \sum_i k_i^{BG} \quad (21)$$

where C_{OMFix}^{BG} is the fixed operation and maintenance cost of photovoltaic panel (R\$/kW), k_i^{BG} is the capacity of the biogas generator installed at house i , C_{OMVar}^{BG} is the variable operation and maintenance cost (R\$/kWh), $E_{i,m,p}^{SELF,BG}$ is the energy produced for self-consumption (kWh), $E_{i,m,p}^{SALE,BG}$ is the energy inserted into the central grid (kWh), $E_{i,j,m,p}^{TRANSFER,BG}$ is the energy transferred from house i to all other houses and $E_{i,m,p}^{STORAGE,BG}$ is the energy stored in house i . In order to find the annual variable cost, the total energy produced is multiplied by the number of months in each season m , number of days in season m and the total of hours within time period p .

- Wind turbine

The operation and maintenance cost of the wind turbine is given by:

$$C_{OM}^{WT} = C_{OMVar}^{WT} \cdot \sum_{i,m,p} (E_{i,m,p}^{SELF,WT} + E_{i,m,p}^{SALE,WT} + \sum_{j(j \neq i)} E_{i,j,m,p}^{TRANSFER,WT} + E_{i,m,p}^{STORAGE,WT}) \cdot day_m \cdot hours_p \cdot season_m + \sum_i A_i^{WT} \cdot kr^{WT} \cdot C_{OMFix}^{WT} \quad (22)$$

where C_{OMVar}^{WT} is the variable maintenance and operation cost (R\$/kWh), which is multiplied by the sum of energy for self-consumption ($E_{i,m,p}^{SELF,WT}$), for insertion into the

central grid ($E_{i,m,p}^{SALE,WT}$), for transfer with other houses ($E_{i,j,m,p}^{TRANSFER,WT}$) and for storage ($E_{i,m,p}^{STORAGE,WT}$). In order to find the variable cost per year, this sum is multiplied by the number of seasons, days in a season and the hours during a day. In addition, the operation and maintenance cost are composed of the fixed cost of operation and maintenance of wind turbine (C_{OMFix}^{WT} , R\$/kW), multiplied by the nominal capacity of the wind turbine unit and the area.

- Biodigester

As previously mentioned, the production of biogas depends on the organic material collected from the houses and, if necessary, an extra amount of residual biomass can be purchased. The organic material (Qow_i , kg) can be bought by each house from companies, so the value considered consists of the price of the organic material plus the cost of transportation to the biodigester (P^{OW} , R\$/kg). In addition, there is the cost of operating the biodigester. Therefore, the operation and maintenance cost of biodigester is given by:

$$C_{OM}^{BT} = C_{OMVar}^{BT} \cdot \sum_{i,m,p} E_{i,m,p}^{STORAGE IN,BT} \cdot day_m \cdot hours_p \cdot season_m \quad (23)$$

which depends on the fixed cost of operation and maintenance of the biodigester (C_{OMFix}^{BD} , R\$/year) and whether or not the biodigester is installed (Y^{BD}).

- Pipeline of the biodigester

The operation and maintenance cost of the piping to collect the organic material from the houses to the biodigester and to distribute the biogas from the biodigester to the houses is given by:

$$C_{OM}^{PPBD} = C_{OMFix}^{PPBD} \cdot Y_i^{PPBIO} \cdot \sum_i lbio_i + C_{OMFix}^{PPOW} \cdot Y^{BD} \cdot \sum_i lbio_i \quad (24)$$

which depends on the fixed O&M cost of a pipeline to distribute the biogas (C_{OMFix}^{PPBD} , R\$/m), the distance from the biodigester to house i ($lbio_i$, m) and whether or not the pipeline to house i is installed (Y_i^{PPBIO}), the fixed O&M cost of a pipeline to collect the organic material from the houses (C_{OMFix}^{PPOW} , R\$/m) and whether or not the biodigester is installed (Y^{BD}).

- Battery for electrical energy storage

The O&M cost of the battery is given by:

$$C_{OM}^{BT} = C_{OMVar}^{BT} \cdot day(m) \cdot hours(p) \cdot season(m) \cdot \sum_{i,m,p} E_{i,m,p}^{STORAGE IN,BT} \quad (25)$$

which is composed of the variable operation and maintenance cost (C_{OMVar}^{BT} , R\$/kWh) multiplied by the amount of energy going into storage ($E_{i,m,p}^{STORAGE IN,BT}$). In order to find the variable cost per year, this is multiplied by the number of days, the period in hours and the number of seasons.

- Microgrid

The operation and maintenance cost of the microgrid is composed of fixed operation and maintenance cost of the microgrid central controller (C_{OMFix}^{MG} , R\$), which can only exist if the microgrid has been installed, according to:

$$C_{OM}^{MG} = C_{OMFix}^{MG} \cdot Z \quad (26)$$

where Z is a binary variable which indicates if the microgrid exists.

- Solar collector for hot water production

The operation and maintenance cost of the solar collector is given by:

$$C_{OM}^{SC} = k^{SC} \cdot C_{OMFix}^{SC} \cdot \sum_i A_i^{SC} \quad (27)$$

which is composed of the fixed operation and maintenance cost of the solar collector (C_{OMFix}^{SC} , R\$/kW), the nominal capacity of the solar collector (k^{SC} , kWp/m²) and the total area.

- Thermal storage of hot water

The operation and maintenance cost of thermal storage (C_{OM}^{TS}) is given by:

$$C_{OM}^{TS} = C_{OMVar}^{TS} \cdot \sum_{i,m,p} HW_{i,m,p}^{STORAGE,SC} \cdot day_m \cdot hours_p \cdot season_m \quad (28)$$

which depends on the variable thermal storage operation and maintenance cost (C_{OMVar}^{TS} , R\$/L/h), together with the amount of hot water for storage in house i coming from the solar collector ($HW_{i,m,p}^{STORAGE,SC}$, L/h). In order to find the variable cost per year, this is multiplied by the number of days, the period in hours and the number of seasons of operation.

- Natural gas heater for hot water production

The operation and maintenance cost of the gas heater is given by:

$$C_{OM}^{GH} = C_{OMVar}^{GH} \cdot \sum_{i,m,p} HW_{i,m,p}^{SELF,GH} \cdot day_m \cdot hours_p \cdot season_m + \sum_i k_i^{GH} \cdot C_{OMFix}^{GH} \quad (29)$$

which depends on the variable O&M cost (C_{OMVar}^{GH} , R\$/L/h), and the amount of hot water produced for self-consumption ($HW_{i,m,p}^{SELF,GH}$). In order to find the variable cost per year, this cost is multiplied by the number of days, the period in hours and the number of seasons of operation. In addition, the operation and maintenance cost are composed of the fixed O&M cost (C_{OMFix}^{GH} , R\$/L/h), and the capacity of the gas heater (k_i^{GH} , L/h).

- Biogas heater for hot water production

The operation and maintenance cost of the biogas heater is given by:

$$C_{OM}^{BH} = C_{OMVar}^{BH} \cdot \sum_{i,m,p} HW_{i,m,p}^{SELF,BH} \cdot day_m \cdot hours_p \cdot season_m + \sum_i k_i^{BH} \cdot C_{OMFix}^{BH} \quad (30)$$

which is composed of the variable O&M cost (C_{OMVar}^{BH} , R\$/L), the amount of hot water produced in house i for self-consumption ($HW_{i,m,p}^{SELF,BH}$). In order to find the variable cost per year, this cost is multiplied by the number of days, the period in hours and the number of seasons of operation. In addition, the operation and maintenance cost are composed of the fixed O&M cost (C_{OMFix}^{BH} , R\$/L) and the capacity of biogas heater (k_i^{BH} , L/h).

- Electric Shower for hot water production

The operation and maintenance cost of electric shower is given by:

$$C_{OM}^{ES} = C_{OMVar}^{ES} \cdot \sum_{i,m,p} HW_{i,m,p}^{SELF,ES} \cdot day_m \cdot hours_p \cdot season_m + \sum_i k_i^{ES} \cdot C_{OMFix}^{ES} \quad (31)$$

which is composed of the variable operation and maintenance cost (C_{OMVar}^{ES} , R\$/L/h), and the amount of hot water produced in house i by the electric shower ($HW_{i,m,p}^{SELF,ES}$). In order to find the variable cost per year, this term multiplies the number of days, the period in hours and the number of seasons of operation. In addition, the operation and maintenance cost is composed of the fixed cost of operation and maintenance (C_{OMFix}^{ES} , R\$/kW), and the capacity of the electric shower (k_i^{ES} , kW).

- Air conditioning

The operation and maintenance cost of air conditioning is given by:

$$C_{OM}^{AC} = C_{OMVar}^{AC} \cdot \sum_{i,m,p} E_{i,m,p}^{AC} \cdot day_m \cdot hours_p \cdot season_m \quad (32)$$

which is composed of the variable operation and maintenance cost (C_{OMVar}^{AC} , R\$/kW), multiplied by the amount of air cooling produced ($E_{i,m,p}^{AC}$, kW). In order to find the variable cost per year, it multiplies the number of days, the period in hours and the number of stations of operation.

c. Environmental Cost

The cost of taxing emissions will depend on the GHG reduction responsibility of each country. The environmental costs are given by the sum of the carbon emission costs of each technology (SIDNELL et al., 2021a):

$$C^{ENV} = CO_2^{GRID} + CO_2^{NG} + CO_2^{WT} + CO_2^{PV} + CO_2^{SC} + CO_2^{BIO} \quad (33)$$

The environmental costs for each energy resource are calculated as following.

- Grid

The carbon cost for energy from the central grid is given by:

$$CO_2^{GRID} = CT \cdot CI^{GRID} \cdot \sum_{i,m,p} E_{i,m,p}^{GRID} \cdot day_m \cdot hours_p \cdot season_m \quad (34)$$

It depends on carbon intensity of electricity from the grid (CI^{GRID} , kg CO₂/kWh), the energy consumed from the central grid ($E_{i,m,p}^{GRID}$), the carbon tax (CT , R\$/ kg CO₂) and the number of days, hours and seasons when this energy is consumed.

- Natural gas

The carbon cost for natural gas from the grid is given by:

$$CO_2^{NG} = CT \cdot CI^{GN} \cdot \sum_{i,m,p} Use_{i,m,p}^{NG} \cdot day_m \cdot hours_p \cdot season_m \quad (35)$$

It depends on the carbon intensity of natural gas (CI^{NG} , kg CO₂/kWh), the carbon tax (CT , R\$/kg CO₂), the number of days, hours and seasons when this gas was consumed and the amount of natural gas consumed from the grid ($Use_{i,m,p}^{NG}$, kW), which will be determined in the session III.4.7.

- Wind

The carbon cost for wind energy is given by:

$$CO_2^{WT} = CT \cdot CI^{WT} \cdot \sum_{i,m,p} E_{i,m,p}^{WT} \cdot day_m \cdot hours_p \cdot season_m \quad (36)$$

It depends on the carbon intensity of wind turbine (CI^{WT} , kg CO₂/kWh), the energy generated by wind turbine ($E_{i,m,p}^{WT}$). In addition, it is considered the carbon tax (CT , R\$/kg CO₂) and the number of days, hours and seasons that this energy is produced.

- Photovoltaic panel

The carbon cost for photovoltaic energy is given by:

$$CO_2^{PV} = CT \cdot CI^{PV} \cdot \sum_{i,m,p} E_{i,m,p}^{PV} \cdot CI^{PV} \cdot day_m \cdot hours_p \cdot season_m \quad (37)$$

It depends on the carbon intensity of photovoltaic panel (CI^{PV} , kg CO₂/kWh), the energy generated by photovoltaic panel ($E_{i,m,p}^{PV}$). In addition, it considers the carbon tax (CT , R\$/kg CO₂) and the number of days, hours and seasons that this energy is produced.

- Solar collector

The carbon cost of the thermal energy produced by the solar collector is given by:

$$CO_2^{SC} = CT \cdot CI^{SC} \cdot \sum_{i,m,p} E_{i,m,p}^{SC} \cdot day_m \cdot hours_p \cdot season_m \quad (38)$$

It depends on the carbon intensity of solar collector (CI^{SC} , kg CO₂/kWh), which is multiplied by the thermal energy ($E_{i,m,p}^{SC}$), the carbon tax (CT , R\$/kg CO₂), and the number of days, hours and seasons that this energy was produced.

- Biogas

The carbon cost of the biogas is given by:

$$CO_2^{BIO} = Qbg \cdot Hb \cdot CI^B \cdot CT \quad (39)$$

It depends on the carbon intensity of biogas (CI^B , kg CO₂/kWh), the volume of biogas produced (Qbg , m³), the calorific capacity of biogas (Hb , kWh/m³) and the carbon tax (CT , R\$/kg CO₂).

d. Electricity Cost

The cost of buying power from the central grid it is given by:

$$C_{BUY}^{GRID} = \sum_{i,m,p} (E_{i,m,p}^{GRID} \cdot P_{m,p}^{Elec} \cdot day_m \cdot hours_p \cdot season_m) \quad (40)$$

which depends on the amount of power purchased from the central grid ($E_{i,m,p}^{GRID}$, kW), the price of electricity for each period of time (m, p) ($P_{m,p}^{Elec}$, R\$/kWh) and the period that the energy was consumed.

e. Natural Gas Cost

The cost of buying natural gas from the grid is given by:

$$C^{NG} = \frac{P^{NG}}{q^{NG}} \cdot \sum_{i,m,p} (Use_{i,m,p}^{NG} \cdot day_m \cdot hours_p \cdot season_m) + \sum_i Y_i^{NG} \cdot C_{Fix}^{NG} \cdot season_m \quad (41)$$

which depends on variable and fixed contributions. The variable cost depends on the volume of gas that is purchased from the grid ($Use_{i,m,p}^{NG}$, kW) the price of gas (P^{NG} , R\$/m³), the calorific capacity of natural gas (q^{NG} , kWh/m³) and the number of hours that the gas has been used. The fixed cost (C_{Fix}^{NG} , R\$/month) exists when natural gas is purchased from the grid and is a monthly amount, so we use the variable Y_i^{NG} to identify whether natural gas is used or not.

f. Policy revenue

In order to define the best incentive policy to be adopted for distributed generation, the Net Metering, Feed in Tariff models were considered. The credits obtained by each policy depends on the total energy sold to the grid and will be detailed next.

- Net Metering

The amount received in energy credits through the Net Metering policy is given by:

$$NEM = \sum_{i,m,p} (E_{i,m,p}^{SALE,PV} + E_{i,m,p}^{SALE,WT} + E_{i,m,p}^{SALE,BG}) \cdot P_{m,p}^{Elec} \cdot day(m) \cdot hours(p) \cdot season(m) \cdot Y^{NEM} \quad (42)$$

which depends on whether the policy is being used or not (Y^{NEM}), the amount of the energy fed into the central grid by the wind turbine ($E_{i,m,p}^{SALE,WT}$, kW) by the photovoltaic panel ($E_{i,m,p}^{SALE,PV}$, kW) and the biogas generator ($E_{i,m,p}^{SALE,BG}$, kW) the price of the central grid energy ($P_{m,p}^{Elec}$, R\$/kWh) and the period of time that this energy is fed into the grid. This equation introduces nonlinearity into the model, due to the multiplication of the binary variable (Y^{NEM}) with the sum of the generated electricity variables.

- Feed in Tariff

The amount received through the Feed in Tariff policy is given by (MEHLERI et al. 2012):

$$FIT = \sum_{i,m,p} (E_{i,m,p}^{SALE,PV} \cdot P^{FIT,PV} + E_{i,m,p}^{SALE,WT} \cdot P^{FIT,WT} + E_{i,m,p}^{SALE,BG} \cdot P^{FIT,BG}) \cdot day(m) \cdot hours(p) \cdot season(m) \cdot Y^{FIT} \quad (43)$$

which depends on whether the policy is being used or not (Y^{FIT}), the amount of the energy fed into the central grid by the wind turbine ($E_{i,m,p}^{SALE,WT}$, kW) by the photovoltaic panel ($E_{i,m,p}^{SALE,PV}$, kW) and the biogas generator ($E_{i,m,p}^{SALE,BG}$, kW) the rate of the sale for the photovoltaic panel ($P^{FIT,PV}$, R\$/kW), the wind turbine ($P^{FIT,WT}$, R\$/kW) and the biogas generator ($P^{FIT,BG}$, R\$/kW) and the period that this energy is fed into the grid. In this equation, it is also possible to observe a non-linearity, due to the multiplication of the binary variable (Y^{FIT}) with the sum of the generated electricity variables.

Considering that only one electricity incentive policy can be chosen, the following constraint is included in the model:

$$Y^{FIT} + Y^{NEM} \leq 1 \quad (44)$$

where Y^{FIT} and Y^{NEM} are binary variables that define whether the policy was adopted or not.

III.4.2. Electricity balance

The electricity demand must be equal to the sum of the electricity generated by the installed energy resources and the electricity consumed from the central grid, for this the energy produced for self-consumption must be equal to the energy demand subtracted from the energy transferred from other houses given by (SIDNELL et al., 2021a):

$$\begin{aligned} Load_{i,m,p}^E + \frac{Load_{i,m,p}^{AC}}{ACCOP} + \frac{E_{i,m,p}^{SELF,ES}}{ne^{ES}} \\ - \sum_j (\beta_{i,j} \cdot E_{j,i,m,p}^{TRANSFER} - E_{i,j,m,p}^{TRANSFER}) \\ = E_{i,m,p}^{GRID} + E_{i,m,p}^{SELF,PV} + E_{i,m,p}^{SELF,WT} + E_{i,m,p}^{SELF,BG} \\ + E_{i,m,p}^{STORAGE\ OUT,BT} \quad i = 1, \dots, n; m = 1, \dots, k; p = 1, \dots, h \end{aligned} \quad (45)$$

where $Load_{i,m,p}^E$ is the electricity load in the residence i at period m, p (kW), $Load_{i,m,p}^{AC}$ is the air conditioning load (kW), $ACCOP$ is the air conditioning power coefficient, $E_{i,m,p}^{SELF,ES}$ is the electricity consumed by the electric shower in the residence i at period m, p (kW), ne^{ES} is electrical efficiency of the electric shower, $\beta_{i,j}$ is energy loss coefficient. The energy loss is accounted for by the difference of the energy transported from house i to house j with the energy arriving at house j . The balance of $E_{i,m,p}^{STORAGE\ OUT,BT}$ is found in Equation (133).

The microgrid cannot feed energy into the central grid before it has met the electricity demand of the residences at every instant of time (SIDNELL et al., 2021a):

$$\begin{aligned}
 E_{i,m,p}^{SALE,PV} + E_{i,m,p}^{SALE,WT} + E_{i,m,p}^{SALE,BG} &\leq \\
 E_{i,m,p}^{GRID} + E_{i,m,p}^{SELF,PV} + E_{i,m,p}^{SELF,WT} + E_{i,m,p}^{SELF,BG} + E_{i,m,p}^{STORAGE\ OUT,BT} & \\
 i = 1, \dots, n; m = 1, \dots, k; p = 1, \dots, h &
 \end{aligned} \tag{46}$$

III.4.3. Hot water balance

The sum of the generation of hot water by energy resources must meet the hot water demand of the residences (SIDNELL et al., 2021a):

$$\begin{aligned}
 Load_{i,m,p}^{HW} - \sum_j (\beta_{i,j} \cdot HW_{j,i,m,p}^{TRANSFER} - HW_{i,j,m,p}^{TRANSFER}) & \\
 = HW_{i,m,p}^{SELF,BH} + HW_{i,m,p}^{SELF,ES} + HW_{i,m,p}^{SELF,GH} & \\
 + HW_{i,m,p}^{SELF,TS} & \\
 i = 1, \dots, n; m = 1, \dots, k; p = 1, \dots, h &
 \end{aligned} \tag{47}$$

where $Load_{i,m,p}^{HW}$ is the hot water demand in the residence i at period m, p , $HW_{i,j,m,p}^{TRANSFER}$ is the hot water transferred from house i to house j (L), $HW_{j,i,m,p}^{TRANSFER}$ is the hot water transferred to house i from houses j , $\beta_{i,j}$ is the thermal energy loss factor from the transfer of hot water between houses i and j , $HW_{i,m,p}^{SELF}$ is the amount of hot water produced for self-consumption by biogas heater (BH), electric shower (ES), gas heater (GH), thermal storage (TS).

Hot water cannot be shared between houses before the house has met its demand, so the hot water transferred must be less than the hot water used for self-consumption:

$$\begin{aligned}
 \sum_j (\beta_{i,j} \cdot HW_{j,i,m,p}^{TRANSFER} - HW_{i,j,m,p}^{TRANSFER}) & \\
 \leq HW_{i,m,p}^{SELF,BH} + HW_{i,m,p}^{SELF,ES} + HW_{i,m,p}^{SELF,GH} & \\
 + HW_{i,m,p}^{SELF,TS} \quad i = 1, \dots, n; m = 1, \dots, k; p = 1, \dots, h &
 \end{aligned} \tag{48}$$

III.4.4. Air cooling balance

The air conditioning generation must be sufficient to meet the demands of the houses:

$$Load_{i,m,p}^{AC} = E_{i,m,p}^{AC} \quad i = 1, \dots, n; m = 1, \dots, k; p = 1, \dots, h \tag{49}$$

III.4.5. Cooking gas balance

The sum of natural gas and biogas used for cooking must equal the gas demand of the household:

$$\begin{aligned} Load_{i,m,p}^C &= G_{i,m,p}^{NG} + Qbgc_{i,j,m} \cdot Hb \quad i = 1, \dots, n; m = 1, \dots, k; p \\ &= 1, \dots, h \end{aligned} \quad (50)$$

where $Load_{i,m,p}^C$ is the demand for cooking gas from households (kW), $G_{i,m,p}^{NG}$ is the natural gas consumed from the grid to meet the demand for cooking (kW), $Qbgc_{i,j,m}$ is the biogas produced to meet the demand for cooking (m³) and Hb is the calorific capacity of biogas (kW/m³).

III.4.6. Natural gas consumption

The natural gas consumption must be equal to the gas used for cooking ($G_{i,m,p}^{NG}$, kW) and the gas used in the gas heater ($E_{i,m,p}^{GH}$, kW):

$$Use_{i,m,p}^{NG} = G_{i,m,p}^{NG} + \frac{E_{i,m,p}^{GH}}{ne^{GH}} \quad i = 1, \dots, n; m = 1, \dots, k; p = 1, \dots, h \quad (51)$$

where ne^{GH} is the natural gas heater efficiency.

The rule NBR 13103 establishes the minimum requirements for the installation of gas appliances for residential use. It dictates that the nominal power must not exceed 80.0 kW in the same place of installation. To meet this rule, the following equation is proposed:

$$\sum_{m,p} Use_{i,m,p}^{NG} \leq 80 \cdot Y_i^{NG} \quad i = 1, \dots, n \quad (52)$$

where Y_i^{NG} indicates whether or not natural gas is being used in the house.

III.4.7. Design and operation constraints

In order to consider the capacity, configuration, and operation limitations of the system, the constraints involved in the operation and design of each technology will be presented. These are essential to achieve a more realistic result.

- Microgrid

The sale of energy to the grid cannot exceed a maximum limit and the house cannot insert energy into the grid and buy from the grid in the same period of time. Therefore, the following constraint is formulated (SIDNELL et al., 2021a):

$$\begin{aligned} E_{i,m,p}^{SALE,PV} + E_{i,m,p}^{SALE,WT} + E_{i,m,p}^{SALE,BG} &\leq Sale_{up} \cdot (1 - Y_{i,m,p}^{GRID}) \quad i \\ &= 1, \dots, n; m = 1, \dots, k; p = 1, \dots, h \end{aligned} \quad (53)$$

where $Y_{i,m,p}^{GRID}$ is a binary variable that defines whether or not energy is bought from the grid for the house i at period m, p and $Sale_{up}$ is the limit amount of energy that can be sold to the grid (kW).

The energy purchased from the grid cannot exceed the house's demand:

$$E_{i,m,p}^{GRID} \leq \left(Load_{i,m,p}^E + \frac{Load_{i,m,p}^{AC}}{ACCOP} + \frac{E_{i,m,p}^{SELF,ES}}{ne^{ES}} \right) \cdot (Y_{i,m,p}^{GRID}) \quad i = 1, \dots, n; m = 1, \dots, k; p = 1, \dots, h \quad (54)$$

Energy cannot be transferred from house i to house j in the same period m, p that energy is being purchased from the central grid:

$$E_{i,j,m,p}^{TRANSFER} \leq \left(Load_{i,m,p}^E + \frac{Load_{i,m,p}^{AC}}{ACCOP} + \frac{E_{i,m,p}^{SELF,ES}}{ne^{ES}} \right) \cdot (1 - Y_{i,m,p}^{GRID}) \quad i = 1, \dots, n; m = 1, \dots, k; p = 1, \dots, h \quad (55)$$

According to Sidnell et al. (2021a) and Clarke et al. (2021), the energy must be transferred only in one direction. This means that if house i shares energy with house j , house j is assigned a higher numerical position (E_j) between them and therefore cannot send energy to house i (E_i):

$$E_j \geq E_i + 1 - i \cdot (1 - Y_{i,j}^{MG}) \quad i, j = 1, \dots, n \quad (56)$$

where E_j is the numerical position of house j , E_i is the numerical position of house i , $Y_{i,j}^{MG}$ is the binary variable that informs whether or not there is a connection between house i and j .

In addition, if there is energy transfer from house i to house j , then there can be no energy transfer from house j to house i , as well as energy sharing from one house at the same time it receives energy from another house:

$$\sum_j Y_{i,j}^{MG} + \sum_j Y_{j,i}^{MG} \leq 1 \quad i, j = 1, \dots, n \quad (57)$$

There can be no electricity line between the same house:

$$Y_{i,i}^{MG} = 0 \quad i = 1, \dots, n \quad (58)$$

$$E_{i,i,m,p}^{TRANSFER} = 0 \quad i = 1, \dots, n; m = 1, \dots, k; p = 1, \dots, h \quad (59)$$

where $E_{i,i,m,p}^{TRANSFER}$ is the energy transferred from house i to house i .

The electricity transferred between houses is the sum of the energy generated by each energy resource that was not used for self-consumption or for insertion into the grid :

$$E_{i,j,m,p}^{TRANSFER} = E_{i,j,m,p}^{TRANSFER,PV} + E_{i,j,m,p}^{TRANSFER,WT} + E_{i,j,m,p}^{TRANSFER,BG} \quad (60)$$

$$i, j = 1, \dots, n; m = 1, \dots, k; p = 1, \dots, h$$

In order to certify that the energy will only be transferred if there is an electric cable, the energy transferred must be less than demand of the microgrid multiplied by the binary variable of existence or not of the electric cable between house i and house j :

$$E_{i,j,m,p}^{TRANSFER} \leq \left(Load_{i,m,p}^E + \frac{Load_{i,m,p}^{AC}}{ACCOP} + \frac{E_{i,m,p}^{SELF,ES}}{ne^{ES}} \right) \cdot Y_{i,j}^{MG} \quad (61)$$

$$i, j = 1, \dots, n; m = 1, \dots, k; p = 1, \dots, h$$

The binary variable Z represents whether there is a microgrid in the system or not (Eq. 26), so it must be greater than or equal to the binary variable of the electrical cable between the houses:

$$Z \geq Y_{i,j}^{MG} \quad i, j = 1, \dots, n \quad (62)$$

- Pipeline

As in the microgrid, the transfer of hot water can only be carried out in one direction (SIDNELL et al., 2021a):

$$O_j \geq O_i + 1 - i \cdot (1 - Y_{i,j}^P) \quad i, j = 1, \dots, n \quad (63)$$

where O_j is the numerical position of house j , O_i is the numerical position of house i , $Y_{i,j}^P$ is the binary variable that informs whether or not there is a connection between house i and j .

The electric shower warms the water by passing electric current through an electrical resistance, brought into contact by a diaphragm. This is activated by the flow of water entering the showerhead, as exemplified in Figure 45. Therefore, the electric shower cannot be installed with any other source:

$$Y_i^{ES} + Y_i^{GH} \leq 1 \quad i = 1, \dots, n \quad (64)$$

$$Y_i^{ES} + Y_i^{SC} \leq 1 \quad i = 1, \dots, n$$

$$Y_i^{ES} + Y_i^{BH} \leq 1 \quad i = 1, \dots, n$$

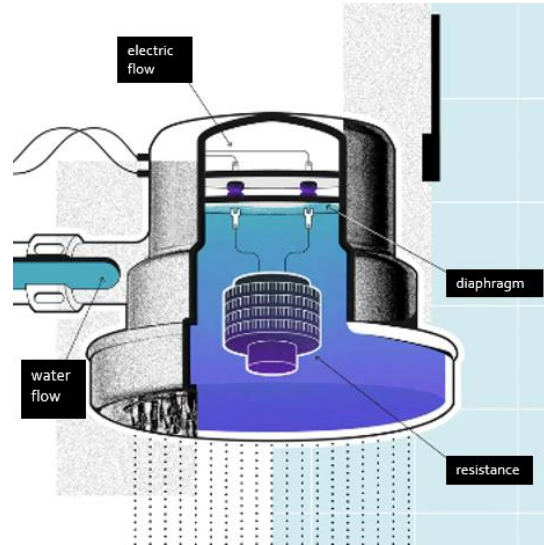


Figure 45 - Operation of an electric shower. Source: Adapted from Lara (2019).

Considering that a house has limited space and can only afford one heater/boiler, the following constraint is imposed:

$$Y_i^{GH} + Y_i^{BH} \leq 1 \quad i = 1, \dots, n \quad (65)$$

Therefore, a single house cannot have more than one of these technologies: biogas heater and natural gas heater.

As in the microgrid, if there is hot water transfer from house i to house j , then there can be no hot water transfer from house j to house i , as well as energy sharing from one house at the same time it receives energy from another house:

$$\sum_j Y_{i,j}^P + \sum_j Y_{j,i}^P \leq 1 \quad i, j = 1, \dots, n \quad (66)$$

A pipeline cannot exist between the same house:

$$Y_{i,i}^P = 0 \quad i = 1, \dots, n \quad (67)$$

$$HW_{i,i,m,p}^P = 0 \quad i = 1, \dots, n; m = 1, \dots, k; p = 1, \dots, h \quad (68)$$

The hot water transferred between the houses is the sum of the hot water produced that is intended for transfer, so it is the amount that has not been used for self-consumption:

$$HW_{i,j,m,p}^{TRANSFER} = HW_{i,j,m,p}^{TRANSFER,GH} + HW_{i,j,m,p}^{TRANSFER,BH} + HW_{i,j,m,p}^{TRANSFER,TS} \quad i = 1, \dots, n; m = 1, \dots, k; p = 1, \dots, h \quad (69)$$

In order to certify that the hot water will only be transferred if there is a pipe between the houses, the sum of the energy transferred must be less than the upper bound of the energy that can be transferred multiplied by the binary variable of existence or not of the pipeline between house i and house j :

$$HW_{i,j,m,p}^{TRANSFER,GH} + HW_{i,j,m,p}^{TRANSFER,BH} + HW_{i,j,m,p}^{TRANSFER,TS} \leq UB^P \cdot Y_{i,j}^P \quad (70)$$

$$i = 1, \dots, n; m = 1, \dots, k; p = 1, \dots, h$$

- Photovoltaic panel

The energy produced by the photovoltaic panel ($E_{i,m,p}^{PV}$, kW) cannot be greater than the production capacity of the photovoltaic panel, this equation considers the time dependent profile of the efficiency associated with the photovoltaic panel, as suggested by Karamov et al. (2021):

$$E_{i,m,p}^{PV} \leq A_i^{PV} \cdot It_{m,p} \cdot ne_{m,p}^{PV} \cdot KL \quad i = 1, \dots, n; m = 1, \dots, k; \quad (71)$$

$$p = 1, \dots, h$$

where $It_{m,p}$ is the time dependent solar radiation at the site (kWh /m²), $ne_{m,p}^{PV}$ is the energy efficiency of the photovoltaic panel per time period and KL is a coefficient to account for power losses in diodes.

The time dependent profile of the efficiency of a photovoltaic panel might be expressed as suggested by Karamov et al. (2021):

$$ne_{m,p}^{PV} = nee^{PV} \cdot \left[(1 - \beta_S) * T_{m,p}^{PV/SC} - 48 \right] \quad m = 1, \dots, k; p = 1, \dots, h \quad (72)$$

$$= 1, \dots, h$$

where nee^{PV} is the nominal energy efficiency of the photovoltaic panel, β_S is temperature coefficient for silicon photovoltaic panel and $T_{m,p}^{PV/SC}$ is the operating temperature of the photovoltaic converter and is expressed as follows:

$$T_{m,p}^{PV/SC} = T_{m,p}^{Env} + \frac{It_{m,p}}{K_0 + K_1 \cdot V_{m,p}^{Env}} \quad m = 1, \dots, k; p = 1, \dots, h \quad (73)$$

where $T_{m,p}^{Env}$ is the ambient air temperature (°C), $V_{m,p}^{Env}$ is wind speed (m/s), K_0 and K_1 are Koehl correlation coefficients.

The energy generated in the photovoltaic panel must be equal to the sum of the PV energy used:

$$E_{i,m,p}^{PV} = E_{i,m,p}^{SELF,PV} + E_{i,m,p}^{SALE,PV} + \sum_j E_{i,j,m,p}^{TRANSFER,PV} + E_{i,m,p}^{STORAGE,PV} \quad (74)$$

$$i = 1, \dots, n; m = 1, \dots, k; p = 1, \dots, h$$

The sale of electricity cannot be greater than is produced for consumption:

$$\begin{aligned} E_{i,m,p}^{SALE,PV} &\leq E_{i,m,p}^{SELF,PV} + \sum_j E_{i,m,p}^{TRANSFER,PV} + E_{i,m,p}^{STORAGE,PV} \quad i \\ &= 1, \dots, n; m = 1, \dots, k; p = 1, \dots, h \end{aligned} \quad (75)$$

The energy storage will be arranged in batteries and detailed in the Eq. 133.

Due to space limitations for the installation of photovoltaic panels and solar collectors, the sum of the areas should not exceed a maximum limit, defined based on the roof area of each house (PV_{up}):

$$A_i^{PV} + A_i^{SC} \leq PV_{up} \quad i = 1, \dots, n \quad (76)$$

- Wind turbine

Considering the fluctuation of energy generated by the wind turbine according to the environmental behavior of the site, when the environmental wind speed ($V_{m,p}^{Env}$) is below the cut off speed of the turbine (V_{co} , m/s) or above the cut in speed (V_{ci} , m/s), the electricity generation is equal to zero according to Pallabazzer (2003), then:

$$E_{i,m,p}^{WT} = 0 \quad \forall V_{co} < V_{m,p}^{Env} \cup 0 < V_{m,p}^{Env} < V_{ci} \quad (77)$$

When the environmental wind speed is greater or equal to the cut off speed and less or equal than the nominal speed (V_r , m/s), the energy produced by the wind turbine is expressed by:

$$\begin{aligned} E_{i,m,p}^{WT} &= \frac{1}{2} \cdot A_i^{WT} \cdot \rho_{wind} \cdot Cp^{WT} \cdot V_r^3 \cdot \frac{V_{m,p}^{Env^2} - V_{ci}^2}{\frac{V_r^2 - V_{ci}^2}{100}} \quad i = 1, \dots, n; m \\ &= 1, \dots, k; p = 1, \dots, h \end{aligned} \quad (78)$$

$$\forall V_{ci} \leq V_{m,p}^{Env} \cap V_{m,p}^{Env} \leq V_r$$

When the wind speed is greater or equal than the rated speed and less or equal than the cut in speed, the energy produced by the wind turbine is expressed by Pallabazzer (2003):

$$\begin{aligned} E_{i,m,p}^{WT} &= \frac{\frac{1}{2} \cdot A_i^{WT} \cdot \rho_{wind} \cdot Cp^{WT} \cdot V_r^3}{100} \quad i = 1, \dots, n; m = 1, \dots, k; p \\ &= 1, \dots, h \end{aligned} \quad (79)$$

$$\forall V_r \leq V_{m,p}^{Env} \cap V_{m,p}^{Env} \leq V_{co}$$

where ρ_{wind} is wind density (kg/m³), Cp^{WT} is power coefficient of the wind turbine.

Two houses adjacent to each other cannot have a wind turbine:

$$Y_{i+1}^{WT} + Y_i^{WT} \leq 1 \quad i = 1, \dots, n \quad (80)$$

The energy generated ($E_{i,m,p}^{WT}$, kW) in the wind turbine must be equal to the sum of the energy for self-consumption:

$$E_{i,m,p}^{WT} = E_{i,m,p}^{SELF,WT} + E_{i,m,p}^{SALE,WT} + \sum_j E_{i,m,p}^{TRANSFER,WT} + E_{i,m,p}^{STORAGE,WT} \quad i = 1, \dots, n; m = 1, \dots, k; p = 1, \dots, h \quad (81)$$

The energy storage will be stored in batteries and detailed in the Eq. 133.

The area of the wind turbine (A_i^{WT} , m²) must not exceed a maximum limit (WT_{up}):

$$A_i^{WT} \leq WT_{up} \cdot Y_i^{WT} \quad i = 1, \dots, n \quad (82)$$

where Y_i^{WT} is indicating whether or not the wind turbine is installed.

The surplus of electricity must not be more than is produced for consumption:

$$E_{i,m,p}^{SALE,WT} \leq E_{i,m,p}^{SELF,WT} + \sum_j E_{i,m,p}^{TRANSFER,WT} + E_{i,m,p}^{STORAGE,WT} \quad i = 1, \dots, n; m = 1, \dots, k; p = 1, \dots, h \quad (83)$$

- Biogas

The correlations and constraints that concern biogas production, as well as the behavior of transport between houses will be presented below. These constraints were modeled for the system in order to provide the novelty of the work in applying biogas to meet the gas demands for food cooking, water heating and power generation.

a. Production

The total biogas produced depends on the organic matter produced in each house per day (Qom_i , kg) and the extra organic matter purchased from an external source per day (Qow_i , kg). The production in m³ per year is found by multiplying the biogas production

rate per organic material (qb , m^3 of biogas/kg of organic waste) by the number of days (30) and months (12) in the year:

$$Qbg = qb \cdot days \cdot \sum_i (Qom_i + Qow_i) \quad (84)$$

The total biogas produced is the sum of the biogas produced for cooking food in each house i and time period (m, p) ($Qbgc_{i,m,p}$, m^3), the biogas produced for electricity generation in each house i and time period (m, p) ($Qbgi_{i,m,p}$, m^3), and the biogas produced for hot water generation in each house i and time period (m, p) ($Qbhw_{i,m,p}$, m^3). In order to find the annual production value, each term is multiplied by the time it was produced:

$$\begin{aligned} Qbg = & \sum_{i,m,p} Qbgc_{i,m,p} \cdot hours_m \cdot day_p \cdot season_m \\ & + \sum_{i,m,p} Qbgi_{i,m,p} \cdot hours_p \cdot day_m \cdot season_m \\ & + \sum_{i,m,p} Qbhw_{i,m,p} \cdot hours_p \cdot day_m \cdot season_m \end{aligned} \quad (85)$$

In order to find the total biogas production for each house i and period (m, p) ($Qbio_{i,m,p}$, m^3), the sum of the biogas used for cooking food, for producing hot water and for generating electricity for each house and period is performed:

$$Qbio_{i,m,p} = Qbgc_{i,m,p} + Qbgi_{i,m,p} + Qbhw_{i,m,p} \quad i = 1, \dots, n; m = 1, \dots, k; p = 1, \dots, h \quad (86)$$

Following the rule NBR 13103, the total biogas produced must be less than or equal to 80 kW and will only be used if the pipeline exists:

$$Qbio_{i,m,p} \leq \frac{80}{Hb} \cdot Y_i^{BIO} \quad i = 1, \dots, n; m = 1, \dots, k; p = 1, \dots, h \quad (87)$$

where Hb is the calorific capacity of the biogas (kW/m^3) and Y_i^{BIO} is a binary variable and indicates whether or not there is a connection between the biodigester and the house i .

b. Biodigester for biogas production

According to Araujo (2017) and Otim et al. (2006), the volume of the biodigester is given by:

$$V^{BD} = \sum_i \frac{(Qom_i + Qow_i) \cdot IS}{DMO} \cdot tr \cdot (1 + 0.3) \quad (88)$$

where Qom_i is the amount of organic material produced by each house (kg/day), Qow_i is the extra organic material purchased from a company (kg/day), IS is the percentage of dry mass in organic material, DMO is the density of the dry material in the fluid (kg/m³), tr is the hydraulic retention time in the biodigester (day). The final volume of the biodigester should be considered 30% larger than calculated due to the gaseous phase that will also be stored in it.

The binary variable (Y^{BD}) indicates whether or not the biodigester is installed within the microgrid and its volume must not exceed a maximum space limit (BD_{up})(m³):

$$V^{BD} \leq BD_{up} \cdot Y^{BD} \quad (89)$$

The binary variable Y^{BD} must be greater than or equal to the binary variable that indicates whether or not there is a connection between the biodigester and the house i :

$$Y^{BD} \geq Y_i^{BIO} \quad i = 1, \dots, n \quad (90)$$

- Biogas electric generator

When operating the biogas generator, the energy produced by the generator for self-consumption ($E_{i,m,p}^{SELF,BG}$), insertion into grid ($E_{i,m,p}^{SALE,BG}$), transferred between houses ($E_{i,j,m,p}^{TRANSFER,BG}$) and storage ($E_{i,j,m,p}^{STORAGE,BG}$) cannot be greater than the production capacity of the generator:

$$E_{i,m,p}^{SELF,BG} + E_{i,m,p}^{SALE,BG} + \sum_j (E_{i,j,m,p}^{TRANSFER,BG}) + E_{i,j,m,p}^{STORAGE,BG} \leq k_i^{BG} \cdot ne^{BG} \quad i = 1, \dots, n; m = 1, \dots, k; p = 1, \dots, h \quad (91)$$

where ne^{BG} is the efficiency of the biogas generator.

The energy generated in the biogas generator ($E_{i,m,p}^{BG}$, kW) must be equal to the sum of the energy for self-consumption :

$$E_{i,m,p}^{BG} = E_{i,m,p}^{SELF,BG} + E_{i,m,p}^{SALE,BG} + \sum_j (E_{i,j,m,p}^{TRANSFER,BG}) + E_{i,j,m,p}^{STORAGE,BG} \quad i = 1, \dots, n; m = 1, \dots, k; p = 1, \dots, h \quad (92)$$

The sale of electricity cannot be more than is produced for consumption:

$$E_{i,m,p}^{SALE,BG} \leq E_{i,m,p}^{SELF,BG} + \sum_j (E_{i,j,m,p}^{TRANSFER,BG}) + E_{i,j,m,p}^{STORAGE,BG} \quad i = 1, \dots, n; m = 1, \dots, k; p = 1, \dots, h \quad (93)$$

The energy storage will be arranged in batteries and detailed in Eq. 133.

The capacity of the biogas generator (k_i^{BG}) (kW) must not be greater than the biogas production capacity of the biodigester system:

$$k_i^{BG} \leq Qbgg_{i,m,p} \cdot Hb \quad i = 1, \dots, n; m = 1, \dots, k; p = 1, \dots, h \quad (94)$$

where Hb is calorific capacity of biogas (kWh/m³).

In addition, the capacity of the generator must be within the capacity limits found in the market, when the equipment is installed (Y_i^{BG}):

$$k_i^{BG} \geq BG_{low} \cdot Y_i^{BG} \quad i = 1, \dots, n \quad (95)$$

$$k_i^{BG} \leq BG_{up} \cdot Y_i^{BG} \quad i = 1, \dots, n \quad (96)$$

where BG_{low} is the lower limit and BG_{up} is the upper limit.

- Biogas heater

As the biogas generator, the thermal energy produced by the biogas heater cannot be greater than the biogas production capacity of the biodigester system:

$$E_{i,m,p}^{BH} \leq Qbhw_{i,m,p} \cdot Hb \cdot ne^{BH} \quad i = 1, \dots, n; m = 1, \dots, k; p = 1, \dots, h \quad (97)$$

where $E_{i,m,p}^{BH}$ is the thermal energy produced (kW), ne^{BH} is the thermal efficiency of the biogas heater, Hb is calorific capacity of biogas (kWh/m³).

It is more common to find information about the capacity of the heating equipment in liters in the market, the energy balance equation represents the energy in kW required to heat a quantity of water in L. This considers the room temperature in each period (m, p) ($T_{m,p}^{Env}$, °C) and the desired temperature of hot water ($T_{storage}$, °C) use and is expressed as:

$$E_{i,m,p}^{BH} = \frac{cp_{water} \cdot HW_{i,m,p}^{BH} \cdot \rho_{water} \cdot (T_{storage} - T_{m,p}^{Env})}{3600} \quad i = 1, \dots, n; m = 1, \dots, k; p = 1, \dots, h \quad (98)$$

where cp_{water} is the heat capacity of water and corresponds to 4.18 kJ/kg, ρ_{water} is the water density and corresponds to 1 kg/L, $HW_{i,m,p}^{BH}$ is the amount of hot water produced (L).

The capacity of the biogas heater must be greater than or equal to the amount of hot water produced:

$$k_i^{BH} \geq HW_{i,m,p}^{BH} \quad i = 1, \dots, n; m = 1, \dots, k; p = 1, \dots, h \quad (99)$$

The hot water produced ($HW_{i,m,p}^{BH}$) can be consumed for own use ($HW_{i,m,p}^{SELF,BH}$) or be transferred to another house ($HW_{i,m,p}^{TRANSFER,BH}$):

$$HW_{i,m,p}^{BH} = HW_{i,m,p}^{SELF,BH} + \sum_j HW_{i,m,p}^{TRANSFER,BH}$$

$$i = 1, \dots, n; m = 1, \dots, k; p = 1, \dots, h \quad (100)$$

Considering that the biogas heater does not store thermal energy and therefore must be activated only when in use, it does not transfer hot water from one house to another:

$$HW_{i,j,m,p}^{TRANSFER,BH} = 0 \quad i = 1, \dots, n; m = 1, \dots, k; p = 1, \dots, h \quad (101)$$

The capacity of the heater must be within the capacity limits found in the market, when the equipment is installed (Y_i^{BH}), hence:

$$k_i^{BH} \geq BH_{low} \cdot Y_i^{BH} \quad i = 1, \dots, n \quad (102)$$

$$k_i^{BH} \leq BH_{up} \cdot Y_i^{BH} \quad i = 1, \dots, n \quad (103)$$

where BH_{low} is the lower limit of capacity (L/h) and BH_{up} is the upper limit of capacity (L/h).

- Solar collector

The solar hot water generation system is composed of a solar collector to capture the energy and a solar tank to store the produced hot water. As in the photovoltaic panel, the thermal energy captured by the solar collector ($E_{i,m,p}^{SC}$) cannot exceed its capacity, hence:

$$E_{i,m,p}^{SC} \leq A_i^{SC} \cdot It_{m,p} \cdot ne_{m,p}^{SC} \cdot KL \cdot Y_i^{ST} \quad i = 1, \dots, n; m = 1, \dots, k; p = 1, \dots, h \quad (104)$$

which is dependent on the solar irradiation ($It_{m,p}$, kWh/m²), solar collector area (A_i^{SC} , m²), collector efficiency ($ne_{m,p}^{SC}$), the coefficient of power losses in diodes (KL) and whether or not the solar collector is installed (Y_i^{ST}). Due to the multiplication of the binary variable (Y_i^{ST}) and the solar collector area (A_i^{SC}) this equation is non-linear.

As the photovoltaic panel, the efficiency of the solar collector ($ne_{m,p}^{SC}$) was also considered to vary with time and is expressed as suggested by Karamov et al. (2021):

$$ne_{m,p}^{SC} = ne^{SC} \cdot \left[(1 - \beta_S) * T_{m,p}^{\frac{PV}{SC}} - 48 \right] \quad m = 1, \dots, k; p = 1, \dots, h \quad (105)$$

where η^{PV} is the rated energy efficiency of the photovoltaic panel and $T_{m,p}^{PV/SC}$ can be found in Eq. (73).

Similarly to the biogas heater, it is more usual to find the capacity of the solar tank in liters, so the energy balance equation represents the energy in kW required to heat a quantity of water in L:

$$E_{i,m,p}^{SC} = \frac{c_{p_{water}} \cdot HW_{i,m,p}^{SC} \cdot \rho_{water} \cdot (T_{storage} - T_{m,p}^{Env})}{3600} \quad i = 1, \dots, n; m = 1, \dots, k; p = 1, \dots, h \quad (106)$$

where $c_{p_{water}}$ is the heat capacity of water and corresponds to 4.18 kJ/kg, ρ_{water} is the water density and corresponds to 1 kg/L, $HW_{i,m,p}^{SC}$ is the amount of hot water produced (L/h), $T_{m,p}^{Env}$ is the room temperature in each period (m, p) (°C) and ($T_{storage}$) is the desired temperature of hot water (°C).

The hot water produced is stored ($HW_{i,m,p}^{STORAGE,SC}$, L/h) to be used later:

$$HW_{i,m,p}^{SC} = HW_{i,m,p}^{STORAGE,SC} \quad i = 1, \dots, n; m = 1, \dots, k; p = 1, \dots, h \quad (107)$$

- Thermal storage

The hot water produced in the solar collector is fed into the thermal storage system:

$$HW_{i,m,p}^{TS,in} = HW_{i,m,p}^{STORAGE,SC} \quad i = 1, \dots, n; m = 1, \dots, k; p = 1, \dots, h \quad (108)$$

where $HW_{i,m,p}^{TS,in}$ is the hot water inserted into thermal storage.

The mass balance at the storage tank might be expressed as (SIDNELL et al., 2021a):

$$HW_{i,m,p}^{TS} = (1 - \zeta) \cdot HW_{i,m,p-1}^{TS} + HW_{i,m,p}^{TS,in} - HW_{i,m,p}^{TS,out} \quad i = 1, \dots, n; m = 1, \dots, k; p = 1, \dots, h \quad (109)$$

where $HW_{i,m,p}^{TS}$ is the hold up of hot water in the tank (L) at any time (m, p), $HW_{i,m,p-1}^{TS}$ (L) is the previous state of the hold up, ζ is the loss coefficient for thermal storage, $HW_{i,m,p}^{TS,in}$ is the mass of hot water that enters the tank at the time (m, p) and $HW_{i,m,p}^{TS,out}$ (L) is the mass of hot water that leaves the tank at the same time instant.

The energy removed from the system cannot be greater than the hot water that was loaded into the system:

$$HW_{i,m,p}^{TS,out} \leq (1 - \zeta) \cdot HW_{i,m,p-1}^{TS} \quad i = 1, \dots, n; m = 1, \dots, k; p = 1, \dots, h \quad (110)$$

The hot water taken from the tank can be shared with the other houses ($HW_{i,j,m,p}^{TRANSFER,TS}$) or can be used for self-consumption ($HW_{i,m,p}^{SELF,TS}$):

$$HW_{i,m,p}^{TS,out} = \sum_j HW_{i,j,m,p}^{TRANSFER,TS} + HW_{i,m,p}^{SELF,TS} \quad i = 1, \dots, n; m = 1, \dots, k; p = 1, \dots, h \quad (111)$$

The installed capacity of the thermal storage tank (k_i^{ST} , L) must be equal to or greater than the amount of hot water entering the unit plus the amount already in it at any given time (m, p):

$$k_i^{TS} \geq (1 - \zeta) \cdot HW_{i,m,p-1}^{TS} + HW_{i,m,p}^{TS,in} \quad i = 1, \dots, n; m = 1, \dots, k; p = 1, \dots, h \quad (112)$$

The volume of hot water stored in the unit cannot exceed its capacity:

$$HW_{i,m,p}^{TS} \leq k_i^{TS} \quad i = 1, \dots, n; m = 1, \dots, k; p = 1, \dots, h \quad (113)$$

In addition, the capacity of the solar tank must be within the capacity limits available in the market, when the equipment is installed (Y_i^{TS}):

$$k_i^{TS} \geq TS_{low} \cdot Y_i^{TS} \quad i = 1, \dots, n \quad (114)$$

$$k_i^{TS} \leq TS_{up} \cdot Y_i^{TS} \quad i = 1, \dots, n \quad (115)$$

where TS_{low} is the lower limit (L) and TS_{up} is the upper limit (L).

- Electric shower

For the electric shower, the thermal energy ($E_{i,m,p}^{ES}$, kW) produced must be less than or equal to the product of the shower's capacity (k_i^{ES}) and efficiency (ne^{ES}):

$$E_{i,m,p}^{ES} \leq k_i^{ES} \cdot ne^{ES} \quad i = 1, \dots, n; m = 1, \dots, k; p = 1, \dots, h \quad (116)$$

The energy produced is used for self-consumption:

$$E_{i,m,p}^{ES} = E_{i,m,p}^{SELF,ES} \quad i = 1, \dots, n; m = 1, \dots, k; p = 1, \dots, h \quad (117)$$

In order to find the amount of hot water in liter corresponding to the thermal energy generated, the energy balance equation was used and represents the energy in kW required to heat a quantity of water in L:

$$E_{i,m,p}^{SELF,ES} = \frac{cp_{water} \cdot HW_{i,m,p}^{SELF,ES} \cdot \rho_{water} \cdot (T_{use} - T_{m,p}^{Env})}{3600} \quad (118)$$

$$i = 1, \dots, n; m = 1, \dots, k; p = 1, \dots, h$$

where $HW_{i,m,p}^{SELF,ES}$ is the hot water produced that can be consumed for own use (L), cp_{water} is the heat capacity of water and corresponds to 4.18 kJ/kg, ρ_{water} is the water density and corresponds to 1 kg/L, T_{use} is the desired temperature of hot water (°C) and $(T_{m,p}^{Env})$ is the room temperature in each period (m, p) (°C).

In addition, the capacity of the electric shower must be within the capacity limits found in the market, when the equipment is installed (Y_i^{ES}):

$$k_i^{ES} \geq ES_{low} \cdot Y_i^{ES} \quad i = 1, \dots, n \quad (119)$$

$$k_i^{ES} \leq ES_{up} \cdot Y_i^{ES} \quad i = 1, \dots, n \quad (120)$$

where ES_{low} is the lower limit (kW) and ES_{up} is the upper limit (kW).

- Gas heater

For the gas heater, the hot water produced ($HW_{i,m,p}^{GH}$, L/h) must be less than or equal to the capacity of the heater (k_i^{GH} , L/h):

$$HW_{i,m,p}^{GH} \leq k_i^{GH} \quad i = 1, \dots, n; m = 1, \dots, k; p = 1, \dots, h \quad (121)$$

The hot water produced can be consumed for own use ($HW_{i,m,p}^{SELF,GH}$, L/h) or to be transferred to another house ($HW_{i,j,m,p}^{TRANSFER,GH}$, L/h):

$$\begin{aligned} HW_{i,m,p}^{GH} &= HW_{i,m,p}^{SELF,GH} + \sum_j HW_{i,j,m,p}^{TRANSFER,GH} \quad i = 1, \dots, n; m \\ &= 1, \dots, k; p = 1, \dots, h \end{aligned} \quad (122)$$

In order to calculate the consumption of natural gas by the heater, the energy balance equation was used and represents the energy in kW required to heat a quantity of water in L:

$$\begin{aligned} E_{i,m,p}^{GH} &= \left(\frac{cp_{water} \cdot HW_{i,m,p}^{GH} \cdot \rho_{water} \cdot (T_{use} - T_{m,p}^{Env})}{3600} \right) \cdot ne^{GH} \\ & \quad i = 1, \dots, n; m = 1, \dots, k; p = 1, \dots, h \end{aligned} \quad (123)$$

where $E_{i,m,p}^{GH}$ is the energy corresponding to the hot water produced (kW), cp_{water} is the heat capacity of water and corresponds to 4.18 kJ/kg, ρ_{water} is the water density and corresponds to 1 kg/L, T_{use} is the desired temperature of hot water (°C) and $(T_{m,p}^{Env})$ is the room temperature in each period (m, p) (°C), ne^{GH} gas heater efficiency.

Considering that the gas heater does not store thermal energy and therefore must be activated only when in use, it does not transfer hot water from one house to another:

$$HW_{i,j,m,p}^{TRANSFER,GH} = 0 \quad (124)$$

The capacity of the gas heater must be within the capacity limits found in the market, when the equipment is installed (Y_i^{GH}):

$$k_i^{GH} \geq GH_{low} \cdot Y_i^{GH} \quad i = 1, \dots, n \quad (125)$$

$$k_i^{GH} \leq GH_{up} \cdot Y_i^{GH} \quad i = 1, \dots, n \quad (126)$$

where GH_{low} is the lower limit (L/h) and GH_{up} is the upper limit (L/h).

- Air conditioning

For the air conditioning, the cooling air produced in each period (m, p) ($E_{i,m,p}^{AC}$, kW) must be less than or equal to the capacity of the air conditioning unit (k_i^{AC} , kW):

$$E_{i,m,p}^{AC} \leq k_i^{AC} \quad i = 1, \dots, n; m = 1, \dots, k; p = 1, \dots, h \quad (127)$$

The capacity of the air conditioning must be within the capacity limits found in the market, when the equipment is installed (Y_i^{AC}):

$$k_i^{AC} \geq AC_{low} \cdot Y_i^{AC} \quad i = 1, \dots, n \quad (128)$$

$$k_i^{AC} \leq AC_{up} \cdot Y_i^{AC} \quad i = 1, \dots, n \quad (129)$$

where AC_{low} is the lower limit (kW) and AC_{up} is the upper limit (kW).

- Battery (electrical storage)

Initially, the state of charge of battery systems found in Mbungu et al. (2020) was considered. However, the computational effort of the model made it impossible to find a solution to the problem. Therefore, the presented model did not consider the state of charge of battery systems as presented in Sidnell et al. (2021a).

The amount of electricity in the storage unit at any time ($E_{i,m,p}^{STORAGE,BT}$, kW), can be expressed a correlation of the amount that was already stored in the battery ($E_{i,m,p-1}^{STORAGE,BT}$) (kW) considering the energy loss due to storage, plus the amount that enters the battery ($E_{i,m,p}^{STORAGE IN,BT}$, kW) considering the charge rate per time, and subtracted from the amount of energy that is removed from the battery ($E_{i,m,p}^{STORAGE OUT,BT}$, kW) considering the discharge rate per time (SIDNELL et al., 2021a):

$$E_{i,m,p}^{STORAGE,BT} = (1 - \theta) \cdot E_{i,m,p-1}^{STORAGE,BT} + hours_p \cdot (1 - X) \cdot E_{i,m,p}^{STORAGE IN,BT} - \frac{hours_p \cdot E_{i,m,p}^{STORAGE OUT,BT}}{(1 - \Delta X)} \quad (130)$$

$$i = 1, \dots, n; m = 1, \dots, k; p = 1, \dots, h$$

where θ is the static loss coefficient (%), X is the load rate (%) and ΔX discharge rate (%).

The maximum amount of electricity stored by the electrical storage unit (k_i^{BT}) must be greater or equal to the sum between the amount of energy that is already stored in the battery and the amount that is charged in the battery:

$$k_i^{BT} \geq hours_p \cdot (1 - X) \cdot E_{i,m,p}^{STORAGE IN,BT} + (1 - \theta) \cdot E_{i,m,p-1}^{STORAGE,BT} \quad (131)$$

$$i = 1, \dots, n; m = 1, \dots, k; p = 1, \dots, h$$

In addition, what is consumed from the battery cannot exceed what is charged inside it:

$$\frac{hours_p \cdot E_{i,m,p}^{STORAGE OUT,BT}}{(1 - \Delta X)} \leq (1 - \theta) \cdot E_{i,m,p-1}^{STORAGE,BT} \quad (132)$$

$$i = 1, \dots, n; m = 1, \dots, k; p = 1, \dots, h$$

The energy charged inside the battery comes from distributed energy resources:

$$E_{i,m,p}^{STORAGE IN,BT} = E_{i,m,p}^{STORAGE,GB} + E_{i,m,p}^{STORAGE,PV} + E_{i,m,p}^{STORAGE,WT} \quad (133)$$

$$i = 1, \dots, n; m = 1, \dots, k; p = 1, \dots, h$$

The energy going into and coming out of the battery is limited by the maximum charge rate and maximum discharge rate, respectively:

$$hours_p \cdot (1 - X) \cdot E_{i,m,p}^{STORAGE IN,BT} \leq k_i^{BT} \cdot X_{up} \quad i = 1, \dots, n; m = 1, \dots, k; p = 1, \dots, h \quad (134)$$

$$\frac{hours_p \cdot E_{i,m,p}^{STORAGE OUT,BT}}{(1 - \Delta X)} \leq k_i^{BT} \cdot \Delta X_{up} \quad i = 1, \dots, n; m = 1, \dots, k; p = 1, \dots, h \quad (135)$$

Furthermore, the battery capacity at any given time can be calculated using Depth of discharge (DOC), which measures the part of the battery capacity that has not been charged:

$$(1 - DOC) \cdot k_i^{BT} \leq E_{i,m,p}^{STORAGE,BT} \quad i = 1, \dots, n; m = 1, \dots, k; p = 1, \dots, h \quad (136)$$

The capacity of the battery must be within the capacity limits found in the market, when the equipment is installed (Y_i^{BT}):

$$k_i^{BT} \geq BT_{low} \cdot Y_i^{BT} \quad i = 1, \dots, n \quad (137)$$

$$k_i^{BT} \leq BT_{up} \cdot Y_i^{BT} \quad i = 1, \dots, n \quad (138)$$

where BT_{low} is the lower limit (kW) and BT_{up} is the upper limit (kW).

III.5. Model Implementation

Since a higher accuracy in the results was prioritized, the Mixed Integer Nonlinear Programming (MINLP) model was deemed more appropriate for capturing the complexities of the incentive policy selection constraints and solar collector operating constraints. Thus, the model includes three nonlinear equations (Eq. 42, 43 and 104) in addition to the linear equations and consists of both discrete and continuous variables that can be found in Appendix E. The general mathematical notation of the problem can be represented as follows:

$$\begin{aligned} & \min. C_{TOTAL}(x, y) \\ & \text{s.t. } x, y \in \Omega \\ & \Omega = \{x \in \mathbb{R}^N, y \in \mathbb{Z}^N \mid g_i(y) \geq 0, i = 1, \dots, s, h_i(x, y) \geq 0, i \\ & \quad = 1, \dots, m, h_i(x) = 0, i = 1, \dots, p\} \end{aligned} \quad (139)$$

where C_{TOTAL} is the objective function, x and y are the continuous and binary decision variables respectively, and these are subject to a set of constraints in Ω .

According to Tan et al. (2013) and considering what was discussed in the previous chapter, MINLP problems can be solved using General Algebraic Modelling System (GAMS) software (GAMS, 2021). This software is integrated with several solvers capable of solving many different types of optimization problems. Among these solvers are BARON, CPLEX, MOSEK, SNOPT. For the present model, the Branch-And-Reduce Optimization Navigator (BARON) solver was used, since this solver is capable to handle a wide range of MINLP problems, including those with nonlinear equations, discrete variables, and multiple local optima (TAWARMALANI, SAHINIDIS, 2005; SAHINIDIS, 2021). To ensure local optimum, upper and lower bond values are entered for all decision variables.

III.6. Conclusion

The proposed model introduces several novel aspects that differentiate it from the state-of-the-art, including: the adoption of a clustering procedure for systematic

determination of the time period for comparison with empirical method; consideration of time-dependent efficiency profiles for renewable resources subject to weather conditions for analysis in energy behavior among houses in the microgrid; investigation of the feasibility of biogas implementation in microgrids; selection of the best renewable energy incentive policy; and consideration of eleven different technologies to meet various energy demands. These aspects make the proposed model more comprehensive and tailored to real-world microgrid configurations, addressing some of the gaps in the literature and providing valuable insights for microgrid design and optimization.

The next chapter will look at each method of splitting the time horizon influences the results. In addition, results and discussions will be presented for different demand and configuration scenarios in order to observe the applicability of the model as well as the advantages of implementing distributed renewable energy resources in a set of houses. This will be done through a detailed analysis of costs, problem size and solution time.

CHAPTER IV – RESULTS AND DISCUSSION

IV.1. Introduction

As discussed in the first chapter, Brazil has a high potential for the use of renewable energy due to its high availability of natural resources. Taking this into consideration and based on the framework presented in the previous chapter, this chapter aims to apply the proposed model to a residential network in the city of Salvador, Bahia, Brazil.

According to the Brazilian Institute of Geography and Statistics (IBGE: Instituto Brasileiro de Geografia e Estatística) in 2020, 7.9 million of Brazilians worked remotely due to the COVID-19 pandemic. According to Manokha (2020), there is a tendency for this method of work to continue being applied even after the pandemic. Therefore, this chapter will analyze the impact of consumption dynamics on the sizing of microgrids in Brazil during the period before and after COVID-19.

Thus, the applicability of the clustering method to define the time horizon in the sizing and selection of distributed energy resources is exposed. This is done by comparing the results of the empirical method and the clustering method for the pre-COVID scenario for 5 houses.

In order to compare the model with the time-dependent efficiency profile and with constant efficiency, the results for the pre-COVID scenario for 5 houses are generated. In addition, the model that considers the time horizon splitting method and time-dependent profile for renewable resource efficiencies is generated for the pre- and post-COVID scenarios for 5 and 10 houses. These results will be compared with each other in terms of total and environmental cost, and energy resource sizing. Finally, a statistical analysis of the model will be performed in order to verify the computational effort for each scenario.

IV.2. Description of the case study

The selected study site was the city of Salvador, Bahia, Brazil. The country currently adopts the renewable resources incentive policy based on Net Metering, hence it will be analyzed whether this option remains viable for all scenarios. Currently, Brazil does not have a well-defined carbon pricing. Therefore, in order to find the environmental costs of the renewable resources, base values were considered in relation to countries that already have well-defined carbon pricing such as the UK, which adopts a carbon tax value of R\$0.12/kg CO₂ using a conversion of R\$6.58/£ (Sidnell et al, 2021). Considering that the GDP in Brazil is approximately half the value of the UK, the carbon tax in Brazil was estimated as R\$0.06/kg CO₂. In addition, for the calculation of the capital recovery factor an interest rate of 0.07 and 20 years was considered.

The upper and lower limits of the model resources were stipulated according to local constraints, capacity limits found in the market and regulations. The fixed costs were estimated according to studies such as Mustafa (2010) and the variable costs, according to the fuel or the water price when the equipment generates hot water. These parameters are presented in Appendix A. This chapter reports the other parameters used for the case study, which include the distance between the residences in the microgrid, the energy demand profile, the environmental data for the region found in the World Bank Group (2022); DTU Wind Energy (2022), the grid energy and natural gas prices.

IV.2.1 Parameters

The case study considered the Rua das Estrelícias in Alphaville 2, Salvador, Bahia to define the average distance between the houses in the model. Table 16 show the distances between the houses, as well as the distance between the houses and the biodigester installed for 10 houses. In addition, the hatched area in the table refers to the distances for the micro-grid of 5 houses.

Table 16 - Distance between houses in meters for the scenario with 10 houses.

	i1	i2	i3	i4	i5	i6	i7	i8	i9	i10
i1	0	5	23	13	18	41	59	54	72	53
i2	5	0	5	18	13	28	46	49	67	58
i3	23	5	0	36	18	8	23	36	54	76
i4	13	18	36	0	5	59	36	69	87	10
i5	18	13	18	5	0	82	59	46	64	15
i6	41	28	8	59	82	0	36	18	41	99
i7	59	46	23	36	59	36	0	13	18	122
i8	54	49	36	69	46	18	13	0	5	109
i9	72	67	54	87	64	41	18	5	0	117
i10	53	58	76	10	15	99	122	109	117	0
Biodigester	36	18	18	23	5	18	41	23	51	28

a. Weather data

Figure 46 shows the behavior of solar irradiation (a), ambient temperature (b), wind speed (c) and wind power (d) in Salvador, Bahia. The data are divided into seasons for better visualization, as follows: m1: January, February, March, April, m2: May, June, July, August, September and m3: October, November, December. The explanation of the division of the year into these seasons will be presented below, in section IV.3.

In season m1 the solar irradiation and consequently the temperature is higher than the other seasons; however, the wind speed and wind power are lower in season m1 than in the other seasons. These variations in weather conditions between seasons can impact the design of the system and will be analyzed later.

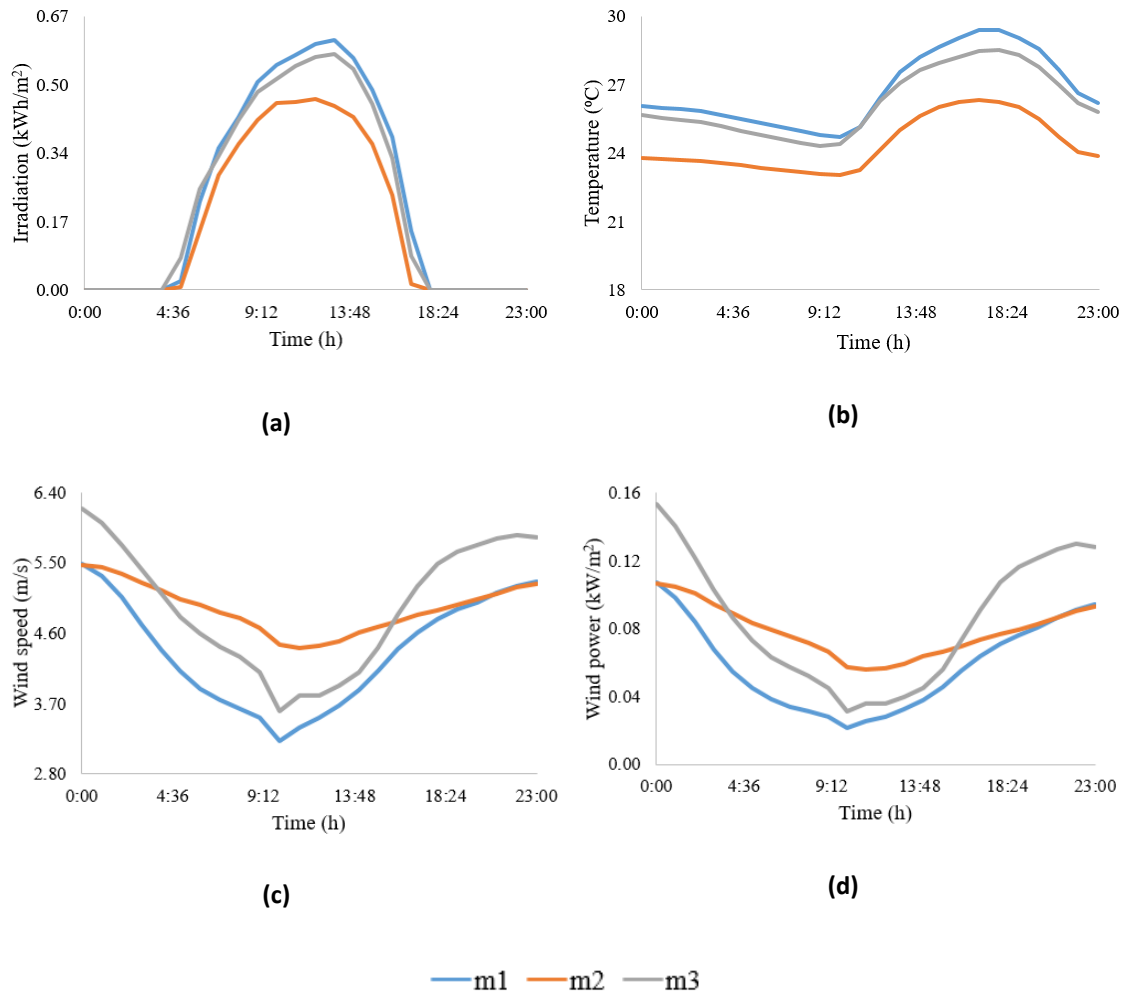


Figure 46 - Behavior of the weather in Brazil: (a) Solar irradiation; (b) Temperature; (c) Wind speed; (d) Wind power. Source: World Bank Group (2022); DTU Wind Energy (2022)

b. Electricity and natural gas prices

In order to avoid overloading the power distribution system, Brazil adopts different electricity rates throughout the day. These are defined as peak, off-peak and intermediate time. Peak time for the state of Bahia is considered to be between 18:00 and 20:59, where there is normally higher energy consumption in households. The intermediate schedule is the 2h before peak time (16:00 to 17:59) which characterizes the period that consumption starts to increase in relation to the off-peak schedule (the remaining hours) (NEOENERGIA COELBA, 2020). Figure 47 shows the variation in the price of electricity obtained from the central grid for both pre- and post-COVID scenarios. In the post-COVID case there was a 15% increase in the electricity rate during the peak period in relation to pre-COVID, a 10% increase in the off-peak period and 16% in the intermediate period, respectively. This increase can be attributed to the consequent increase in grid usage due to the COVID-19 pandemic.

The same behavior is observed with the prices for natural gas. As illustrated in Table 17, the value of natural gas per m³ was 53% higher in the post- than the pre-COVID scenario. In addition, the price of the fixed amount paid per month increased by 25%.

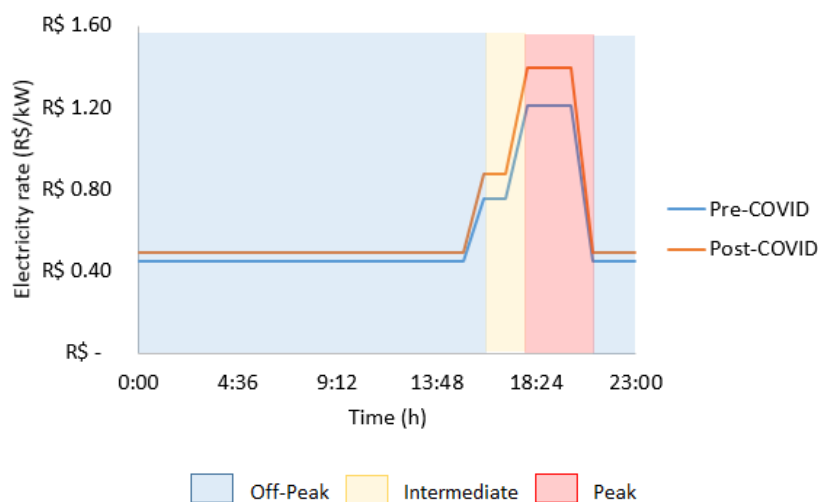


Figure 47 - Electricity rate (R\$/kW) from the central grid in Bahia for the pre- and post-COVID scenario. Source: BRASIL, 2019; BRASIL, 2022.

Table 17- Cost of natural gas in Bahia for the pre-covid and post-covid states

Gas Cost	Pre-COVID	Post-COVID	References
Natural Gas (R\$/m ³)	0.40	0.52	BAHIAGAS (2019)
Fix Gas (R\$/month)	6.81	8.53	BAHIAGAS (2022)

c. Demands

The demands adopted in the model were electricity, cooling, hot water and gas for cooking. Because there are no studies that analyze the average Brazilian energy demand after COVID-19, the demands for the post-COVID scenario were estimated in relation to the pre-COVID case. For the electricity demand this value was 25% higher, with a continuous behavior during the day, due to the remote work often adopted at this time (MACEDO, 2021). Due to the lack of data and information on how the other demand profiles perform in the post-COVID scenario, only the percentage increase over the pre-COVID profile was considered.

For hot water demand an increase of 15% was considered, for cooling demand, an increase of 50%, and for cooking gas, an increase of 25%. The behavior of the demands per season during the day is shown in Figure 48.

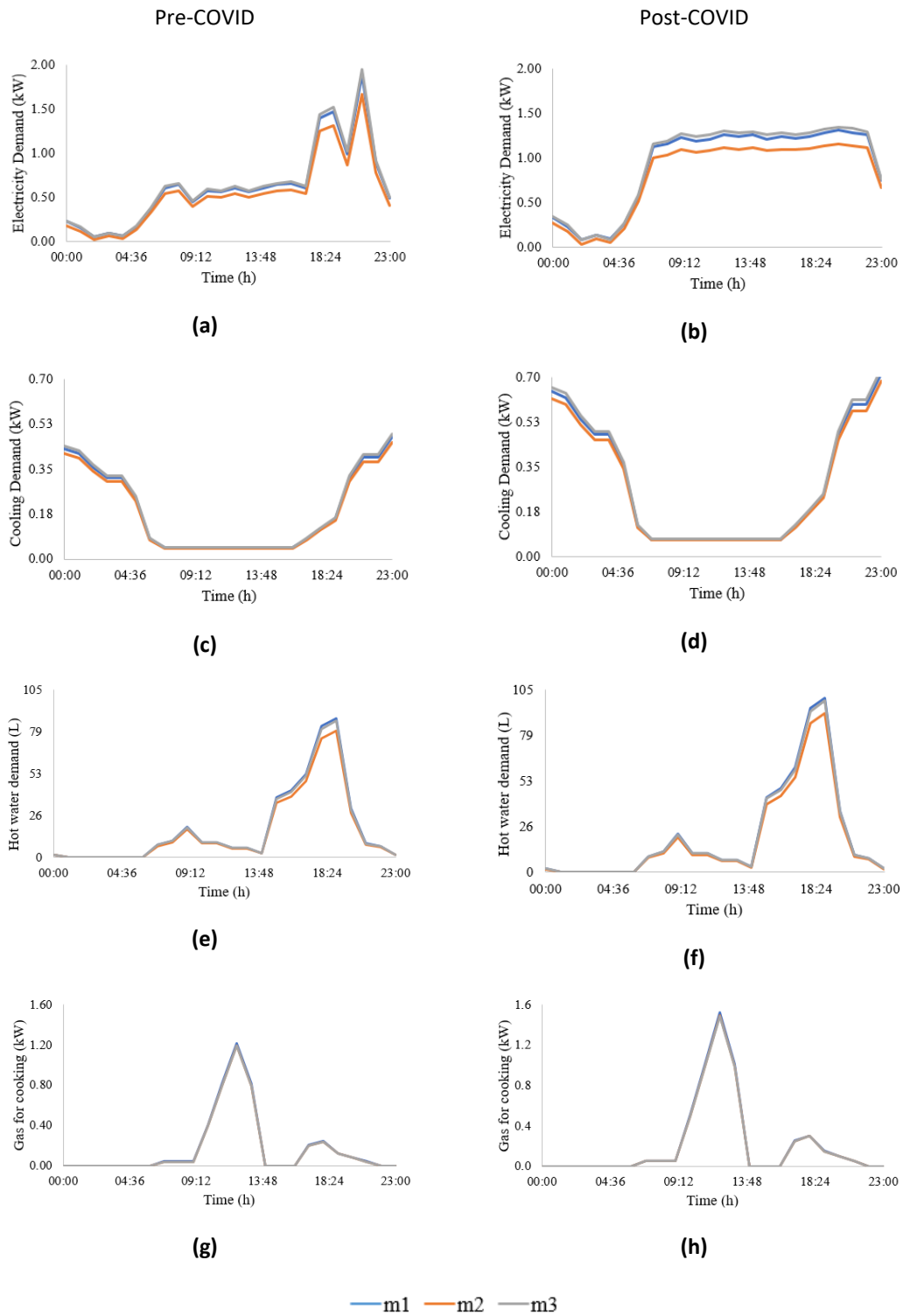


Figure 48 - Average energy demand in Salvador, Brazil in the pre- and post-COVID scenarios for: (a-b) electrical demand (kW); (c-d) cooling demand (kW); (e-f) hot water (L); (g-h) gas for cooking (kW). Source: Baptista (2006); EPE (2018); EPE (2021).

Each household has a different consumption profile which depends on the number of people residing in the residence, and their way of life. To consider different profiles, a variation in demand was considered for each residence. Therefore, the average

demand presented in Figure 48 was multiplied by the scalars in Table 18 and thus the demand for each residence was estimated.

Table 18 - Scalar of the demand for each house

Houses	Scalar
i1, i6	0.2
i2, i7	0.6
i3, i8	1.0
i4, i9	1.4
i5, i10	1.8

IV.3. Splitting the Time Horizon

In order to separate the time horizon of the optimization problem, the methods (empirical and clustering) proposed in the previous chapter were applied to data of electric demand, solar irradiation and wind speed and electric energy price for a residence in Salvador, Bahia, Brazil. The definitions of each season as well as the time periods will be detailed below for each method.

IV.1. The Empirical Method

For comparison purposes with the systematic clustering method, the empirical method was applied only for the pre-COVID state. Thus, the division of the time horizon by this method is expressed in Figure 49. In this distribution, the year was divided into two seasons and seven periods of various durations in hours.

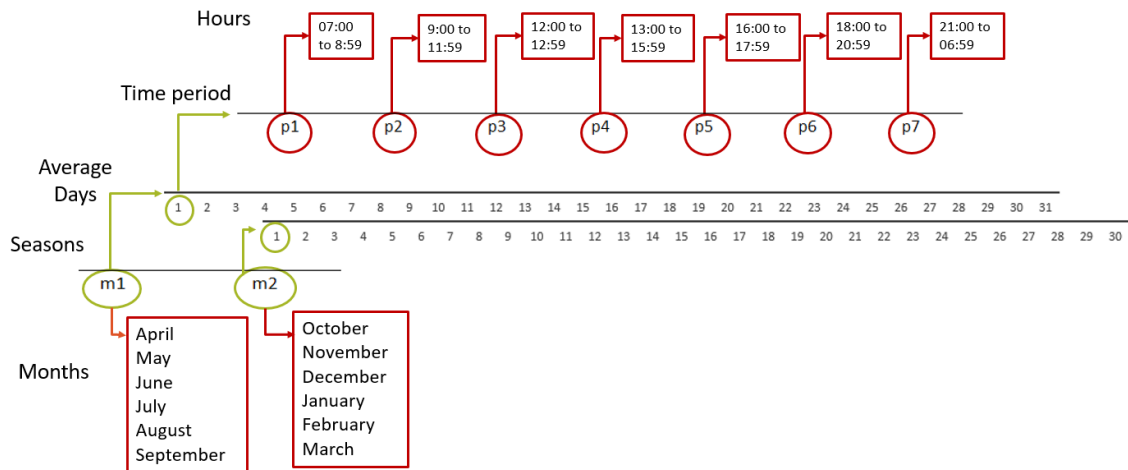


Figure 49 - Time period during the year and the day for the pre-COVID state with empirical method.

IV.2. The Clustering Method

The methodology for the clustering of time periods, explained in the previous chapter, was adopted for both the pre- and post-COVID scenarios. Figure 50 shows the time division found for the pre-COVID case. This was divided into three seasons and eighth periods.

Figure 51 illustrates the distribution of time periods for the post-COVID scenario. This was divided into three seasons and five periods. The analysis performed to determine the time periods according to the methodology exposed in the previous chapter is in Appendix C, as well as the code used in the Python language is presented in Appendix B.

It is observed that there was a reduction in the number of time periods from the Pre-COVID to the Post-COVID scenario. This can be attributed to the fact that the Post-COVID scenario had a constant distribution of electrical demand throughout the day, allowing these periods to be aggregated into the same time cluster.

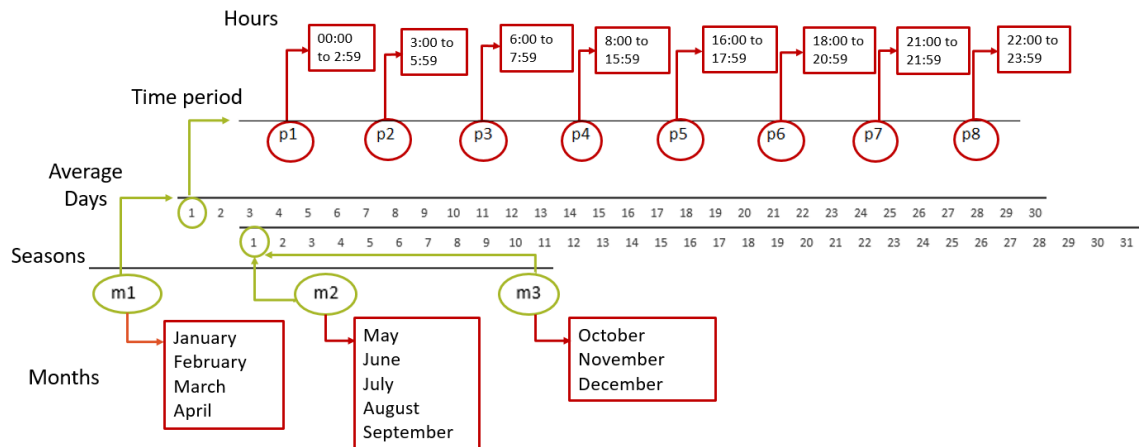


Figure 50 - Time period during the year for the pre-COVID scenario.

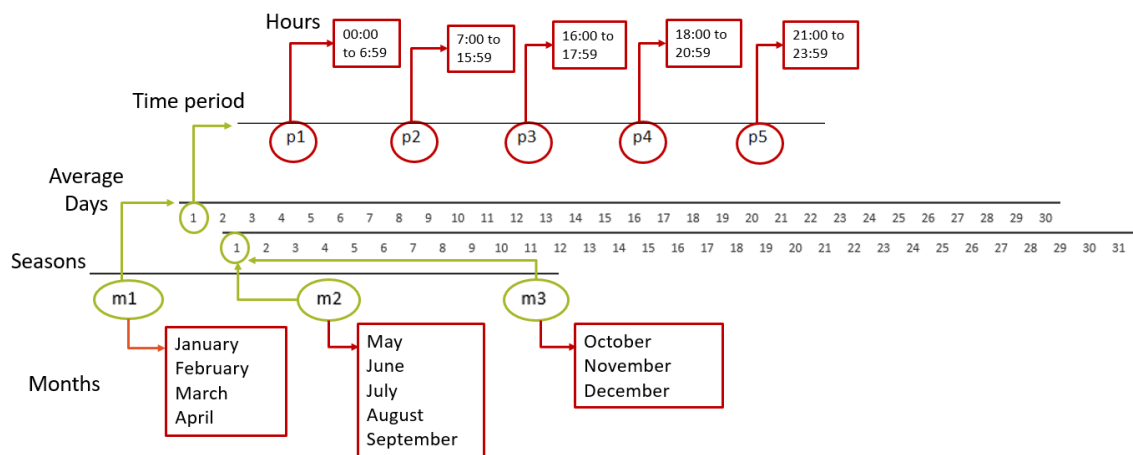


Figure 51 - Time period during the day for the post-COVID state.

IV.4. Results and discussions

The following sections will present the microgrid configuration for different scenarios to show how the model implementation influence the microgrid design, namely: time horizon splitting method; time-dependent profile for efficiencies in wind and photovoltaic generation; demand profile; number of houses. Three different scenarios are considered, in addition to the baseline for each scenario, i.e. without distributed energy resources only considering the use of the central grid:

- Scenario 1: time-dependent profiles for efficiency of the solar panel, solar collector and wind turbine were neglected; time domain was splitted using the clustering method.
- Scenario 2: time-dependent profile for efficiencies of the solar panel, solar collector and wind turbine were considered; time domain was splitted using empirical method;

- Scenario 3: time-dependent profile for efficiencies of the solar panel, solar collector and wind turbine were considered; clustering of the time periods was carried out.

In addition, the simulations consider two situations: pre-COVID (E) and post-COVID (O) in the characterization of the energy demand. Scenarios 1, 2 and 3 is evaluated during pre-COVID with 5 houses (S1E5, S2E5, S3E5), whereas Scenario 3 is further modeled for 5 houses during post-COVID (S3O5), 10 houses during pre-COVID (S3E10) and post-COVID (S3O10). For the baseline (B), since the distinction between S1E5 and S3E5 lies in the operation of renewable resources, and the baseline does not incorporate their use, the same baseline was used for both (B13E5). For the S2E5 scenario the corresponding baseline is B2E5. For S3O5 the corresponding baseline is B3O5. For S3E10 the corresponding baseline is B3E10. For S3O10 the corresponding baseline is B3O10. This information is summarized in the Table 19.

Table 19 – Simulated cases

Scenario	Empirical method	Cluster method	Time-dependent profiles for efficiency of the DER	Pre-COVID	Post-COVID	Houses	Acronym
1	No	Yes	No	Yes	No	5	S1E5
2	Yes	No	Yes	Yes	No	5	S2E5
3	No	Yes	Yes	Yes	No	5	S3E5
						10	S3E10
	No	Yes	Yes	No	Yes	5	S3O5
						10	S3O10
Baseline1,3	No	Yes	No	Yes	No	5	B13E5
						10	B13E10
	No	Yes	No	No	Yes	5	B13O5
						10	B13O10
Baseline 2	Yes	No	No	Yes	No	5	B2E5

The impact on cost and desing for each scenario will be explained in the following sections. Finally, a model statistics analysis will be performed in order to verify the computational effort for each proposed model. The description of the behavior profile of energy generation and consumption for each scenario is explained in Appendix D.

IV.4.1. S1E5: Scenario without time-dependent profile for efficiency of the DER and cluster method during pre-COVID for five houses

Figure 52 depicts the optimal configuration for Scenario 1 (time-constant profiles and clustering) during pre-COVID for 5 houses. For all the houses, air conditioning is

installed to supply the cooling demand. Regarding electricity generation, only houses i1, i3 and i5 adopted the wind turbine. This can be attributed to the restriction of wind turbine allocation that cannot occur in neighboring houses.

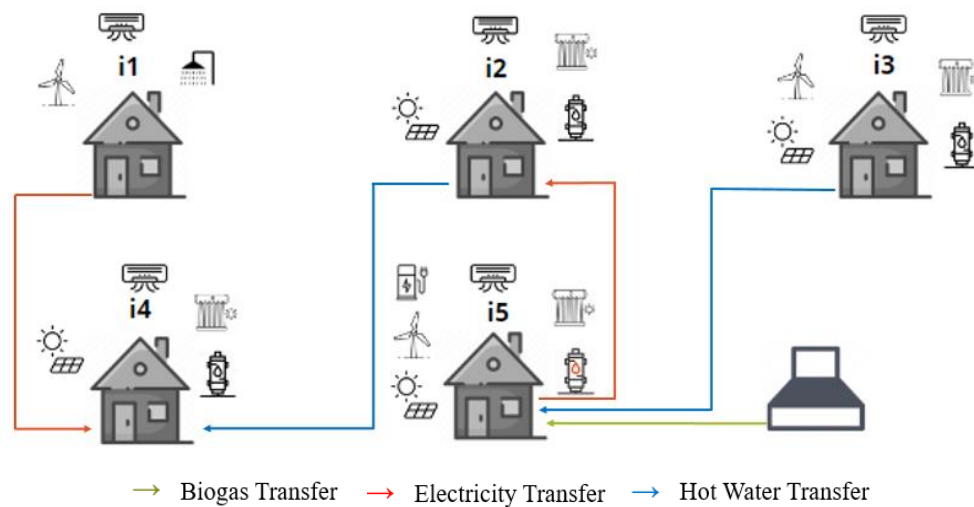


Figure 52 - Optimal energy resources and connections between houses for Scenario 1 during pre-COVID for five houses (S1E5).

The photovoltaic panel was installed in all houses except house i1. In this scenario, the variation in the efficiency of the photovoltaic panel and wind turbine was not considered and this may have caused an overestimated utilization for the wind turbine and photovoltaic panel. This can be seen in the generation profiles for these resources in Appendix D. Due to this behavior, the energy generation was overestimated and therefore only the installation of the battery in the house i5 was considered, since this house has a higher electrical demand.

Regarding hot water demand, house i1 is supplied by an electric shower, due to its lower demand, and all other houses have a solar collector coupled with a natural gas or biogas heater. The optimal microgrid shares energy and hot water. Houses i1 and i5 transfer electricity to houses i4 and i2, respectively. This may happen because house i1 has a lower demand, being able to share its surplus energy with house i4, which has a higher demand; while the larger equipment in house i5 can share energy with house i2. In addition, to meet the demand of house i5, hot water needs to be transferred from house i3. House i4 also receives excess of hot water produced by house i2. The results indicate that it is more feasible to receive hot water from another house than to install a bigger equipment in the residence. The sizing of each equipment will be discussed in more detail in sub-section IV.7.

A biodigester with a volume of 0.84 m³ was installed to supply the gas demand for cooking food and the biogas for the biogas heater in house i5. The amount of organic material produced per day in the household is sufficient to generate the biogas volume required to meet the demand for cooking-gas and biogas heater. Hence, purchasing

extra organic material is not required. In order to fulfill their gas for cooking needs, houses i1, i2, i3, and i4 opted for natural gas due to their lower demand compared to house i5. On the other hand, in house i5 some of the cooking gas demand was met by utilizing the biogas produced. In this situation it has become more feasible to use part of the biogas produced to meet the gas demand for cooking, in order to reduce the use of natural gas, than to use it completely for hot water demand, since the biogas produced was not enough to meet the entire hot water demand. In Appendix D, the optimal yearly profiles of electricity, hot water and gas for cooking production are discussed facing the demands of the households in the microgrid in more detail.

IV.4.2. S2E5: Scenario with time-dependent profiles for efficiency of the DER and empirical method during pre-COVID for five houses

Figure 53 represents the optimal configuration of the microgrid for Scenario 2 (time-dependent profiles and no clustering) during pre-COVID for 5 houses. Air conditioning was used to meet the cooling demand in all the houses. In this scenario, due to the difference in the method of splitting the time horizon, the period of sunlight in the region is distributed over more than one-time period (p1 to p5), therefore the optimal solution considered the installation of solar panels for electricity generation and solar collectors for hot water generation in all the residences. In addition, wind turbines are considered in houses i1, i3 and i5 to meet the demand of electric energy. House i1 produces more than necessary to meet its own demand, then it transfers energy to house i5. The same happens with house i3 that transfer energy to house i4.

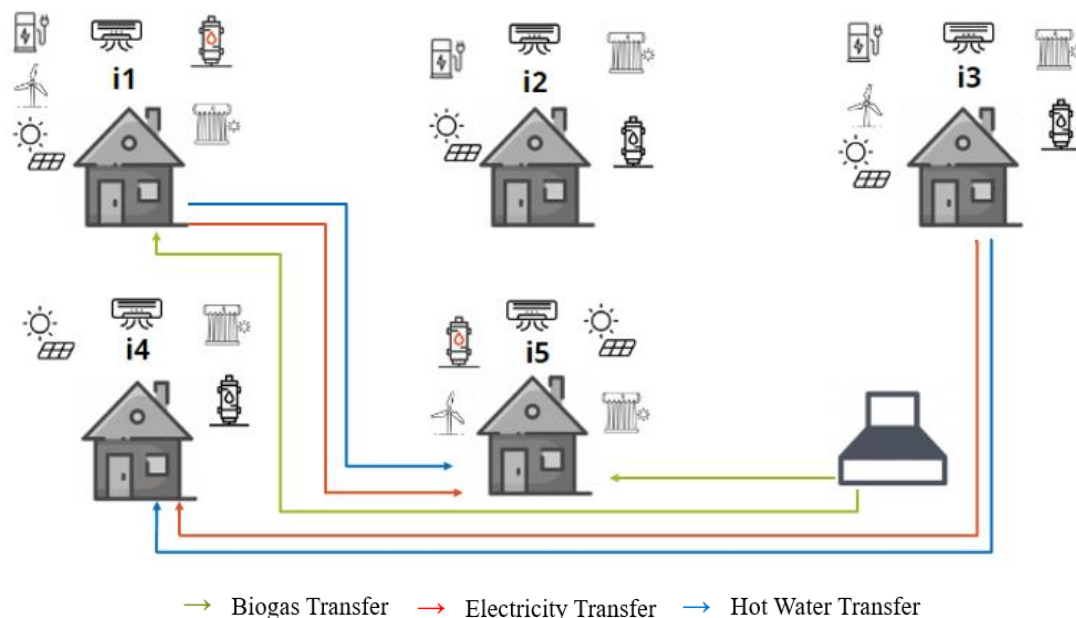


Figure 53 - Optimal energy resources and connections between houses for Scenario 2 during pre-COVID for five houses (S2E5).

The battery was installed in houses i1, i2 and i3. Installing a smaller battery in houses i1 and i3, which share energy with houses of higher demand i4 and i5, is more profitable than installing a larger battery in these houses (i4 and i5). Since house i2 has only photovoltaic energy to meet the demand, the battery was installed to meet the self-demand when energy from the central network is more expensive. This will be discussed in more detail in the following sections.

A biodigester was installed in the microgrid, with a volume of 0.86 m³, requiring 0.0757 kg/day of extra organic matter. Under these conditions the demand of gas for cooking from house i1 in all seasons and time periods is supplied by biogas, as well as part of the hot water generation in the i1 and i5 houses. This suggests that using biogas is a more feasible option than buying natural gas from the grid for cooking purposes in house i1. However, only natural gas was used for cooking in houses i2, i3, i4, and i5, as the limited production of biogas could not meet the demand of all households.

For hot water generation, besides the solar collector, a biogas heater was installed in houses i1 and i5 and a natural gas heater in houses i2, i3 and i4. Due to the limited biogas production, it can be used in house i5, which has the highest energy demand, and the rest in house i1, which has the lowest. With this, house i1 can share the excess hot water produced with house i5. This is because it is more feasible to install a smaller capacity biogas heater unit in each house, rather than a larger capacity unit in house i5.

The capacities of the equipment will be discussed in more detail in section IV.7. Because natural gas has a continuous supply, it was used in the other houses to meet the rest of the demand that the solar collector could not meet. Also, the hot water was shared from house i3 to house i4 which has a higher demand than houses i1, i2 and i3.

IV.4.3. S3E5: Scenario with time-dependent profile for efficiency of the DER and clustering method during pre-COVID for five houses

Figure 54 expresses the optimal configuration for scenario 3 (time-dependent profiles and clustering) during pre-COVID for the microgrid with 5 houses. Air conditioning was used to meet the cooling demand in all the houses. In this scenario, due to the time horizon being divided by the clustering method, the period of sunlight in the region is distributed in 3 periods (p3 to p5), ensuring the best use of sunlight and, therefore, the installation of solar panels for electricity and solar collectors for hot water production in all homes was considered. In addition, for the generation of electric energy, wind turbines were considered in houses i1, i3 and i5. As well as in the previous scenario, because house i1 produced more than necessary to meet its own demand, it shares energy with house i5, and the same happened with house i3, sharing energy with house i4.

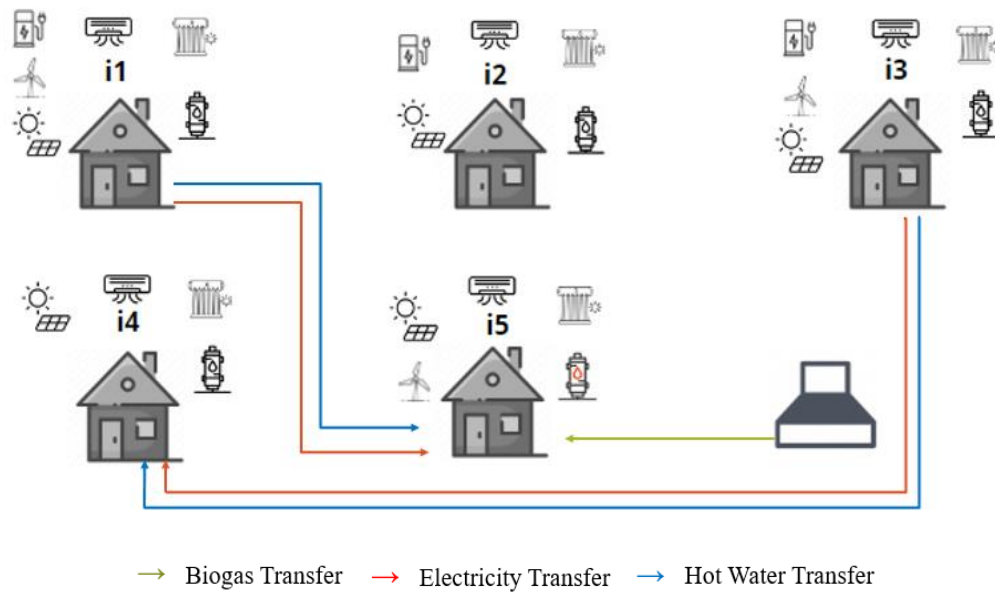


Figure 54- Optimal energy resources and connections between houses for Scenario 3 during pre-COVID for five houses (S3E5).

The battery was installed in houses i1, i2 and i3. It seems to be more profitable to install a smaller battery in the houses (i1 and i3) which transfer energy to the houses of higher demand (i4 and i5) than to install a larger battery in these houses (i4 and i5). As in the previous scenario, because house i2 has only photovoltaic energy to meet the demand, the battery was considered to meet the demand at times when energy from the central grid is more expensive, as will be shown in more detail below.

For the generation of hot water, besides the solar collector, a biogas heater was installed in house 5 and a natural gas heater in houses i1, i2, i3 and i4. This is due to the limited biogas production, preferably sent to house i5 because of its higher demand. The biodigester allocated in the system has 0.84 m³ and the biogas was distributed to house i5 to meet not only the gas demand for hot water generation, but also for cooking food, the generation profile can be found in Appendix D. The amount of organic matter produced per day in the household is sufficient to generate the volume of biogas needed to meet the gas demand for cooking and biogas heater. Since natural gas has a continuous supply, it was used in the other houses to meet the remaining hot water demand not met by the solar collector and the cooking gas demand in houses i1, i2, i3 and i4. In addition, house i5 receives hot water from house i1, and house i4, which has the highest demand among houses i1, i2 and i3, receives hot water from house i3.

Finally, it was observed that there was a greater amount of resources installed in this scenario than scenario 1, for instance. This is due to the fact that this scenario considers the time-dependency of the energy resource efficiencies, so more energy capacity was needed to supply the demand. A more detailed analysis of this will be made in the section IV.8.

IV.4.4. S305: Scenario with time-dependent profile for efficiency of the DER and clustering method during post-COVID for five houses

Figure 55 illustrates the optimal configuration of the microgrid for 5 houses post-COVID in scenario 3 (time-dependent profiles and clustering). For this particular scenario, it is important to remember that due to the change in the energy consumption profile, the day was distributed in 5 periods.

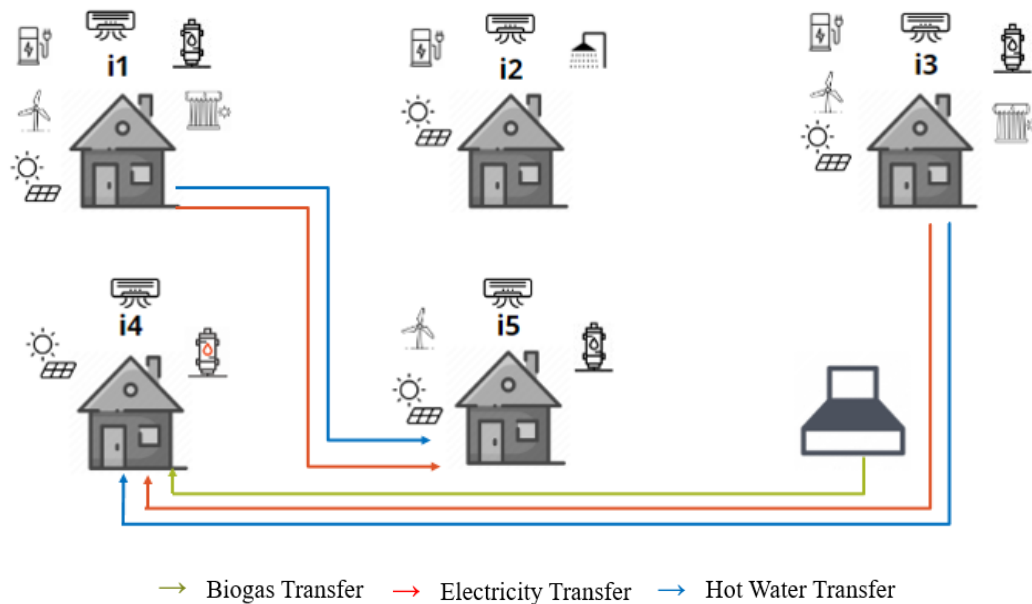


Figure 55 - Optimal energy resources and connections between houses for Scenario 3 post-COVID for five houses (S305).

Solar panels are installed in all residences to supply electrical energy, and houses i1, i3 and i5 further adopt the wind turbine. Because houses i4 and i5 have a higher demand for electricity, they receive electricity from houses i3 and i1, respectively.

As in the previous scenarios, the battery is installed in houses i1, i2 and i3. This is because it is more profitable to install a smaller battery in the houses i1 and i3, with lower demand which then transfer energy to the houses with higher demand (i4 and i5) than to install a larger battery in these houses (i4 and i5). House i2 has only photovoltaic energy to meet its requirements, then battery is considered to meet the demand when energy from the central grid is more expensive.

To meet the hot water demand, the natural gas heater and the solar collector are installed in houses i1 and i3. Houses i1 and i3 share hot water with houses i5 and i4, respectively. Since they have a lower hot water demand than houses i5 and i4, the results indicate that it is more profitable to install the two technologies to meet the demands of the 4 houses than to install, for example, a bigger equipment in house i4 and house i5. A biogas heater is further installed in house i4 to supply the rest of the hot

water demand and the natural gas heater is installed in house i5. In house i2 the electric shower is sufficient to meet all its hot water demand.

Furthermore, air conditioning is used to meet the cooling demand in all houses. A biodigester with a volume of 1.48 m³ was installed, requiring 12.72 kg of organic material per day in one house, to supply the biogas heater of the house i4. Due to the increased consumption compared to the pre-COVID scenarios and due to the limited biogas production, in this case it became more feasible to be used in house i4 which has a lower demand compared to house i5, for example. In all houses, natural gas was used to supply the gas for cooking demand because, under the assumptions considered, it is more profitable to use natural gas than to increase the production of biogas. Furthermore, in this scenario there are fewer equipment than in the respective scenario for pre-COVID, however the capacities of resources (photovoltaic panel, wind turbine, battery and air conditioning) are higher than those found pre-COVID as can be observed in the section IV.7. This is due to the increased energy demand and behavior change in the post covid state.

IV.4.5. S3E10: Scenario with time-dependent profile for efficiency of the DER and clustering method during pre-COVID for ten houses

For the microgrid with 10 houses in Scenario 3 pre-COVID, the optimal configuration is illustrated in Figure 56. Regarding to the electricity demand, photovoltaic panels were installed in all of the houses. In addition, wind turbines were also installed in houses i1, i3, i5, i7 and i9. This can be explained either because they share energy with other houses, as is the case with house i1, i3, i7, i9, thus needing more capacity than their electricity demand, or because the electricity demand of this house is high in relation to the others, as is the case with house i5.

The transfer of electricity was observed from house i1 to house i8, from house i3 to house i10, from house i6 to house i2, from house i7 to house i5, and from house i9 to house i4, respectively. It was found that most of the electricity sharing occurred from houses with lower demand to houses with higher demand and according to the distance between them. For house i9, although it has the same electricity demand as house i4, it presents a greater installed capacity, being able to meet its demand and share the excess energy.

In addition, the battery was considered for the houses that are sharing electricity with others (i1, i3, i6, i7 and i9) and for the house i2 that the installed capacity is not enough to cover all its demand. The sizing values for each technology will be seen in more detail in section IV.7.

To meet the hot water demand, all the houses had the solar collector installed. This can be explained by the fact that in this scenario the periods of solar incidence are

distributed in more than one cluster, allowing a greater exploitation of the solar resources available. Moreover, natural gas heaters were used in all houses except for house i6, which used the biogas heater instead.

Furthermore, air conditioning was used to meet the air cooling demand in all the houses. A biodigester of size 1.68 m³ was installed in the microgrid and is connected to houses i5 and i6, this provides biogas for cooking gas demand and the biogas heater. For this there was no need for the houses to purchase extra organic material other than that produced in the households.

A 1.68 m³ biodigester was installed in the microgrid, providing biogas for cooking gas demand in houses i5 and i6 and for the biogas heater in house i6. No additional organic material needed to be purchased as the households produced enough for their needs. Natural gas supplied the cooking gas demand in houses i1, i2, i3, i4, i7, i8, i9, and i10, while biogas was exclusively used in house i6. In house i5, however, it was more cost-effective to use both natural gas and biogas, as shown in Appendix D. The limited use of biogas in this case could be due to its higher cost compared to natural gas from the grid. Biogas was only supplied to the houses nearest to the biodigester (house i5 and i6), possibly due to lower transportation costs and less loss of biogas during transportation.

The main difference from the microgrid of 10 houses to the 5 houses, when comparing the five equivalent houses in both situations, is the energy sharing between them. As the present scenario has the possibility of connection with other five houses, there was a change in the behavior of both electrical and thermal energy transfer. Furthermore, in this scenario house i6 generates hot water through the biogas heater instead of house i5. This occurs because the new configuration allows house i6 to share hot water with house i5, indicating that it is more feasible to install a smaller capacity water heater unit in each house, rather than a larger capacity unit in house i5. The capacities of the equipment will be discussed in more detail in section IV.7.

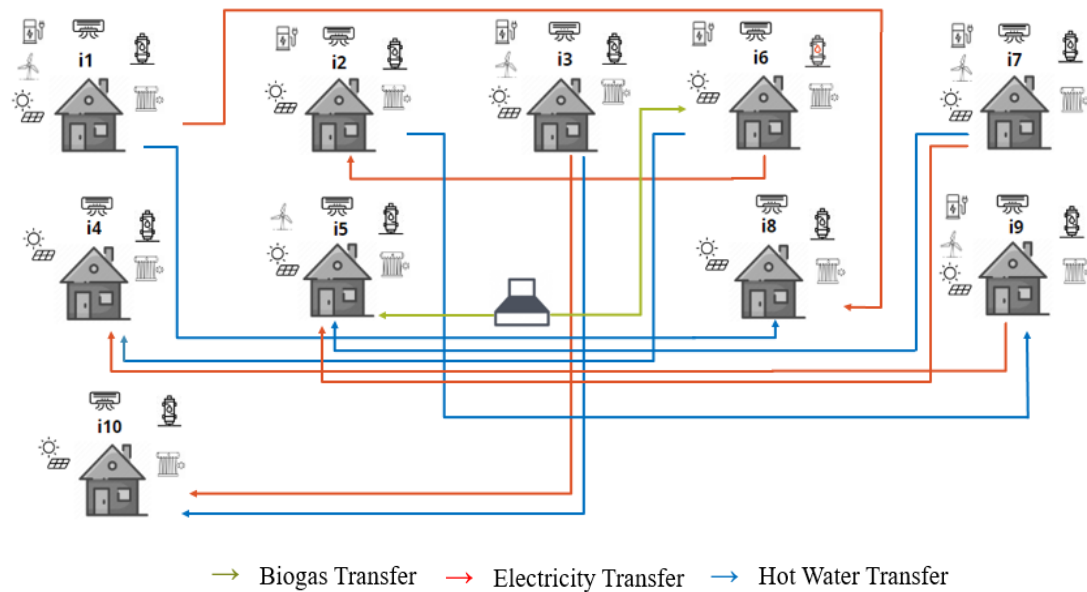


Figure 56 - Diagram of energy resources and connections between houses for the microgrid with 10 houses pre-COVID for Scenario 3 (S3E10).

IV.4.6. S3010: Scenario with time-dependent profile for efficiency of the DER and clustering method during post-COVID for ten houses

For the microgrid with 10 houses in the Scenario 3 post-COVID, the optimal configuration is illustrated in Figure 57. Regarding to the electricity demand, photovoltaic panels were installed in all of the houses. In addition, wind turbines were also installed in houses i1, i3, i6, i8 and i10. This can be explained either because they share energy with other houses, as is the case with house i1, i3, i6, i8, thus needing more capacity than their electricity demand, or because the electricity demand of this house is high in relation to the others, as is the case with house i10.

The transfer of electricity was observed from the house i1 to house i5, from house i3 to house i10, from house i6 to house i9, from house i7 to house i2, and from house i8 to house i4, respectively. As in the other scenario, it was found that the sharing of electricity happened from houses of lower demand to houses of higher demand and according to the distance between them. In addition, because houses i3 and i6 are separated by a small street, they were not considered adjacent houses and therefore it was possible to install the wind turbines in both houses.

In addition, the battery was considered for the houses that are sharing electricity with others (i1, i3, i6, i7 and i8) and for the house i2, for which the installed capacity is not enough to cover all its demand. The sizing values for each technology will be seen in more detail in section IV.7.

To meet the hot water demand, natural gas heater was used in all houses except house i5, which used the biogas heater instead. In addition, all the houses that share hot

water with other houses also had the solar collector installed (i1, i2, i3, i6 and i7). Since these houses have lower hot water demand compared to the houses that are receiving the hot water, it became more feasible to implement two technologies in these houses than to install a larger technology in the houses with higher demand, since there is a limitation in the capacity of the equipment.

Furthermore, air conditioning was used to meet the cooling demand in all the houses. To provide biogas for the biogas heater installed in house i5 a biodigester of 1.90 m³ was used, with the need to acquire 4.30 kg of organic material per day in a house. This can be explained by the limited biogas production. For the gas demand for cooking, all the houses use natural gas, indicating its profitability. Under the assumptions considered for this scenario, using natural gas is better than increasing the production of biogas to meet the gas demand for cooking.

Because this scenario has the possibility of different connections between the other houses, as well as the energy profile enables the use of different technologies, some changes in the configuration of the five equivalent houses were observed between this scenario and the one with 5 houses. Among them are: in house i2, the installation of a solar collector and gas heater instead of an electric shower; in house i4, the installation of a gas heater instead of a biogas heater; in house i5, the non-installation of a wind turbine and the installation of a biogas heater instead of a gas heater.

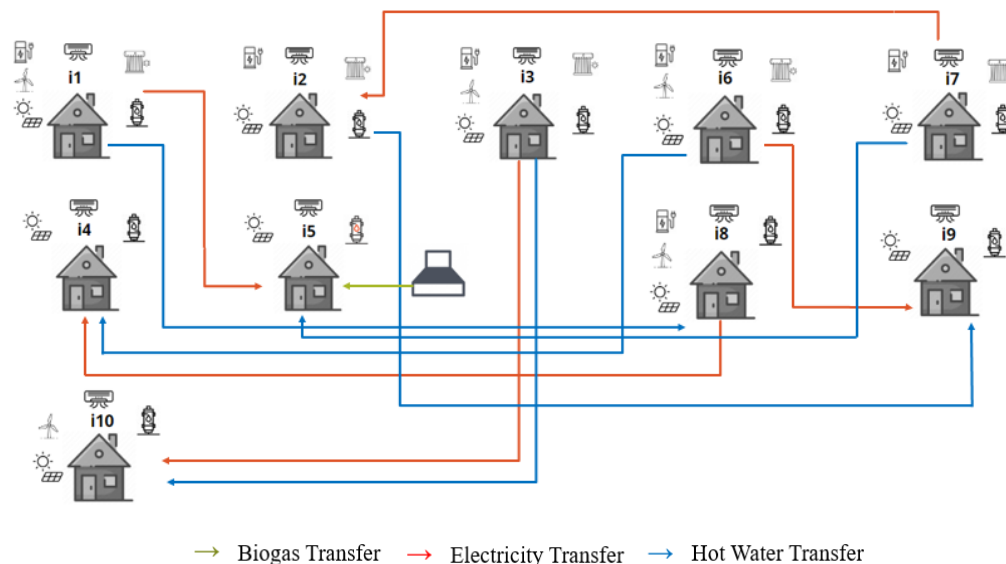


Figure 57 - Diagram of energy resources and connections between houses for the microgrid with 10 houses post-COVID for Scenario 3 (S3O10).

IV.5. Costs and revenues

For all scenarios investigated, the incentive policy selected for the systems was Net Metering. This is the current policy adopted in the country and confirms that, in the

current conditions of technology and local electricity prices, this policy continues to be the most advantageous for Brazil.

Table 20 and Figure 58 shows the costs and revenues found for all scenarios investigated, which will be analyzed below. Because the difference between S1E5 and S3E5 is in the operation of the renewable resources (considering or not time-dependent profile for efficiencies of the resources), the baseline for these two scenarios is the same, as it does not include the use of renewable resources.

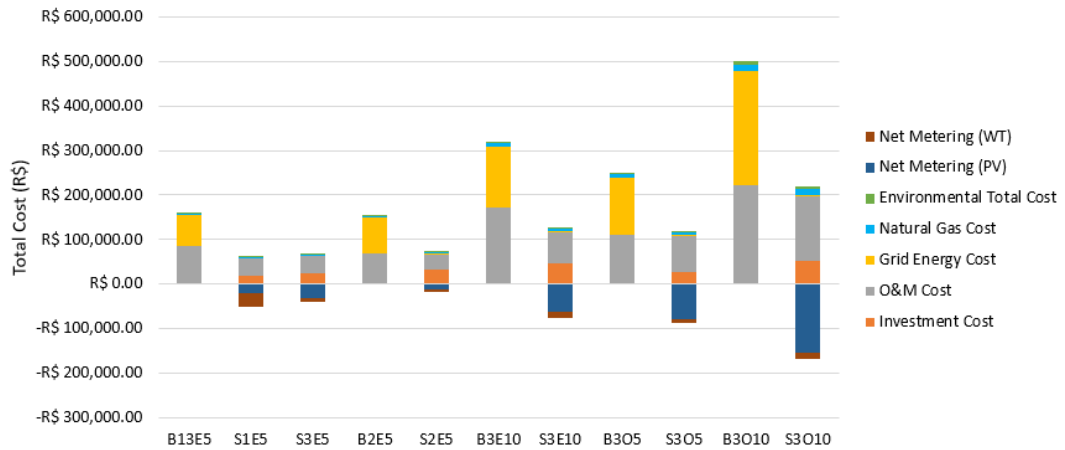


Figure 58 - Total cost for each scenario and its respective baseline.

Table 20 - Costs and revenues for all scenarios

Stage	#	Scenario	Houses	Total Cost (R\$)	Investment Cost (R\$)	O&M Cost(R\$)	Grid Energy Cost (R\$)	Natural Gas Cost (R\$)	Environmental Total Cost (R\$)	Net Metering (PV)	Net Metering (WT)
Pre-COVID	B13E5	Baseline of scenario 1,3	5	160,210.26	990.15	84,672.04	68,722.25	3,809.99	2,015.82	-	-
	S1E5	Scenario 1	5	10,261.60	18,090.40	39,108.92	-	2,557.95	1,256.69	20,680.62	30,071.75
	S3E5	Scenario 3	5	28,956.95	24,450.86	38,539.39	845.82	2,599.89	1,428.47	31,004.54	7,902.94
	B2E5	Baseline of scenario 2	5	154,151.17	1,430.53	66,499.38	83,043.32	1,766.99	1,410.94	-	-
	S2E5	Scenario 2	5	52,458.11	32,224.66	33,506.08	4,139.58	693.10	554.72	11,640.61	7,019.43
	B3E10	Baseline of scenario 3	10	320,420.51	1,980.30	169,344.09	137,444.50	7,619.99	4,031.64	-	-
	S3E10	Scenario 3	10	50,434.78	47,079.12	70,171.55	1,117.29	5,122.33	2,846.50	62,623.51	13,278.50
Post-COVID	B3O5	Baseline of scenario 3	5	249,889.14	1,398.02	109,351.27	128,398.45	7,595.89	3,145.50	-	-
	S3O5	Scenario 3	5	31,596.10	28,056.46	80,756.17	1,755.81	5,985.75	2,562.79	77,561.29	9,959.60
	B3O10	Baseline of scenario 3	10	499,757.41	2,775.18	218,702.54	256,796.90	15,191.78	6,291.01	-	-
	S3O10	Scenario 3	10	50,370.09	51,037.36	146,725.13	2,637.08	12,629.48	5,176.71	153,671.66	14,164.02

IV.5.1. The impact of Time-Dependent Efficiency Profile of the renewable resources on Costs and Revenues

When incorporating RES in S1E5, despite neglecting time-dependent efficiencies, it presented a 94% reduction in total cost compared to B13E5, with a further 38% reduction in environmental cost. When further considering time-dependent efficiencies in S3E5, there was an 82% reduction in total cost compared to B13E5 and a 29% reduction in environmental cost. S1E5 produced a better environmental cost and a higher gain in economic terms. However, because this scenario does not consider time-dependent profile for efficiencies of the photovoltaic panels and wind turbines as S3E5, it cannot be said to reliably represent real systems. In addition, these better values may be due to overestimated energy generation.

Regarding the generation of credit for the sale of energy to the grid, R\$50,752.37 in credits were generated in S1E5 versus only R\$38,907.48 in S3E5. Revenue from the sale of electricity to the central grid provided compensation for the expenses of installing the equipment. In addition, with the use of renewable resources the purchase of energy from the central grid in most houses was no longer necessary, as can be seen in the generation profiles in Appendix D. This may explain the cost reduction between the scenarios and the baseline.

With regard to the other costs compared to the B13E5, S1E5 and S3E5 present similar costs of operation and maintenance, environmental cost, purchase of electricity and natural gas from the central grid. On the other hand, investment cost presents shows a significant difference. The investment for S1E5 (constant efficiency) is lower than investment for S3E5 (time-dependent efficiency) due to the poor dimensioning of energy resources when the time-dependent profile for efficiencies in the energy generation process are not considered.

IV.5.2. The impact of the clustering method to split the time horizon on Costs and Revenues

The S2E5 scenario showed a 66% reduction in total cost compared to the baseline and a 61% reduction in environmental costs. This suggests that using the empirical method for determining time periods can significantly improve environmental outcomes. However, when compared to the S3E5 scenario, which used the clustering method, it appears that the latter scenario achieved better economic results.

Analysis of the energy injected into the grid indicates that the S2E5 scenario, despite having a higher generation capacity (as detailed in section IV.7), produced less energy than the S3E5 scenario. This explains why the S2E5 scenario had lower emissions, as the environmental cost is directly proportional to energy production. However, this implies that the empirical method was not effective in optimizing the use of energy resources.

IV.5.3. The impact of pre- and post-COVID demands on costs and revenues

In the S3O5 there was a 87% reduction in the total cost in relation to the B3O5. When all the parts that make up the cost are analyzed, it can be observed that, despite the increase of more than 1,900% in the investment cost, there was a reduction of 99% in the energy consumption of the central grid, 21% in the use of natural gas and 19% reduction in the environmental cost. As the operation and maintenance cost is composed of variable costs, which depend on energy generation, and fixed costs, it was observed that there was a 26% reduction in relation to the baseline. This infers that with the adoption of renewable resources there is a reduction in operational costs. Besides this, there was the insertion of energy in the grid that generated R\$ 87,520.89 in credits. When compared with S3E5, an increase of only 9% in total cost was observed post-COVID. This infers that despite the 25% increase in electricity demand and 50% increase in air cooling demand, along with the increased cost of electricity and natural gas, the use of the technologies installed in the scenario was optimized.

IV.5.4. The impact of the increase of houses in the microgrid on costs and revenues

- *Pre-COVID*

For the 10 houses microgrid in S3E10 there was an 84% reduction in total cost compared to the baseline and a 29% reduction in environmental cost, 33% in natural gas cost and 99% in grid energy cost. When compared to the scenario equivalent with 5 houses (S3E5), S3E10 shows a 74% increase in total cost, with no reduction in the other costs. This indicates that even with the doubling of the number of houses, the costs will not necessarily increase proportionately, due to the optimal use of resources and cost composition.

- *Post-COVID*

For the 10 houses microgrid in S3O10 there was a 90% reduction in total cost compared to the baseline with 18% reduction in environmental cost, 17% reduction in natural gas purchase cost, 99% reduction in grid electricity purchase cost and 33% reduction in operation and maintenance cost. Despite the increase in investment cost, in this scenario there was the generation of R\$ 167,835.68 credits for the energy fed into the central grid. When compared to the scenario equivalent with 5 houses, there was an increase of approximately 60% in the total cost, with no reduction in the other costs. As the post-COVID scenario has more constant energy consumption during the day (Figure 48), different technologies are required as the number of the houses increases, reflecting in a higher total cost.

IV.6. Sensitivity analysis for battery use

Given the limited feasibility of battery use in microgrids as identified in the literature review, a sensitivity analysis was performed for the S3E5 to determine its viability under different conditions (Figure 59). To do this, one-at-a-time analysis, a methodology described by Khalid et al. (2016), was utilized. The approach involves adjusting a single input variable at a time, while keeping all others constant, in order to assess its impact on a specific parameter, such as costs. This analysis considered constant operating and maintenance costs, as well as the costs of the battery controller, which are outlined in Appendix A. The aim of the sensitivity analysis was to compare the feasibility of battery use for the microgrid under varying capital costs.

The first value considered for the capital cost of the battery was the one adopted in the scenarios above. It can be observed that from this first value up to a battery investment cost of R\$3,000.00 the number of units installed drops from 3 to 2. From R\$33,100.00 on the battery units are no longer installed and therefore the objective function becomes constant. Thus, it is observed that under the conditions analyzed, the installation of batteries would become unfeasible only by an increase in capital cost above R\$31,600.00. This is likely because of the high cost of electricity from the central grid, which makes battery usage economically feasible.

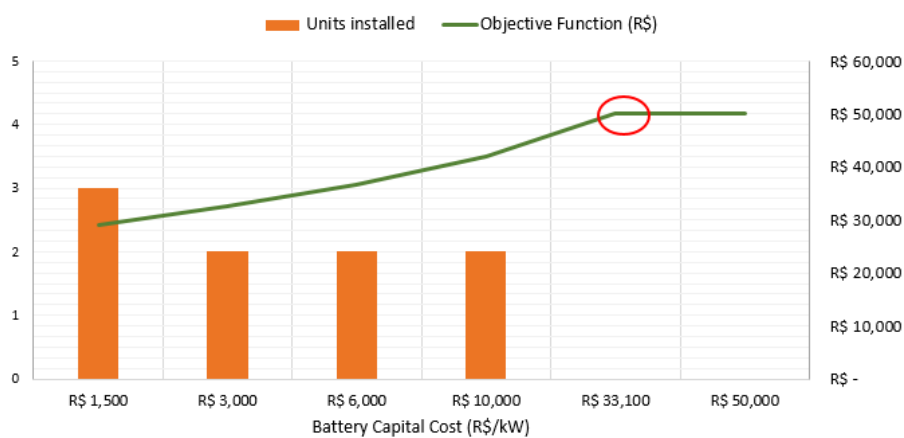


Figure 59 - Impact of battery capital cost on the objective function and number of batteries installed in S3E5.

IV.7. Sizing

The energy resources were sized for all the cases expressed in Table 19. The dimensioning of each renewable resource for each case is shown below, along with an analysis of how the novel aspects in the model impacted the sizing of renewable resources.

IV.7.1. Baseline

The sizing of the selected resources in the baseline scenario, which does not have renewable resources, are expressed in Table 21. For all scenarios the gas heater was selected to supply the hot water demand, indicating that using natural gas to heat water is more profitable than the use of electricity for the electric shower.

Table 21 - Resource size at baseline for all scenarios

Stage	Scenario	Houses	Gas Heater (L)	Air Conditioning (kW)	Stage	Scenario	Houses	Gas Heater (L)	Air Conditioning (kW)
Pre-COVID	B13E5	1	400.00	2.20	Post-COVID	B3O5	1	400.00	2.20
		2	400.00	2.20			2	400.00	2.20
		3	400.00	2.20			3	400.00	3.31
		4	400.00	2.20			4	400.00	4.63
		5	400.00	2.21			5	413.39	5.96
	B2E5	1	400.00	2.20		B3O10	1	400.00	2.20
		2	400.00	2.20			2	400.00	2.20
		3	400.00	3.46			3	400.00	3.31
		4	400.00	4.84			4	400.00	4.63
		5	400.00	6.22			5	413.39	5.96
	B3E10	1	400.00	2.20		6	400.00	2.20	
		2	400.00	2.20		7	400.00	2.20	
		3	400.00	2.20		8	400.00	3.31	
		4	400.00	2.20		9	400.00	4.63	
		5	400.00	2.21		10	413.39	5.96	
		6	400.00	2.20					
		7	400.00	2.20					
		8	400.00	2.20					
		9	400.00	2.20					
		10	400.00	2.21					

IV.7.2. Scenarios incorporating renewable sources

The dimensioning of the selected resources in the scenarios that have renewable sources is shown in Table 22. The results show that most of the resource capacities were sized according to the energy demand of the house and whether or not the house shares

energy with other houses. The capacity of batteries, solar panels, solar collectors, and wind turbines is higher in houses with higher demand or that share energy. This is evident from the increased capacity observed in these systems.

Regarding the air conditioning, in the pre-COVID scenarios, in which the time periods were divided by the clustering method (S1E5, S3E5 and S3E10), the capacity of each household was similar. In S2E5, where the division of time periods was empirically performed, the capacity of the air conditioning varied with the increase in demand. This may have occurred because the choice of time periods concentrated the demand in a single period, therefore requiring a larger capacity, which was also observed in the baseline scenario.

Most wind turbines installed were sized near the upper bound, i.e. the maximum area allowed in the model. This infers that the generation of wind energy could be greater if more space were available for installation or if other turbine types that use less space were installed.

Regarding the gas heater, biogas heater and solar tank capacities, the minimum capacity for these resources were observed in S1E5 and S3E5. This is due to the fact that the time periods were divided in a way that there was no concentration of a large demand in a single period, and because of this there was no need for a larger capacity.

It was found that the capacity of the biodigester varied based on the number of houses and method used to divide the time period, as well as its energy demand. For the scenarios with the same number of houses and clustering in the division of the time horizon, the capacity was the same (S1E5, S3E5). However, there was a non significant difference in capacity between the scenario using an empirical time division method (S2E5) and S1E5 and S3E5, suggesting that the number of houses has the greatest impact on the capacity of biodigester. The capacity was higher in scenarios with more houses (S3E10 and S3O10) compared to those with fewer houses (S3E5 and S3O5) due to higher energy demand, as well as between the pre-(S3E5) and post-COVID(S3O5) scenarios.

It was observed that additional organic matter needed to be acquired only in the scenarios S2E5, S3O5, and S3O10 in order to meet biogas production. This is due to the fact that in these scenarios, there is a higher demand for biogas during the same period, resulting in the need for increased production and the purchase of additional materials. It is worth mentioning that scenario S2E5 has the same energy demand as S1E5 and S3E5, showing that the distribution of time periods by the clustering method optimized the available resources in the microgrid, with no need to purchase additional organic material in these scenarios.

Table 22 - Size of renewable resources distributed for all scenarios

Stage	Scenario	Houses	Electric Shower (kW)	Natural Gas Heater (L)	Biogas Heater (L)	Solar collector (m ²)	Solar Tank (L)	Air Conditioning (kW)	Wind Turbine (m ²)	Photovoltaic Panel (m ²)	Battery (kW)	Biodigester (m ³)	Extra organic material acquired by the microgrid (kg/day)
Pre-COVID	S1E5	1	2.50	-	-	-	-	2.20	2.91	-	-	0.84	-
		2	-	400.00	-	14.06	200.00	2.20	-	8.88	-		
		3	-	400.00	-	20.72	200.00	2.20	5.00	3.87	-		
		4	-	400.00	-	14.21	200.00	2.20	-	20.73	-		
		5	-	-	400.00	16.01	200.00	2.21	5.00	15.09	15.34		
	S2E5	1	-	-	400.00	5.62	200.00	2.20	5.00	2.06	5.93	0.86	0.076
		2	-	400.00	-	10.66	200.00	2.20	-	17.63	9.92		
		3	-	400.00	-	18.57	232.99	3.46	5.00	45.97	46.32		
		4	-	400.00	-	12.44	200.00	4.84	-	20.24	-		
		5	-	-	400.00	15.99	200.27	6.22	5.00	22.56	-		
	S3E5	1	-	400.00	-	6.54	200.00	2.20	2.74	2.60	4.22	0.84	-
		2	-	400.00	-	11.16	200.00	2.20	-	12.20	10.23		
		3	-	400.00	-	19.70	200.00	2.20	5.00	16.56	15.16		
		4	-	400.00	-	13.02	200.00	2.20	-	22.26	-		
		5	-	-	400.00	16.74	200.00	2.21	5.00	26.29	-		
	S3E10	1	-	400.00	-	4.24	200.00	2.20	2.00	2.60	2.48	1.68	-

		2	-	400.00	-	11.75	200.00	2.20	-	11.96	9.32		
		3	-	400.00	-	19.27	200.00	2.20	5.00	16.34	14.45		
		4	-	400.00	-	13.02	200.00	2.20	-	22.27	-		
		5	-	400.00	-	16.74	200.00	2.21	5.00	26.29	-		
		6	-	-	400.00	4.39	200.00	2.20	-	4.08	3.47		
		7	-	400.00	-	12.02	200.00	2.20	5.00	8.08	6.60		
		8	-	400.00	-	9.30	200.00	2.20	-	15.90	-		
		9	-	400.00	-	13.02	200.00	2.20	5.00	25.59	23.48		
		10	-	400.00	-	16.74	200.00	2.21	-	28.63	-		
		1	-	400.00	-	3.67	200.00	2.20	4.83	4.48	2.73		
		2	2.50	-	-	-	-	2.20	-	25.67	19.45		
	S305	3	-	400.00	-	1.43	200.00	3.31	5.00	34.18	20.35	1.48	12.72
		4	-	-	400.00	-	-	4.63	-	39.77	-		
		5	-	400.00	-	-	-	5.96	5.00	48.95	-		
Post-COVID		1	-	400.00	-	0.68	200.00	2.20	5.00	4.42	2.43		
		2	-	400.00	-	0.77	200.00	2.20	-	18.75	8.02		
	S3010	3	-	400.00	-	0.87	200.00	3.31	5.00	32.17	19.44	1.90	4.30
		4	-	400.00	-	-	-	4.63	-	39.77	-		
		5	-	-	400.00	-	-	5.96	-	51.14	-		

6	-	400.00	-	0.87	200.00	2.20	3.80	4.54	1.74
7	-	400.00	-	1.12	200.00	2.20	-	40.76	8.53
8	-	400.00	-	-	-	3.31	5.00	32.26	19.43
9	-	400.00	-	-	-	4.63	-	39.77	-
10	-	400.00	-	-	-	5.96	5.00	48.95	-

IV.8. The Effect of Time-Varying Efficiency Profiles on power generation

In order to analyze the effect of time-varying efficiency profiles on DER (Distributed Energy Resources) sizing, Figure 60 compares the profile of resources used in Scenario S1E5 (houses i1 and i4) with Scenario S3E5 (houses i1 and i5). When time-varying efficiency profile was neglected in S1E5, only wind turbine was installed in house i1 but it could still transfer energy to house i4 (Figure 52). When time-varying efficiency profiles are considered in S3E5, though, two additional technologies were installed in house i1, namely the photovoltaic panel and the battery. In this Scenario, house i1 exports energy to house i5, which demands 22% more energy than house i4. During periods such as p6, for instance, the wind turbine of the house i1 in Scenario S1E5 was able to meet the entire self-demand and part of the demand from house i4. When time-varying efficiency profiles were considered in Scenario S3E5, though, stored energy in batteries had to be used instead, although the electrical demand of house i1 in previous scenario (S1E5) is higher. This higher energy demand in house i1 is due to the use of the electric shower when time-dependent profile for efficiencies were neglected.

This example illustrates that, despite the similar wind turbine dimensions in both S1E5 and S3E5, when efficiency does not vary over time (S1E5), the energy generation is overestimated. This overestimation allowed for the practical fulfillment of all the residences' demands without the need to increase production capacity of these houses, which may have also been the reason for the different connections observed between the two scenarios.

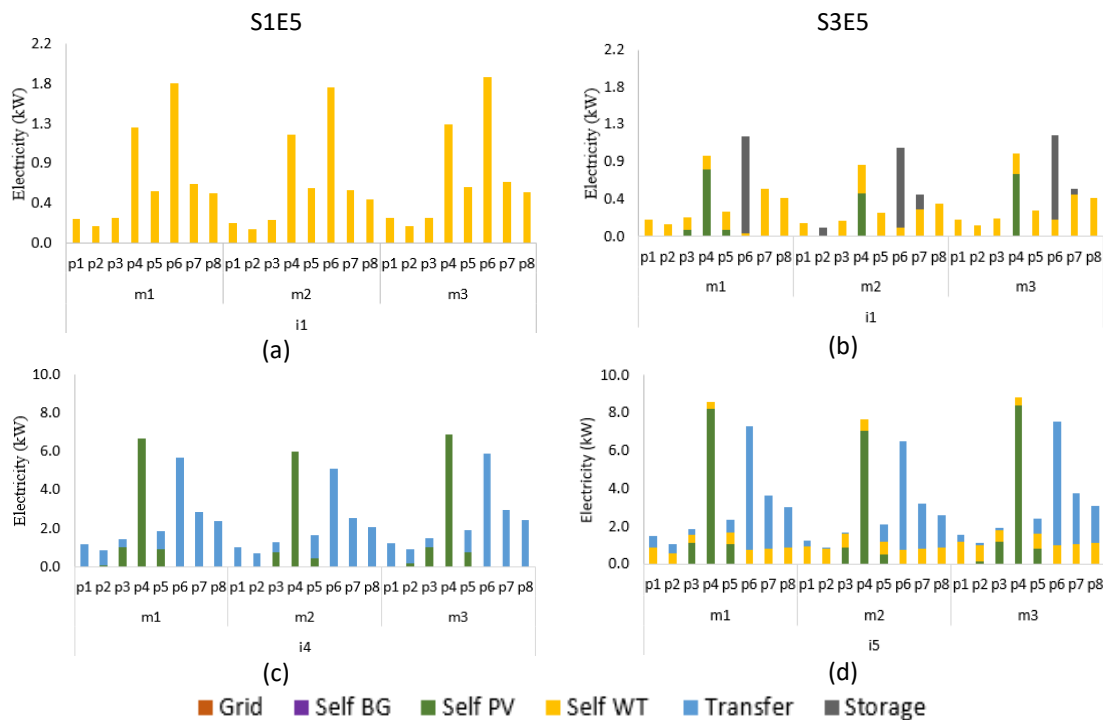


Figure 60 - Profile of resources used to meet the electrical demand: a) house i1 in Scenario S1E5; b) house i1 in Scenario S3E5; c) house i4 in Scenario S1E5; d) hose i5 in Scenario S3E5.

The same was observed in the hot water generation profile, although in a smoother way, since only the efficiency of the solar collector is able to vary with the climatic conditions over time. Figure 61 compares the distribution of resources at house i5 for both scenarios S1E5 and S3E5, as they have the same energy demand. As can be observed in Table 22, the solar collector was dimensioned with similar capacities, nearly 16 m². However, in the p6 periods of season m1 and m3, the solar collector produced more hot water when time-varying efficiency was neglected: 41% and 35% in m1 and m3, respectively, in S1E5 compared to 38% and 33% in S3E5. This confirms that disregarding the variation of the solar panel efficiency caused an overestimation of the real capacity to meet the demand in the S1E5 scenario.

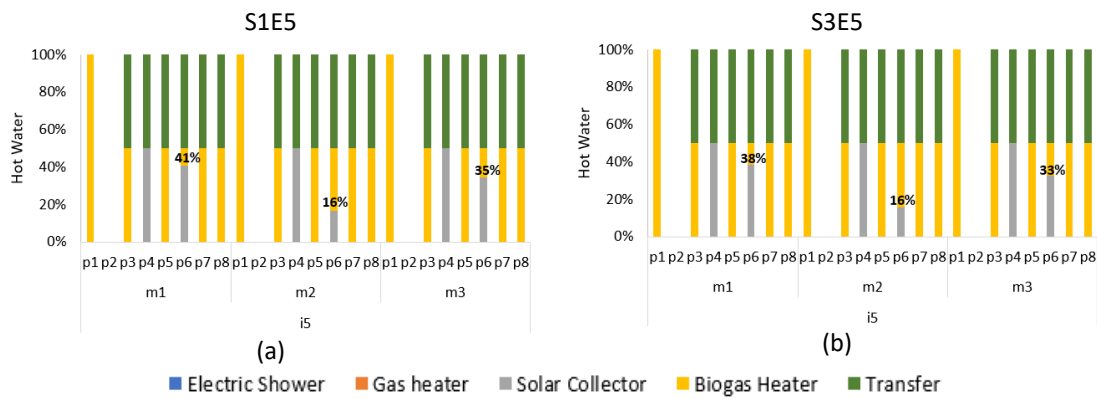


Figure 61 - Distribution of resources used to meet the hot water demand for house i5 in the case: a) S1E5; b) S3E5.

IV.9. The Effect of Time Horizon Division with the Clustering Method on power generation

To analyze the effect of the clustering method in splitting the time horizon on power generation, Figure 62 compares the resources profile of house i1 in S2E5 (empirical method) and in S3E5 (clustering method). In both scenarios, house i1 shares energy with houses i5. The results indicated that house i1 in S3E5 had a greater utilization of solar panels and generated more energy compared to the same house in S2E5, despite having similar dimensions, as shown in Table 22. This observation highlights the effectiveness of the clustering method in optimizing the installed resources.

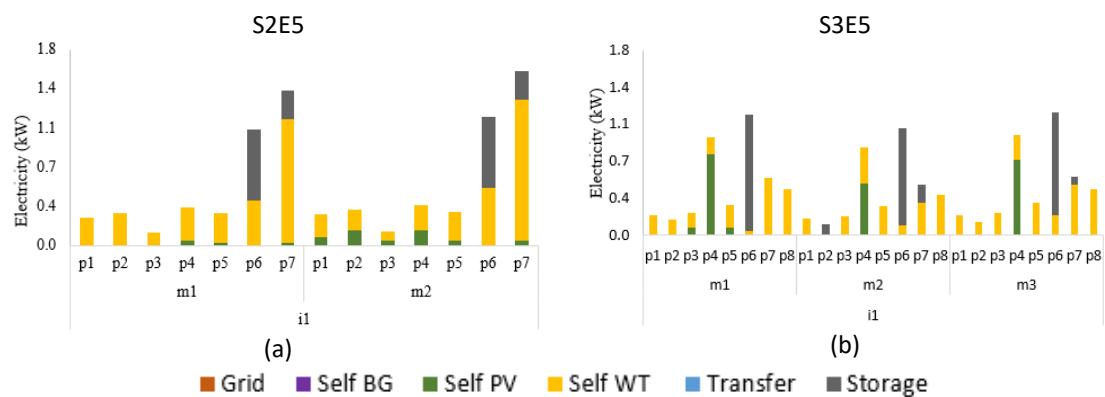


Figure 62 - Profile of resources used to meet the electrical demand in house i1 in the case: a) S2E5; b) S3E5.

IV.10. Differences between Pre and Post-COVID on power generation

In order to analyze the impact of the increase in energy demand from the pre-COVID to the post-COVID scenario on the sizing and utilization profile of available renewable resources, the electrical consumption profile of house i2 in both S3E5 and S3O5 is presented in Figure 63. The profiles for the other houses in both scenarios are included in Appendix D.

As shown in Table 22, the solar panel sizing doubled from the post-COVID to the pre-COVID scenario (from 26 to 49 m²) to meet a 25% increase in electricity demand and a 50% increase in air cooling demand. As a result, when comparing proportional energy demand in Figure 63, the post-COVID scenario (d) reduced the amount of electricity purchased from the central grid compared to the pre-COVID scenario (Figure 63c). This can be attributed to the greater utilization of the solar panels, which were favored by the consumption profile in this scenario due to more consistent demand during the day. Therefore, despite the cost increases in the post-COVID scenario discussed in the section IV.5.3, there was a more optimized use of resources in the post-COVID scenario, which can be attributed mainly to its consumption profile.

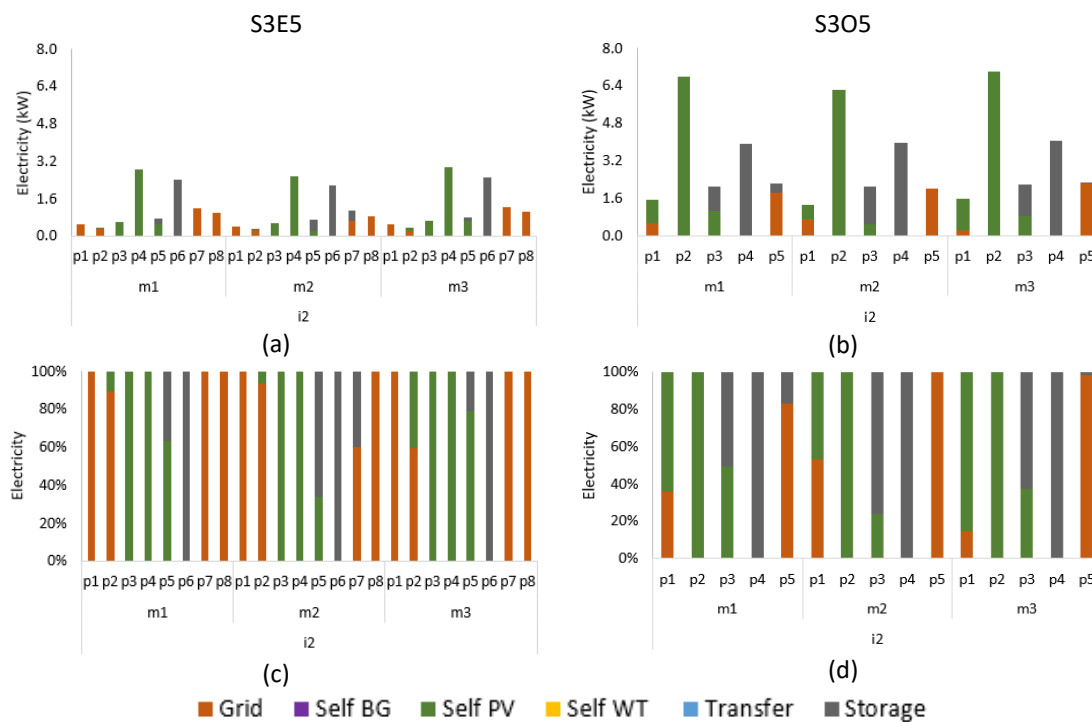


Figure 63 - Profile of the resources used to meet the electrical demand in house i2 expressed in kW and percentage: a) Scenario S3E5 (kW); b) Scenario S3O5 (kW); c) Scenario S3E5 (percentage); d) Scenario S3O5 (percentage).

IV.11. The Influence of the Number of Houses on Power Generation

In order to analyze the differences in energy generation with increasing number of houses, the energy consumption profile of house i2 for the pre-COVID state with 5 and 10 houses are expressed in Figure 64. As house i2 in the microgrid with 10 houses has a slightly smaller installed capacity than in the microgrid with 5 houses (Table 22), a different behavior in the consumption profile was observed. Part of the demand in periods p3 and p5 during all seasons was imported from another house (blue bar in Figure 64b). This suggests that it was more profitable in this scenario to share energy between houses i6 and i2 than to acquire equipment of greater capacity, since the distance between these houses is not great and, therefore, the loss of energy in its transport is not significant.

However, in general due to the similarity of demand and the use of the same technologies in houses 5 and 10, similar behaviors in the energy consumption profile were observed for both pre- and post-COVID and can be found in Appendix D. On the other hand, the differences found when increasing the number of houses can be explained by the layout of the additional houses facilitating new connections between

pre-existing houses. This explains the sharing of electricity from house i6 to house i2 in S3E10.

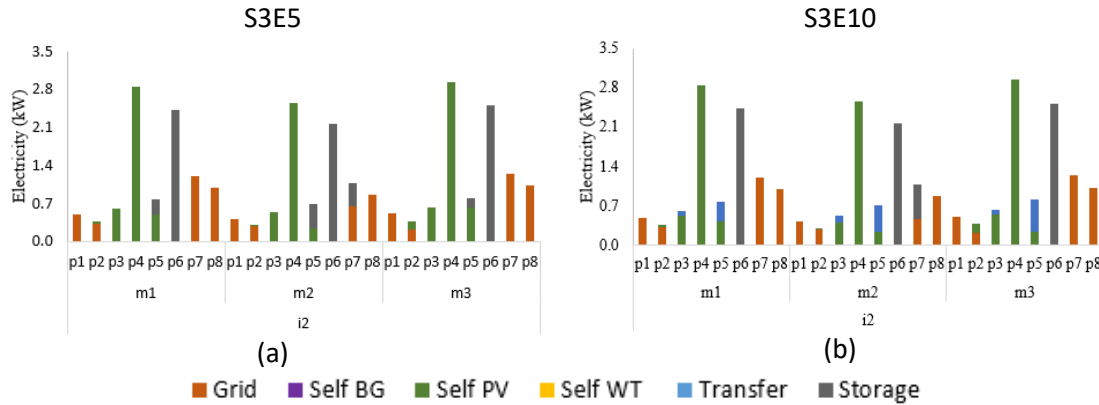


Figure 64 - Profile of resources used to meet the electrical demand in house i2 in the case: a)S3E10; b)S3E5.

IV.12. Numerical Statistics

The results were generated on an Intel(R) Core(TM) i9-9900K CPU 3.60GHz computer using GAMS Studio 0.8.6 64 bit. Table 23 shows the results for the scenarios with 5 and 10 houses with a gap of 0% between the solution found and the best possible.

The number of single equations, single variables, discrete variables increased on average 170% from S3E5 and S3E10, due to the increase in the number of houses. This caused an increase of over 124 hours in CPU time. For the post-COVID scenario, the number of equations and variables increased 175% from S3O5 to S3O10. This caused an increase of over 20 hours in CPU time. Therefore, the amount of houses in a model will impact the computational time. The same can be observed when comparing scenarios 1 to scenario 3, since scenarios 1 have fewer single equations and single variables which resulted in a lower CPU time.

When comparing S2E5 to S3E5, which have the same number of discrete variables but 10% more single equations and 1% fewer single variables, a reduction of 12 minutes in CPU time was observed. This suggests that the number of single variables has a greater impact on CPU time, as the reduction was observed even with a larger number of single equations.

Table 23 - Results for the scenarios with energy resources distributed at a 0% gap

Stage	Scenario	Houses	Single equations	Single variables	Discrete variables	CPU time (s)	Objective Function (R\$)
Pre-COVID	S1E5	5	12,203	8,504	224	263.93	10,261.60
	S2E5	5	6,895	5,096	174	59.64	52,458.11
	S3E5	5	11,100	8,576	224	968.59	28,956.95
	S3E10	10	31,770	24,321	544	446,850.31	50,434.78
Post-COVID	S3O5	5	7,023	5,444	179	164.23	31,596.10
	S3O10	10	20,043	15,384	454	71306.31	50,370.09

IV.13. Conclusion

This chapter presents the results and discussion for the case study in the city of Salvador - Bahia, Brazil. The study was developed for 3 different scenarios that correspond to the model: without time-dependent profile for efficiencies in energy resources (scenario 1), with the time period divided with the empirical method (scenario 2) and with the clustering method and with time-dependent profile for efficiencies in energy resources (scenario 3). Scenario 3 was applied to 2 states of energy demand, pre- and post-COVID. These states were considered for microgrids of 5 and 10 houses.

The model presented was able to attest the high economic gain with the adoption of renewable energy resources, as well as environmental gains for all scenarios, states and number of houses. In addition, it was observed that the method used to divide the time periods, as well as the behavior of the energy demand of the houses in the microgrid influence the sizing and design of the microgrid resources.

By not considering time-dependent efficiency in the analysis, there may have been a positive impact on the economic gain, but it may also have contributed to the underestimation of power generation. Furthermore, it is important to point out that the method of splitting the time horizon impacted the total and environmental costs differently. In fact, the empirical method showed a greater reduction in environmental costs, while the clustering method had a greater reduction in total system costs. However, it is noted that although the environmental cost was higher in the scenario that used the clustering method, the amount of energy injected into the grid was higher. This indirectly contributed to the reduction of greenhouse gas emissions in the overall system (microgrid-central grid), since by transferring more energy generated by renewable sources to the central grid, there is a partial replacement of non-renewable

sources, which are generally more polluting. This study introduced a novel viewpoint on the topic that was not previously explored in the literature.

The difference between the pre-COVID and post-COVID scenarios can be seen in the energy consumption patterns. In the post-COVID scenario, there is a more consistent level of energy consumption throughout the day, which means that different technologies become necessary as the number of houses increases. This results in a higher total cost. Therefore, it can be inferred that the new trend of remote working has an effect on the design and size of a microgrid.

Moreover, it is important to keep in mind that the renewable energy resources used in this study can be implemented in countries beyond those with tropical climates, as highlighted in the literature review. Therefore, the model presented here can be applied to other locations. However, it is important to take into account the costs of renewable resources, as well as the specific rates and restrictions in each country before implementing the model.

Furthermore, the proposed optimization model was able to provide information regarding the best renewable energy incentive policy for the country and the viability of using biogas, solar and wind energy to meet the electrical, hot water, air cooling and gas for cooking demands. Therefore, the results emphasize the contribution of this work for a better understanding of the dimensioning of renewable resources in a microgrid.

In the course of this work, the main points raised in the literature review (regarding the incorporation of time-dependent energy demand patterns and renewable resource efficiency, the use of a systematic time period splitting method, and the combination of different renewable resources) were addressed. Nevertheless, further enhancements can be made to enhance the analysis. To increase the accuracy of the results, the actual performance and degradation of components over time should be taken into account, as well as uncertainties in energy generation, as these factors can have a large impact on the efficiency and overall cost of the system. In addition, applying the model using real energy data for the post-COVID scenario would improve the analysis. To further streamline the model, reducing the variables related to time periods can help decrease the resolution time and make it more suitable for systems with a larger number of households. Also, consider other renewable energy incentive policies for selection in the model.

CHAPTER V – CONCLUSIONS AND FUTURE WORK

V.1. Conclusion

The present work aimed to fill the gaps in the literature regarding the particularities in modeling distributed energy systems. This included analyzing the effect of changing energy demand on system sizing to minimize costs, the use of clustering to divide time horizons, the impact of time-dependent profile for efficiencies of renewable resources on system costs, and the sizing and profile of energy generation from renewable resources for 5 and 10 houses in a microgrid. The feasibility of using biogas for cooking gas, hot water, and electricity was also investigated.

Furthermore, because Brazil has an energy potential in solar irradiation and wind speed and since there is a limited exploration of these systems in the country and limited research on optimizing microgrids in this context, the city of Salvador in Bahia was chosen to perform the case study of the proposed model.

Thus, it was found that the use of distributed energy resources is beneficial in economic and environmental terms when compared to the use of non-renewable resources alone. In the context of Brazil, Net Metering was determined to be the most favorable incentive policy for reducing overall costs when compared to the Feed in Tariff policy under the specific conditions studied. However, if the FIT rates were increased to cover the high cost of investing in renewable energy sources in Brazil, the outcome could be different. It is important to note that the impact of incentive policies can vary greatly depending on the specific circumstances of a country, and what may be the most favorable policy in one country may not be the case in another.

The energy demand of a house, as well as the division of time periods and the dynamics of energy sharing between other houses, have an influence on the sizing of energy resource generation technologies. It was observed that for the division of the time horizon using the empirical method, the resource capacity tended to be larger and with lower energy production than for the clustering method. This shows that the use of the systematic method for splitting the time horizon of the model provided a better

optimization of energy resource sizing than the use of the empirical method. In addition, the scenario using the empirical method showed a greater gain in environmental cost because of lower energy generation. On the other hand, the scenario using the clustering method had higher energy injection into the central grid, which led to a decrease in greenhouse gases emitted by the entire system (microgrid – central grid).

For houses that shared energy with other houses, as expected, in general, more energy resources were installed or, if not, they had equipment of higher capacity to meet their demand and the demand of the other house. In the pre- and post-COVID scenarios, due to the difference in the energy demand profile, the dimensioning of energy resources differed in capacity and in the number of installed equipment.

Similarly, the impact of increasing the number of houses in the microgrid on the sizing of renewable resources varies according to the energy consumption profile. In the pre-COVID scenarios, which have a lower consumption during the day the comparison between the scenario with 5 houses and the scenario with 10 houses revealed little variation in capacity and energy resource selection. On the other hand, for the post-COVID scenario, due to the higher consumption and more constant distribution during the day, as the number of houses increased, different combinations of resources were used.

Furthermore, it was observed that neglecting time-dependent profile for efficiencies of the renewable resource generation technologies tends to overestimate energy generation. This may imply installing equipment with lower capacity that indeed would not be sufficient to meet the entire energy demand, and different distribution of energy among the houses in the microgrid.

The feasibility of using biogas was established, as it was chosen in all the scenarios studied. However, it was not employed in all the houses because the primary option was the natural gas to meet the demand for cooking gas and hot water and photovoltaic or wind energy to meet the demand for electricity. This suggests that based on current economic conditions and the configuration of the microgrid studied, using natural gas resulted in lower overall costs for most houses. However, if biogas were provided by the central grid, its investment cost would be lower due to large-scale use, making it even more competitive compared to natural gas. The capacity of the biodigester was influenced by both the number of houses and the way the time periods were divided. Additionally, the need for extra organic matter was mainly determined by the division of the scenario by time horizon, as high demand for biogas may have been concentrated in a single time period.

Finally, it was determined that battery use was feasible in all the scenarios studied. This suggests that in Brazil's current energy tariff system, this storage technology can be a substitute for energy from the central grid in some periods of time.

In conclusion, this work provides a comprehensive analysis of the different factors that influence the sizing and sharing of energy in microgrids, and it proposes a systematic approach to optimize energy resource sizing. The novelty of this work lies in its focus on the specificities of modeling distributed energy systems filling research gaps identified in the state-of-the-art. It addresses key points such as the impact of the empirical method versus the clustering method for dividing the time horizon on microgrid sizing, the effects of changes in energy demand after the COVID-19 pandemic on microgrid sizing, and the behavior of microgrids when considering electricity demand, air cooling, gas for cooking, and hot water. Additionally, the work investigates the impact of time-dependent efficiency profiles of renewable resources on energy sharing behavior in microgrids and explores the feasibility of utilizing biogas as a renewable energy source in microgrids.

V.2. Suggestions for future work

In order to continue the present work, future studies can be performed on:

1. **Improving the Clustering Method:** One way to improve the clustering method used in this study is to incorporate all energy demands into the analysis. This could contribute to a more optimal choice of energy resources.
2. **Multi-Objective Optimization:** The single objective approach utilized in this study may not be sufficient to fully capture the complexities of microgrid systems. It may be useful to consider multi-objective optimization techniques that can take into account multiple factors such as energy production, cost, and environmental impact.
3. **Uncertainty in Energy Generation and demand:** Incorporating proper uncertainty in energy generation and demand is important in order to accurately model the behavior of microgrid systems. Future research could consider techniques such as stochastic optimization to capture the uncertainty in these variables.
4. **Reducing Computational Effort:** Due to the high computational demands of the model presented in this study, it was not feasible to apply it to a scenario of 20 houses. Thus, to make the model more suitable for larger microgrid systems, it may be necessary to reduce the computational effort required to run the simulation. This could include reducing the number of variables related to time periods.

5. Renewable Energy Incentive Policies: Future research could explore the impact of different policy options, including tax credits, subsidies, and others, and how they can impact the cost and efficiency of microgrid systems.
6. Consider new renewable sources: Incorporating additional renewable sources into the model enables the assessment of the potential for future implementation of innovative technologies like green hydrogen and hydrogen fuel cells in microgrid systems.

In conclusion, while the case study on Salvador is a useful starting point, further research is needed to fully understand the complex interactions between time-dependent renewable resource efficiency patterns as well as variations in the price of central grid power. By exploring the areas listed above, future research can help to improve the accuracy and usefulness of microgrid modeling and optimization techniques.

APPENDIX A- Parameters and Costs

In this section the input costs and parameters for the model expressed in Chapter III are set out. Table 24 shows the costs and operational parameters for each resource considered in the model. Table 25 shows the carbon intensity for each resource. Finally, Table 26 presents the Feed in Tariff for generating electricity for each resource.

Table 24 – Costs of energy resources and their operational parameters

Source	Item	Value	Reference
Electric Shower (ES)	Capital cost of ES (R\$/kW)	24.37	Lorenzetti (2022)
	ES Electric Efficiency	0.98	Lorenzetti (2022)
	Variable OM cost of ES (R\$/L)	0.029	Embasa (2022)
	Fixed cost of OM of ES (R\$/kW)	0.975	Mustafa (2010)
	Upper bound of ES (kW)	5.5	Lorenzetti (2022)
	Lower bound of ES (kW)	2.5	Lorenzetti (2022)
Gas Heater (GH)	Capital cost of GH (R\$/L/h)	2.0	Lorenzetti (2022) and Komeco (2022)
	GH Electric Efficiency	0.84	Lorenzetti (2022) and Komeco (2022)
	Variable OM cost of GH (R\$/L)	0.029	Embasa (2022)
	Fixed cost of OM of GH (R\$/kW)	0.08	Mustafa (2010)
	Upper bound of GH (L/h)	1200	Lorenzetti (2022) and Komeco (2022)
	Lower bound of GH (L/h)	400	Lorenzetti (2022) and Komeco (2022)
Air conditioning (AC)	Capital cost of AC (R\$/kW)	583.18	Fontaine (2022)
	AC coefficient of power	3	Sidnell et al. (2021a)
	Variable OM cost of AC (R\$/kW)	0.023	Sidnell et al. (2021a)
	Fixed cost of OM of AC (R\$/kW)	0	Sidnell et al. (2021a)
	Upper bound of AC (kW)	8.0	Fontaine (2022)
	Lower bound of AC (kW)	2.2	Fontaine (2022)
Photovoltaic (PV)	Capital cost of PV (R\$/kWp)	5,825	DAH Solar (2022)
	Nominal capacity(kWp/m ²)	0.16	DAH Solar (2022)
	Nominal Value of PV Efficiency	0.17	DAH Solar (2022)
	Variable OM cost of PV (R\$/kWp / year)	0	DAH Solar (2022)
	Fixed cost of OM of PV (R\$/kWp/year)	62.5	Mustafa (2010)
	Koehl correlation 1	30.02	Karamov et al. (2021)
	Koehl correlation 2	6.28	Karamov et al. (2021)
	Power losses in diodes coefficient	0.85	Karamov et al. (2021)
	Temperature coeficiente for silicone PV	0.004	Karamov et al. (2021)
Solar Collector (SC)	Capital cost of SC (R\$/kW/day)	359.84	Via Sol (2022)
	Nominal capacity of SC (kWh/day/m ²)	2.42	Via Sol (2022)
	Nominal Value of SC Efficiency	0.538	Via Sol (2022)

APPENDIX

	Fixed cost of OM of SC (R\$/kWh/year)	14.39	Mustafa (2010)
Solar Tank (ST)	Capital cost of ST (R\$/L)	10.0	Komeco (2022)
	Storage temperature (°C)	60	Komeco (2022)
	Variable OM cost of ST (R\$/L)	0.029	Embasa (2022)
	Upper bound of ST (kW)	200	Komeco (2022)
	Lower bound of ST (kW)	700	Komeco (2022)
	Calorific capacity of the water (J/kg.°C)	4.2	Guimarães (1997)
	Density of the water (kg/L)	1	Guimarães (1997)
Microgrid	Capital Cost of central controller (R\$)	7817.02	Sidnell et al. (2021a)
	OM cost of central controller (R\$)	137.99	Sidnell et al. (2021a)
	Capital Cost of an electricity line (R\$/m)	5.75	SIL (2022)
Pipeline	Capital Cost (R\$/m)	19.31	Krona (2022)
	Heat and electric loss	0.00004	Sidnell et al. (2021a)
Electrical Storage (Est)	Capital cost of Est (R\$/kW)	1,500	Lopes (2019)
	Capital cost of charge controller (R\$/battery)	6,000	Portal Solar (2022)
	OM cost of Est (R\$/kWh)	0.031	Sidnell et al. (2021a)
	Static loss of battery (%)	0.05	Sidnell et al. (2021a)
	Percentage charge rate	0.1	Sidnell et al. (2021a)
	Discharge rate	0.15	Sidnell et al. (2021a)
	Maximum charge rate	1	Sidnell et al. (2021a)
	Maximum discharge rate	1	Sidnell et al. (2021a)
	Depth of charge	1	Sidnell et al. (2021a)
	Upper bound of Est (kW)	100	Sidnell et al. (2021a)
Lower bound of Est (kW)	1	Sidnell et al. (2021a)	
Wind Turbine (WT)	Nominal wind speed (m/s)	10	Enersud (2022)
	Turbine cutting speed (m/s)	40	Enersud (2022)
	Turbine starting speed (m/s)	2	Enersud (2022)
	Rated capacity of WT (kW/m ²)	0.25	Enersud (2022)
	Capital cost of WT (R\$/kW)	8,883.33	Enersud (2022)
	Wind density (kg/m ³)	1.29	Cardoso et al. 2015
	Power coefficient	0.22	Cardoso et al. 2015
	Rotor Area limit	5	Assumed
	Fixed cost of OM from WT (R\$/kW/year)	355.33	Mustafa (2010)
	Variable OM cost of WT (R\$/kW/year)	0	Mustafa (2010)
Biogas biodigestor(BgBd)	Cost of BgBd (R\$/m ³)	3,600	Fortlev (2022)
	OM cost of BgBd (R\$/year)	72.0	Mustafa (2010)
	Calorific capacity of biogás (kW/m ³)	6.332	Lessly et al. 2020
	Number of people in the household	3	Agência Brasil, 2020
	Amount of organic material produced per person per day (kg)	1.125	Assumed
	Biogas production rate (m ³ of biogas/kg of organic waste)	0.04	BARROS (2021)
	Density of the dry material in the fluid (kg/ m ³)	211	Li et al. (2020)

	Hydraulic retention time in the BgBd (days)	30	Assumed
	Percentage of dry mass in organic material	0.27	Li et al. (2020)
	Maximum volume BgBd (m ³)	5	Assumed
	Price of organic waste (R\$/kg)	1.0	Assumed
	OM pipeline cost percentage of biogas and organic material(%)	2	Mustafa (2010)
	Cost of pipeline for biogas (R\$/m) OM cost	6.5	Johann (2012)
Biogas Generator (BgG)	Capital cost of BgG (R\$/ kW)	440	Souza et al. (2019)
	BgG efficiency	0.25	Souza et al. (2019)
	Maximum BgG power	308	ENERMAC (2022)
	Minimum BgG power	20	ENERMAC (2022)
	Fixed cost of OM of BgG (R\$/ kW/year)	17.6	Souza et al. (2019)
	Variable cost of OM of BgG (R\$/ kW/year)	0	Souza et al. (2019)
Biogas Heater (BgH)	Capital cost of BgH (R\$/L/h)	2.0	Lorenzetti (2022) and Komeco (2022)
	BgH efficiency	0.68	Silva et al. (2005)
	Upper bound of BgG (L/h)	1,200	Lorenzetti (2022) and Komeco (2022)
	Lower bound of BgG (L/h)	400	Lorenzetti (2022) and Komeco (2022)
	Fixed cost of OM of BgG (R\$/year)	0.08	Mustafa (2010)
	Variable cost of OM of BgG (R\$/ L/year)	0.029	Embasa (2022)

Table 25 – Carbon intensity for each resource

Resource	Carbon Intensity (kg CO ₂ /kWh)	Reference
Grid electricity	0.1000	EPE, 2021
Natural Gas	0.2020	MCTI, 2010
Wind	0.0066	Wang et al. 2012
Photovoltaic	0.0550	De Wild et al. 2014
Solar collector	0.0390	Milousi et al. 2019
Biogas Generator, Heater	0.1680	Paolini et al. 2018

Table 26 – Feed in Tariff for generating electricity for each resource

Resource	Value (R\$/ kWh)	References
Photovoltaic Panel	0.1293	OFGEM, 2020
Wind Turbine	0.2694	OFGEM, 2020
Biogas electric generator	0.2151	OFGEM, 2020

APPENDIX B- Python code for period clustering

The separation into clusters of the months and days for the post and pre covid states in the model was developed in Python language in the Spyder solver (Anaconda) (ROSSUM, DRAKE, 1995; RAYBAUT, 2009; ANACONDA, 2020). Below is expressed the code used to find both the clusters for the months and day in both states.

```
# Native libraries
import os
import math
# Essential Libraries
import pandas as pd
import matplotlib.pyplot as plt
import numpy as np
# Preprocessing
from sklearn.cluster import KMeans
import matplotlib.pyplot as mtp
#Collecting dataset
directory1 = 'H:\\demand_month\\'

for Data_month in os.listdir(directory1):
    if Data_month.endswith(".xlsx"):
        dff1 = pd.read_excel(directory1+Data_month)
        dff = dff1.loc[:, ['Demand', 'Solar', 'Wind']]

dff = pd.DataFrame(dff)

#Data normalization
def minmax_norm(dff_input):
    return (dff - dff.min()) / (dff.max() - dff.min())

dff_minmax_norm = minmax_norm(dff)

print(dff_minmax_norm)
fig, axs = plt.subplots()
fig.suptitle('Solar and wind data by month normalized')
axs.plot(dff_minmax_norm)
axs.set_xlabel('Month')
plt.show()

# The Elbow Method Graph
wcss_list= [] #Initializing the list for the values of WCSS
#Using for loop for iterations from 1 to 11.
for i in range(1, 11):
    kmeans = KMeans(n_clusters=i, init='k-means++', random_state= 42)
    kmeans.fit(dff_minmax_norm)
    wcss_list.append(kmeans.inertia_)
```

```
mtp.plot(range(1, 11), wcss_list)
mtp.title('The Elbow Method Graph')
mtp.xlabel('Number of clusters')
mtp.ylabel('Sum of squared errors')
mtp.show()

#training the K-means model on a dataset
kmeans = KMeans(n_clusters=3, init='k-means++', random_state= 42)
y_predict= kmeans.fit_predict(dff_minmax_norm)

dff_minmax_norm = dff_minmax_norm.values

month = [1,2,3,4,5,6,7,8,9,10,11,12]
dff_minmax_norm = np.insert(dff_minmax_norm, 0, month, axis=1)
print(dff_minmax_norm)

print(y_predict)

#visulaizing the clusters
mtp.scatter(dff_minmax_norm[y_predict == 0, 0],
dff_minmax_norm[y_predict == 0, 1], s = 100, c = 'blue', label =
'Cluster 1') #for first cluster
mtp.scatter(dff_minmax_norm[y_predict == 1, 0],
dff_minmax_norm[y_predict == 1, 1], s = 100, c = 'green', label =
'Cluster 2') #for second cluster
mtp.scatter(dff_minmax_norm[y_predict== 2, 0],
dff_minmax_norm[y_predict == 2, 1], s = 100, c = 'red', label =
'Cluster 3') #for third cluster
mtp.scatter(dff_minmax_norm[y_predict == 3, 0],
dff_minmax_norm[y_predict == 3, 1], s = 100, c = 'cyan', label =
'Cluster 4') #for fourth cluster
mtp.scatter(kmeans.cluster_centers[:, 0], kmeans.cluster_centers[:,
1], s = 300, c = 'yellow', label = 'Centroid')
mtp.title('Solar and wind - Clustering the period during the year')
mtp.xlabel('Month')
mtp.ylabel('Variable')
mtp.legend()
mtp.show()
```

APPENDIX C - Discussion of the Time Clustering Result

The methodology for the clustering of time periods, explained in the III.3, was adopted for both the pre- and post-COVID scenarios. Below are the results found and the analysis performed to determine the time periods that were used in the models of the scenarios with clustering.

a. Pre-COVID

For the division of seasons in the pre-COVID scenario, the solar irradiation, wind speed and electricity demand data were normalized. After this the graph obtained with the elbow method for the period was found (Figure 65). When number of clusters equals to 3, the reduction of the sum of the squared errors becomes less pronounced, so according to the method this point is ideal for the choice of the cluster number.

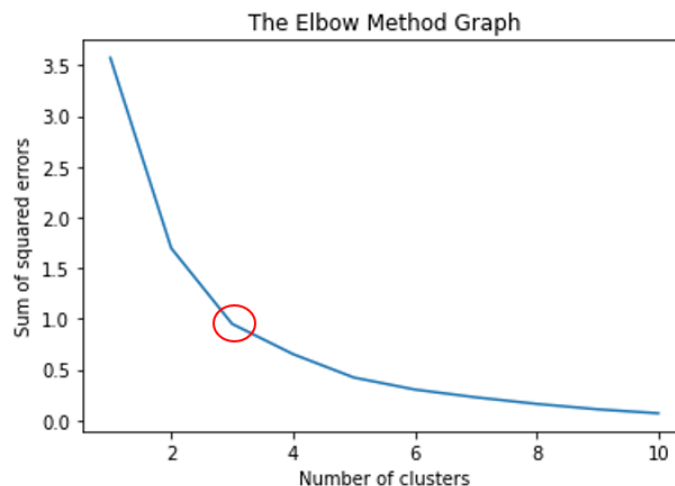


Figure 65- Graphical method for selecting the best amount of clusters during the year in the pre-COVID scenarios.

After the cluster number was chosen according to the elbow method, the choice was tested to see if the time periods would be presented consecutively in the clusters. As observed in the Figure 66, with 3 clusters it was possible to find consecutive time periods. Therefore, the number of 3 clusters was considered for the pre-COVID scenarios, and the year is split into the seasons illustrated in Table 27.

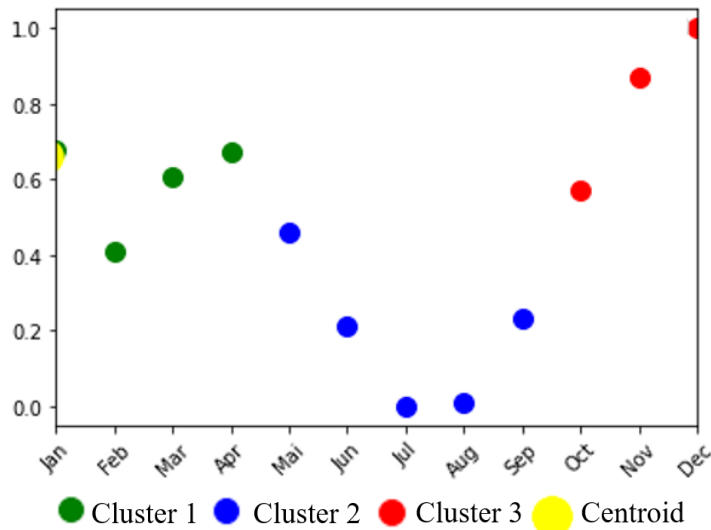


Figure 66 – Clustering the period during the year in the pre covid state

Table 27 - Time period during the year for the pre-COVID scenarios

Season	m1	m2	m3
Period of the year	January, February, March, April	May, June, July, August, September	October, November, December

To determine the time periods during the day, the data was divided into the seasons found previously and, in addition, data on the electricity rate was added for the clustering algorithm, as explained earlier. After normalizing the data, the graph obtained from the Elbow method was again generated and is shown in Figure 67.

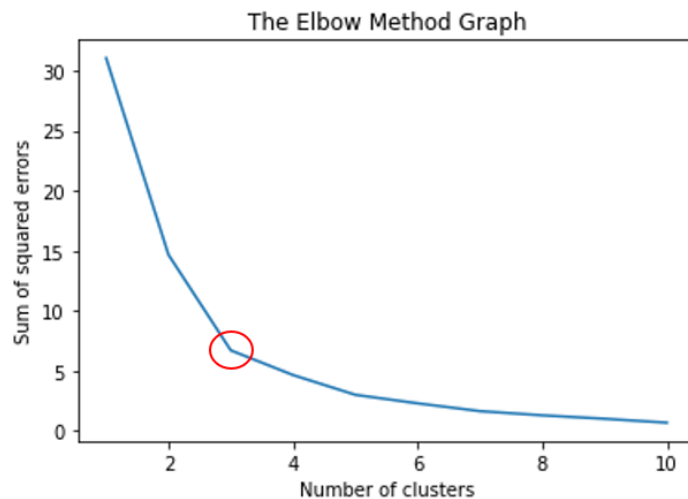


Figure 67 - Graphical method for selecting the best amount of clusters during the day in the pre-COVID scenarios

Figure 67 indicates that 3 clusters would be the optimal number. However, when performing the test for 3 clusters, non-consecutive periods were found in the same cluster. Therefore, a new test for 4, 5, 6 and 7 clusters were performed, which showed similar behavior to 3. Finally, for 8 clusters, consecutive periods were found as observed in Figure 68. Therefore, the day is split into the time periods presented in Table 28 for the pre-COVID scenarios.

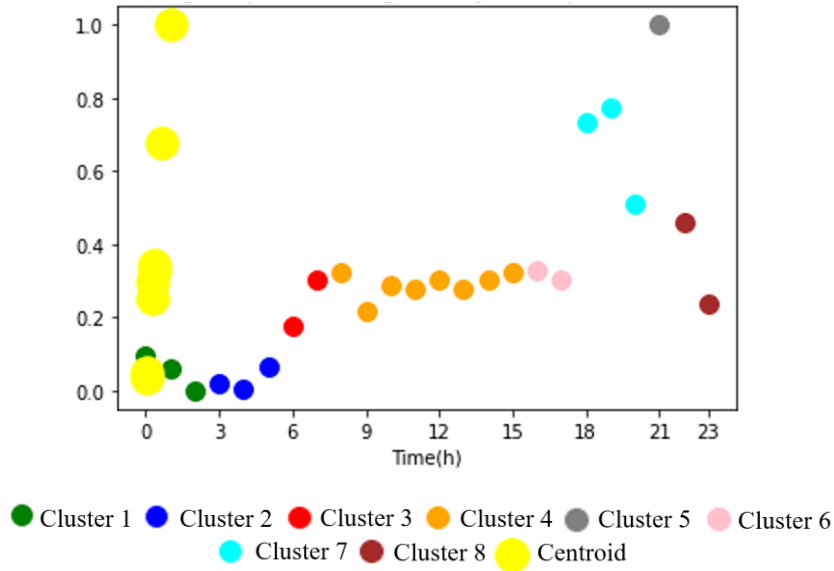


Figure 68 - Clustering the period during the day in the pre-COVID scenarios

Table 28 - Time period during the day for the pre-COVID scenarios

Period of the day	p1	p2	p3	p4	p5
Pre-COVID	0:00 – 2:59	3:00– 5:59	6:00 – 7:59	8:00 – 15:59	16:00 – 17:59
Period of the day	p6	p7	p8		
Pre-COVID	18:00 – 20:59	21:00 – 21:59	22:00 – 23:59		

b. Post-COVID

For the division of seasons in the post-COVID scenarios, the electricity demand data was grouped with the solar irradiation and wind speed data. After normalizing the data, the graph in Figure 69 for the Elbow method was obtained.

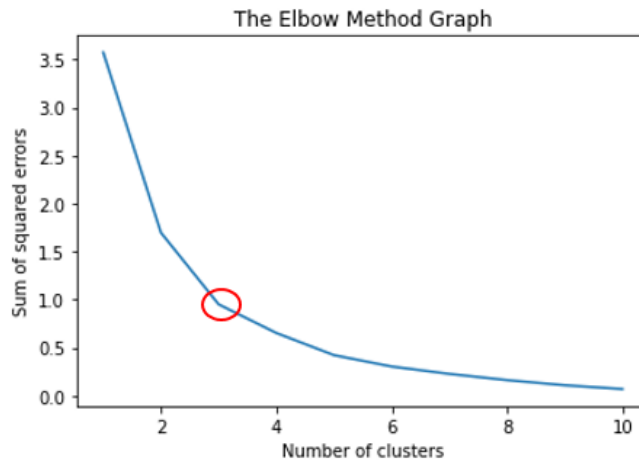


Figure 69 - Graphical method for selecting the best amount of clusters during the year in the post-COVID scenarios

The graph indicates that the best number of clusters for this data set is 3, because the sum of the square of the errors starts to reduce more smoothly once this value is reached. Figure 70 shows that for this number of clusters the time periods are consecutive. Therefore, the year is split into the periods summarise in Table 29 for the post-COVID scenarios.

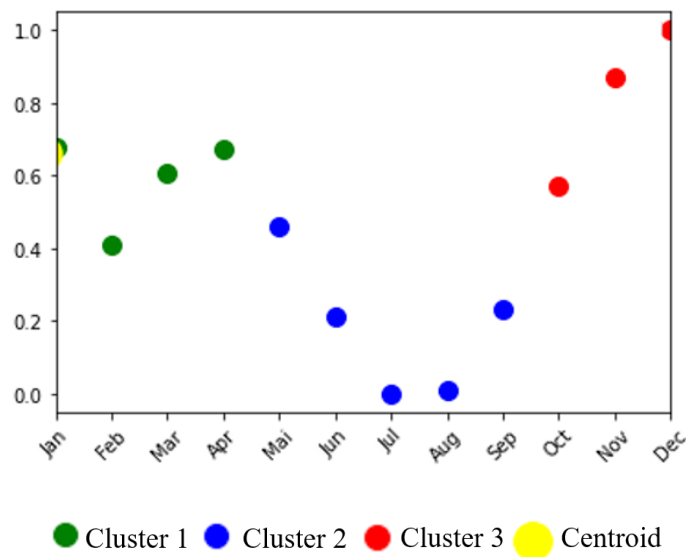


Figure 70 - Clustering the period during the year in the post-COVID scenarios

Table 29 - Time period during the year for the post-COVID scenarios

Season	m1	m2	m3
Post-COVID	January, February, March, April	May, June, July, August, September	October, November, December

To determine the time periods during the day, the electricity rate in the post-COVID scenarios was added to the data and this was organized according to the seasons found in the previous step. The graph for the elbow method in Figure 71 is obtained.

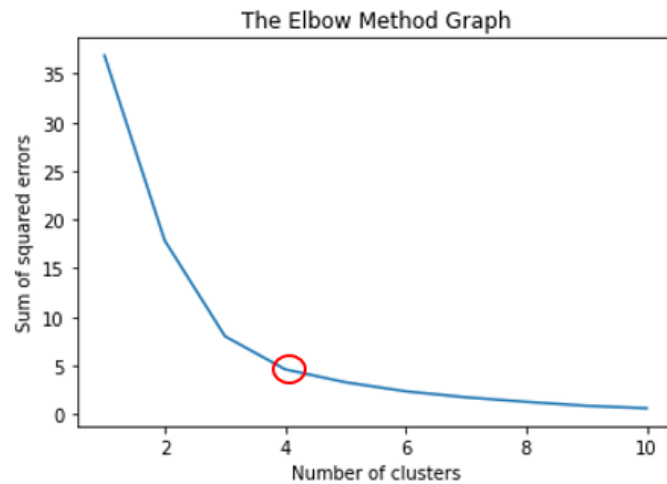


Figure 71- Graphical method for selecting the best amount of clusters during the day in the post-COVID scenarios

The elbow method indicates that the optimal number of clusters for the data set under this scenarios is 4; however with this number, the time periods were not distributed consecutively in the same cluster. Thus, the number of 5 clusters was considered as shown in Figure 72. Therefore, the day for the post-COVID scenarios is split into the periods presented in Table 30.

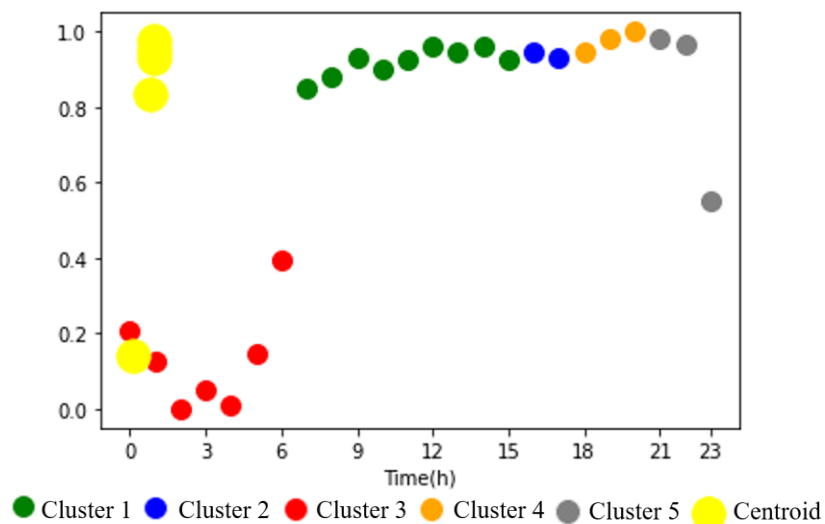


Figure 72 - Clustering the period during the day in the post-COVID scenarios

Table 30 - Time period during the day for the post-COVID scenarios

Period of the day	p1	p2	p3	p4	p5
Post-COVID	0:00 - 6:59	7:00 - 15:59	16:00 - 17:59	18:00 - 20:59	21:00 - 23:59

APPENDIX D - Discussion of the results for each scenario

S1E5: Scenario 1 during pre-COVID for five (5) houses

- *Electricity demand*

The corresponding yearly profiles of energy resources usage to satisfy the electricity demand for each house is illustrated in Figure 73. The photovoltaic panel was installed in all houses except for house i1, which can be explained by the lowest electricity demand of house i1, already supplied by the wind turbine.

Only house i5 had a battery installed because this house has a higher electricity demand and, therefore, storing energy becomes feasible. The use of the battery in house i5 is observed in the period of highest demand (p6), as shown in Figure 73 (e), illustrating that the cost of using stored energy is lower than buying energy from the central grid in this time period.

Additionally, the yearly profiles evidence that the energy demand of houses i2 and i4 is mostly supplied by the transferred energy from the wind energy produced in houses i3 and i5, besides the photovoltaic panels which operate in the periods of greater solar irradiation (p3 to p4). The results indicate that the wind turbine is the preferable source of electric energy.

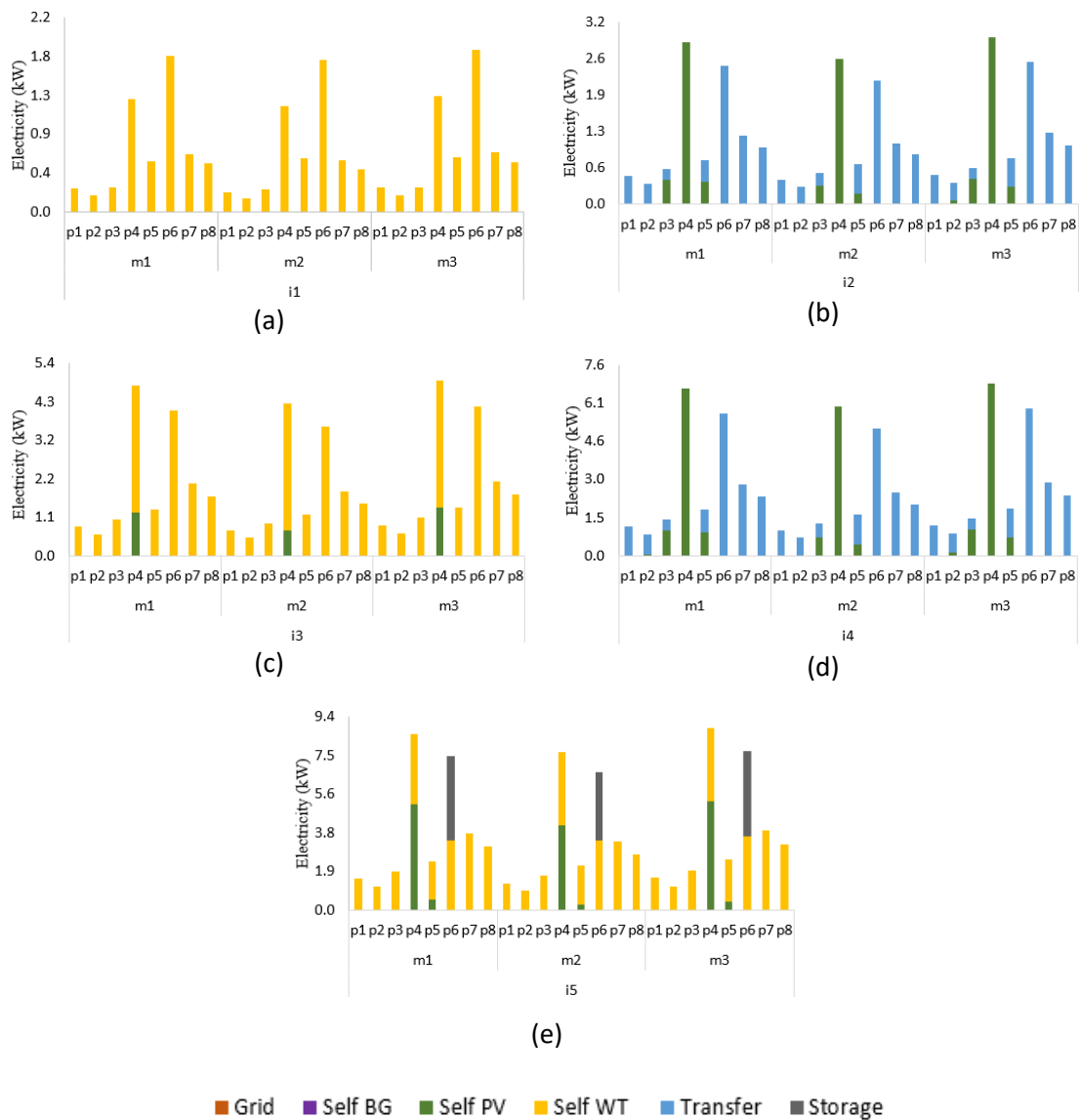


Figure 73 - Profile of resources used to meet the electrical demand in Scenario 1 pre-COVID for a microgrid with 5 houses: a) i1; b) i2; c) i3; d) i4; e) i5.

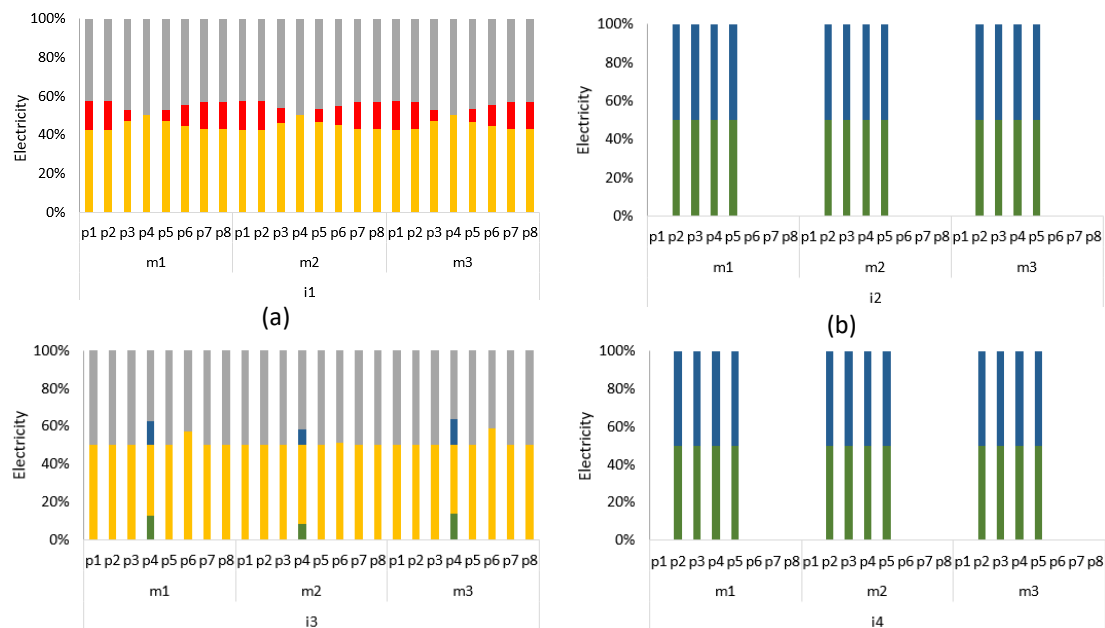
Figure 74 shows the power generation profile of distributed energy resources for each household in the microgrid. It illustrates the share of self-consumption (Self PV, Self WT, Self BG), storage (Storage PV, Storage WT, Storage BG), transfer (Transfer PV, Transfer WT, Transfer BG) and sale to the central grid (Sale PV, Sale WT, Sale BG) for each period along the year.

In house i1, only the wind turbine is installed, then its production is used for self-consumption, a large share (about 40%) is sold to the central grid and a small share (about 15%) is transferred to other houses, i.e. house i4. This suggests that inserting the excess energy produced into the central grid brings a greater benefit than transferring it within the microgrid.

In houses i2 and i4, the energy produced by the solar panel was used to meet the electricity demand and sell to the central energy grid. The photovoltaic panel only operates during p2 to p6, when the solar radiation is available; therefore the energy produced is not enough to supply the entire demand, especially during the night periods. During p2 and p6 the solar radiation is too low, then almost all the demand is supplied by the microgrid, as indicated in Figure 73.

In house i3 the wind generation is mostly used, but during period p4 in all seasons, photovoltaic is further used. The optimal choice for two energy sources can be explained by the fact that this period is characterized by the highest demand for electricity, as can be seen in Figure 73. Besides this, excess energy is produced by both sources and sold to the central grid. In the other periods, only the energy generated by the wind turbine is used for self-consumption, as it is sufficient to meet the demand of the residence, and the surplus energy is sold to the central network.

In house i5 during periods p3 and p5 in seasons m1 and m2 and during periods p2, p3 and p5 in season m3 the largest percentage (about 45%) of energy generated is destined to storage, since, as can be observed in Figure 73, these are periods which present lower demands. Therefore, the energy generated is sufficient to supply the demand in the period and its excess can be either stored or sold to the central grid. In the p4 period, which has the highest demand, the energy generated was used for self-consumption, as well as for transfer to other houses and sale to the central grid. In the other periods, the largest percentage of the energy generated was destined for self-consumption and sale to the central grid. The high percentage of wind power generation in this scenario may have been favored due to neglecting variations in energy supply.



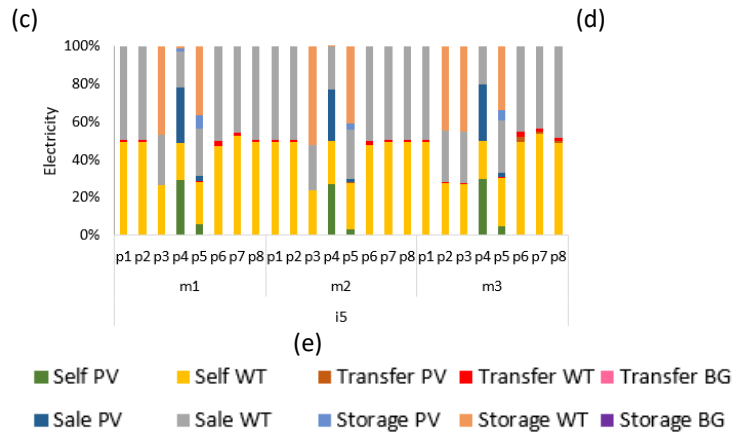


Figure 74 - Distribution of electricity generation by distributed renewable resources for Scenario 1 pre-COVID for a microgrid with 5 houses: a) i1; b) i2; c) i3; d) i4; e) i5.

- *Hot water demand*

Regarding the hot water demand, house 1 is supplied by an electric shower (which cannot be coupled with other source of hot water) since this house has the lowest demand. All other houses have a solar collector which is also coupled to thermal energy storage. Figure 75 illustrates the yearly profiles of hot water supply for houses i1 to i5.

Although the thermal energy storage can provide hot water when there is no solar radiation (p6), due to energy losses over time, a natural gas heater is further installed in houses i2, i3 and i4 and, in house i5, a biogas heater is chosen. The biogas may have been chosen for house i5 instead of the natural gas heater due to its lower cost and because this house demands a larger amount of hot water. Nevertheless, to meet the demand of house i5, hot water needs to be transferred from house i3. House i4 also receives excess of hot water produced by house i2. As discussed in IV.4, the results indicate that it is more feasible to receive hot water from another house than to install a bigger equipment in the residence.

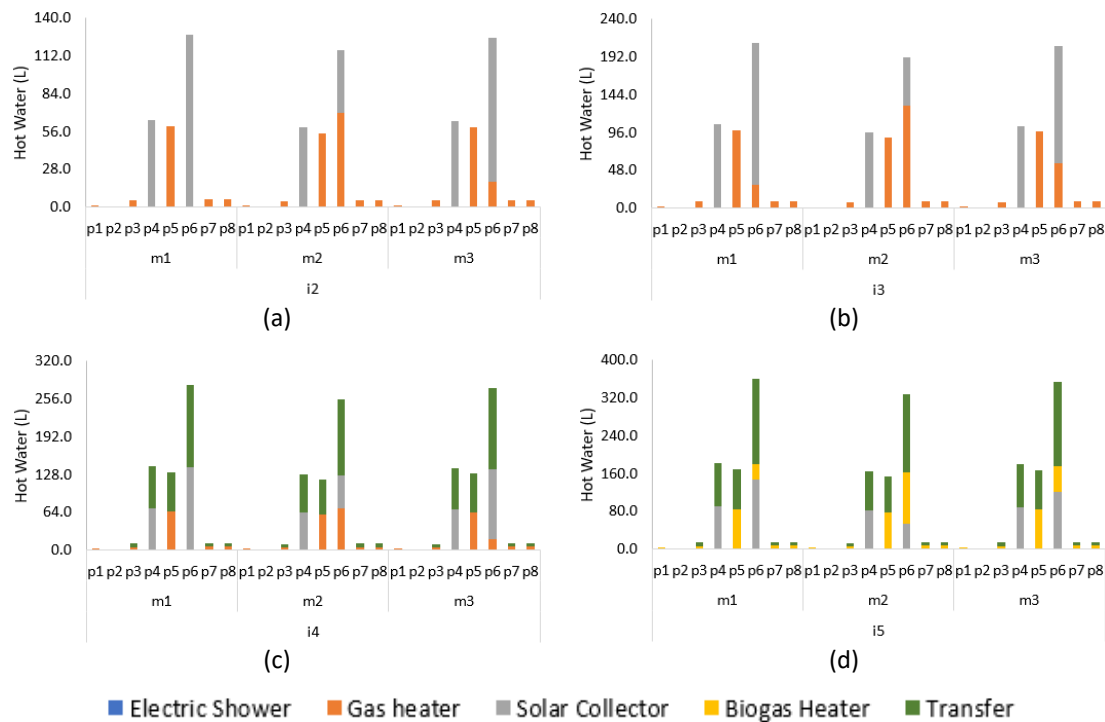


Figure 75 - Profile of resources used to meet the hot water demand for Scenario 1 pre-COVID for a microgrid with 5 houses: a) i2; b) i3; c) i4; d) i5.

- *Cooking-gas demand*

The optimal configuration installs a biodigester to supply the demand for biogas, which is used in i5 for cooking and for hot water production in the biogas heater. The amount of organic material produced per day in the household is sufficient to generate the biogas volume required to meet the demand for cooking-gas and biogas heater. Hence, purchasing extra organic material is not required.

Figure 76 shows that, despite having the highest percentage coming from natural gas, biogas is also used in house i5 for cooking. In houses i1, i2, i3 and i4 natural gas was chosen to supply all the gas demand for cooking food because they have a lower demand than house i5, as seen before.

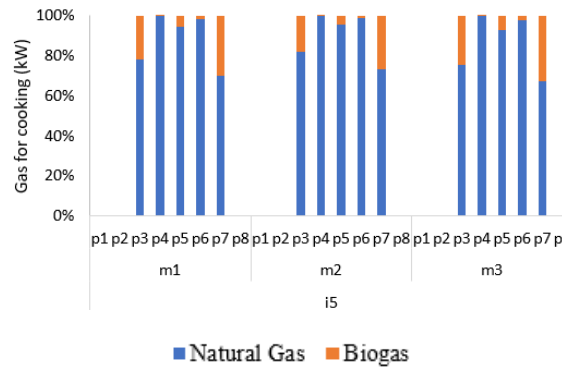


Figure 76 - Biogas and natural gas consumption behavior for Scenario 1 pre-COVID for a microgrid with 5 houses for house i5.

S2E5: Scenario 2 during pre-COVID state for five (5) houses

- *Electricity demand*

Figure 77 illustrates the profile of resources used to meet the electricity demand in the microgrid. House i1 is mostly supplied by wind turbines and the stored energy in batteries. This residence has a lower demand, thus the self-generation of energy is sufficient to meet its demand. Although house i2 has a battery installed, during the p7 period of the two seasons it purchases energy from the central grid. The p7 period is characterized as off-peak by the energy concessionaire, consequently the purchase of energy seems to be more profitable than the implementation of larger batteries to supply the demand during this period. On the other hand, house i2 uses energy stored in batteries mainly in the p6 period. This suggests that the cost of using battery is lower than buying energy from the central grid in this period, since p6 is characterized by the higher sales rate by the energy concessionaire.

Although house i3 has the same technologies for electricity production as house i1, in house i3 there was a greater use of photovoltaic panels to meet the electric demand than the wind turbine because the installed capacity of the PV panel is larger than the wind turbine in this house. This can be explained by the capacity limitation of the wind turbine and the higher electrical demand of house i3 in relation to house i1.

Furthermore, the higher capacity of the PV makes possible for house i3 to transfer energy to house i4. Houses i4 and i5 receive a significant share of energy in periods with higher demand, p5, p6 and p7, from houses i3 and i1, respectively. These results suggest that it is less expensive to receive energy from another house than to install equipment with higher capacities or to purchase energy from the grid.

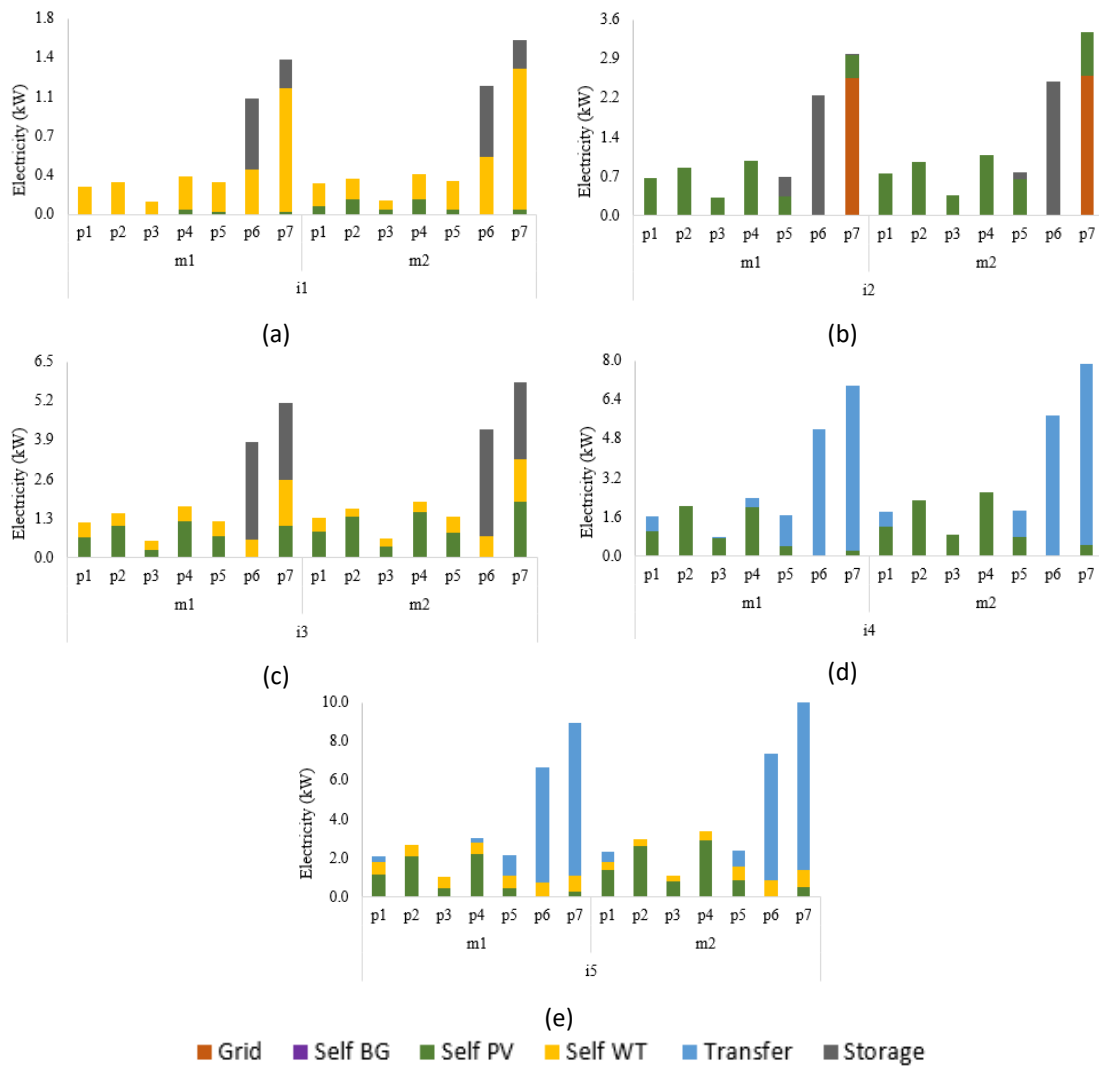


Figure 77 - Profile of resources used to meet the electrical demand in Scenario 2 pre-COVID for five houses: a) i1; b) i2; c) i3; d) i4; e) i5.

Figure 78 shows the share of electricity generation by distributed renewable resources. In house i1, characterized by a low demand, most of the energy produced is sold to the grid, stored in batteries, or transferred to another house. For houses i1, i2 and i3 a greater energy storage was observed in the periods of low demand (p1, p2, p3 and p4). The sale of energy to the grid obtained a lower percentage in these same periods (p1, p2, p3 and p4) and a higher percentage in period p5. The latter was possible because in this period (p5) the energy produced was higher and thus generated more credits to be used at the energy concessionaire. During periods p6 and p7 of both seasons, around 20% and 10% of the generated electrical energy in houses i1 and i3, respectively, is intended for transferring to other houses. This is mainly due to three reasons:

- these periods are marked by a higher demand for energy in the houses receiving the energy;
- both houses that are transferring energy have a lower electrical demand than the houses that are receiving it;
- houses i1 and i3 have batteries installed, making it possible to use the energy both for own consumption and for transfer to other houses.

Regarding house i2 during period p7 of both seasons, the energy produced is completely used for self-consumption because this period has a high demand. During period p6 there is no solar irradiation, therefore there is no energy generation in houses i2 and i4, which have only the photovoltaic panel installed.

In house i3 there are several uses of energy resources, transfer to other houses, self-consumption, sale to the grid and storage. Although house i3 has the same number of energy resources as house i1, the different profiles reflect the demand of the residence, which required equipment with higher capacities, as discussed in more detail in section IV.7.

The energy generated in house i4 was divided between sale to the grid and self-consumption, since this house has a greater demand in relation to houses i1, i2 and i3 and receives energy from house i3, as can be seen in Figure 77. The same behavior is observed for house i5, in which the energy generated in the residence by PV and wind turbine is used for self-consumption and sale to the grid. Moreover, this house has the highest demand of the microgrid, thus it receives energy produced by house i1 to meet its demand.

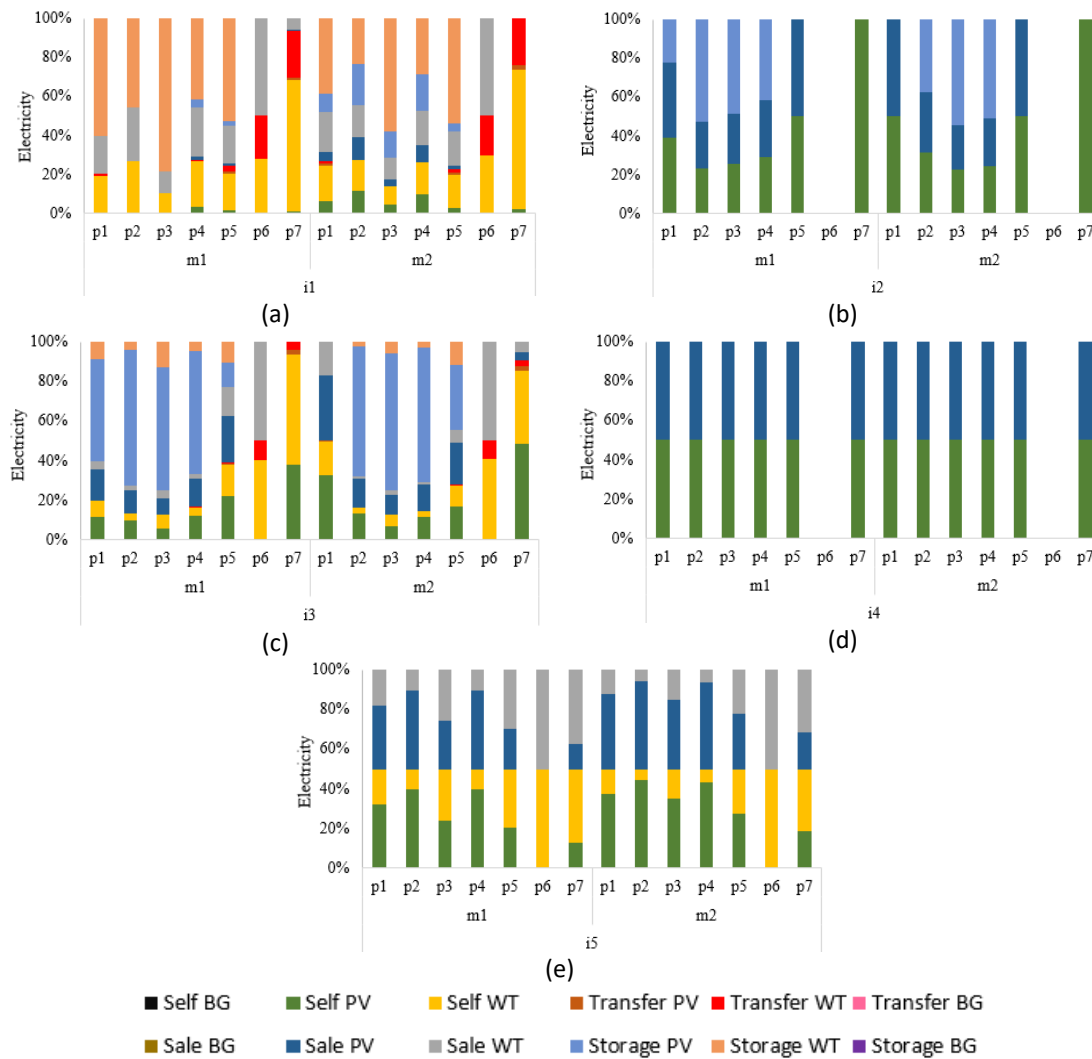


Figure 78 - Distribution of electricity generation by distributed renewable resources for Scenario 2 pre-COVID for a microgrid with five houses: a) i1; b) i2; c) i3; d) i4; e) i5.

- *Hot water demand*

Figure 79 illustrates the resources used to supply the hot water demand. House i1 is supplied by the solar collector and biogas heater. A similar consumption behavior is observed in houses i2 and i3; however, instead of using the biogas heater, the natural gas heater is used. The natural gas is continuously supplied through the central network, which could meet the demand, unlike the solar collector. Furthermore, because the solar collector has thermal energy storage, hot water could be used in periods when there was no solar radiation (p6) for all houses.

Besides the natural gas heater and solar collector, house i4 also receives hot water from house i3 to supply its demand. Therefore, it is more profitable to receive hot water from another house than to install a bigger equipment in the residence, as observed in the previous scenario, as discussed in section IV.7.

In house i5, a biogas heater and solar collector were installed. The biogas may have been chosen instead of the natural gas heater due to its lower cost and because this house demands a larger amount of hot water. However, due to the limited biogas production, it was not enough to meet all the demand, which was supplied by the solar collector and also by the transfer of hot water from house i1, as in the previous scenario.

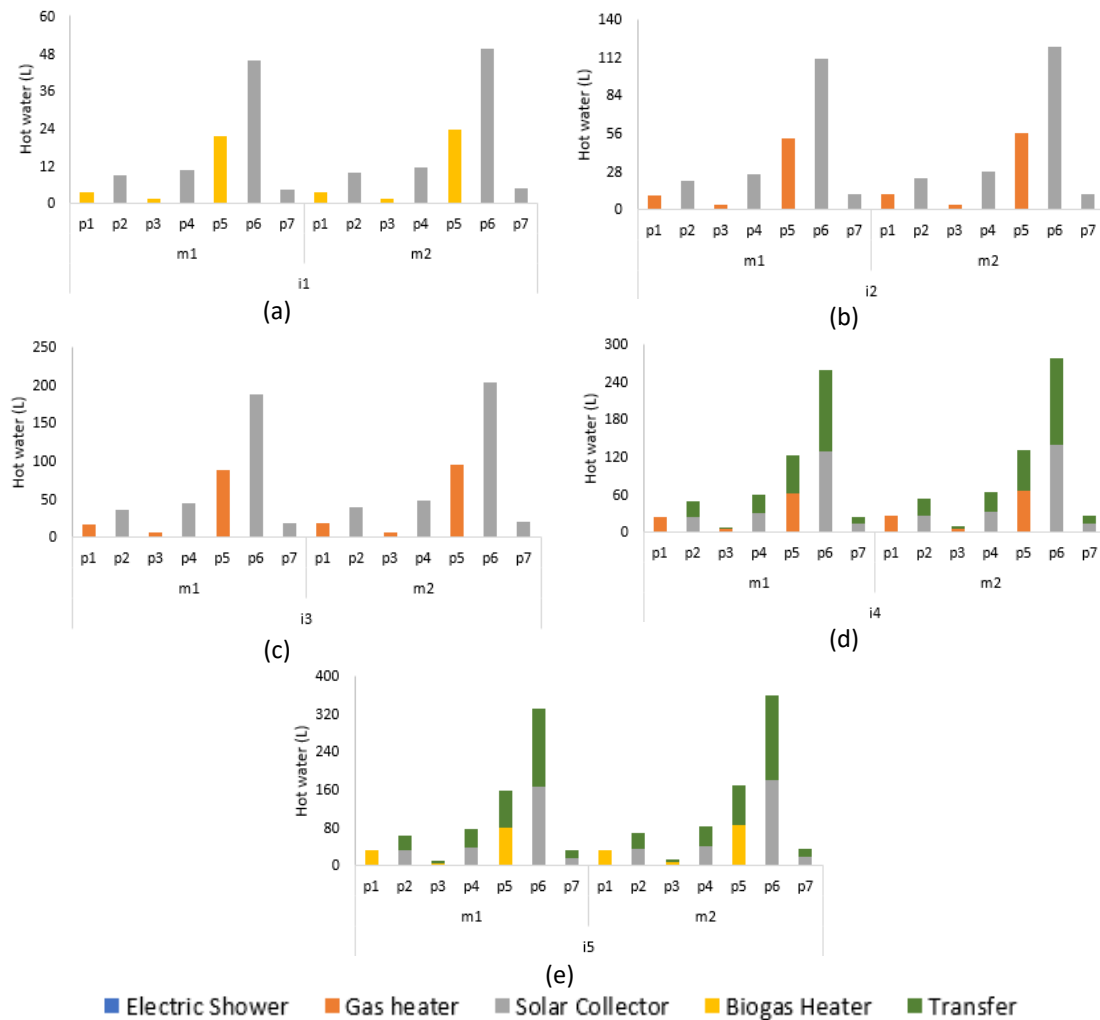


Figure 79- Profile of resources used to meet the hot water demand in Scenario 2 pre-COVID for a microgrid with five houses: a) i1; b) i2; c) i3; d) i4; e) i5.

S3E5: Scenario 3 pre-COVID for five (5) houses

- *Electricity demand*

The yearly profile of resources used to meet the electrical demand is expressed in the Figure 80. In house i1 there is a predominance of wind energy but, during the period of highest solar irradiation (p4), the photovoltaic panel is preferentially used. Since house i1 has the lowest demand, the surplus energy is stored for transferred to house i5 in the microgrid.

House i2 consumes energy from the central grid during some periods, but these are off peak billing. In sunny periods, photovoltaic energy is predominantly used (p3, p4 and p5). During the period of highest energy consumption (p6) in all seasons, stored energy is used instead. The use of battery afforded optimal solution since this period (p6) corresponds to the highest electricity rate of the grid. Therefore, using the battery presented a greater advantage compared to purchasing energy at a higher price from the grid. The same behavior is observed for houses i1 and i3 in this time period.

House i3 presented a similar behavior to house i1; however, as detailed in Table 22 the capacities of the installed equipment were higher, since the electrical demand of house i3 is higher than house i1. Houses i4 and i5 are mostly supplied by other houses in the microgrid. This may be associated with a lower cost of transferring energy between houses instead of implementing of a bigger energy resource.

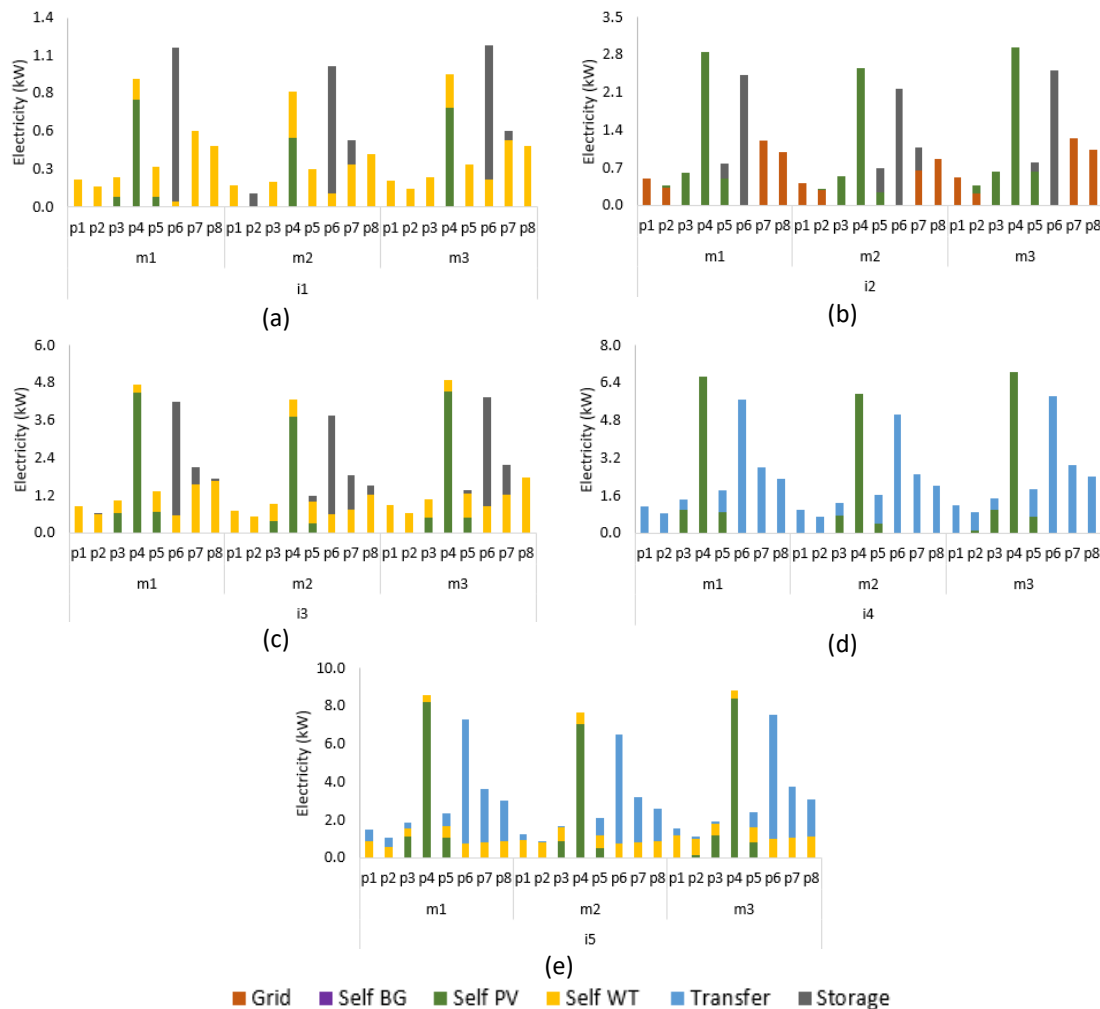


Figure 80 - Profile of resources used to meet the electrical demand in Scenario 3 pre-COVID for a microgrid with five houses: a) i1; b) i2; c) i3; d) i4; e) i5.

Figure 81 shows the share of electricity generation by distributed renewable resources. In house i1, the distribution of each percentage of energy produced changed for each season and time period. However, periods p6, p7 and p8 of seasons m2 and m3 follow a similar behavior. Around 40% of the energy from the wind turbine is inserted into the grid and the rest is divided into self-consumption and transfer to other houses. During periods p1 and p2 in each season there is a greater storage of energy from the wind turbine than for self-consumption because in these periods the demand is lower, but the wind energy production is higher than in the other seasons. In general, in this house the generation of energy by the wind turbine is higher than the generation by solar panels, which may be due to the production capacity of the installed wind turbine and the climatic conditions of the location that favor the use of wind turbines.

In house i2 it was noticed that in the p4 period of each season there was around 50% self-consumption and around 50% for insertion in the central grid. This occurs because of the less electrical demand in this period so that more energy can be fed into the central grid or stored for use in periods of higher demand. In period 2 for all seasons, all the energy produced is self-consumed. During period p5 and all seasons, house i2 inserted almost 50% of all energy produced into the grid. Hence, the energy generated in this period seems sufficient to supply the demand and export the surplus to the grid. The same occurred for all periods of energy generated in house i4. There are some periods when house i2 and i4 do not produce energy. As illustrated in Figure 80 (b), the demand of house i2 is supplied by the stored energy and by the grid, whereas house i4 receives energy from house i3.

For house i3 it was observed that in period p8 for all the seasons the highest percentage of wind power generation corresponds to self-consumption, since in this period there is a higher demand. Besides this, for the p4 period for all seasons, about 80% of the energy production corresponded to photovoltaic panels, it is divided between energy for self-consumption and for sale to the grid since in this period the electric demand is low. House i3 sells energy to the grid, mainly produced by the wind turbine in all periods. This can be explained due to the availability of the generating agent (wind speed) in all periods and the capacity of the wind turbine, providing a higher generation potential of the wind turbine than the photovoltaic panel.

In house i5, during periods p1, p6, p7 and p8 for all seasons, about 50% of all the energy produced by the wind turbine is destined for its own consumption and the remainder is sold to the central grid. Period p4 is characterized by a higher production from photovoltaic panels, with about 45% for own consumption and 45% for sale to the central grid. This is possible because this period has a lower demand for electricity and a higher availability of solar energy. Similar behavior is observed in house i3.

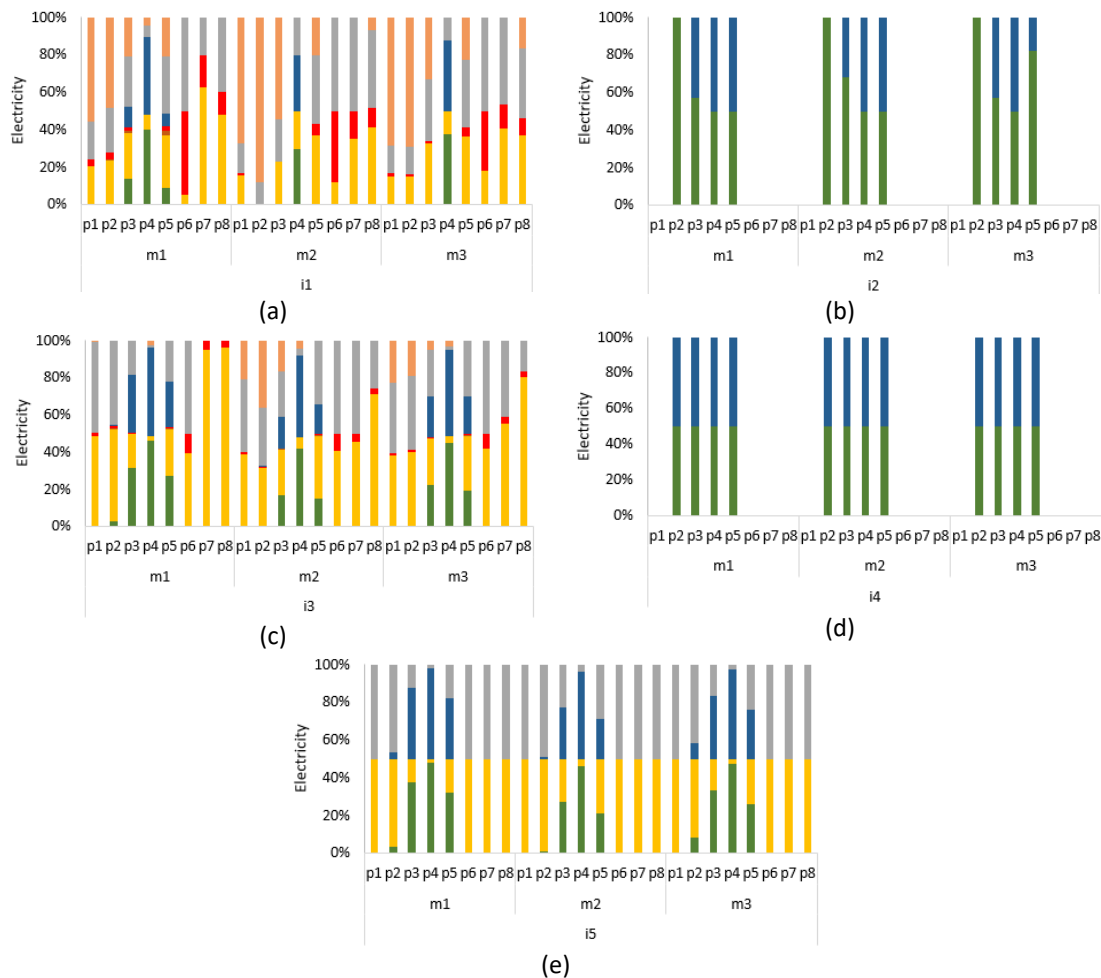


Figure 81 - Distribution of electricity generation by distributed renewable resources in Scenario 3 pre-COVID for a microgrid with five houses: a) i1; b) i2; c) i3; d) i4; e) i5.

- *Hot water demand*

According to the profile of resources used to satisfy the hot water demand expressed in Figure 82, houses i1, i2 and i3 were supplied by the solar collector and natural gas heater. In these houses, similar behavior in the use of energy resources was observed. Because the natural gas heater has a continuous supply coming from the central grid, it can be used when the solar collector cannot meet the demand. Furthermore, because the solar collector has thermal energy storage, hot water could be used in periods when there was no solar radiation (p6) for all houses.

In house i4 the natural gas heater and solar collector are used. Because this house had a higher demand than the other ones, it received hot water from house i3 to supply its demand. Therefore, receiving hot water from another house is more profitable than installing an equipment with higher capacity in the residence, as observed in the

previous scenarios. The sizing of each equipment will be approached in more detail in section IV.7.

In house i5, the biogas heater is installed besides the solar collector. The biogas may have been chosen instead of the natural gas heater due to its lower cost and because this house demands a larger amount of hot water. Due to the limited biogas production, though, it was not enough to meet all the demand, so that it receives hot water from house i1, as observed in the previous scenarios.

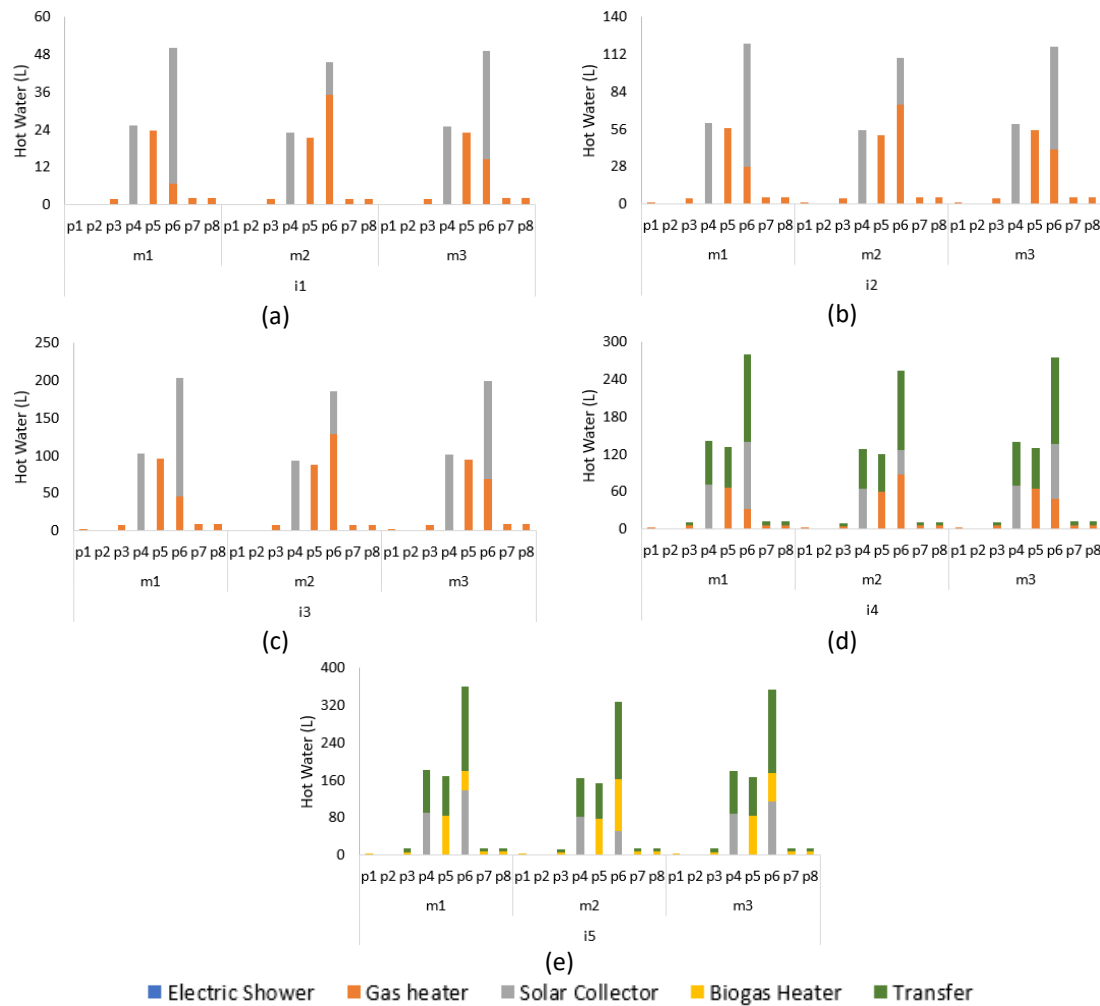


Figure 82 - Profile of resources used to meet the hot water demand in Scenario 3 pre-COVID for a microgrid with five houses: a) i1; b) i2; c) i3; d) i4; e) i5.

- *Cooking-gas demand*

For the supply of gas for cooking and for the biogas heater, there was no need for the houses to purchase extra organic material other than that produced in the households. Figure 83 shows the profiles of resources use to meet the gas demand for

cooking in the house i5. It is observed that more than 80% of the cooking gas demand is supplied by natural gas because of the biogas produced is mostly used to generate hot water.

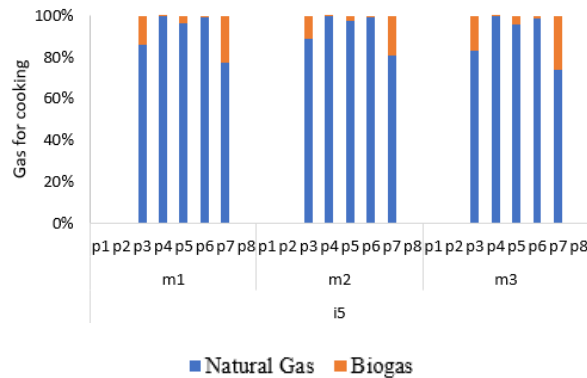


Figure 83 - Biogas and natural gas consumption behavior in Scenario 3 pre-COVID for a microgrid with five houses for house i5.

S305: Scenario 3 post-COVID for five (5) houses

- *Electricity demand*

Figure 84 shows the yearly profile of resources used to meet the electricity demand of this scenario. All the demand of house i1 is satisfied by the photovoltaic panels, the wind turbine and the energy stored in the battery. Because the residence has a low demand, there is no need to buy energy from the central grid. In period p2 of all the seasons a higher use of photovoltaic energy is observed because this period has the highest solar irradiation as observed in Figure 46 (a) between the hours of 7:00 and 16:00 (p2), and also because of the increase in electrical demand in the post-covid state during the day. The same behavior is observed for the other houses in this scenario. During the other periods energy from the wind turbine is used, besides the stored energy in the battery in the periods p4 and p5, with the largest quantity in the period p4. Period p4 is characterized as a peak period by the central energy grid and, therefore, it is more profitable to use the battery than purchase energy from the grid.

In house i2, during periods p1 and p5, the energy produced is not enough to meet all the demand, therefore energy from the grid needs to be purchased. In the periods p4 and p3 the stored energy is used to supply the energy demand, since the energy purchase rate is high in these periods, which made the use of stored energy more viable.

House i3 has a higher demand than house i1, then the utilization behavior of the installed technologies is different, with a higher utilization of the photovoltaic panel. In

addition, as in the previous houses in period p4 there is a greater use of the energy coming from the battery and to a lesser extent in periods p3 and p5.

Houses i4 and i5 received energy from other houses in periods p1, p3, p4 and p5. This can be explained by the fact that these houses have the highest demand of the microgrid. The results suggest, then, that it is more profitable to use energy from other houses than to buy equipment of higher capacity or from the grid.

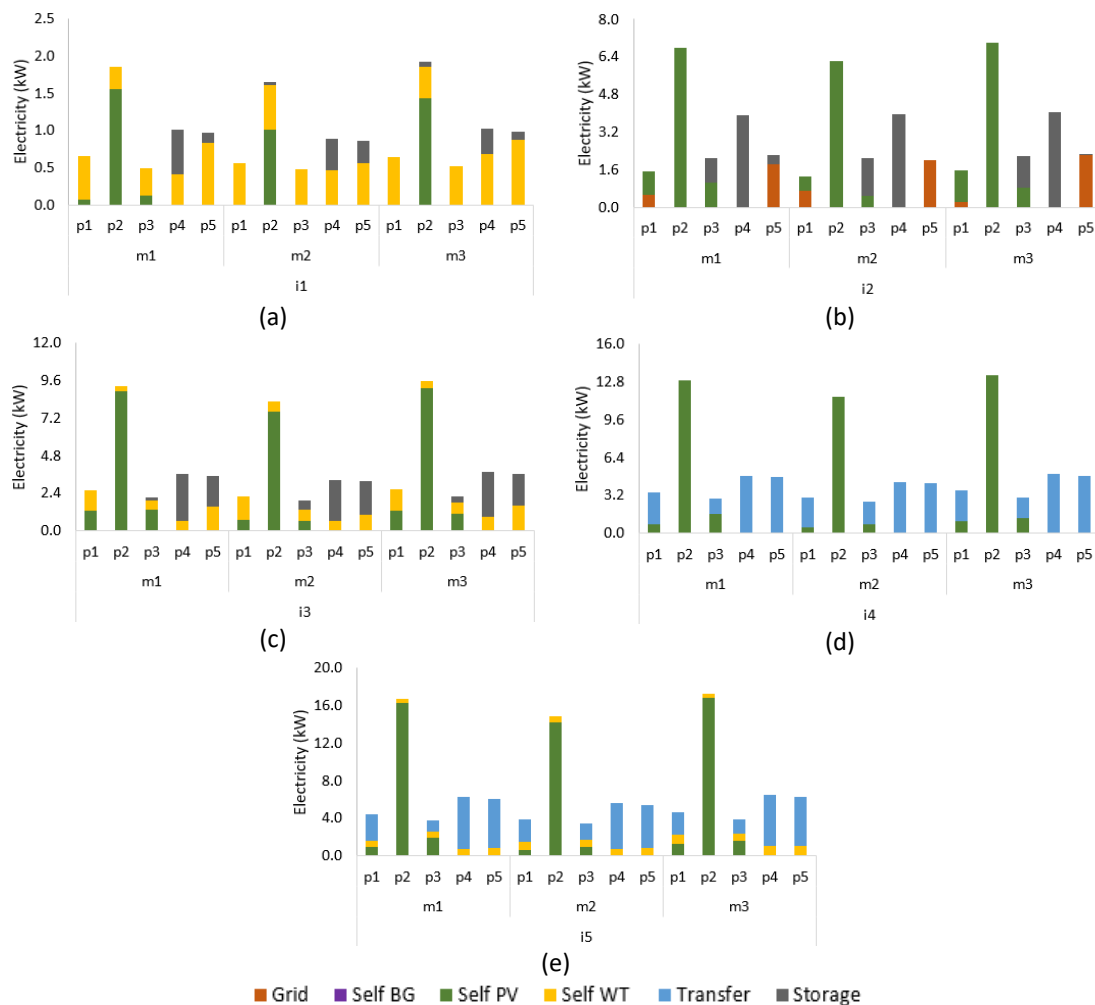


Figure 84 - Profile of resources used to meet the electrical demand for Scenario 3 post-COVID for five houses: a) i1; b) i2; c) i3; d) i4; e) i5.

Figure 85 shows the share of generation profile of each distributed energy resource. House i1 inserts energy into the grid during all periods. Since house i1 has the lowest demand among the houses, the productive capacity is higher than the house's demand; therefore, besides inserting energy into the central grid, it also shares energy in the same periods.

House i2, during the period p2 of each season, stores around 20% of energy coming from the photovoltaic panels and sells around 40% to the central grid because

in this period there is a high energy generation from photovoltaic panels. Around 40% of energy is self-consumed. In period p1 for all seasons, all the energy produced is used for self-consumption. In the p3 period for all seasons the insertion of energy into the grid is almost 50% of all energy produced. The same occurred for all periods of energy generated in house i4.

For house i3 during period p5 in all seasons, a greater proportion of wind energy production corresponded to self-consumption, since in this period there is a higher demand. For the other periods, around 50% of the energy generated from both technologies is self-consumed, while the rest is distributed to the central grid, to another house and stored in the battery because these periods have lower demands and, therefore, a greater surplus of energy generated.

In house i5 there is a higher consumption of energy coming from the wind turbine in the periods when there is not enough solar irradiation (p4, p5). Furthermore, approximately 50% of the energy produced by both installed resources is used for self-consumption and the other 50% for insertion into the central grid.

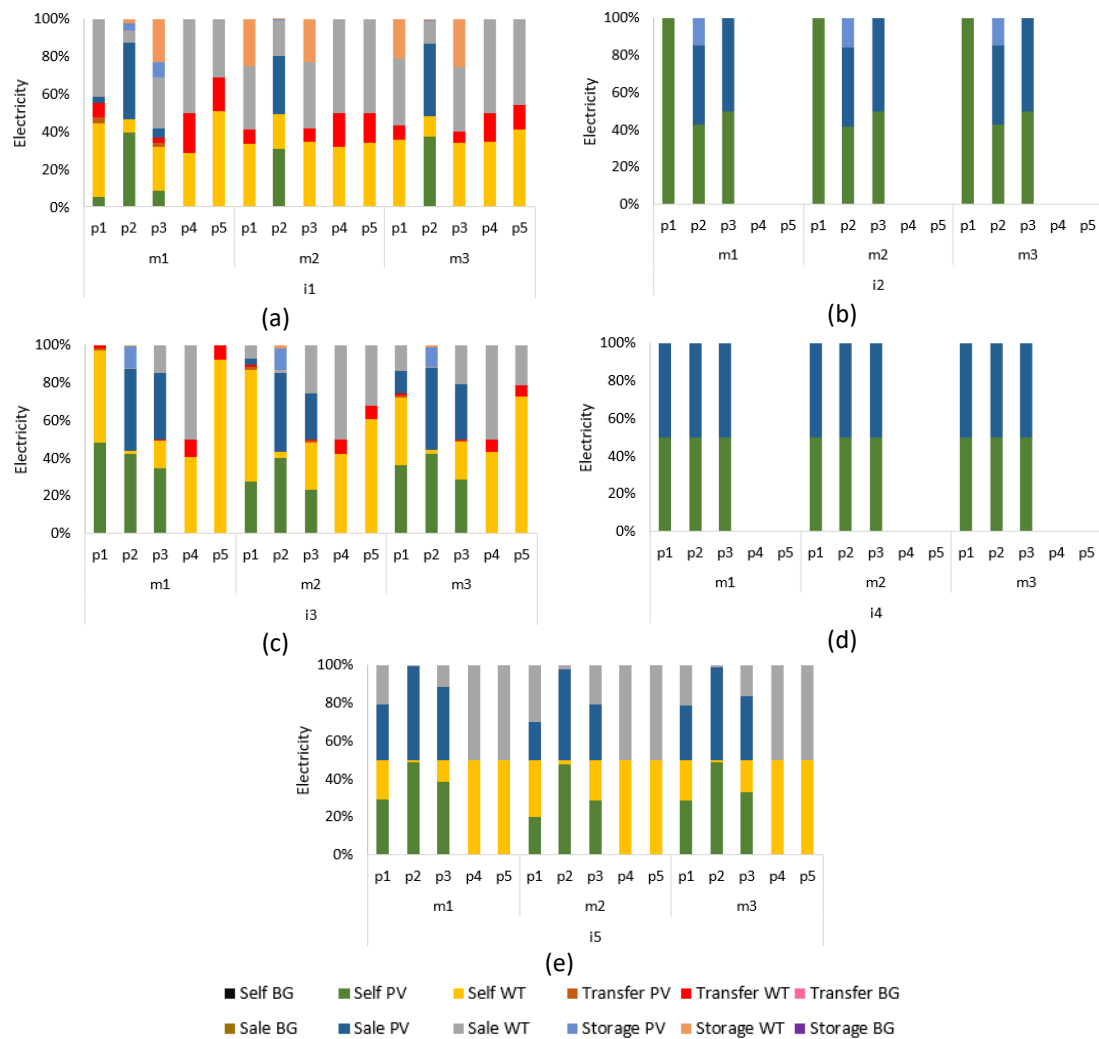


Figure 85 - Distribution of electricity generation by distributed renewable resources for Scenario 3 post-COVID state for five houses: a) i1; b) i2; c) i3; d) i4; e) i5.

- *Hot water demand*

According to the profile of resources used to satisfy the hot water demand expressed in Figure 86, house i1 is served in the periods of highest demand (p2 and p4) by the solar collector and the natural gas heater. As the natural gas heater has a continuous supply coming from the central grid, it can be used when the solar collector cannot meet the demand. House i2 has its hot water demand completely satisfied by the electric shower, since there is no possibility of installing another technology together with the electric shower.

House i3 is primarily served by the natural gas heater, due to the smaller capacity of the solar collector installed in the residence. Houses i4 and i5 present similar behavior: during periods p2, p3, p4 and p5 they receive hot water from another

residence and the rest is supplied by the biogas heater (house i4) and by the natural gas heater (house i5).

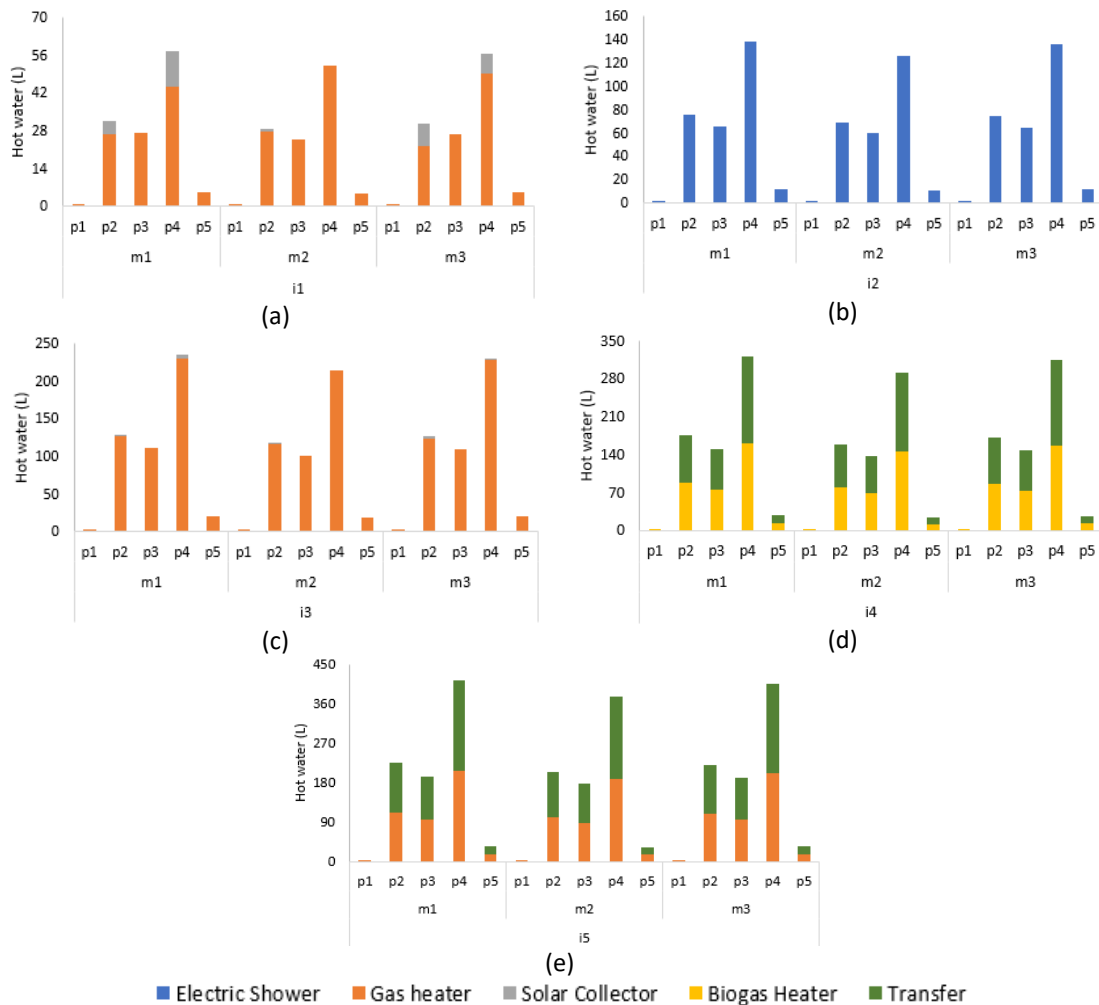


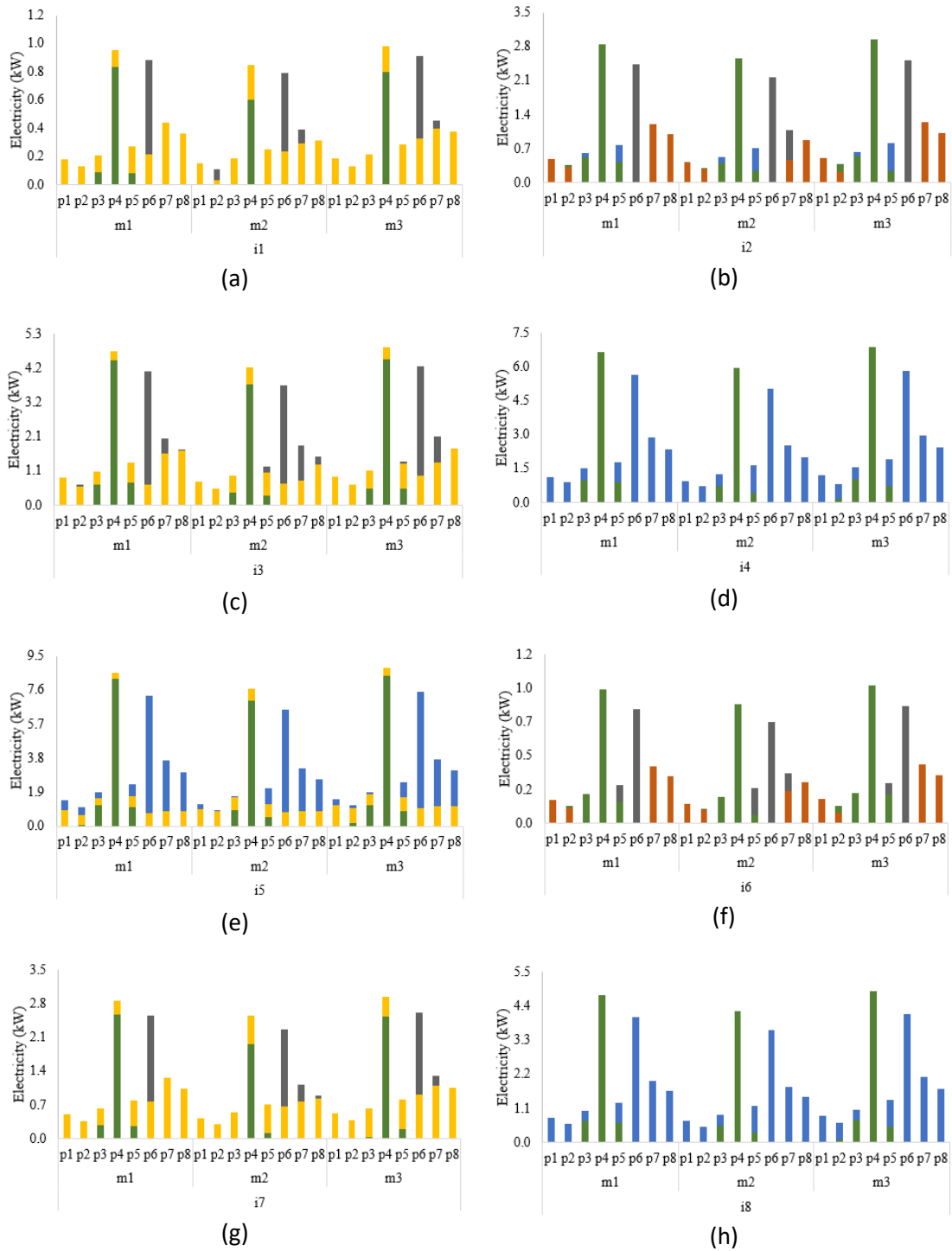
Figure 86 - Profile of resources used to meet the hot water demand for Scenario 3 post-COVID state for five houses: a) i1; b) i2; c) i3; d) i4; e) i5.

S3E10: Scenario 3 during pre-covid state for ten (10) houses

- Profile of use of energy resources to meet electrical demand

Figure 87 shows the profile of resources used to meet the electricity demand of this scenario. Thus, the electricity demands are equivalent to S3E5 as follows: houses i1 and i6 are equal to house i1 in the 5 houses scenario, houses i2 and i7 are equal to house i2 in the 5 houses scenario, houses i3 and i8 are equal to house i3 in the 5 houses scenario, house i4 and i9 are equal to house i4 in the 5 houses scenario, houses i5 and i10 are equal to house i5 in the 5 house scenario. Thus, similar behaviors were observed with the scenario of 5 houses in houses i1, i3, i4, i5.

Furthermore, similar behavior was observed with S3E5, houses i8 and i10 in S3E10 with house i4 in the S3E5, house i6 with house i2 for the S3E5, house i7 with house i1 for the S3E5, house i9 with house i3 for the S3E5. This can be explained due to the same number of technologies used and same behavior regarding energy sharing between houses.



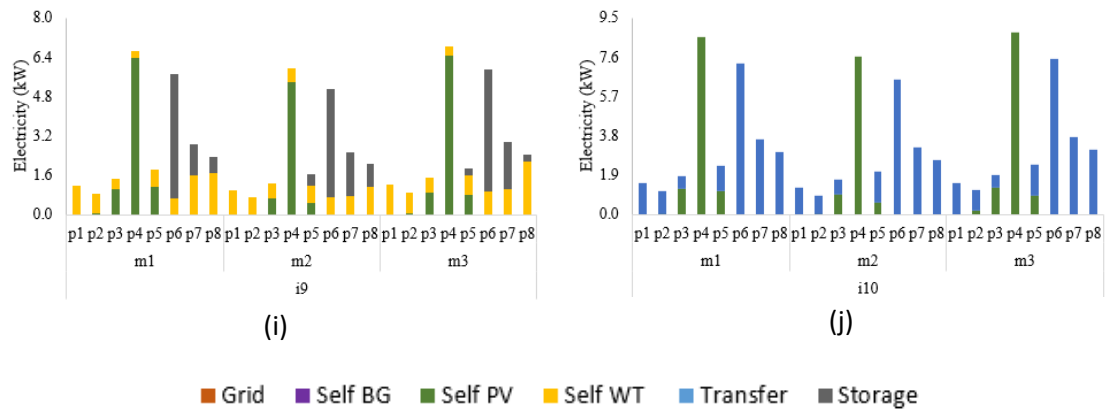


Figure 87 - Profile of resources used to meet the electrical demand in the pre-COVID scenario 3 for ten houses: a) i1; b) i2; c) i3; d) i4; e) i5; f) i6; g) i7; h) i8; i) i9; j) i10

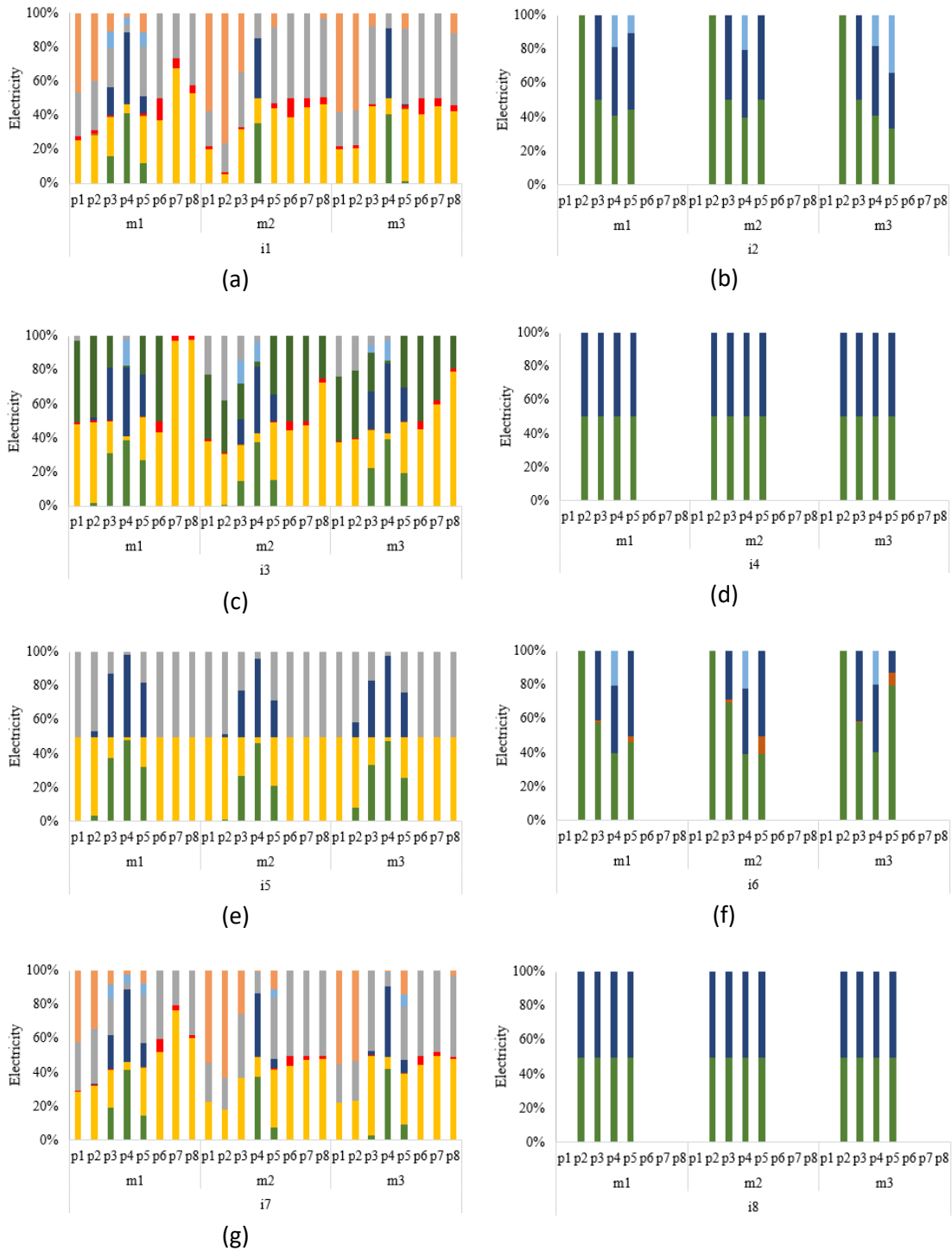
- *Power generation profile of distributed energy resources*

Figure 88 shows the generation profile of each distributed energy resource. Regarding electric energy generation, a similar behavior was observed for houses i4, i8, i10 with house i4 in the 5 houses scenario and house i5 with house i5 in the 5 houses scenario. This is because these houses have the same amount of technologies installed and also receive energy from other houses.

When comparing the houses in the same scenario, it is observed that for houses i1 and i6, despite having the same demand for electric energy, the production capacity of house i1 is higher than that of house i6. This is due to the dynamics of wind turbine installation, which considers the configuration of the microgrid and the electrical demand of the houses. This way, it becomes more viable to adopt the wind turbine in house i1 to share energy to house i8 than to adopt in house i8 a higher capacity. As for house i6, although it also shares energy with another house, the house it shares has a lower demand than house i8, so there is no need for a larger production capacity in house i6. A similar explanation can be attributed to the i2 and i7 houses that have the same demand, but different installed capacities and with this, different behaviors in the use of the energy generated.

For house i2 the wind turbine was not installed, being more viable to receive energy from house i6. Because of that, in periods p3 and p5 of all the seasons, when energy is received from house i6, it was possible to insert in the central grid the excess of energy produced or store it in battery to be used in the period of greatest demand, as observed in the profile of Figure 48. For house i7, with the installation of the wind turbine and solar panel, it was possible to share energy with house i5 in periods p1, p2, p3, p5, p6, p7 and p8 for all seasons, as well as feed energy into the grid and store energy.

Thus, as in house i7, for houses i3 and i9, because they have both technologies (wind turbine and photovoltaic panel), it was observed a distribution between stored energy, inserted in the central network, used for own consumption and transferred to another residence. The difference between the percentage destined to each category is due to the installed capacity of both houses, as well as the demand of each house and the demand of the houses that receive energy.



(h)

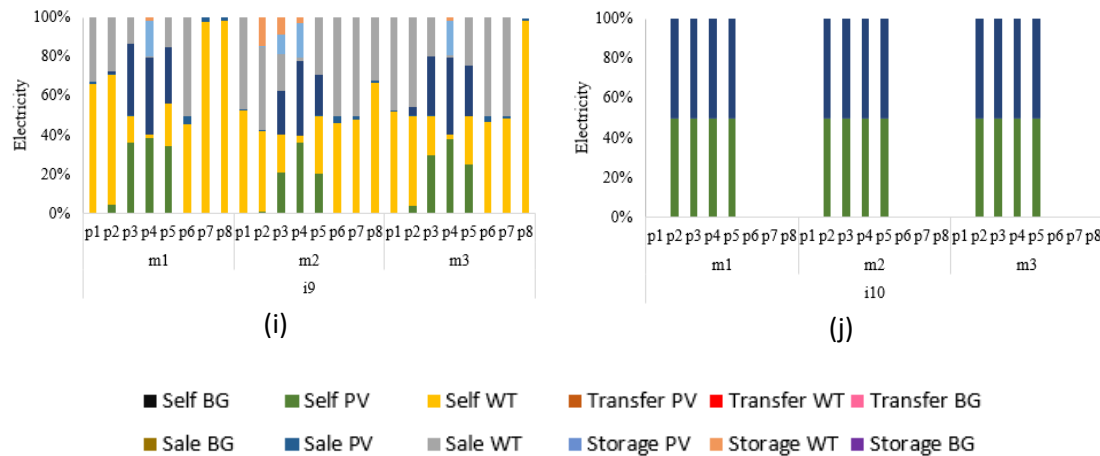


Figure 88 - Distribution of electricity generation by distributed renewable resources in the pre-COVID scenario 3 for ten houses: a) i1; b) i2; c) i3; d) i4; e) i5; f) i6; g) i7; h) i8; i) i9; j) i10

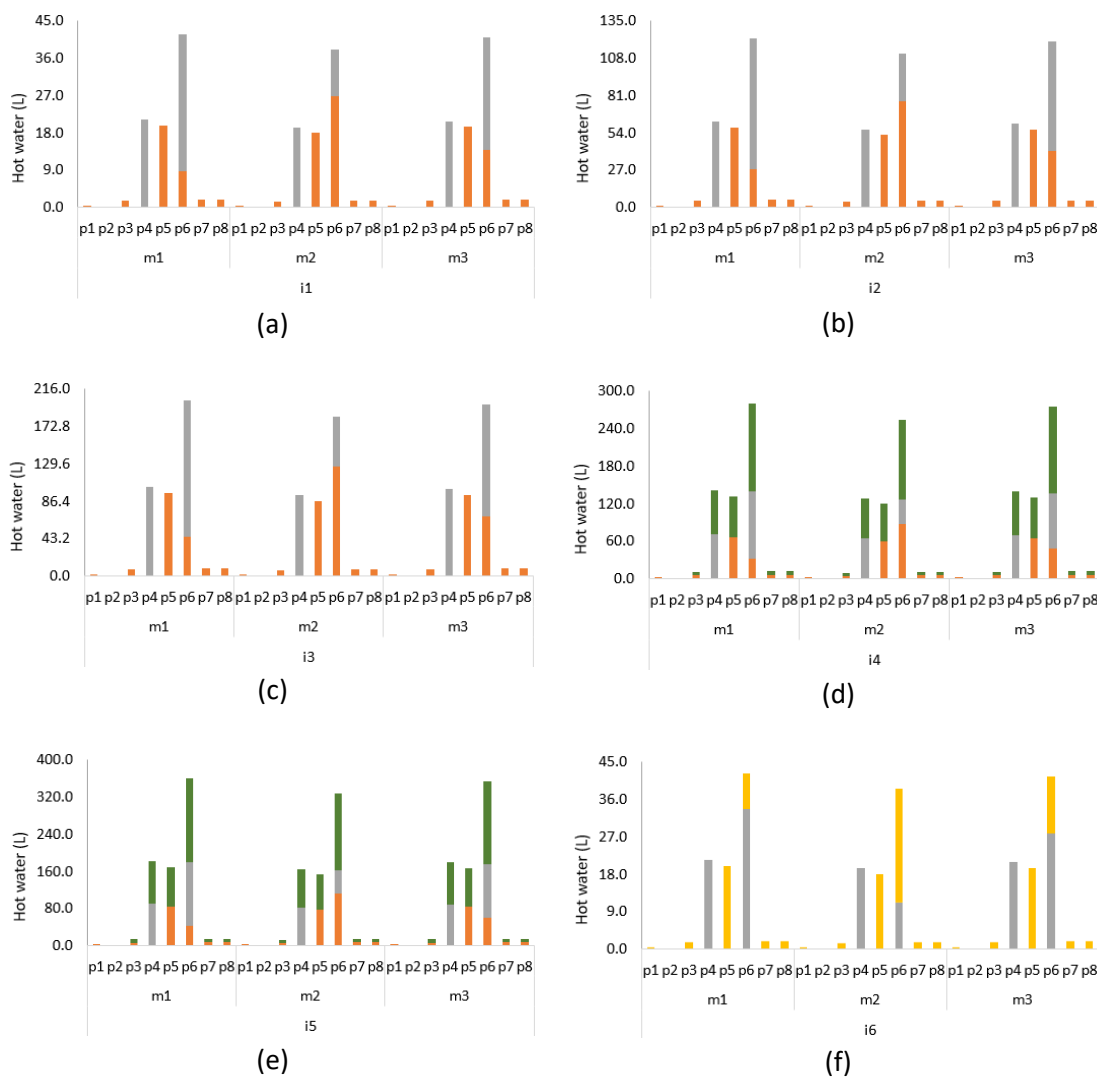
- *Profile of use of energy resources to meet hot water demand*

Figure 89 shows the profile of resources used to satisfy the hot water demand. In this scenario, the hot water demands are equivalent to the S3E5 as follows: houses i1 and i6 are equal to house i1 in the 5 houses scenario, houses i2 and i7 are equal to house i2 in the 5 houses scenario, houses i3 and i8 are equal to house i3 in the 5 houses scenario, house i4 and i9 are equal to house i4 in the 5 houses scenario, houses i5 and i10 are equal to house i5 in the 5 house scenario. Thus, a similar behavior is observed as in the scenario of 5 houses in houses i1, i2, i3, i4, i7 and i9, due to the similarity of hot water demand and installed equipment.

On the other hand, for the other houses the behavior differed from that observed in the 5 houses scenario. This is due to the installed capacity or the installed resource being different. However, a similar behavior between them was observed in houses i5 and i10, due to both having the same hot water demand and the same hot water generation technologies. Due to these houses having a high demand, both received hot water from another house to supply their demand. This infers that it was more feasible to receive hot water from another house than to install larger equipment in the residence. As for the sizing of each equipment, this is expressed in more detail in item IV.7.

Despite different capacities, house i8 has similar behavior as i4, i5, i9 and i10. This can be explained by the fact that all houses also receive hot water from other houses and use the same energy resources. When the transferred hot water cannot supply the entire demand of the house, the natural gas heater is used, as observed in periods p1, p3, p5, p6, p7 and p8 for all seasons.

House i6 has a different profile from the others, because it uses the biogas heater and hot water from the solar collector to supply its energy. When the hot water from the solar collector cannot supply the demand, the biogas heater is used. The use of biogas heater only in this residence can be explained by the limited production of biogas in the microgrid, as well as because it is located close to the biodigester, reducing the cost of transporting the biogas.



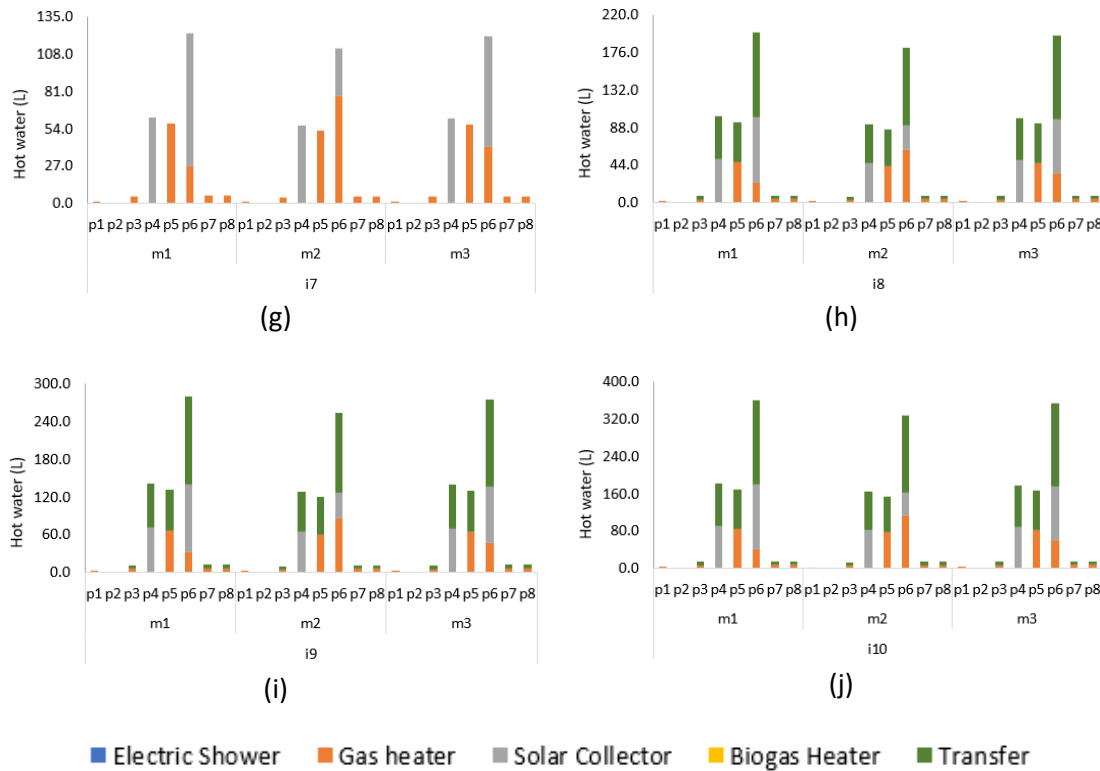


Figure 89 - Profile of resources used to meet the hot water demand in the pre-COVID scenario 3 for ten houses: a) i1; b) i2; c) i3; d) i4; e) i5; f) i6; g) i7; h) i8; i) i9; j) i10.

- *Profile of use of energy resources to meet gas for cooking demand*

For the supply of gas for cooking and for the biogas heater there was no need for the houses to purchase extra organic material other than that produced in the households. The profile of biogas and natural gas consumption by the i5 house is shown in Figure 90. As can be observed, natural gas represented the largest percentage in all periods (more than 55%). As explained earlier the reduction of biogas use in this scenario is due to its higher cost compared to natural gas from the grid.

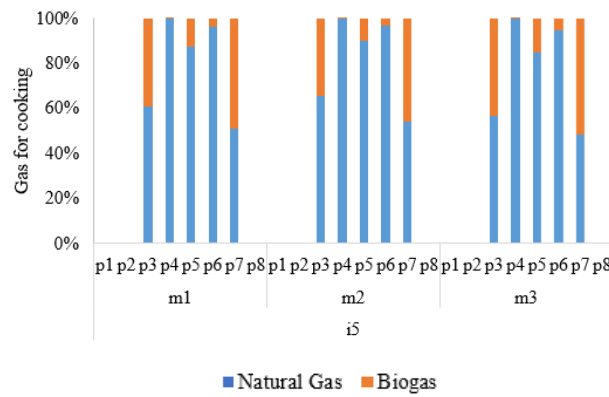


Figure 90 - Biogas and natural gas consumption behavior for house i5 for the microgrid of 10 houses in the pre-COVID scenario 3

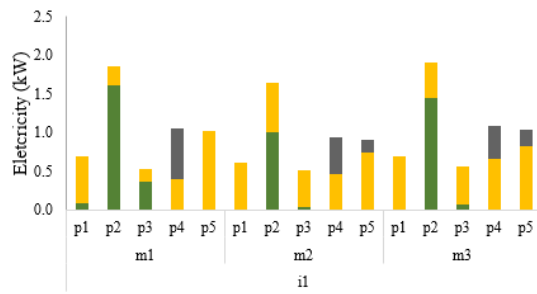
S3010: Scenario 3 during post-COVID state for ten (10) houses

- *Profile of use of energy resources to meet electrical demand*

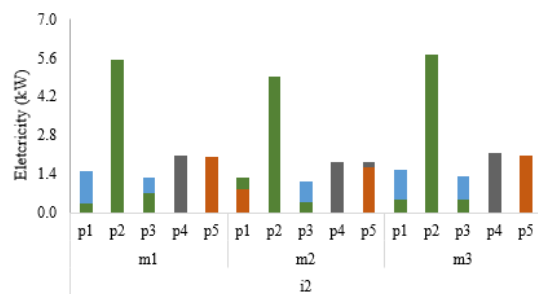
Figure 91 shows the profile of resources used to meet the electricity demand of this scenario. In this scenario, the electricity demands are equivalent to S305 as follows: houses i1 and i6 are equal to house i1 in the 5 houses scenario, houses i2 and i7 are equal to house i2 in the 5 houses scenario, houses i3 and i8 are equal to house i3 in the 5 houses scenario, house i4 and i9 are equal to house i4 in the 5 houses scenario, houses i5 and i10 are equal to house i5 in the 5 house scenario. Thus, a similar behavior is observed with the scenario of 5 houses in houses i1, i3, i4, i6, i7, i8, i9 and i10.

However, for house i2, due to the fact that it receives electricity from house i7, in periods p2 and p3 there is a greater use of energy coming the house i7 to meet its demand. This infers that it was more viable in this scenario to share energy between houses i7 and i2, since the distance between these houses is not high, and, therefore, without a great loss of energy in its transportation. In addition, the house i7 has a larger installed capacity than the house i2, as will be detailed later in section IV.7.

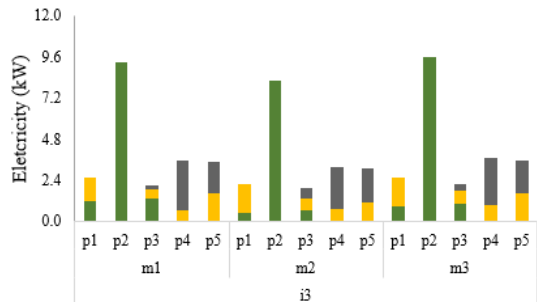
Because house i1 in this scenario has a larger capacity wind turbine than house i1 in the scenario for 5 houses, it was able to transfer a larger amount of energy to house i5. Thus, house i5 did not need to install a wind turbine to supply its electrical demand. It only used the energy transferred from house i1 and its photovoltaic panel to meet its electrical demand.



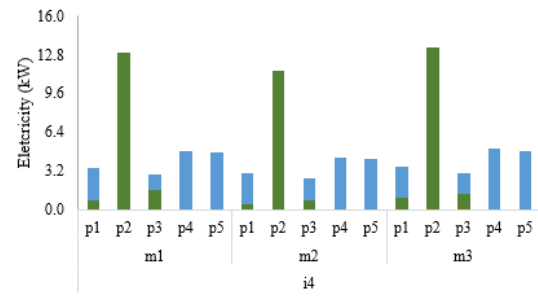
(a)



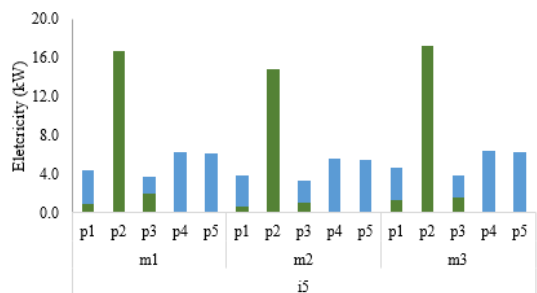
(b)



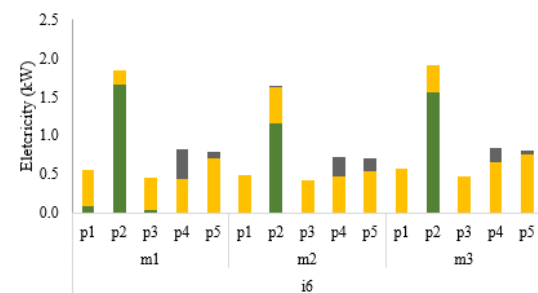
(c)



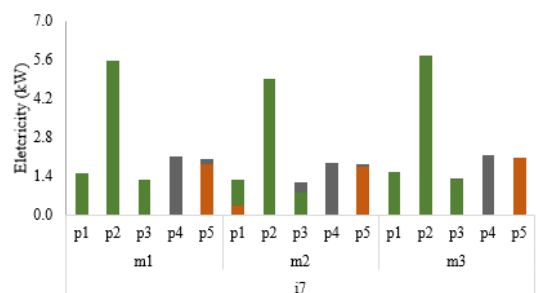
(d)



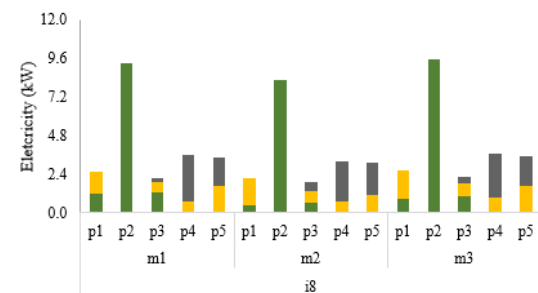
(e)



(f)



(g)



(h)

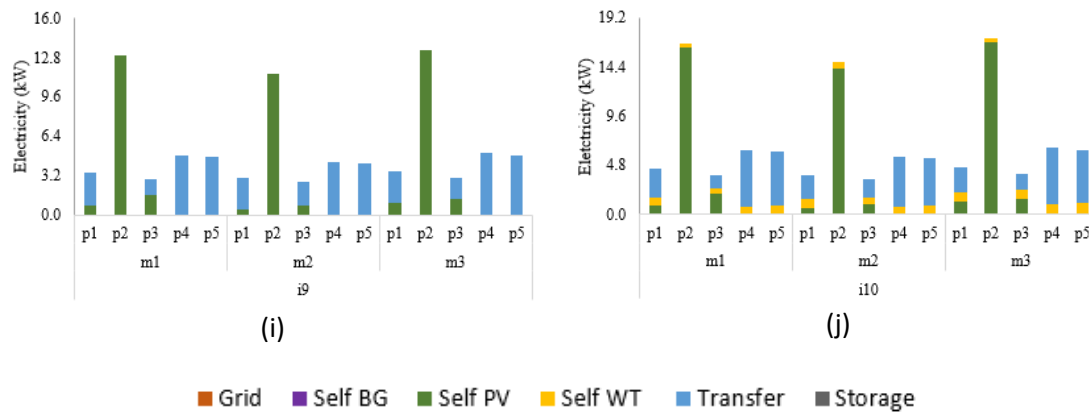


Figure 91 - Profile of resources used to meet the electrical demand in the post-COVID scenario 3 for ten houses: a) i1; b) i2; c) i3; d) i4; e) i5; f) i6; g) i7; h) i8; i) i9; j) i10.

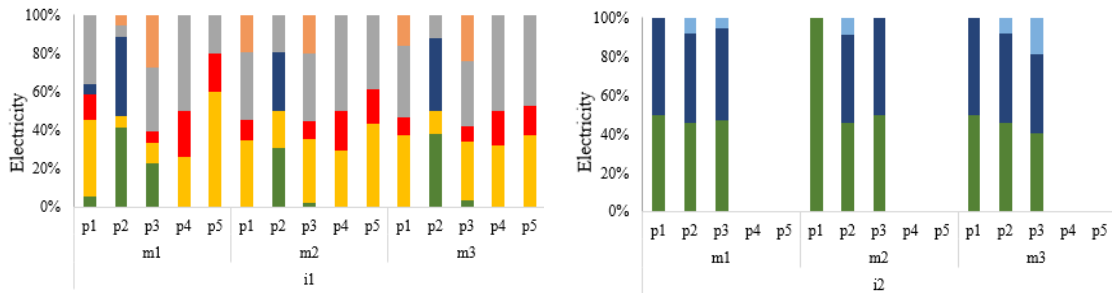
- *Power generation profile of distributed energy resources*

Figure 92 shows the generation profile of each distributed energy resource. Regarding electric energy generation, a similar behavior was observed for houses i3 and i8 with house i3 in the 5 houses scenario, houses i4 and i9 with house i4 in the 5 houses scenario and, finally, house i10 with house i5 for the 5 houses scenario.

For houses i1 and i6, despite having the same electric energy demand, the production capacity of house i1 is bigger than that of i6. In this way, there is a greater transfer of energy from this house to another house in all periods.

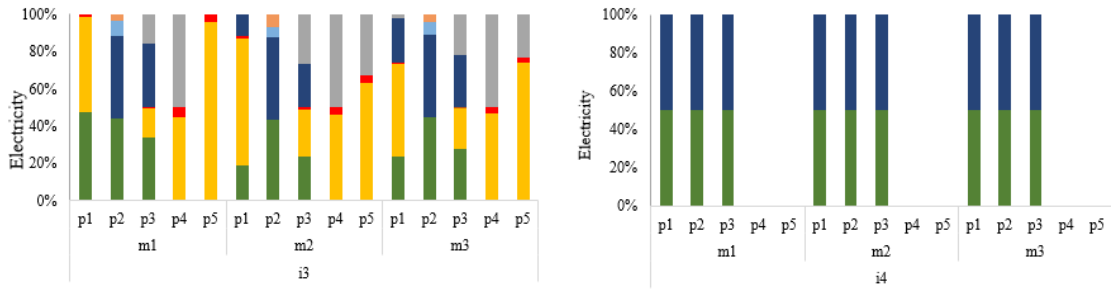
Besides this, because house i2 received energy from house i7 in period p1 it was able to insert energy into the grid. This was possible due to the consideration that a house can only insert energy into the central grid when all the demand of the residence is satisfied by the microgrid. The same is valid for house i5 that received most of the energy it needed to meet its demand from house i1, this way it could sell energy to the central grid.

Although the quantity of energy transferred from house i7 to house i2 was sufficient to supply the electrical demand in the residence in the periods of lower demand (p1 and p3 of season m1 and m3 and in period p3 in season m2), as observed in Figure 91, this quantity was not significant in relation to the total energy generated by house i7. This infers that in this house it was more viable to insert more energy in the central network than to transfer energy to another house.



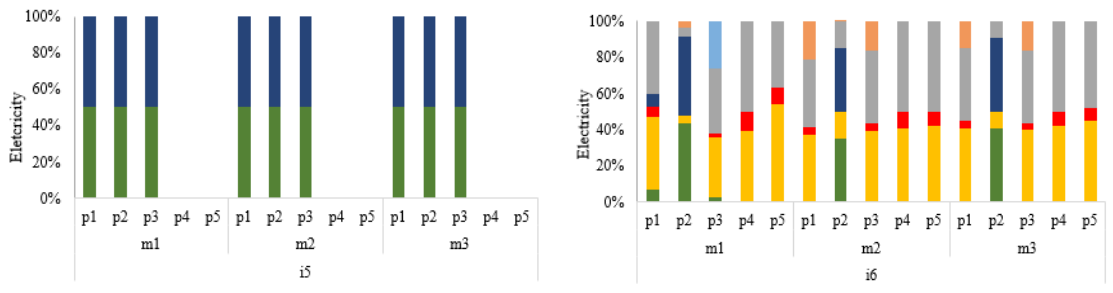
(a)

(b)



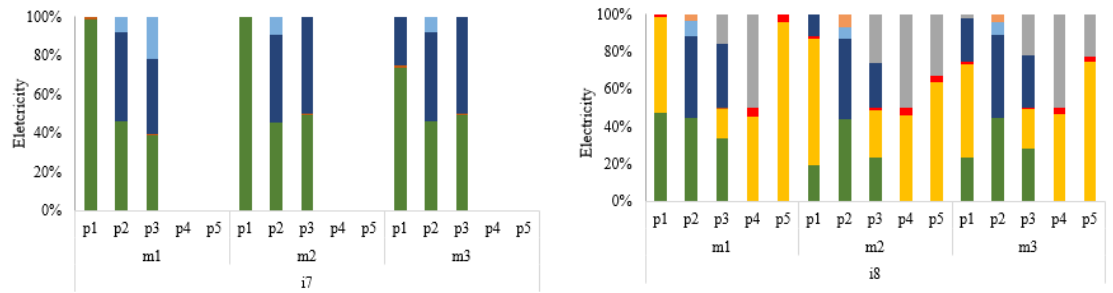
(c)

(d)



(e)

(f)



(g)

(h)

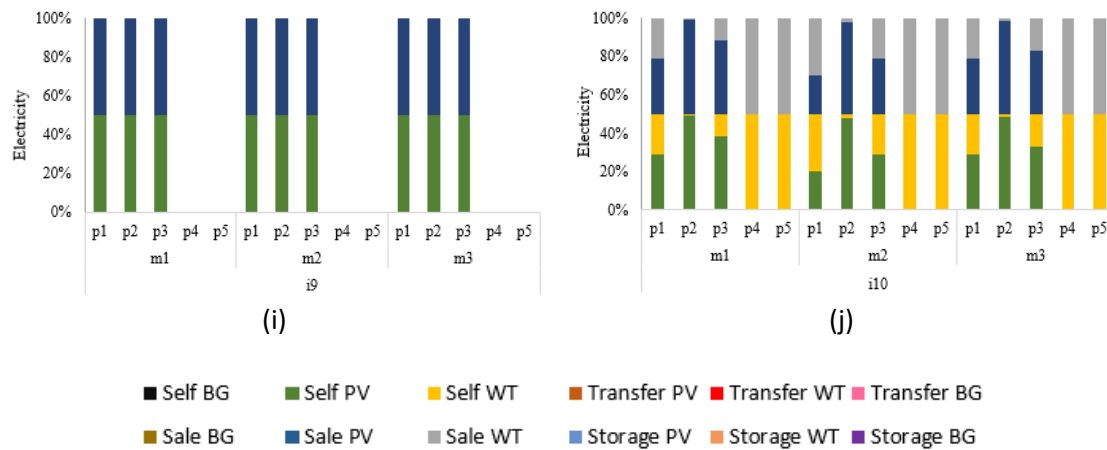


Figure 92 - Distribution of electricity generation by distributed renewable resources in the post-COVID scenario 3 for ten houses: a) i1; b) i2; c) i3; d) i4; e) i5; f) i6; g) i7; h) i8; i) i9; j) i10.

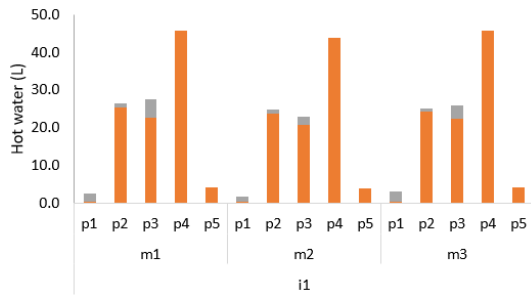
- *Profile of use of energy resources to meet hot water demand*

Figure 93 shows the profile of resources used to satisfy the hot water demand. A similar behavior was observed in houses i1 and i6, due to both having the same hot water demand and the same hot water generation technologies. Thus, it is observed that in period p1 of all seasons practically all the hot water coming from the photovoltaic panel was used, due to the lower demand in this period. In the periods when the solar collector was not able to meet the demand, the natural gas heater was used, because the natural gas has a continuous supply coming from the central network. Moreover, houses i2 and i7, due to having the same technologies and the same hot water demand, obtained a similar resource utilization profile to meet their demand.

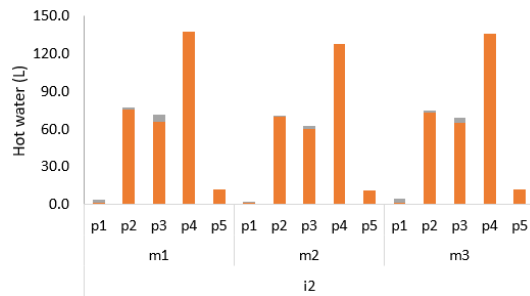
When analyzing houses i1, i6, i2, i7 and i3 that used the natural gas heater and solar collector, it can be inferred that the natural gas heater becomes more viable to be used in most of the periods that its use is demanded. This can be explained using the same argument exposed above, because natural gas has a continuous supply and the solar collector depends on the climatic conditions of the region. For houses i4, i8, i9 and i10, similar behavior is observed, since all these houses receive hot water from other residences. When the hot water transfer cannot supply the entire demand of the residence, the natural gas heater is used in these houses, as observed in periods p2, p3, p4 and p5 for all seasons.

House i5 has a different profile from the others, because it uses the biogas heater and hot water transferred from another residence to supply its energy. It can be observed that when the hot water transferred from another house cannot supply the demand, the biogas heater is used. The use of biogas heater only in this residence can be explained by the limited production of biogas in the micro-grid, as well as the high

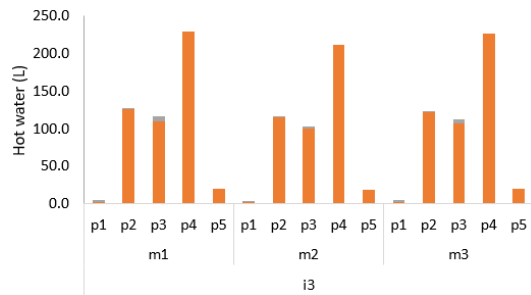
demand for hot water of the i5 house and because it is located close to the biodigester, reducing the cost of transporting the biogas.



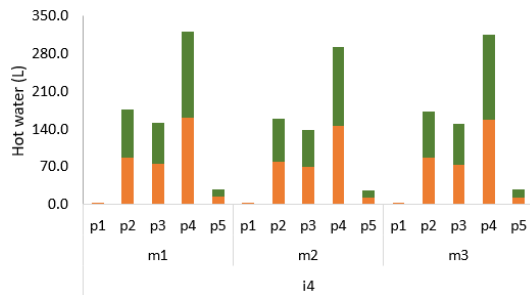
(a)



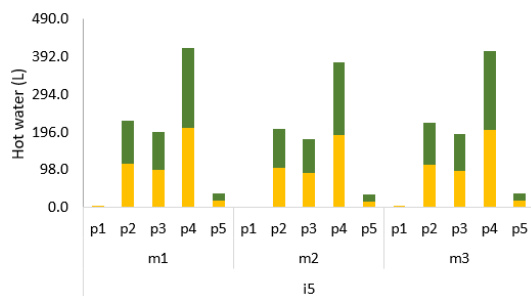
(b)



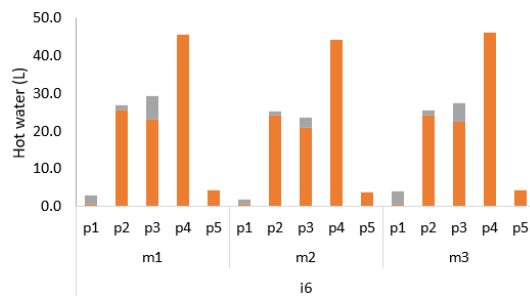
(c)



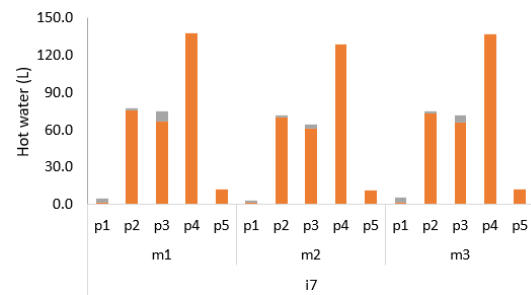
(d)



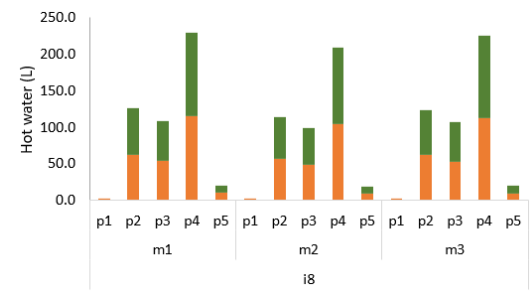
(e)



(f)



(g)



(h)

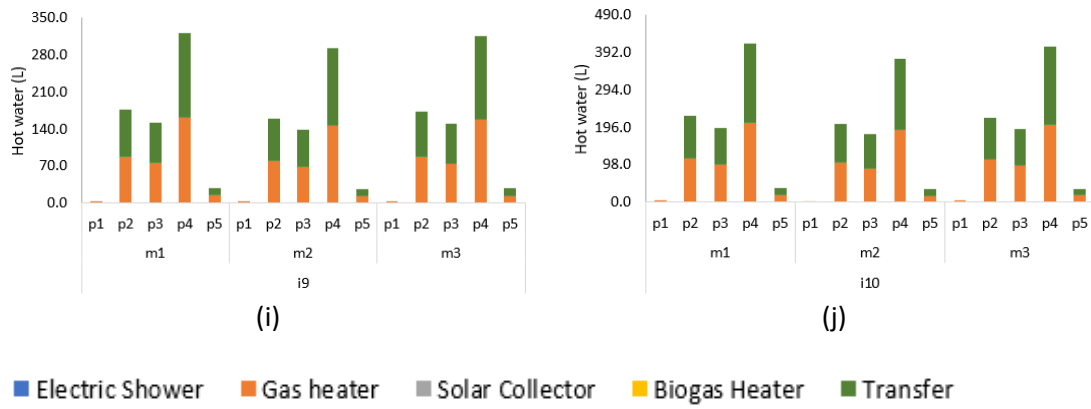


Figure 93 - Profile of resources used to meet the hot water demand in the post-COVID scenario 3 for ten houses: a) i1; b) i2; c) i3; d) i4; e) i5; f) i6; g) i7; h) i8; i) i9; j) i10.

APPENDIX E – Variables and Parameters

The variables are the unknowns that need to be determined by the solution of the model. For the optimization problem, both continuous and discrete variables were proposed. The continuous variables are summarized in Table 31. The subscripts i and j represent the houses, the season is indicated by the letter m and the time period in hours, by the letter p . The variables that are related to the photovoltaic panel have the superscript PV , the wind turbine, WT , the biogas electricity generator BG , the solar collector, SC , the electric shower, ES , the biogas heater, BH , the gas heater, GH , the air conditioning, AC , the storage tank, ST , the battery, BT , and the biodigester, BD . The superscript $SELF$ represents all the energy used for self-consumption, the superscript $SALE$ represents energy that is fed into the central grid, the superscript $STORAGE$ represents energy that is stored and the superscript $TRANSFER$ represents energy that is transferred between houses.

Regarding costs, investment, operational, maintenance, and environmental costs are considered. The investment costs are expressed with superscripts indicating each of the technologies which are: PV for photovoltaic, BG for biogas electric generator, WT for wind turbine, BD for the biodigester, $PPBD$ for the pipes that make up the biodigester system, which includes the pipe to bring the biogas to the houses and the pipe that leads the organic material from the houses to the biodigester, BT is used for battery, MG for the cost with the microgrid, which includes the cost of controlling the sharing of energy between the houses, EL for electricity line for sharing electricity between the houses, PP for hot water piping for sharing hot water between the houses, SC for solar collector, TS for thermal storage, GH for gas heater, BH for biogas heater, ES for electric shower and AC for air conditioning.

The model considers the environmental impact of each technology through its carbon footprint and corresponding cost. This is represented as CO_2 with the superscript corresponding to the energy source: $GRID$ for grid energy, BIO for biogas energy, PV for photovoltaic energy, SC for solar collector energy, WT for wind energy, NG for natural gas energy. Furthermore, the model considered time-dependent profile for efficiencies ne of photovoltaic panels, solar collectors and wind turbines. Thus, the efficiency of the photovoltaic panels and solar collectors varies over time (m, p), whereas for the wind turbine this is expressed in terms of the wind conditions of the region and the operating intervals of the turbine.

Regarding the generation of biogas, the amount of biogas produced in the biodigester is divided between gas for cooking food, for electricity generation and for heating water. In addition, the amount of raw material that can be purchased from an external source is determined by the needs of the households.

Table 31 - Continuous variables for the model.

Symbol	Continuous variable
A_i^{PV}	Area of the photovoltaic panel in house i (m ²)
A_i^{SC}	Solar collector area for thermal energy generation in house i (m ²)
A_i^{WT}	Wind turbine area in house i (m ²)
k_i^{ST}	Amount of hot water produced for storage in each house i (L)
k_i^{BG}	Power of the biogas generator in house i (kW)
k_i^{ES}	Power of the electric shower in house i (kW)
k_i^{GH}	Power of the gas heater in house i (kW)
k_i^{AC}	Power of the air conditioning in house i (kW)
k_i^{BH}	Power of the biogas heater in house i (kW)
k_i^{TS}	Storage tank capacity for the thermal storage unit in house i (L)
k_i^{BT}	Battery capacity in house i (kW)
V^{BD}	Volume of the biodigester (m ³)
$E_{i,m,p}^{GRID}$	Amount of energy purchased from the central grid by house i in period m, p (kW)
$E_{i,m,p}^{SELF}$	Amount of energy generated for self-consumption by house i in period m, p (kW)
$E_{i,m,p}^{SALE}$	Amount of energy inserted into the central grid by house i in period m, p (kW)
$E_{i,j,m,p}^{TRANSFER}$	Amount of energy transferred from house i to house j in period m, p (kW)
$E_{i,m,p}^{STORAGE}$	Amount of stored energy in house i in period m, p (kW)
$E_{i,m,p}^{STORAGE IN}$	Amount of energy going into storage (kW)
$E_{i,m,p}^{STORAGE OUT}$	Amount of energy that is removed from storage (kW)
$Use_{i,m,p}^{NG}$	Amount of natural gas purchased from the grid by house i in period m, p (kW)
Q_{bg}	Amount of biogas produced (m ³)
Q_{ow_i}	Amount of organic material purchased from house i (kg)
$HW_{i,m,p}^{SELF}$	Amount of hot water generated for self-consumption in house i in period m, p (L)
$HW_{i,m,p}^{STORAGE}$	Amount of hot water stored by house i in periods m, p (L)
$HW_{i,j,m,p}^{TRANSFER}$	Amount of hot water transferred from house i to house j (L)
CO_2^{GRID}	Carbon cost of the energy from grid (R\$)
CO_2^{NG}	Carbon cost of the energy from the natural gas (R\$)
CO_2^{WT}	Carbon cost of the energy produced by the wind turbine (R\$)
CO_2^{PV}	Carbon cost of the energy produced by the photovoltaic panel (R\$)
CO_2^{SC}	Carbon cost of the thermal energy produced by the solar collector (R\$)
CO_2^{BIO}	Carbon cost of the energy from the biogas (R\$)
C_{INV}	Total investment (R\$)
C_{OM}	Operating and maintenance cost (R\$)
C_{BUY}^{GRID}	Total cost of electricity purchased from the grid (R\$)
C^{NG}	Cost to purchase natural gas from the grid (R\$)
C^{ENV}	Total environmental costs (R\$)
NEM	Credit revenue obtained by using the Net Metering policy
FIT	Revenue received for adopting Feed in Tariff (R\$)
C_{INV}^{PV}	Investment of photovoltaic panel (R\$)

C_{INV}^{BG}	Investment of biogas electric generator (R\$)
C_{INV}^{WT}	Investment of wind turbine (R\$)
C_{INV}^{BD}	Investment of biodigester (R\$)
C_{INV}^{PPBD}	Investment of biodigester pipeline (R\$)
C_{INV}^{BT}	Investment of battery (R\$)
C_{INV}^{MG}	Investment of microgrid (R\$)
C_{INV}^{EL}	Investment of electricity line (R\$)
C_{INV}^{PP}	Investment of hot water pipeline (R\$)
C_{INV}^{SC}	Investment of solar collector (R\$)
C_{INV}^{TS}	Investment of thermal storage (R\$)
C_{INV}^{GH}	Investment of gas heater (R\$)
C_{INV}^{BH}	Investment of biogas heater (R\$)
C_{INV}^{ES}	Investment of electric shower (R\$)
C_{INV}^{AC}	Investment of air conditioning (R\$)
C_{OM}^{PV}	Operation and maintenance cost of photovoltaic panel (R\$)
C_{OM}^{BG}	Operation and maintenance cost of biogas electric generator (R\$)
C_{OM}^{WT}	Operation and maintenance cost of wind turbine (R\$)
C_{OM}^{BD}	Operation and maintenance cost of biodigester (R\$)
C_{OM}^{PPBD}	Operation and maintenance cost of biodigester pipeline (R\$)
C_{OM}^{BT}	Operation and maintenance cost of battery (R\$)
C_{OM}^{MG}	Operation and maintenance cost of microgrid (R\$)
C_{OM}^{SC}	Operation and maintenance cost of solar collector (R\$)
C_{OM}^{TS}	Operation and maintenance cost of thermal storage (R\$)
C_{OM}^{GH}	Operation and maintenance cost of gas heater (R\$)
C_{OM}^{BH}	Operation and maintenance cost of biogas heater (R\$)
C_{OM}^{ES}	Operation and maintenance cost of electric shower (R\$)
C_{OM}^{AC}	Operation and maintenance cost of air conditioning (R\$)
$G_{i,m,p}^{NG}$	Natural gas consumed from the grid in each house and time period (m, p) (kw)
$ne_{i,m,p}^{PV}$	Energy efficiency of the photovoltaic panel
$ne_{i,m,p}^{SC}$	Energy efficiency of the solar collector
$T_{i,m,p}^{PV/SC}$	Operating temperature of photovoltaic panel and solar collector (°C)
$Q_{bio_{i,m,p}}$	Total biogas production by house i in time period (m, p) (m ³)
$Q_{bgc_{i,m,p}}$	Biogas production for cooking food for house i in time period (m, p) (m ³)
$Q_{bg_{i,m,p}}$	Biogas production for hot water for house i in time period (m, p) (m ³)
$Q_{bg_{i,m,p}}$	Biogas production for electricity generation for house i in time period (m, p) (m ³)
$HW_{i,m,p}^{BH}$	Amount of hot water produced by the biogas heater in house i in time period (m, p) (L)
$E_{i,m,p}^{BH}$	Thermal energy produced by the biogas heater in house i in time period (m, p) (kW)
$HW_{i,m,p}^{GH}$	Amount of hot water produced by the gas heater in house i in time period (m, p) (L)
$E_{i,m,p}^{GH}$	Thermal energy produced by the gas heater in house i in time period (m, p) (kW)
$HW_{i,m,p}^{ES}$	Amount of hot water produced for the solar collector (L)
$E_{i,m,p}^{ES}$	Thermal energy produced for the electric shower in house i in time period (m, p) (kW)
$HW_{i,m,p}^{SC}$	Amount of hot water produced by the solar collector in house i in time period (m, p) (L)
$E_{i,m,p}^{SC}$	Thermal energy produced by the solar collector in house i in time period (m, p) (kW)
CRF	Capital Recovery Factor

The discrete variables in the model are binary, or in other words, they can only assume the value 0 or 1. The binary variables are summarized in Table 32. They were used in the problem to define whether a technology is installed or not in the system, as well as whether an energy generation incentive policy was adopted or not. Regarding the incentive policy, the Feed in Tariff (FIT) and Net metering (NEM) might be selected, taking into consideration the prices that will be received with the adoption of each of the policies. For the Net Metering policy, the credits obtained with the insertion of the extra energy produced in the central energy grid is considered. These credits are calculated according to the price of energy from the central network and can be used when it is necessary to purchase energy from the central network at another time. For the Feed in Tariff policy, the revenue acquired with the sale of energy to the central grid is considered, and this value varies according to each technology used.

Table 32 - Binary variables used in the model.

Symbol	Binary Variable
Y_i^{WT}	whether or not the wind turbine exists in the house i
$Y_{i,j}^{MG}$	whether or not an electricity line between houses i and j exists
Z	whether or not a microgrid exists
Y^{BD}	whether or not the biodigester exists
Y_i^{PPBIO}	whether or not biogas pipeline exists between house i and the biodigester
Y_i^{BT}	whether or not the battery exists in the house i
Y^{NG}	whether or not natural gas from the grid is consumed
$Y_{i,j}^{PP}$	whether or not the pipeline exists from house i to house j
Y_i^{BH}	whether or not there is energy produced in house i by biogas heater
Y_i^{SC}	whether or not there is energy produced in house i by solar collector
Y_i^{ES}	whether or not there is energy produced in house i by electric shower
Y_i^{GH}	whether or not there is energy produced in house i by gas heater
$Y_{i,m,p}^{GRID}$	whether or not energy is purchased from the central grid by house i and periods m and p
Y^{FIT}	whether or not the feed-in tariff policy has been implemented
Y^{NEM}	whether or not the net metering policy has been implemented

In addition, parameters and input variables are required to solve the problem. The parameters and input variables considered for this model are shown in Table 33 and Table 34, respectively. Regarding energy demands, they are expressed as *Load* with the superscript E for electric power, HW for hot water, C for cooking gas and AC for air cooling and with the subscript indicating the correspondence for each house i in each time period (m, p). The environmental data depend on the installation site and are: solar irradiation data (kW/m^2); ambient temperature ($^{\circ}\text{C}$); wind speed (m/s); wind power (kW/m^2). In addition, the prices of electricity purchased from the grid, as well as the price of natural gas are considered.

The other parameters are the values of each technology such as maintenance and operation costs, capacity limits, CO_2 emissions, and their respective prices. All these parameters were quoted with companies in the region or found in databases applied to the case study site. Data that could not be found was estimated according to similar

works (MUSTAFA, 2010; KARAMOV et al., 2021; SIDNELL et al., 2021a; LOPES, 2019; BARROS, 2021; SOUZA et al., 2019).

Table 33 – Parameters used in the model.

Symbol	Input parameter	Symbol	Input parameter
C_c^{ES}	Capital cost of ES (R\$/kW)	DMO	Density of the dry material in the fluid (kg/ m ³)
ne^{ES}	ES Electric Efficiency	BD_{up}	Maximum volume Biodigester (m ³)
C_{OMVar}^{ES}	Variable OM cost of ES (R\$/L)	C_{Fix}^{NG}	Fixed price of natural gas per month (R\$)
C_{OMFix}^{ES}	Fixed OM cost of ES (R\$/kW)	AC_{up}	Upper bound of AC (kW)
ES_{up}	Upper bound of ES (kW)	AC_{low}	Lower bound of AC (kW)
ES_{low}	Lower bound of ES (kW)	C_c^{PV}	Capital cost of PV (R\$/kWp)
C_c^{GH}	Capital cost of GH (R\$/L/h)	Cn^{PV}	Nominal capacity of PV (kWp/m ²)
ne^{GH}	GH Electric Efficiency	nee^{PV}	Nominal Value of PV Efficiency
C_{OMVar}^{GH}	Variable OM cost of GH (R\$/L)	C_{OMVar}^{PV}	Variable OM cost of PV (R\$/ kWp / year)
C_{OMFix}^{GH}	Fixed cost of OM of GH (R\$/kW)	C_{OMFix}^{PV}	Fixed cost of OM of PV (R\$/kWp/year)
GH_{up}	Upper bound of GH (L/h)	β_s	Temperature coefficient for silicon photovoltaic panel
GH_{low}	Lower bound of GH (L/h)	K_0	Koehl correlation 1
C_c^{AC}	Capital cost of AC (R\$/kW)	K_1	Koehl correlation 2
AC_{COP}	AC coefficient of power	KL	Power losses in diodes coefficient
C_{OMVar}^{AC}	Variable OM cost of AC (R\$/ kW)	C_c^{SC}	Capital cost of SC (R\$/kW/day)
C_{OMFix}^{AC}	Fixed cost of OM of AC (R\$/kW)	Cn^{SC}	Nominal capacity of SC (kWh/day/m ²)
$T_{storage}$	Storage temperature (°C)	nee^{SC}	Nominal Value of SC Efficiency
C_c^{TS}	Capital cost of TS (R\$/L)	C_{OMFix}^{SC}	Fixed cost of OM of SC (R\$/kWh/year)
C_{OMVar}^{TS}	Variable OM cost of TS (R\$/L)	V_{ci}	Turbine cut off speed (m/s)
TS_{up}	Upper bound of TS (kW)	V_{co}	Turbine cut in speed (m/s)
TS_{low}	Lower bound of TS (kW)	V_r	Turbine nominal speed (m/s)
C_c^{PP}	Capital Cost pipeline (R\$/m)	kr^{WT}	Rated capacity of WT (kW/m ²)
$\beta_{i,j}$	Heat and electric loss	C_c^{WT}	Capital cost of WT (R\$/kW)
C_c^{BT}	Capital cost of battery (R\$/kW)	ρ_{wind}	Wind density (kg/m ³)
$C_c^{CONTROLLER,BT}$	Capital cost of charge controller (R\$/battery)	Cp^{WT}	Power coefficient of WT
C_{OMFix}^{BT}	OM cost of battery (R\$/kWh)	WT_{up}	Rotor Area limit (m ²)
ϑ	Static loss of battery (%)	C_{OMFix}^{WT}	Fixed cost of OM from WT (R\$/kW/year)
X	Percentage charge rate (%)	C_{OMVar}^{WT}	Variable OM cost of WT (R\$/ kW/year)
ΔX	Discharge rate (%)	C_c^{BD}	Capital cost of Biodigester (R\$/ kW)
X_{up}	Maximum charge rate	C_{OMFix}^{BD}	OM cost of Biodigester (R\$/year)
ΔX_{up}	Maximum discharge rate	P^{OW}	Price of organic waste (R\$/kg)
DOC	Depth of charge	Hb	Calorific capacity of biogas (kW/ m ³)
BT_{up}	Upper bound of battery (kW)	qb	Biogas production rate (m ³ of biogas/kg of organic waste)
BT_{low}	Lower bound of battery (kW)	tr	Hydraulic retention time in the Biodigester (days)
cp_{water}	Calorific capacity of the water	IS	Percentage of dry mass in organic material
ρ_{water}	Density of the water	r	Interest rate
C_c^{PPBio}	Cost of pipeline for biogas (R\$/m)	n	Period in years
C_c^{BG}	Capital cost of BG (R\$/L/h)	C_c^{PPOW}	Cost of pipeline for organic material (R\$/m)
ne^{BG}	BG efficiency	C_c^{CC}	Capital Cost of central controller (R\$)
BG_{up}	Maximum BG power	C_{OMFix}^{CC}	OM cost of central controller (R\$)
BG_{low}	Minimum BG power	C_c^{EL}	Capital Cost of an electricity line (R\$/m)
C_{OMFix}^{BG}	Fixed cost of OM of BG (R\$/ kW/year)	C_c^{PP}	Cost of pipeline for hot water (R\$/m)
C_{OMVar}^{BG}	Variable cost of OM of BG (R\$/ kW/year)	CI^{GRID}	Carbon Intensity of grid electricity (kg CO ₂ /kWh)
C_c^{BH}	Capital cost of BH (R\$/L/h)	CI^{NG}	Carbon Intensity of Natural Gas (kg CO ₂ /kWh)
ne^{BH}	BH efficiency	CI^{WT}	Carbon Intensity of Wind (kg CO ₂ /kWh)
BH_{up}	Upper bound of BH (L/h)	CI^{PV}	Carbon Intensity of Photovoltaic (kg CO ₂ /kWh)
BH_{low}	Lower bound of BH (L/h)	CI^{SC}	Carbon Intensity of Solar collector (kg CO ₂ /kWh)
C_{OMFix}^{BH}	Fixed cost of OM of BH (R\$/year)	CI^B	Carbon Intensity of biogas (kg CO ₂ /kWh)
C_{OMVar}^{BH}	Variable cost of OM of BH (R\$/ L/year)	CT	Carbon Tax (R\$/kg CO ₂)

Table 34 – Input variables used in the model.

Symbol	Input variables
$P_{m,p}^{Elec}$	Electricity price (R\$/kWh)
P^{NG}	Natural gas price (R\$/m ³)
$It_{m,p}$	Solar irradiation at the site in the time (m,p) (kWh/m ²)
Qom_i	Amount of organic material produced per house per day (kg)
l_{bio_i}	Distance between houses and biodigester (m)
$l_{i,j}$	Distance between houses (m)
$Load_{i,m,p}^E$	Demand of electricity per house i in period (m, p) (kW)
$Load_{i,m,p}^{AC}$	Demand of air cooling per house i in period (m, p) (kW)
$Load_{i,m,p}^C$	Demand of gas for cooking per house i in period (m, p) (kW)
$Load_{i,m,p}^{HW}$	Demand of hot water per house i in period (m, p) (L)
$V_{m,p}^{Env}$	wind speed of the environmental (m/s)
$T_{m,p}^{Env}$	Room temperature (°C)

REFERENCES

ABSOLAR. **Energia Solar Fotovoltaica no Brasil**: infográfico ABSOLAR. São Paulo: Associação Brasileira de Energia Solar Fotovoltaica, 2021b.

ABSOLAR. **Energia Solar Fotovoltaica no Brasil: Infográfico ABSOLAR**. 2021. São Paulo: Associação Brasileira de Energia Solar Fotovoltaica.

ABSOLAR. **Setor fotovoltaico gerou mais de 86 mil empregos no Brasil em 2020**. 2021a. Available at: <https://www.absolar.org.br/noticia/setor-fotovoltaico-gerou-mais-de-86-mil-empregos-no-brasil-em-2020/>. Accessed 10 mai. 2021.

ABSOLAR. **Geração distribuída fotovoltaica cresce 230% ao ano no Brasil**. 2020. Available at: <https://www.absolar.org.br/noticia/geracao-distribuida-fotovoltaica-cresce-230-ao-ano-no-brasil/>. Accessed 23 jul. 2021.

ABU-BAKAR, S. H. et al. Is Renewable Heat Incentive the future? **Renewable and Sustainable Energy Reviews**, v. 26, p. 365–378, out. 2013.

ABU-MOUTI, FS; EL-HAWARY, ME. Optimal distributed generation allocation and sizing in distribution systems via Artificial Bee Colony Algorithm. **IEEE Transactions on Power Delivery** **2011**; v.26, n.4, p.2090–101. 2011.

ACHARYA, N; MAHAT, P; MITHULANANTHAN, N. An analytical approach for DG allocation in primary distribution network. **International Journal of Electrical Power and Energy Systems** **2006**, v. 28, n. 10, p.669–78.2006.

AGÊNCIA BRASIL. **Majoria dos brasileiros mora em casa e é dona do imóvel, mostra IBGE**. 2020. Available at: <https://www.istoedinheiro.com.br/majoria-dos-brasileiros-mora-em-casa-e-e-dona-do-imovel-mostra-ibge/>. Accessed: 14 mai. 2022.

ALVES, Janaina. **O que é célula a combustível?** 2012. Available at: <http://www.usp.br/portabiossistemas/?p=4316>. Accessed 23 jul. 2021.

AMATO, F. **Menor nível de chuvas em 91 anos obriga governo a preparar plano para evitar falta de energia**. 2022. Available at: <https://g1.globo.com/economia/noticia/2021/05/14/menor-nivel-de-chuvas-em-91-anos-obriga-governo-a-preparar-plano-para-evitar-falta-de-energia.ghtml>. Accessed 8 March 2022.

ANACONDA SOFTWARE DISTRIBUTION. Anaconda Documentation. **Anaconda Inc.** 2020. Available: from <https://docs.anaconda.com/>. Accessed 5 apr. 2022.

ANEEL. **Atlas de Energia Elétrica do Brasil**. Brasília: Agência Nacional de Energia Elétrica, 2002. 199 p.

ANEEL. **No Dia Mundial da Água, ANEEL publica infográfico sobre hidrelétricas no Brasil**. 2021. Available at: <https://www.aneel.gov.br/>. Accessed 12 may 2021.

APETRO. O BioGPL. **APETRO**, [S. l.], v. 96, p. 3, 2019.

AQUILA, Giancarlo; PAMPLONA, Edson de Oliveira; QUEIROZ, Anderson Rodrigo de; JUNIOR, Paulo Rotela; FONSECA, Marcelo Nunes. An overview of incentive policies for the expansion of renewable energy generation in electricity power systems and the Brazilian experience. *Renewable and Sustainable Energy Reviews*, v. 70, p. 1090–1098, abr. 2017.

ARAUJO, Ana Paula Caixeta. **Produção de biogás a partir de resíduos orgânicos utilizando biodigestor anaeróbico**. 42 f. TCC (Bachelor) – Curso de Engenharia de Engenharia Química. Universidade Federal de Uberlândia, Uberlândia, 2017.

ARBOIT, Nathana Karina Swarowski; DECEZARO, Samara Terezinha; DO AMARAL, Gilneia Mello; LIBERALESSO, Tiago; MAYER, Vinicio Michael; KEMERICH, Pedro Daniel da Cunha. Potencialidade De Utilização Da Energia Geotérmica No Brasil – Uma Revisão De Literatura. **Geography Department, University of Sao Paulo**, [S. l.], v. 26, n. 2013, p. 155–168, 2013.

ATWA, Y. M.; EL-SAADANY, E. F.; SALAMA, M. M. A.; SEETHAPATHY, R. Optimal renewable resources mix for distribution system energy loss minimization. **IEEE Transactions on Power Systems**, [S. l.], v. 25, n. 1, p. 360–370, 2010.

AUGUSTO, Otávio. **Brasil sofreu seis apagões de energia elétrica nos últimos 35 anos**. 2020. Available at: <https://www.metropoles.com/brasil/brasil-sofreu-seis-apagoes-de-energia-eletrica-nos-ultimos-35-anos>. Accessed 11 may 2021.

BAHIA GAS. **Tabela tarifária**. 2019. Available: <http://bahiagas.com.br/homologacao/tabela_tarifaria/>. Accessed 5 apr. 2022.

BAHIA GAS. **Tabela tarifária**. 2022. Available: <<https://www.bahiagas.com.br/gas-natural/tabela-tarifaria>>. Accessed 5 mai. 2022.

BAPTISTA, A. S. C. **Análise da viabilidade econômica da utilização de aquecedores solares de água em resorts no Nordeste do Brasil**. 171 f. Thesis—Universidade Federal do Rio de Janeiro, Rio de Janeiro, 2006.

BARROS, Talita Delgrossi. **Biogás**. AGEITEC: Brasília. 2021. Available:<<https://www.agencia.cnptia.embrapa.br>>. Accessed: 15 jun. 2021.

BITENCOURT, L.; SCHETINGER, A.M.; BORBA, B.s.M.C.; DIAS, D.H.N.; MACIEL, R.s.; DIAS, B.H.. Maximum PV Penetration Under Voltage Constraints Considering Optimal Sizing of BESS on Brazilian Secondary Distribution Network. **Ieee Latin America Transactions**, [S.L.], v. 14, n. 9, p.

4063-4069, set. 2016. Institute of Electrical and Electronics Engineers (IEEE). <http://dx.doi.org/10.1109/tla.2016.7785934>

BORGES, CLT; FALCAO, DM. Optimal distributed generation allocation for reliability, losses, and voltage improvement. **International Journal of Electrical Power and Energy Systems** 2006;v.28, n.6, p.413–20. 2006.

BOUCHEKARA, Houssef Rafik El Hana; JAVAID, Muhammad Sharjeel; SHAABAN, Yusuf Abubakar; SHAHRIAR, Mohammad Shoaib; RAMLI, Makbul Anwari Muhammad; LATRECHE, Yaqoub. Decomposition based multiobjective evolutionary algorithm for PV/Wind/Diesel Hybrid Microgrid System design considering load uncertainty. **Energy Reports**, [S. l.], v. 7, p. 52–69, 2021.

BRASIL. MCTI. Emissões de Dióxido de Carbono por Queima de Combustíveis: Abordagem Top-Down. Relatórios de Referência: Setor Energia. **2º Inventário Brasileiro de Emissões e Remoções Antrópicas de Gases de Efeito Estufa**. Brasília, DF: MCTI, 2010.

BRASIL. RESOLUÇÃO HOMOLOGATÓRIA Nº 2.533 DE 16 DE ABRIL DE 2019. Homologa o resultado do Reajuste Tarifário Anual de 2019 da Companhia de Eletricidade do Estado da Bahia - Coelba, a vigorar a partir de 22 de abril de 2019. **Diário Oficial da União, n. 76, 22 apr. 2019**. Available: <www.aneel.gov.br/biblioteca>. Accessed: 25 apr. 2022.

BRASIL. RESOLUÇÃO HOMOLOGATÓRIA No 2.857 DE 22 DE ABRIL DE 2021. Homologa o resultado do reajuste tarifário anual, as Tarifas de Energia - TE e as Tarifas de Uso dos Sistemas de Distribuição - TUSD, referentes à Companhia de Eletricidade do Estado da Bahia - Coelba. **Diário Oficial da União, 22 apr. 2021**. Available: <www.aneel.gov.br/biblioteca>. Accessed: 25 apr. 2022.

BRASIL. **Tribunal de Contas da União. Relatório de Políticas e programas de governo 2017**. Brasília. 2017.

CAMPOS, Adriana Fiorotti; SCARPATI, Cynthia de Barros Lima; DOS SANTOS, Luan Tolentino; PAGEL, Uonis Raasch; DE SOUZA, Victor Hugo Alves. Um panorama sobre a energia geotérmica no Brasil e no Mundo: Aspectos ambientais e econômicos. **Espacios, [S. l.]**, v. 38, n. 1, 2017.

CCEE. **PROINFA**: Tratamento da energia do Proinfa na CCEE. Tratamento da energia do Proinfa na CCEE. 2010. Available at: <https://www.ccee.org.br/>. Accessed 4 aug. 2020.

CCEE. **Comercialização**. 2004. Available at: <https://www.ccee.org.br/>. Accessed 20 jul. 2021.

CHEQUER, T.; BROWN, M. **Informativo Energia Elétrica. Lei nº 14.300/2022: Marco Legal da Geração Distribuída**. 2022.

CHIAPPINI, Gabriel. **HVO desponta como tendência para produção de diesel renovável**. 2020. Available at: <https://epbr.com.br/hvo-desponta-como-tendencia-para-producao-de-diesel-renovavel/>. Accessed 25 may 2021.

CIA. **Electricity – consumption**. 2015. Available at: <https://www.cia.gov/the-world-factbook/field/electricity-consumption/>. Accessed 12 may 2021.

CLARKE, Fiona; DORNEANU, Bogdan; MECHLERI, Evgenia; ARELLANO-GARCIA, Harvey. Optimal design of heating and cooling pipeline networks for residential distributed energy resource systems. **Energy**, [S.L.], v. 235, p. 121430, nov. 2021. Elsevier BV. <http://dx.doi.org/10.1016/j.energy.2021.121430>.

COELHO, José Mauro. Biogás no Brasil: visão atual. **Vii Fórum Do Biogás**, [S. l.], p. 13, 2020.

COELHO, Suani Teixeira (coord); GARCILASSO, Vanessa Pecora; JUNIOR, Antônio Djalma Nunes Ferraz; SANTOS, Marilin Mariano dos; JOBERT, Caio Luca. **Tecnologias de produção e uso de biogás e biometano**. São Paulo: IEE-USP, p. 216, 2018.

CORRÊA, Amanda. (2019). **Energia geotermal – o que é, usos e presença no Brasil – Igeológico**. Available at: [https://igeologico.com.br/energia-geotermal-o-que-e-usos-e-presenca-no-brasil/#:~:text=C\)%20foi%20identificado%20na%20%C3%A1rea,em%20%C3%A1reas%20de%20Obacias%20sedimentares](https://igeologico.com.br/energia-geotermal-o-que-e-usos-e-presenca-no-brasil/#:~:text=C)%20foi%20identificado%20na%20%C3%A1rea,em%20%C3%A1reas%20de%20Obacias%20sedimentares). Accessed 27 may 2022.

COSTA, Rafael Alves da; CASOTTI, Bruna Pretti; AZEVEDO, Rodrigo Luiz Sias de. Um panorama da indústria de bens de capital relacionados à energia eólica. **BNDES Setorial**, Rio de Janeiro, n. 29, p. 229-277, mar. 2009.

CUNHA, Paulo; WEISS, Mariana. **Energia Heliotérmica: uma nova aposta**. Uma Nova Aposta. 2021. Available at: <https://cenariosolar.editorabrasilenergia.com.br/energia-heliotermica-uma-nova-aposta/>. Accessed 23 jul. 2021.

DAH SOLAR. **Products**. 2022. Available:< www.dahsolarpv.com>. Accessed: 15 mai. 2022.

DALVI, Giovanni Gueler; OLIVEIRA FILHO, Delly; RODRIGUES, Élide Maria Bezerra. Feed-in tariff como alternativa de incentivo ao desenvolvimento da geração de energia elétrica por fontes renováveis no Brasil. **Revista Brasileira de Energia**, Viçosa, v. 23, n. 2, p. 20-31, jun. 2017.

DANTAS, Djolse Nascimento. **Uso da biomassa da cana-de-açúcar para geração de energia elétrica: análise energética, exegética e ambiental de sistemas de cogeração em sucroalcooleiras no interior paulista**. 2010. 131 f. Dissertação (Mestrado) - Curso de Ciências da Engenharia Ambiental, Escola de Engenharia de São Carlos, Universidade de São Paulo, São Carlos, 2010.

DE FARIA, Felipe A. M.; JARAMILLO, Paulina; SAWAKUCHI, Henrique O.; RICHEY, Jeffrey E.; BARROS, Nathan. Estimating greenhouse gas emissions from future Amazonian hydroelectric reservoirs. **Environmental Research Letters**, [S. l.], v. 10, n. 12, p. 124019, 2015.

DE MEL, Ishanki; DEMIS, Panagiotis; DORNEANU, Bogdan; KLYMENKO, Evgenia Mechleri; ARELLANO-GARCIA, Harvey. Global Sensitivity Analysis for Design and Operation of Distributed Energy Systems. In: **30 European Symposium on Computer th Aided Process Engineering (ESCAPE30)**, May 24-27, 2020, Milano, Italy. <http://dx.doi.org/10.1016/B978-0-12-823377-1.50254-8>

DE MIRANDA, Ronaldo Leão; MARTINS, Eliane Maria; LOPES, Kamila. A potencialidade energética da biomassa no Brasil. **Desenvolvimento Socioeconômico em Debate**, [S. l.], v. 5, n. 1, p. 94, 2019. DOI: 10.18616/rdsd.v5i1.4829.

DTU Wind Energy. **GLOBAL WIND ATLAS**. 2019. Available at: <https://globalwindatlas.info/>. Accessed 20 Apr. 2021.

DTU Wind Energy. **Global Wind Atlas**. Available: <<https://globalwindatlas.info/>>. Accessed 15 mar. 2022.

EDENHOFER, Ottmar et al. **Renewable Energy Sources and Climate Change Mitigation**. Cambridge: Cambridge University Press, 2011.

ELETRONBRAS. **Plano anual do PROINFA: PAP 2020**. Rio de Janeiro: Eletrobras, 2020. 72 p.

ELINOFF, G., 2019. Microgrids vs. the Macrogrid: The Applications of Microgrids in Today's Power Systems. [online] **All about circuits**. Available at: <<https://www.allaboutcircuits.com/news/microgrids-vs-macrogrid-applications-power-systems/>> [Accessed 15 April 2022].

EL-KHATTAM, W; HEGAZY, YG; SALAMA, MMA. An integrated distributed generation optimization model for distribution system planning. **IEEE Transactions on Power Systems** 2005, v.20, n.2, p.1158–65. 2005.

ELURI, Himabindu; NAIK, M. Gopichand. Challenges of RES with Integration of Power Grids, Control Strategies, Optimization Techniques of Microgrids: A Review. **International Journal of Renewable Energy Research**, [S. l.], v. 11, n. 1, p. 1–19, 2021.

Embasa. **Tarifas da Embasa**. 2022. Available: <<https://agenciavirtual.embasa.ba.gov.br/>>. Accessed 03 apr. 2022.

ENERGIZECT, 2022. Geothermal Basics | Energize Connecticut. [online] **Energizect.com**. Available at: <https://energizect.com/events-resources/energy-basics/geothermal>. Accessed 27 April 2022.

ENERMAC. **ENERMAC: Soluções com Energia**. 2022. Available: <<https://www.enermac.com.br/>> Accessed 05 apr. 2022.

ENERSUD. **Turbina eólica gerar extreme**. 2022. Available: <<https://www.enersud.com.br/produtos/turbina-eolica-gerar-extreme/>>. Accessed 11 apr. 2022.

ENGIE. **Matriz energética brasileira: Fique por dentro de sua evolução ao longo dos anos**. 2022. Available at: <https://www.alemnaenergia.engie.com.br/matriz-energetica-brasileira/>. Accessed 1 August 2022.

EPBR. **Geração distribuída atinge 11GW no Brasil**. 2022. Available at: <https://epbr.com.br/geracao-distribuida-atinge-11-gw-no-brasil/>. Accessed 1 August 2022.

EPBR. **A energia do gás que move o país**. 2021. Available at: <https://epbr.com.br/glp-a-energia-do-gas-que-move-o-pais/>. Accessed 25 may 2021.

EPE. Uso de Ar Condicionado no Setor Residencial Brasileiro: Perspectivas e contribuições para o avanço em eficiência energética. Empresa de Pesquisa Energética. Brasília - DF: **Ministério de Minas e Energia**, 13 dez. 2018.

EPE. Statistical Yearbook of electricity 2020 baseline year. Empresa de Pesquisa Energética. Brasília - DF: **Ministério de Minas e Energia**, 2021.

EPE. **Matriz Energética e Elétrica**. Available at: <https://www.epe.gov.br/pt/abcdenergia/matriz-energetica-e-eletrica>. Accessed 24 may 2021.

EULER, Ana Margarida Castro. O Acordo de Paris e o futuro do REDD+ no Brasil. **Cadernos Adenauer**, [S. l.], v. XVII, n. 2, p. 1–12, 2016.

FERREIRA, Bruna Durieux. **Dimensionamento do aquecedor de passagem a gás**. 2022. Available: <<https://suporte.altoqi.com.br/hc/pt-br/articles/360007842414-Dimensionamento-do-aquecedor-de-passagem-a-g%C3%A1s>>. Accessed 4 mai. 2022.

FLEMING, Fernanda Pereira. **Avaliação do potencial de energias oceânicas no Brasil**. 2012. Dissertação (Mestrado) - Universidade Federal do Rio de Janeiro, [S. l.], 2012.

FNR. **Guia Prático do Biogás: Geração e Utilização**. Gülzow: Fachagentur Nachwachsende Rohstoffe, v.5, p. 236, 2010.

FOCUS ENERGIA. **Consumo**. 2021. Available: <<https://www.focusenergia.com.br/consumo-ponta-e-fora-ponta-o-que-e/#:~:text=O%20hor%C3%A1rio%20fora%20ponta%20corresponde,e%20das%2021h%20C3%A0s%2023h59>>. Accessed 6 mai. 2022.

FONTAINE. **Produtos**. 2022. Available: <<https://www.fontainebrasil.com.br/>>. Accessed 30 apr. 2022

FOREST RESEARCH. **Tools and Resources: Typical calorific values of fuels**. Available: <<https://www.forestresearch.gov.uk/tools-and-resources/fthr/biomass-energy-resources/reference-biomass/facts-figures/typical-calorific-values-of-fuels/>>. Accessed 6 jun.2022.

FORTLEV. **Reservatórios**. 2022. Available: <<https://www.fortlev.com.br/>>. Accessed 10 apr. 2022.

FREITAS, Bruno M. R. de; HOLLANDA, Lavinia. Micro e Minigeração no Brasil: Viabilidade Econômica e Entraves do Setor. **FGV Energia**. Rio de Janeiro, p. 1-22. may 2015.

GABRIELLI, P.; GAZZANI, M.; MARTELLI, E.; MAZZOTTI, M. Optimal design of multi-energy systems with seasonal storage. **Applied Energy**, v. 219, p. 408–424, jun. 2018.

GAMARRA, C.; GUERRERO, J. M., Computational optimization techniques applied to microgrids planning: A review, *Renew. Sustain. Energy Rev.*, vol. 48, pp. 413–424, 2015.

GAMS Development Corporation. General Algebraic Modeling System (GAMS) Release 36.1.0, **Fairfax**, VA, USA, 2021.

GAMS. 2023. **GAMS Output**. Available at: <https://www.gams.com/latest/docs/UG_GAMSOutput.html>. Accessed 23 jan. 2023.

GBS, 2022. Renewable Energy Storage System Solution - LFP Battery Leading Manufacturer. [online] **LFP Battery Leading Manufacturer**. Available at: <https://gbsystem.com/our-solutions/renewable-energy-storage-system-solution/>. Accessed 12 April 2022.

GODOI, Maurício. **Energia eólica chega a 18 GW de capacidade instalada no Brasil**. 2021. Available at: <https://www.canalenergia.com.br/noticias/53163929/energia-eolica-chega-a-18-gw-de-capacidade-instalada-no-brasil>. Accessed 26 jul. 2021.

GREENRIVERSIDE, 2022. Solar Water Heating. [online] **Energydepot.com**. Available at: <<https://www.energydepot.com/RPUres/library/Swaterheater.asp>>. Accessed 14 April 2022.

GUAREZI, Natália Julia. **Dimensionamento do boiler para acumulação de água quente**. 2022. Available: <<https://suporte.altoqi.com.br/hc/pt-br/articles/360001907214-Dimensionamento-do-boiler-para-acumula%C3%A7%C3%A3o-de-%C3%A1gua-quente>>. Accessed 5 mai. 2022.

GUAREZI, Natália Julia. **Dimensionamento do boiler para acumulação de água quente**. 2022. Available at: <https://suporte.altoqi.com.br/hc/pt-br/articles/360001907214-Dimensionamento-do-boiler-para-acumula%C3%A7%C3%A3o-de-%C3%A1gua-quente>. Accessed 1 jun. 2022.

Guimarães, L. A. M; Boa, M. C. F. **Termologia e óptica**. São Paulo: Editora Harbra, 1997.

GUNDA, J; KHAN, NA. Optimal location and sizing of DG and shunt capacitor using differential evolution. **International Journal of Soft Computing** 2011; v.6, n. 4, p.128–35. 2011.

GWEC. Global Wind Report | Gwec. **Global Wind Energy Council**, [S. l.], p. 75, 2021. Available at: <http://www.gwec.net/global-figures/wind-energy-global-status/>. Accessed 12 may 2021.

HARRISON, GP; PICCOLO, A; SIANO, P; WALLACE, AR. Distributed generation capacity evaluation using combined Genetic Algorithm and OPF. **International Journal of Emerging Electric Power Systems** 2007; v.8, n.2, p.1–13.2007.

HAWKES, A. D.; LEACH, M. A. Modelling high level system design and unit commitment for a microgrid. **Applied Energy**, [S. l.], 2009.

HERSCHEL INFRARED, 2022. Biomass Boilers compared with Herschel Infrared heating. [online] **Herschel Infrared Ltd**. Available at: <<https://www.herschel-infrared.co.uk/infrared-heater-comparisons/biomass-boilers-comparison/>> [Accessed 23 April 2022].

HOPWOOD, Lucy, MITCHELL, Edward, SOURMELIS, Sotirios . Biopropane: Feedstocks, Feasibility and our Future Pathway. **NNFCC**, [S. l.], p. 26, 2019.

- HOUGHTON, J., 2005. Global warming. **Reports on Progress in Physics**, 68(6), pp.1343-1403.
- IBGE. **O IBGE apoiando o combate à COVID-19**. 2020. [Online]. Available: <https://covid19.ibge.gov.br/pnad-covid/trabalho.php>. Accessed 2 mar. 2022
- ICOS, 2022. Data supplement to the Global Carbon Budget 2021. [online] **ICOS**. Available at: <<https://www.icos-cp.eu/science-and-impact/global-carbon-budget/2021>> [Accessed 7 April 2022].
- IEA, 2021. Trends in photovoltaic applications. [online] **Enerdeal**. Available at: <<https://iea-pvps.org/wp-content/uploads/2022/01/IEA-PVPS-Trends-report-2021-4.pdf>> [Accessed 9 April 2022].
- IEA. **Hydropower is not fully on track with the Sustainable Development Scenario**. 2020. Available at: <https://www.iea.org/fuels-and-technologies/hydropower>. Accessed 24 jul. 2021.
- IRENA. Bioenergy. **International Renewable Energy Agency**. 2020. Available at at: <<https://www.irena.org/bioenergy>>. Accessed 27 jul. 2021.
- KARAMOV, D.N., SIDOROV D. N., MUFTAHOV, I.R., ZHUKOV, A. V., LIU, F. Optimization of isolated power systems with renewables and storage batteries based on nonlinear Volterra models for the specially protected natural area of lake Baikal. **Journal of Physics: Conference Series**, v.1847, n. 1, p. 012037. 2021. <http://dx.doi.org/10.1088/1742-6596/1847/1/012037>.
- KEATING, David. **Por que a energia geotérmica ainda não decolou?** 2017. Available at: <https://www.dw.com/pt-br/por-que-a-energia-geot%C3%A9rmica-ainda-n%C3%A3o-decolou/a-40568715>. Accessed 28 may 2021.
- KËRÇI, T.; TZOUNAS, G.; MILANO, F. A dynamic behavioral model of the long-term development of solar photovoltaic generation driven by feed-in tariffs. **Energy**, v. 256, p. 124506, out. 2022.
- KHALID, K.; ALI, M.F.; ABD RAHMAN, N.F. Application on One-at-a-Time Sensitivity Analysis of Semi-Distributed Hydrological Model in Tropical Watershed. **International Journal of Engineering and Technology**, v. 8, n. 2, p. 132–136, fev. 2016.
- KHARRICH, Mohammed; MOHAMMED, Omar Hazem; ALSHAMMARI, Nahar; AKHERRAZ, Mohammed. Multi-objective optimization and the effect of the economic factors on the design of the microgrid hybrid system. **Sustainable Cities and Society**, [S. l.], v. 65, p. 102646, 2021.
- KISOLTEC AQUECEDOR SOLAR. **Como dimensionar instalação do aquecedor solar**. 2019. Available: <<https://blog.kisoltec.com.br/como-dimensionar-instalacao-do-aquecedor-solar/>>. Accessed 3 apr. 2022.
- KISOLTEC AQUECEDOR SOLAR. **Descubra como é feito o dimensionamento de aquecimento solar**. 2019. Available at: <https://blog.kisoltec.com.br/como-dimensionar-instalacao-do-aquecedor-solar/>. Accessed 7 jun. 2022.
- KOMEKO. **Produtos**. 2022. Available: <<https://www.komeco.com.br/>>. Accessed 30 apr. 2022

KRONA. **Tubos e conexões**. 2022. Available: < <https://www.krona.com.br/>>. Accessed 3 apr. 2022.

KUMAR, Rajesh; AGARWALA, Arun. Energy certificates REC and PAT sustenance to energy model for India. **Renewable And Sustainable Energy Reviews**, [S.L.], v. 21, p. 315-323, may 2013.

LALITHA, MP; REDDY, VCV; USHA, V; REDDY, NS. Application of fuzzy and Pso for Dg placement for minimum loss in radial distribution system. **ARPN Journal of Engineering and Applied Sciences** 2010; v. 5, n.4, p.30–7. 2010.

LARA, Rodrigo, 2022. Como funcionam os chuveiros elétricos que garantem seu banho quentinho?. [online] **Uol.com.br**. Available at: <<https://www.uol.com.br/tilt/noticias/redacao/2019/08/15/a-tecnologia-por-tras-dos-chuveiros-eletricos.htm>> [Accessed 24 July 2022].

LEE, J.; GUO, J.; CHOI, J. K.; ZUKERMAN, M. Distributed energy trading in microgrids: A game-theoretic model and its equilibrium analysis. **IEEE Trans. Ind. Electron.**, vol. 62, no. 6, pp. 3524–3533, 2015.

LIMA, Williams da Silva Guimarães de; BARROSO, Fábio de Andrade; SILVA, José Martinho de Albuquerque; OLIVEIRA, Jefferson Cardoso; MACIEL, Tuanny da Silva; SOUZA, George Henriques de. IMPACTOS AMBIENTAIS NA PRODUÇÃO DE ENERGIA NA HIDROELÉTRICA. **Revista Campo do Saber**, Paraíba, v. 4, n. 4, p. 106-132, 01 jul. 2018.

LOPES, Igor. **Quanto custa o armazenamento solar por baterias? Compreenda os preços da bateria solar**. 2019. Available: <<https://institutosolar.com/precos-da-bateria-solar/>> .Accessed: 15 mai. 2022.

LORENZETTI. **Produtos**. 2022. Available: <<https://www.lorenzetti.com.br/>>. Accessed 25 apr. 2022.

MACEDO, Bruna. Home office fica mais caro com nova bandeira tarifária, diz pesquisa da FGV, São Paulo: **CNN**. 2021. Available: <<https://www.cnnbrasil.com.br/business/home-office-fica-mais-caro-com-nova-bandeira-tarifaria-diz-pesquisa-da-fgv/>>. Accessed 3 apr. 2022.

MACEDO, Isaias C. Geração de energia elétrica a partir de biomassa no Brasil : situação atual, oportunidades e desenvolvimento. **Centro de Gestão e Estudos Estratégicos**, [S. l.], p. 12, 2001.

MACHADO, Carolina T.; MIRANDA, Fabio S. Photovoltaic solar energy: A briefly review. **Revista Virtual de Química**, [S. l.], v. 7, n. 1, p. 126–143, 2015.

MANOKHA, Ivan. Covid-19: Teleworking, Surveillance and 24/7 Work. Some Reflexions on the Expected Growth of Remote Work After the Pandemic, **Political Anthropological Research on International Social Sciences**, vol.1, no. 2, p. 273-287,2020.

MAPPR. Brazil Regions Map. 2023. Available:< <https://www.mappr.co/counties/brazil-regions-map/>> . Accessed 28 jan. 2023.

MARTINEZ, Simon; MICHAUX, Ghislain; SALAGNAC, Patrick; BOUVIER, Jean Louis. Micro-combined heat and power systems (micro-CHP) based on renewable energy sources. **Energy Conversion and Management**, [S. l.], v. 154, n. September, p. 262–285, 2017.

MARTINS, Juliana Marinho Cavalcanti. **Estudo dos principais mecanismos de incentivo às fontes renováveis alternativas de energia no setor elétrico**. 2010. 114 f. Dissertação (Mestrado) - Curso de Engenharia Mecânica, Universidade Estadual de Campinas, Campinas, 2010.

MARYAMA, Victor. **Gerenciamento Energético para Microrredes Inteligentes**. 2013. 80 f. TCC (Graduação) - Curso de Engenharia de Controle e Automação, Universidade Federal de Santa Catarina, Florianópolis, 2013.

MASHAYEKH, Salman et al. Security-Constrained Design of Isolated Multi-Energy Microgrids. **IEEE Transactions on Power Systems**, [S. l.], v. 33, n. 3, p. 2452–2462, 2018.

MASSON. G.; KAIZUKA. I.; BOSCH E.; DETOLLENAERE A.; NEUBOURG G.; VAN WETTER J. **PVPS: trends in photovoltaic applications 2020**. Suécia: IEA, 2020. 88 p.

MAVROMATIDIS, Georgios; OREHOUNIG, Kristina; CARMELIET, Jan. Design of distributed energy systems under uncertainty: A two-stage stochastic programming approach. **Applied Energy**, v. 222, p. 932-950, 2018.

MBUNGU, N. T.; BANSAL, R. C.; NAIDOO, R. M.; BETTAYEB, M.; SITI, M.W.; BIPATH, M.A dynamic energy management system using smart metering. **Applied energy**, v. 280, n. 115990, p. 115990, 2020.

MECHLERI, Evgenia; DORNEANU, Bogdan; ARELLANO-GARCIA, Harvey. A Model Predictive Control-Based Decision-Making Strategy for Residential Microgrids. **Eng**, [S.L.], v. 3, n. 1, p. 100-115, 9 feb. 2022. MDPI AG. <http://dx.doi.org/10.3390/eng3010009>.

MEHLERI, Eugenia D.; SARIMVEIS, Haralambos; MARKATOS, Nikolaos C.; PAPAGEORGIOU, Lazaros G. A mathematical programming approach for optimal design of distributed energy systems at the neighbourhood level. **Energy**, [S. l.], v. 44, n. 1, p. 96–104, 2012.

MENEGUELLO, Luiz Augusto; CASTRO, Marcus Cesar Avezum Alves De. O Protocolo de Kyoto e a geração de energia elétrica pela biomassa da cana-de-açúcar como mecanismo de desenvolvimento limpo. **Interações (Campo Grande)**, [S. l.], v. 8, n. 1, p. 33–43, 2007.

MME. **Guia de Habilitação Biomassa**. Brasília: Ministério de Minas e Energia, 2004. 42 p.

MME. ProGD Programa de Desenvolvimento da Geração Distribuída de Energia Elétrica. **Brazil. Governo Federal.**, [S. l.], p. 1–17, 2015. Available at: <http://www.mme.gov.br/documents/10584/3013891/15.12.2015+Apresentação+ProGD/bee12bc8-e635-42f2-b66c-fa5cb507fd06?version=1.0>. Accessed 27 apr. 2021.

MME. **Resenha Energética Brasileira**. Brasília: Ministério de Minas e Energia, 2021. 31 p.

MME. **Programa de incentivo às fontes alternativas de energia elétrica**. Brasília: Secretaria de Planejamento e Desenvolvimento Energético, 2009. 39 slides, color.

MME. Resenha Energética Brasileira. [online] **Ministério de Minas e Energia**. 2021. Available at: <<https://www.gov.br/mme/pt-br/assuntos/noticias/ResenhaEnergéticaExercicio2020final.pdf>> [Accessed 10 March 2022].

MOHAMMED, Omar Hazem; AMIRAT, Yassine; BENBOUZID, Mohamed. Particle swarm optimization of a hybrid wind/tidal/PV/battery energy system. Application to a remote area in Bretagne, France. **Energy Procedia**, [S. l.], v. 162, p. 87–96, 2019.

MORAVEJ, Z; AKHLAGHI, A. A novel approach based on cuckoo search for DG allocation in distribution network. **International Journal of Electrical Power and Energy Systems** 2013;v.44, n.1, p.672–9.2003.

MOREIRA, Helena Margarido; GIOMETTI, Analúcia Bueno dos Reis. Protocolo de Quioto e as possibilidades de inserção do Brasil no Mecanismo de Desenvolvimento Limpo por meio de projetos em energia limpa. **Contexto Internacional**, [S. l.], v. 30, n. 1, p. 9–47, 2008.

MOTEVASEL, Mehdi; SEIFI, Ali Reza; NIKNAM, Taher. Multi-objective energy management of CHP (combined heat and power)-based micro-grid. **Energy**, [S. l.], v. 51, p. 123–136, 2013.

MUSTAFA, George de Souza. Avaliação Econômica de Projetos Industriais. Universidade Salvador: Salvador.v. 1, p. 53. 2010.

NASIR, Mohamad Naim Mohd; MUTALE, Joseph. Optimal sizing of solar FV/battery and biogas generator in remote microgrid. 2016. **51st International Universities Power Engineering Conference (UPEC)**, 2016, pp. 1-6, doi: 10.1109/UPEC.2016.8114136.

NASSA, Thiago. **Energia solar cresce 22,5% no mundo com mais de 115 gigawatts instalados no último ano**. 2020. Available at: <https://www.ecodebate.com.br/>. Accessed 11 may 2021.

NEOENERGIA COELBA. Serviços: Residencial. 2020. Available:<<https://servicos.neoenergiacoelba.com.br/residencial-rural/Pages/Baixa%20Tens%C3%A3o/tarifa-branca.aspx>>. Accessed 5 mai. 2022.

NIKOLAIDIS, Pavlos; POULLIKKAS, Andreas. A comparative review of electrical energy storage systems for better sustainability. **Journal of Power Technologies**, [S.l.], v. 97, n. 3, p. 220–245, nov. 2017. ISSN 2083-4195. Available at: <<https://papers.itc.pw.edu.pl/index.php/JPT/article/view/1096>>. Date accessed: 2 may 2022.

NUNEZ, Christina. **Hydropower, explained**: learn about the benefits and pitfalls of generating electricity from waterways. Learn about the benefits and pitfalls of generating electricity from waterways. 2019. Available at: <https://www.nationalgeographic.com/environment/article/hydropower>. Accessed 11 may 2021.

OFGEM. **Feed in Tariffs (FIT)**. 2020. Available: <www.ofgem.gov.uk/environmental-and-social-schemes/feed-tariffs-fit/tariffs-and-payments>. Accessed 27 mar. 2022.

OLIVEIRA, Rafael M.; SAAVEDRA, Osvaldo R. Energias Oceânicas: Arcabouço Legal E Entraves a Serem Superados Para O Desenvolvimento No Brasil. **PCH Notícias SHP News**, [S. l.], v. 70, n. 18, p. 05–11, 2016.

OLIVEIRA, S., MIRANDA, A., KLEPA, R. and SANTANA, J., 2017. Energia Híbrida e suas aplicações em sistemas Fotovoltáicos. In: **International Symposium on Project Management, Innovation and Sustainability**. [online] São Paulo: VI SINGEP. Available at: <<http://www.singep.org.br/6singep/resultado/156.pdf>> [Accessed 15 April 2022].

OMU, A.; CHOUDHARY, R.; BOIES, A. Distributed energy resource system optimisation using mixed integer linear programming. **Energy Policy**, v. 61, p. 249–266, 2013.

ONS. **Boletim Mensal de Geração Eólica Dezembro / 2020**. Brasília: Operador Nacional do Sistema Elétrico. 2020. 46p.

OTIM, George, OKAKA, David, KAYIMA, John. Design of biogás plant for rural households in Uganda(Case Study: Apac District). **Second International Conference on Advances in Engineering and Technology**. p. 544-550. 2006.

PALLABAZZER, Rodolfo. Parametric Analysis of Wind Siting Efficiency. **Journal of Wind Engineering and Industrial Aerodynamics**, v. 91, n. 11, Nov. 2003, pp. 1329–1352, 10.1016/j.jweia.2003.08.002.

PECENAK, Zachary K.; STADLER, Michael; MATHIESEN, Patrick; FAHY, Kelsey; KLEISSL, Jan. Robust design of microgrids using a hybrid minimum investment optimization. **Applied Energy**, [S. l.], v. 276, n. February, p. 115400, 2020.

PEREIRA, Lucas B; DE SÁ, Bruno Gomes; DIAS, Francisco; SAAVEDRA, Osvaldo R.; GOMES, Thiago Luis C.; DE LIMA, Shigeaki Leite; NETO, Pedro Bezerra L.; TORRES JR., Audalio Rebelo. **Sizing Multiple Non-Conventional Renewable Sources for Isolated Microgrids**. Ixtapa, México: IEEE International Autumn Meeting On Power, Electronics And Computing (Ropec 2019)., 2019. 6 p.

PORKAR, S.; POURE, P.; ABBASPOUR-TEHRANI-FARD, A.; SAADATE, S. Optimal allocation of distributed generation using a two-stage multi-objective mixed-integernonlinear programming. **European Transactions on Electric Power**, v. 21, n. 1 p.1072–87, 2010.

Portal Solar. **Controlador de carga: o que é, qual a função, como funciona, tipos e quanto custa**. 2022. Available: <<https://www.portalsolar.com.br/controlador-de-carga>>. Accessed: 15 mai. 2022.

RAMOS, Alba; CHATZOPOULOU, Maria Anna; GUARRACINO, Ilaria; FREEMAN, James; MARKIDES, Christos N. Hybrid photovoltaic-thermal solar systems for combined heating, cooling and power provision in the urban environment. **Energy Conversion And Management**, [S.L.], v. 150, p. 838-850, out. 2017. Elsevier BV. <http://dx.doi.org/10.1016/j.enconman.2017.03.024>.

RAYBAUT, P. **Spyder-documentation**. 2009. Available at: Pythonhosted. Org. Accessed 5 apr. 2022.

RECALDE, Angel A.; ALVAREZ-ALVARADO, Manuel S. Design optimization for reliability improvement in microgrids with wind – tidal – photovoltaic generation. **Electric Power Systems Research**, [S. l.], v. 188, n. February, p. 106540, 2020.

REURASIA. (2022). Green energy from waste and biogas energy solutions. Available at: <https://reurasia.com/green-energy-from-waste-and-biogas-energy-solutions/>. Accessed 12 May 2022.

RITCHIE, H., ROSER, M. AND ROSADO, P., 2021. **CO₂ and Greenhouse Gas Emissions**. **Our World in Data**, [online] Available at: <<https://ourworldindata.org/co2-and-other-greenhouse-gas-emissions>> [Accessed 2 Apr 2022].

RITCHIE, H., ROSER, M. AND ROSADO, P., 2021. **Fossil Fuels**, [online] Available at: <<https://ourworldindata.org/fossil-fuels>> [Accessed 11 Nov 2022].

RITCHIE, H.; ROSER, M., 2020. Emissions by sector. **Our World in Data**, [online] Available at: <<https://ourworldindata.org/emissions-by-sector>> [Accessed 1 Apr 2022].

RITCHIE, Hannah; ROSER, Max. **Energy mix**. 2019. Available at: <https://ourworldindata.org/energy-mix>. Accessed 23 jul. 2021.

ROSSUM , Van G, DRAKE JR, FL. Python reference manual. **Centrum voor Wiskunde en Informatica Amsterdam**; 1995.

ROUX, A.; SHANKER, A. **Net metering and PV self-consumption in emerging countries**. 2018. Available at: <https://iea-pvps.org/key-topics/t9-net-metering-and-pvdevelopment-in-emerging-countries-en-report/>. Accessed 24 mar. 2023.

ROWAN HOUSE, 2022. January 2018 – ROWAN HOUSE. [online] **Rowanhouseonline.org**. Available at: <<https://www.rowanhouseonline.org/2018/01/>> [Accessed 22 April 2022].

SAAVEDRA, Osvaldo R. Potencial Energético do Maranhão: Energias Oceânicas Osvaldo Ronald Saavedra O potencial Energético. **Universidade Federal do Maranhão – UFMA**, [S. l.], 2016.

SACHS, Julia; SAWODNY, Oliver. Multi-objective three stage design optimization for island microgrids. **Applied Energy**, [S. l.], v. 165, p. 789–800, 2016.

SAHINIDIS, N. V., BARON 21.1.13: Global Optimization of Mixed-Integer Nonlinear Programs, **User's manual**, 2021.

SALIX RENEWABLE. 2018. **Biomass** – Salix Renewable Energy BV. [online] Available at: <<https://salixrenewable.com/biomass/>> [Accessed 12 May 2022].

SCHÜTZ, Thomas; HU, Xiaolin; FUCHS, Marcus; MÜLLER, Dirk. Optimal design of decentralized energy conversion systems for smart microgrids using decomposition methods. **Energy**, [S. l.], v. 156, p. 250–263, 2018.

SERGICI, Sanem; YANG, Yingxia; CASTANER, Maria; FARUQUI, Ahmad. Quantifying net energy metering subsidies. **The Electricity Journal**, [S.L.], v. 32, n. 8, p. 106632, out. 2019.

SHARMA, Pranshu. 2022. **K Means Clustering Simplified in Python | K Means Algorithm**. [online] **Analytics Vidhya**. Available at: <https://www.analyticsvidhya.com/blog/2021/04/k-means-clustering-simplified-in-python/>. Accessed 27 July 2022.

SIDNELL, Tim; CLARKE, Fiona; DORNEANU, Bogdan; MECHLERI, Evgenia; ARELLANO-GARCIA, Harvey. Optimal design and operation of distributed energy resources systems for residential neighbourhoods. **Smart Energy**, [S.L.], v. 4, p. 100049, nov. 2021. Elsevier BV. <http://dx.doi.org/10.1016/j.segy.2021.100049>.

SIDNELL, Tim; CLARKE, Fiona; DORNEANU, Bogdan; MECHLERI, Evgenia; ARELLANO-GARCIA, Harvey. Optimal design and operation of distributed energy resources systems for residential neighbourhoods. **Smart Energy**, [S.L.], v. 4, p. 100049, nov. 2021a. Elsevier BV. <http://dx.doi.org/10.1016/j.segy.2021.100049>.

SIDNELL, Tim; DORNEANU, Bogdan; MECHLERI, Evgenia; VASSILIADIS, Vassilios S.; ARELLANO-GARCIA, Harvey. Effects of Dynamic Pricing on the Design and Operation of Distributed Energy Resource Networks. **Processes**, [S.L.], v. 9, n. 8, p. 1306, 28 jul. 2021b. MDPI AG. <http://dx.doi.org/10.3390/pr9081306>.

SIL. **Cabos**. 2022. Available: <<https://www.sil.com.br/>>. Accessed 25 apr. 2022

SINDIGÁS. Gás LP no Brasil: Perguntas frequentes. **Sindicato Nacional das Empresas Distribuidoras de Gás Liquefeito de Petróleo**, [S. l.], v. 1, p. 44, 2008.

SINDIGÁS. GLP em movimento: Panorama do setor de GLP em movimento. **Sindicato Nacional das Empresas Distribuidoras de Gás Liquefeito de Petróleo**, [S. l.], v. 45, p. 26, 2021.

SÖNNICHSEN, N. **Capacity of bioenergy power plants in selected countries and worldwide in 2019**. 2020. Available at: <https://www.statista.com/statistics/264637/world-biomass-energy-capacity/>. Accessed 26 jul. 2021.

SORIA, Rafael; SCHAEFFER, Roberto; SZKLO, Alexandre. Configurações Para Operação De Plantas Heliotérmicas Csp Com Armazenamento De Calor E Hibridização No Brasil. **V Congresso Brasileiro de Energia Solar**, [S. l.], v. V, p. 10, 2014.

SOROUDI, A; EHSAN, M. Imperialist competition algorithm for distributed generation connections. **IET Generation, Transmission & Distribution** 2012;v.6, n.1, p.21–9. 2012.

STATISTA. (2021). **Global geothermal power installed cost 2010-2020**. Available at: <https://www.statista.com/statistics/1027751/global-geothermal-power-installation-cost-per-kilowatt/>. Accessed 27 may 2022.

STAUFFER, N., 2009. **Capturing the energy in ocean waves**. [online] Main. Available at: <https://energy.mit.edu/news/capturing-the-energy-in-ocean-waves/>. Accessed 20 April 2022.

STECANELLA, Priscilla A. Juá; CAMARGOS, Ronaldo S.C.; VIEIRA, Daniel; DOMINGUES, Elder G.; FILHO, Anésio de L. F. A methodology for determining the incentive policy for photovoltaic distributed generation that leverages its technical benefits in the distribution system. **Renewable Energy**, v. 199, n. 0960-1481, p. 474–485, 2022.

SULAIMAN, MH; MUSTAFA, MW; AZMI, A; ALIMAN, O; ABDUL RAHIM, SR. Optimal allocation and sizing of Distributed Generation in distribution system via Firefly Algorithm. In: **IEEE international power engineering and optimization conference (PEOCO)**; 2012. p. 84–9.

SUTTHIBUN, T.; BHASAPUTRA, P. Multi-objective optimal distributed generation placement using simulated annealing. In: **International conference on electrical engineering/electronics computer telecommunications and information technology (ECTI-CON)**; 2010. p. 810–3.

TAN, Wen Shan; HASSAN, Mohammad Yusri; MAJID, Md Shah; ABDUL RAHMAN, Hasimah. Optimal distributed renewable generation planning: A review of different approaches. **Renewable and Sustainable Energy Reviews**, [S. l.], v. 18, p. 626–645, 2013.

TAWARMALANI, M. and N. V. Sahinidis, A polyhedral branch-and-cut approach to global optimization, **Mathematical Programming**, v. 103, n.2, p. 225-249, 2005.

TEICHGRAEBER, H.; LINDENMEYER, C. P.; BAUMGÄRTNER, N.; KOTZUR, L.; STOLTEN, D.; ROBINIUS, M.; BARDOW, A.; BRANDT, A. R. Extreme events in time series aggregation: A case study for optimal residential energy supply systems. **Applied Energy**, v. 275, p. 115223, out. 2020.

TOKE, D. Renewable Energy Auctions and Tenders: How good are they? **International Journal of Sustainable Energy Planning and Management**, v. 8, p. 43–56, 2015.

TOLMASQUIM, MAURICIO Tiomno. **Energia Termelétrica: Gás Natural, Biomassa, Carvão, Nuclear** / Mauricio Tiomno Tolmasquim (coord). – EPE: Rio de Janeiro, 2016 417p.

U.S. DEPARTMENT OF ENERGY, 2022. Types of Hydropower Plants. [online] **Energy.gov**. Available at: <<https://www.energy.gov/eere/water/types-hydropower-plants>> [Accessed 1 May 2022].

UNICA. (2020). **BIOELETRICIDADE EM NÚMEROS – junho/2020**. São Paulo: União da Indústria de Cana de Açúcar. 2020. 6 p.

VAIDYA, Dheeraj. Industrial Revolution. 2023. Available: <<https://www.wallstreetmojo.com/industrial-revolution/>>. Accessed: 29 jan. 2023.

VIA SOL. **Via Sol: Energia Solar**. 2022. Available: <<https://viasolenergiasolar.com.br/>>. Accessed 27 apr. 2022

VIEIRA, Leonardo Santos Reis; GUIMARÃES, Ana Paula Cardoso; LISBOA, Paulo Abreu. Renováveis, Energias Complementares - Energia Solar Heliotérmica. **Renováveis, Energias Complementares - Energia Solar Heliotérmica**, [S. l.], p. 44–51, 2018.

VISHNUHOTLA, V. Renewable Heat Incentive (Updated 2022 Guide), **Greenmatch.co.uk**, 2022. [Online]. Available: <https://www.greenmatch.co.uk/green-energy/grants/rhi>. [Accessed: 08-May- 2022].

VOVOS, PN; HARRISON, GP; WALLACE, AR; BIALEK, JW. Optimal power flow as a tool for fault level-constrained network capacity analysis. **IEEE Transactions on Power Systems** 2005, v.20, n.2, p.734–41. 2005.

WAKUI, Tetsuya; YOKOYAMA, Ryohei. Optimal structural design of residential cogeneration systems in consideration of their operating restrictions. **Energy**, [S. l.], v. 64, p. 719–733, 2014.

WEBER, C.; SHAH, N. Optimisation based design of a district energy system for an eco-town in the United Kingdom. **Energy**, [S. l.], v. 36, n. 2, p. 1292–1308, 2011.

WEBER, Céline; MARÉCHAL, François; FAVRAT, Daniel. Design and optimization of district energy systems. *In*: **Computer Aided Chemical Engineering**. [s.l: s.n.]. v. 24p. 1127–1132.

WEISS, W.; SPÖRK-D. Solar Heat Worldwide 2020 - Global market development and trends in 2019. **Science and Technology for the Built Environment**, [S. l.], v. 24, n. 8, p. 819–819, 2019.

WILLIS, HL. Analytical methods and rule of thumb for modeling DG- distribution interaction. **IEEE PES Summer Meeting 2000**. v. 1643, n.4, 2000.

WORLD BANK GROUP. Global Solar Atlas. Available: <<https://globalsolaratlas.info/map?c=-13.859414,-42.220459,7&s=-12.972442,-38.441162&m=site&pv=small,0,12,1>>. Accessed 15 mar. 2022.

WORLD NUCLEAR ASSOCIATION, 2022. Electricity and Energy Storage - World Nuclear Association. [online] **World-nuclear.org**. Available at: <<https://world-nuclear.org/information-library/current-and-future-generation/electricity-and-energy-storage.aspx#:~:text=Electricity%20cannot%20itself%20be%20stored,air%2C%20and%20pumped%20hydro%20storage>> [Accessed 1 May 2022].

WORLD NUCLEAR, 2022. Carbon Dioxide Emissions From Electricity. [online] **World-nuclear.org**. Available:<<https://www.world-nuclear.org/information-library/energy-and-the-environment/carbon-dioxide-emissions-from-electricity.aspx>> . Accessed 6 jun.2022.

YSE, Diego Lopez. **The Anatomy of K-means: A complete guide to K-means clustering algorithm. Medium**. 2019. Available at: <https://towardsdatascience.com/the-anatomy-of-k-means-c22340543397>. Accessed 26 jun. 2022.

ZATTI, Matteo; GABBA, Marco; FRESCHINI, Marco; ROSSI, Michele; GAMBAROTTA, Agostino; MORINI, Mirko; MARTELI, Emanuele. k-MILP: A novel clustering approach to select typical and extreme days for multi-energy systems design optimization. **Energy**, v. 181, n. [], p. 1051–1063, 2019.

ZHANG, Di; EVANGELISTI, Sara; LETTIERI, Paola; PAPAGEORGIU, Lazaros G. Optimal design of CHP-based microgrids: Multiobjective optimisation and life cycle assessment. **Energy**, [S. l.], v. 85, p. 181–193, 2015.

ZHU, Q.; CHEN. X.; SONG, M.; XINGCHEN, L.; SHEN, Z. Impacts of renewable electricity standard and Renewable Energy Certificates on renewable energy investments and carbon emissions. **Journal of Environmental Management**, v. 306, p. 114495, mar. 2022.

UFBA
UNIVERSIDADE FEDERAL DA BAHIA
ESCOLA POLITÉCNICA

PROGRAMA DE MESTRADO EM ENGENHARIA INDUSTRIAL - PEI

Rua Aristides Novis, 02, 6º andar, Federação, Salvador BA
CEP: 40.210-630
Telefone: (71) 3283-9800
E-mail: pei@ufba.br
Home page: <http://www.pei.ufba.br>

